SQT

NASA Technical Memorandum

NASA TM-82556

BELLOWS FLOW-INDUCED VIBRATIONS

By P. J. Tygielski and H. M. Smyly
Structures and Propulsion Laboratory

and Dr. C. R. Gerlach
Gerlach Products, Inc.

October 1983

National Aeronautics and Space Administration

George C. Marshall Space Flight Center

TECHNICAL REPORT STANDARD TITLE PAGE

1. REPORT NO.	2. GOVERNMENT ACCESSION NO.	3. RECIPIENT'S CATALOG NO.
NASA TM-83556		

4. TITLE AND SUBTITLE	5. REPORT DATE
Bellows Flow-Induced Vibrations	October 1983
	6. PERFORMING ORGANIZATION CODE MSFC/EP36
7. AUTHOR(S) Dr. C. R. Gerlach,* P. J. Tygielski, and H. M. Smyly	8. PERFORMING ORGANIZATION REPORT # CDDF: 80-5
9. PERFORMING ORGANIZATION NAME AND ADDRESS George C. Marshall Space Flight Center Marshall Space Flight Center, Alabama 35812	10. WORK UNIT NO. 11. CONTRACT OR GRANT NO. 13. TYPE OF REPORT & PERIOD COVERED Technical Memorandum
12. SPONSORING AGENCY NAME AND ADDRESS National Aeronautics and Space Administration Washington, D.C. 20546	14. SPONSORING AGENCY CODE

15. SUPPLEMENTARY NOTES

Prepared by Structures and Propulsion Laboratory, Science and Engineering Directorate.

*Dr. C. R. Gerlach of Gerlach Products, Inc., served as Consultant for this project.

16. ABSTRACT

This report summarizes the present understanding of the bellows flow excitation mechanism and of results of a comprehensive test program conducted at MSFC. This, along with other existing test data, is used to refine the analytical model for predicting bellows flow-induced stress. This model includes the effects of an upstream elbow, arbitrary geometry, and multiple plies. A refined computer code for predicting flow-induced stress is described which allows life prediction if a material S-N diagram is available.

17. KEY WORDS		18. DISTRIBUTION STATEMENT
bellows	flow excitation	Unclassified – Unlimited
expansion joints	bellows vibration	
flow-induced vibrations	convolute stress	
flow-induced stress		
vortex		

19. SECURITY CLASSIF. (of this report)	20. SECURITY CLASSIF. (of this page)	21. NO. OF PAGES	22. PRICE
Unclassified	Unclassified	232	NTIS

For sale by National Technical Information Service, Springfield, Virginia 22161

TABLE OF CONTENTS

TABLE OF CONTENTS (Concluded)

LIST OF ILLUSTRATIONS

LIST OF ILLUSTRATIONS (Concluded)

LIST OF TABLES

DEFINITION OF SYMBOLS

Symbol	Definition
a	Mean convolute radius $(\sigma - tN_p)/2$ (in.)
D_i	Inside diameter (in.)
D_o	Outside diameter (in.)
D_m	$(D_o + D_i)/2$ (in.)
h	Mean inside disc height (in.)
L.L.	Live length (in.)
N_c	Number of convolutes
N_p	Number of plies
t	Ply thickness (in.)
σ	Inside convolute tip width (in.)
δ	Internal convolute gap (in.)
δ'	Non-standard internal convolute gap (in.)
λ	Internal convolute pitch (in.)
λ'	Non-standard internal convolute pitch (in.)
f	Frequency (cycles/sec)
f(N)	Modal frequency (cycles/sec)
f_{ml}	Lowest mode frequency (cycles/sec)
f_{mn}	Highest mode frequency (cycles/sec)
k	Elemental spring rate (lbs/in.)
K_a	Overall bellows spring rate (lbs/in.)
ζ_{IV}	Salzmann spring rate shape factor
S.S.R.	Specific Spring Rate

DEFINITION OF SYMBOLS (Continued)

Symbol	Definition
m	Elemental mass (lb sec^2/in.)
m_m	Elemental metal mass (lb sec^2/in.)
m_f	Elemental fluid mass (lb sec^2/in.)
$m_{f_e}{}^*$	Experimental normalized fluid mass
m_{f_e}	Experimental fluid mass (lb sec^2/in.)
ρ_m	Metal mass density (lb $sec^2/in.^4$)
ρ_f	Fluid mass density (lb $sec^2/in.^4$)
S	Strouhal number
$S_{\sigma\ell}$	Lower Strouhal limit
$S_{\sigma c}$	Critical Strouhal value
$S_{\sigma u}$	Upper Strouhal limit
V	Fluid free stream velocity (in./sec)
V'	V/V_c
V_c	Critical velocity for mode $N = N_c$ (in./sec)
v	Convolute fluid velocity amplitude
V_F	Failure velocity of bellows (in./sec)
g	Acceleration (gravity) (in./sec^2)
N	Mode number (1, 2, 3, ..., $2N_c$-1)
A_p	Projected area ($in.^2$)
CSFQ	$\pi/4\ C_S\ C_F\ Q$
E	Young's modulus of elasticity ($lb/in.^2$)
F	Vortex force (lb)
P_d	Fluid free stream dynamic pressure ($1/2\ \rho\ V^2$) (psig)

DEFINITION OF SYMBOLS (Concluded)

Symbol	Definition
x	Convolute dynamic displacement (in.)
B_N	Dimensionless frequency factor
C_E	Elbow factor
C_F	Vortex force coefficient
C_m	Vibration mode factor
C_{NP}	Damping modifier coefficient for multi-ply bellows
C_S	Geometric stress factor
C*	Force and damping coefficient
C_F*	Force coefficient parameter
Q	Dynamic amplification factor
BOP	Bellows Operational Parameter
CTF	Cycles to failure
TTF	Time to failure (sec)
S.I.	Stress Indicator

TECHNICAL MEMORANDUM

BELLOWS FLOW-INDUCED VIBRATIONS

I. INTRODUCTION

It is well known that the occurrence of flow-induced vibrations in metal bellows can cause premature failure because of coupling of fluid vortices with the natural frequency of the bellows. The problem is especially acute in aerospace components where the diameters are kept small (with correspondingly high velocities) to reduce weight and size. The use of internal liners has not been a completely satisfactory solution because this increases weight and cost. Even the use of multiple plies has not been entirely satisfactory for resonance suppression. The ultimate goal, of course, would be to develop an accurate analytical method which predicts the susceptibility of a particular design to flow-induced vibration. If a particular bellows design is susceptible, then calculation of the predicted life would be a desirable goal.

This report concerns the phenomena of flow excitation of metal bellows for spacecraft applications and has a two-fold purpose. First, this report will describe the current understanding of bellows flow excitation, and define updated analytical methods for frequency and stress prediction. Secondly, this report will summarize results of recent extensive spring rate deflection tests, static pressure tests, and flow and failure tests performed at Marshall Space Flight Center and Wyle Laboratories. Results of these tests plus those earlier performed at Southwest Research Institute (SwRI) [1,2] will be used to validate and empirically refine the analytical prediction methods.

II. DESCRIPTION OF BELLOWS FLOW EXCITATION

A. Coupled Fluid-Structure Instability

Bellows "flow excitation" is not the result of a fluid flow-imposed forcing function in the classical linear vibrations sense. Rather, it is a coupled fluid-structure instability problem, nonlinear in nature. For years the term "bellows flow-induced vibration" has been used to identify this phenomena and while not a totally accurate description, we will continue to use the term herein.

Figure 1 shows the measured convolute tip dynamic stress as a function of internal mean fluid velocity for a typical test bellows. As the fluid velocity is increased from zero, successive longitudinal vibratory modes of the bellows are excited. This excitation is the result of periodic formation and shedding of vortices near the convolute tips as illustrated in Figure 2. A key feature of this phenomena is that the structure (convolutes) must be in motion to cause the dynamic vortex activity, but in turn the dynamic vortex activity must exist to cause structural vibration. The above describes a coupled fluid-structural instability problem.

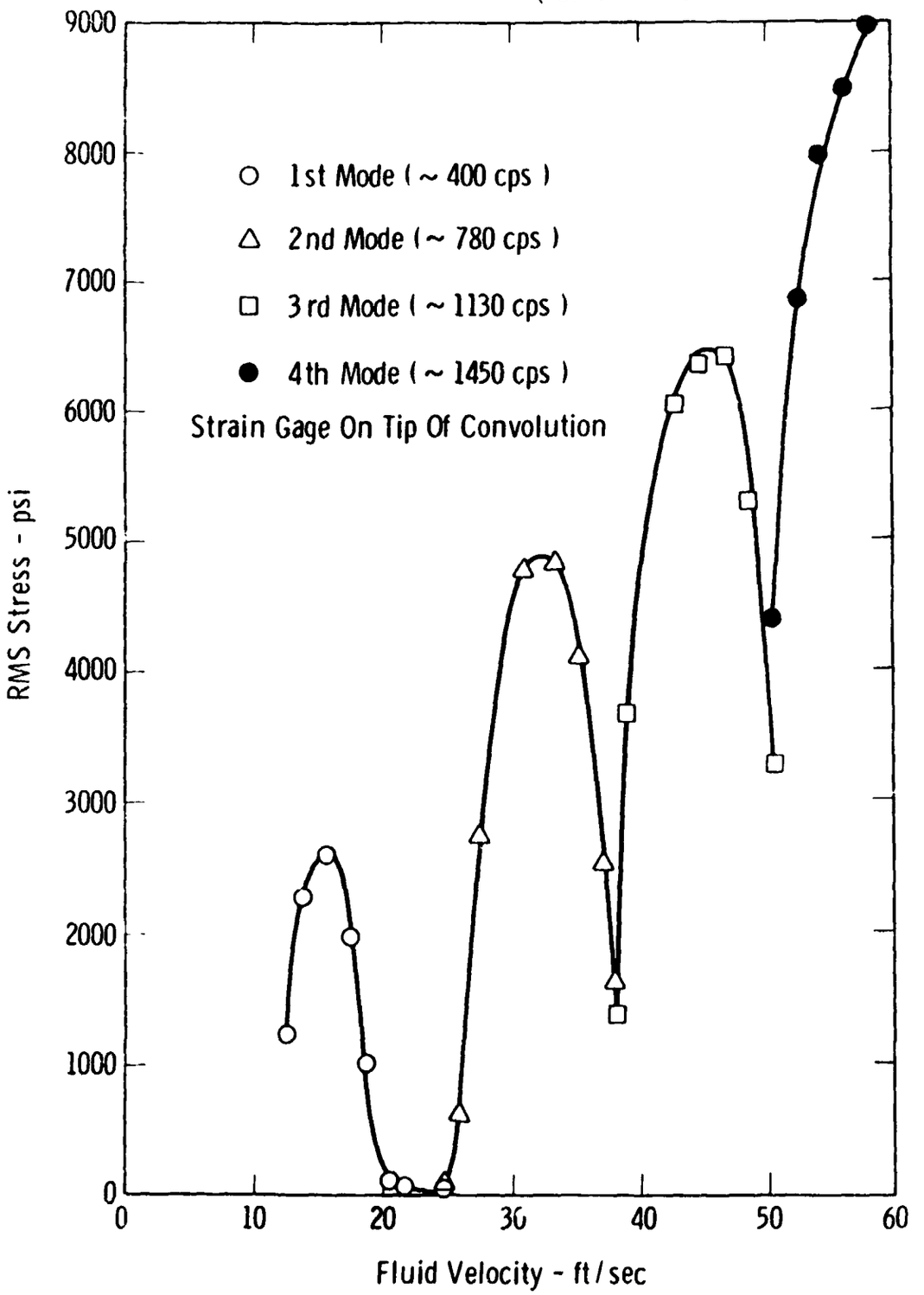

Figure 1. Bellows stress as a function of flow rate for four flow excited modes of vibration, PN 08046.

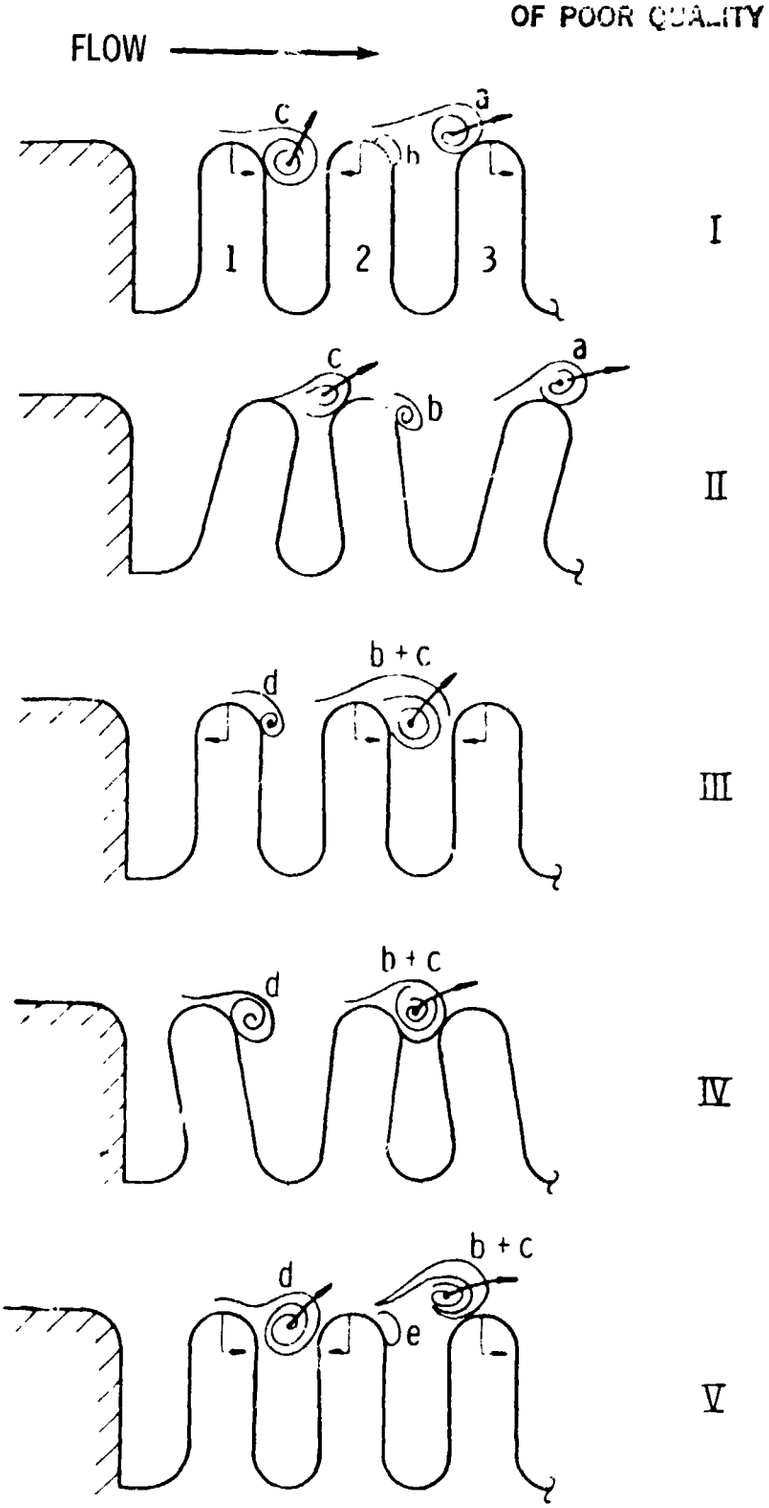

Figure 2 Sequence of coupled fluid-convolution events observed with SwRI two-dimensional bellows flow visualization model.

B. Strouhal Number

As shown in Figure 1, the vortex activity couples with given structural modes over limited velocity ranges, called lock-in ranges. For example, structural longitudinal mode number two, shown in Figure 1, is flow-excited over a range of about 25 ft/sec to 38 ft/sec fluid velocity. Optimum or peak excitation occurs at about 32 ft/sec. The fluid velocity, frequency, and convolute geometry at which the fluid-structure coupling occurs may be related by a Strouhal number of dimensionless quantity of the form

$$S = \frac{f\sigma}{V} \tag{1}$$

Ideally, the Strouhal number is descriptive only of the vortex phenomena and defines the frequency at which vortex shedding and formation would like to occur (if the structure also vibrates) for a given convolute tip width σ and fluid velocity V. As used herein, the Strouhal number concept allows prediction of the velocity or the velocity range of coupling for each bellows mode, defined by a mode frequency f(N).

C. Flow-Excited Modes

Experimentally, flow excitation has been observed for three different kinds of structural modes. Figure 3 illustrates the axisymmetric longitudinal or accordion modes which are most prevalent. For this case relative axial-symmetric motion of adjacent convolute roots and/or crowns occurs. For the first mode, all convolutes move axially back and forth in-phase. For the second mode, convolutes over one-half the bellows length move back and forth in-phase but out-of-phase with convolutes moving in unison over the second half of the bellows.

Figure 4 illustrates nonsymmetric longitudinal or cocking modes which have been occasionally observed interspersed between successive symmetric longitudinal modes. This observed interspersion is illustrated by Figure 5. Response of cocking modes is not observed in all bellows for which the symmetric longitudinal modes are observed. Figure 4 also illustrates a local convolute bending mode which has been observed to date only with high velocity gaseous media and with radial acoustic resonance.

D. Preferred Modes

The frequencies of all possible longitudinal modes for a given bellows are predictable mathematically and each would be observed during a mechanical excitation study of that bellows. Not all of these modes, however, will couple with the dynamic vortex activity to result in flow excitation. There are two explanations for failure of certain modes to be flow-excited. First, the periodic formation and shedding of vortices (Fig. 2) requires an opening and closing action between adjacent convolutes and this may not occur in all possible mechanical modes.

Secondly, vortices displaced from a convolute and washed downstream may have a cancellation or suppression effect upon the vortex forming at the downstream location. Experimental evidence of this phenomena exists.

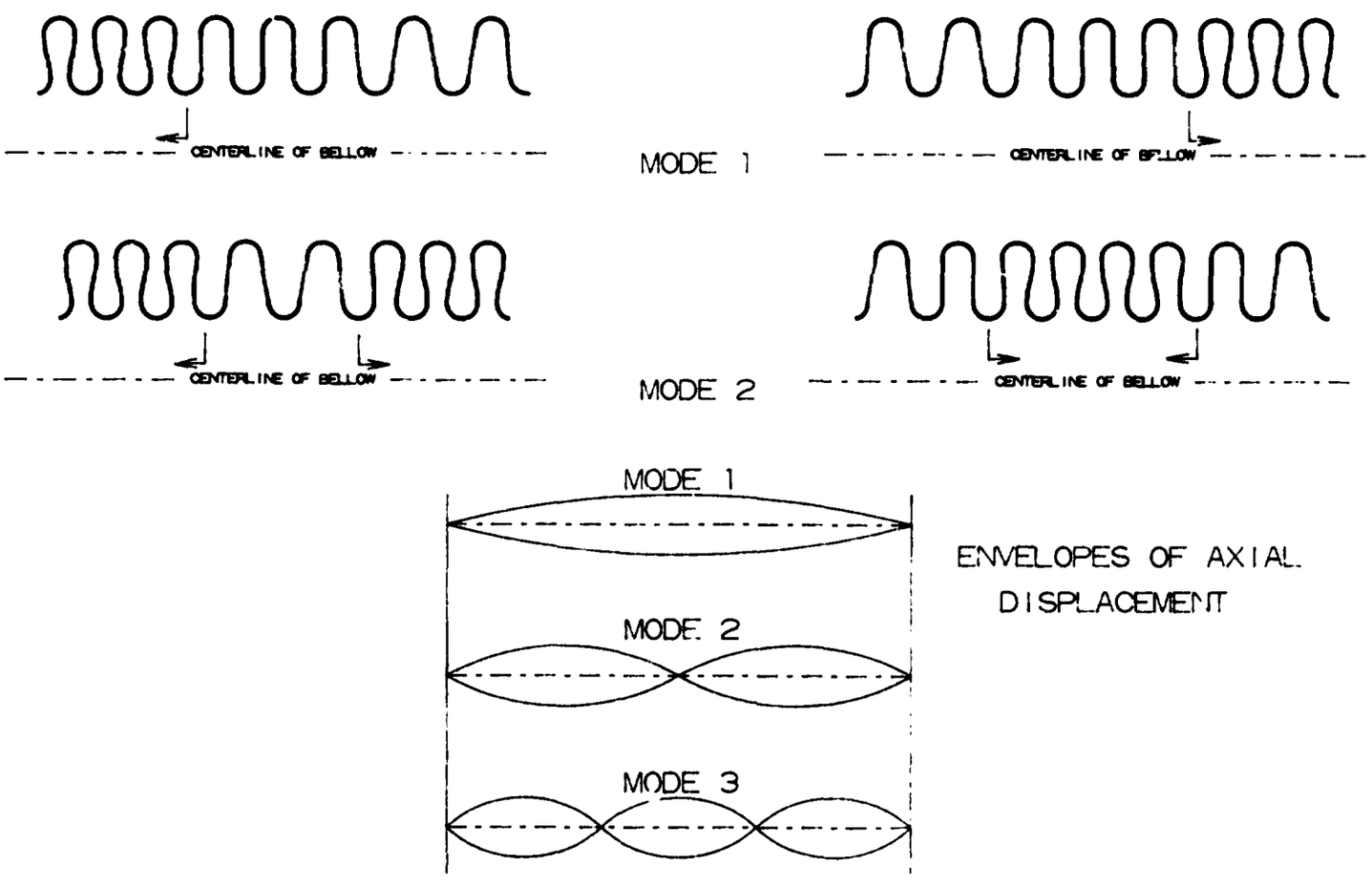

Figure 3. Illustration of axisymmetrical longitudinal modes.

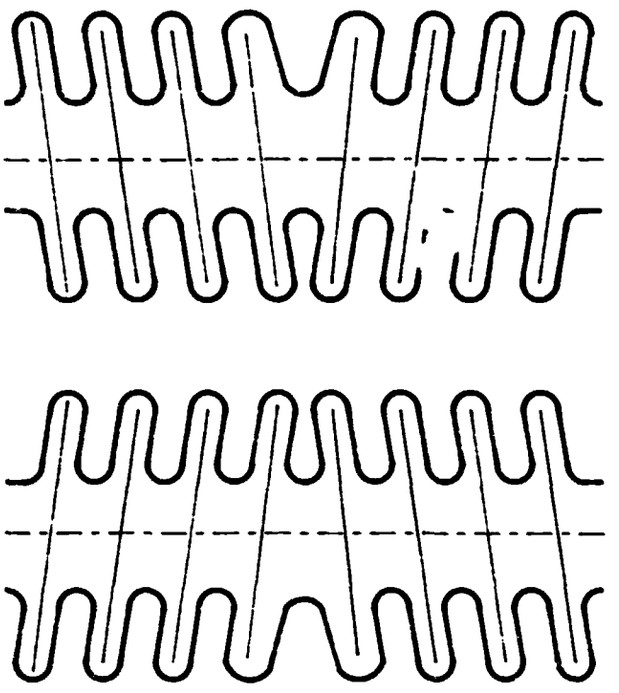

ILLUSTRATION OF SECOND NONSYMMETRICAL LONGITUDINAL MODE

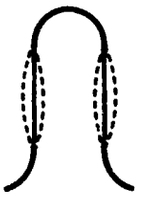

ILLUSTRATION OF LOCAL CONVOLUTE BENDING MODE

Figure 4. Nonsymmetric and local convolute bending modes.

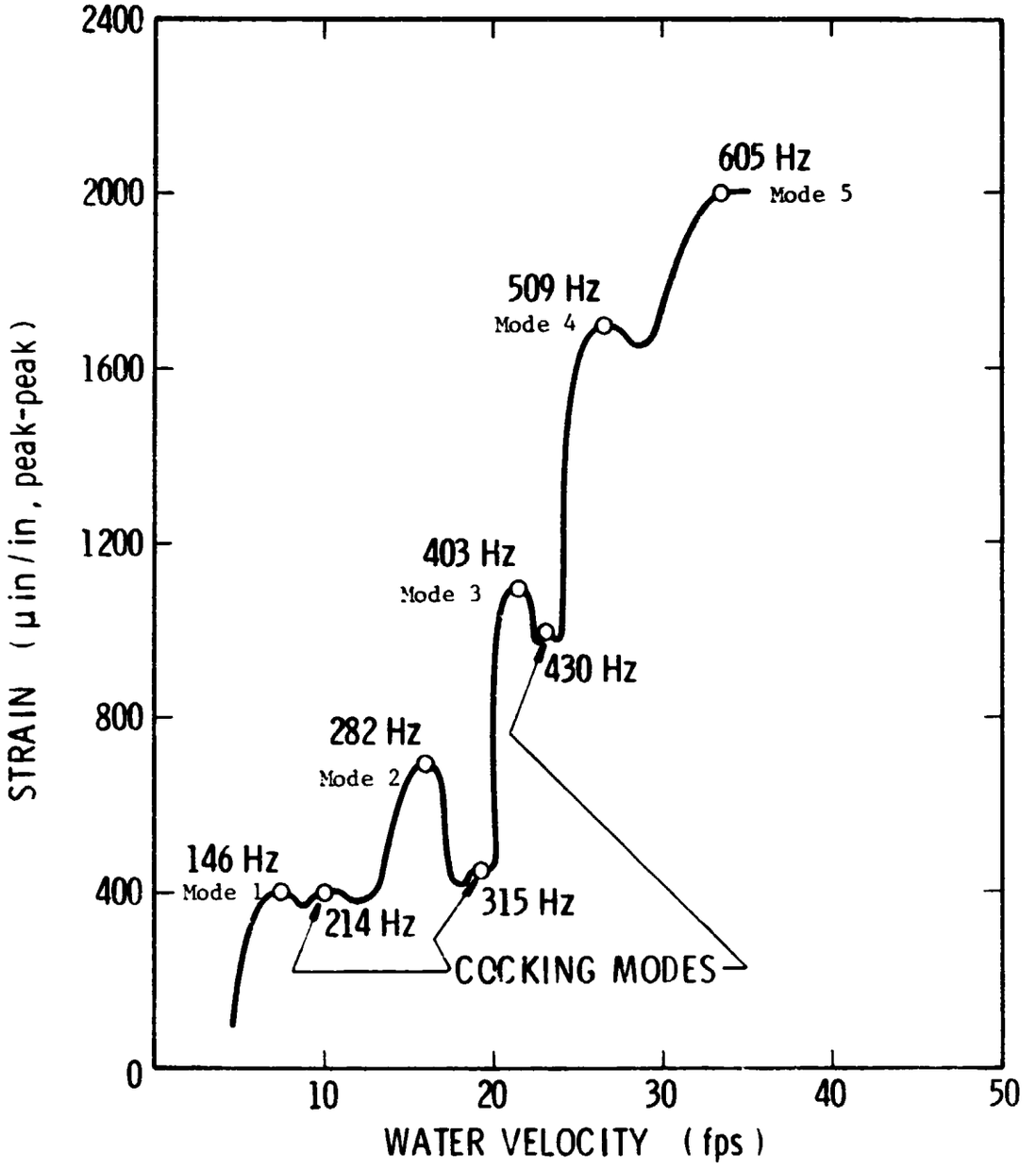

Figure 5. Mean flow velocity versus dynamic strain for SwRI-E bellows (typical).

In earlier reports, we assumed that all predicted bellows modes could be flow-excited This is not necessarily true, and in this report we will attempt to indicate those modes which are suppressed.

E. Other Factors

There are several factors which can significantly modify or change the general bellows flow-induced vibration phenomena described above. First, the presence of an elbow or other flow skewing device upstream of the bellows can cause a shift in the critical velocities where excitation occurs (Fig. 6). Note also that the presence of an elbow can cause a higher convolute stress level for a given fluid velocity.

A second modifying factor is acoustic resonance. For the case of gaseous flows acoustic resonance can couple with vortex shedding from the convolutes to produce extraordinarily high stress levels.

A third modifying factor is the action of local boiling in the convolutes (for the case of cryogenic flows) or cavitation (for high velocity, low absolute pressure normal liquid flows). In both cases, boiling or cavitation, the flow-induced response levels (stresses) are reduced or completely suppressed. Figure 7 illustrates this phenomena.

III. FREQUENCY AND LOCK-IN RANGE PREDICTION

A. Mechanical Model

The bellows symmetric longitudinal mode frequencies are predictable through the use of a lumped spring-mass model. Figure 8 gives pertinent nomenclature which will be used for frequency calculation purposes. Figure 9 shows the lumped spring-mass model used. In this model the bellows is assumed divided into $2N_c-1$ elemental masses of mass m and $2N_c$ elemental springs of rate k. Each elemental spring is related to the overall bellows spring rate K_a by the equation

$$k = 2\, N_c\, K_a \tag{2}$$

Each elemental mass is given by the equation

$$m = {}_m + m_f \tag{3}$$

where m_m, which represents the elemental metal mass, is given by

$$m_m = \pi\, \rho_m + N_P\, D_m\, [\pi a + (h - 2a)] \tag{4}$$

and m_f represents an apparent elemental fluid mass to be discussed below.

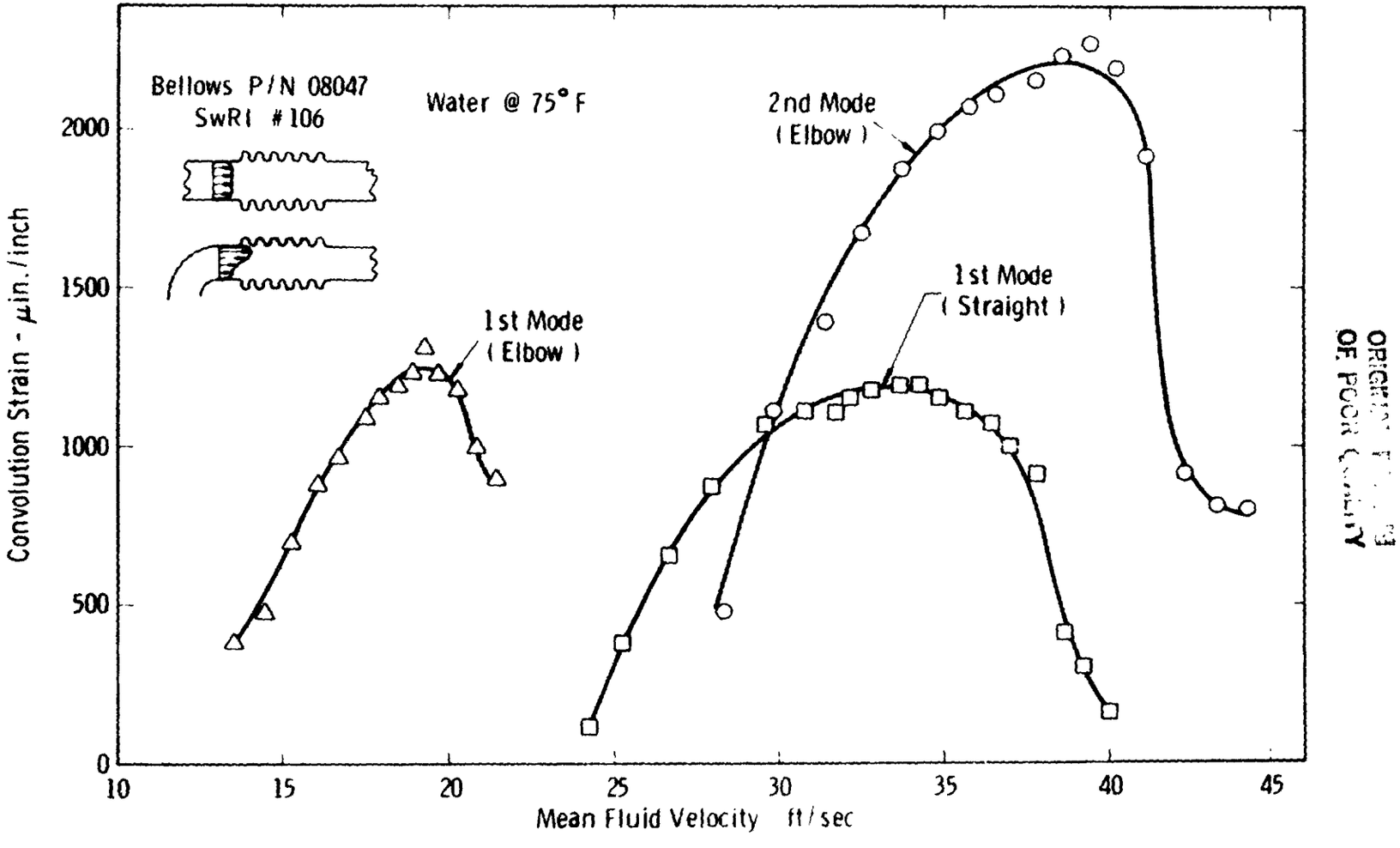

Figure 6. Bellows flow-induced strain with and without upstream elbow.

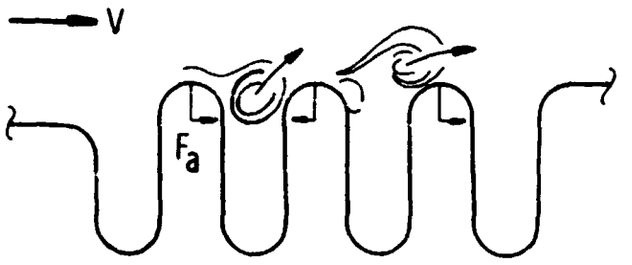

(a) NO HEAT INPUT - CONVENTIONAL VORTEX PHENOMENA

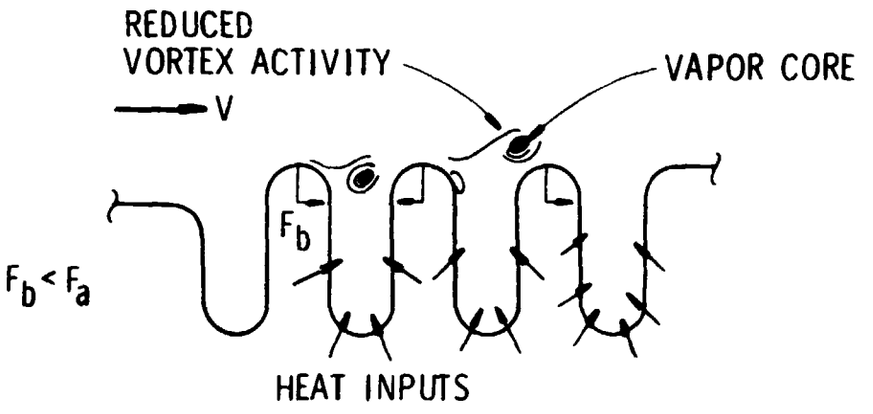

(b) EXTERNAL HEATING - VAPOR CORE IN VORTEXES

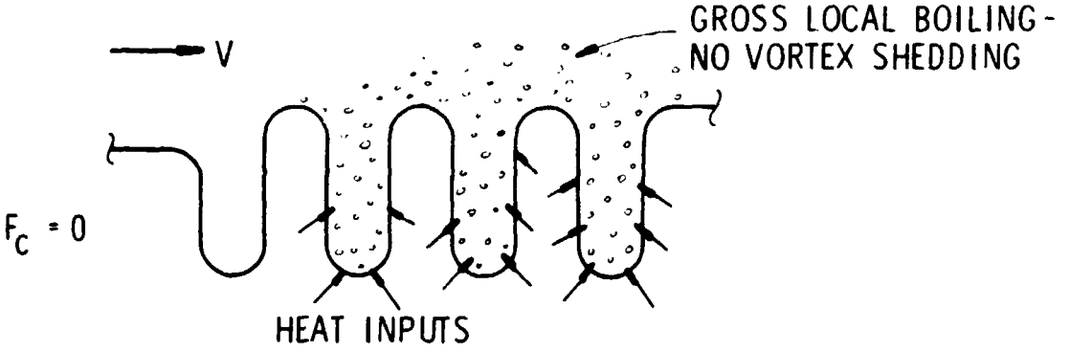

(c) EXTERNAL HEATING - GROSS BOILING

Figure 7. Illustration of heating effect on bellows vortex shedding flow excitation.

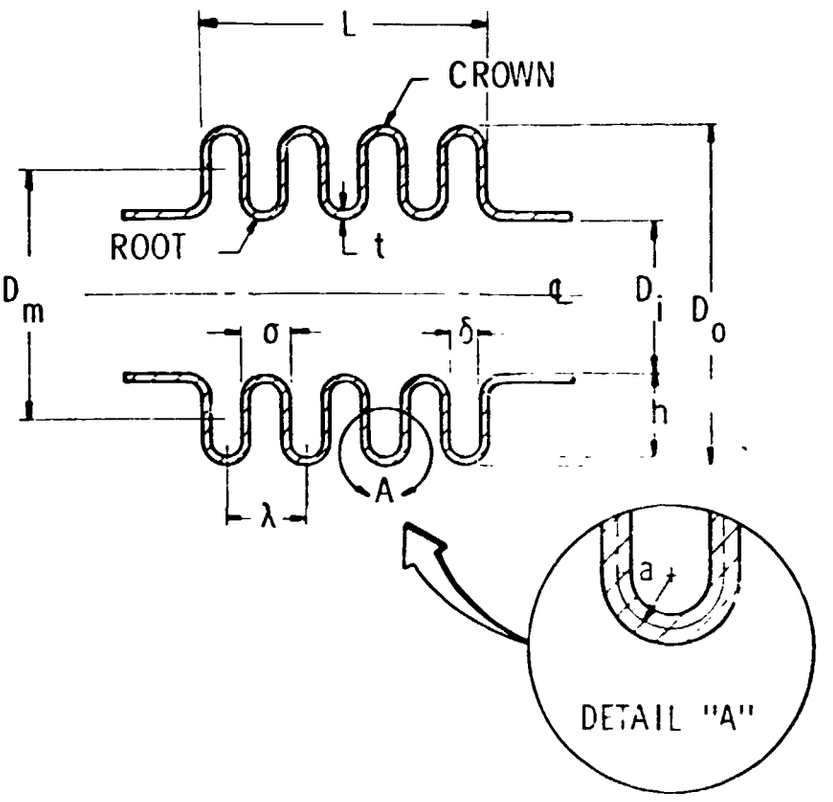

N_c = NUMBER OF CONVOLUTIONS COUNTED FROM THE OUTSIDE

N_p = NUMBER OF PLYS

D_m = MEAN BELLOWS DIAMETER

t = WALL THICKNESS (THICKNESS PER PLY IF MULTI-PLY)

λ = CONVOLUTE PITCH

σ = CONVOLUTE WIDTH

a = MEAN FORMING RADIUS

h = MEAN DISC HEIGHT

Figure 8. Bellows nomenclature.

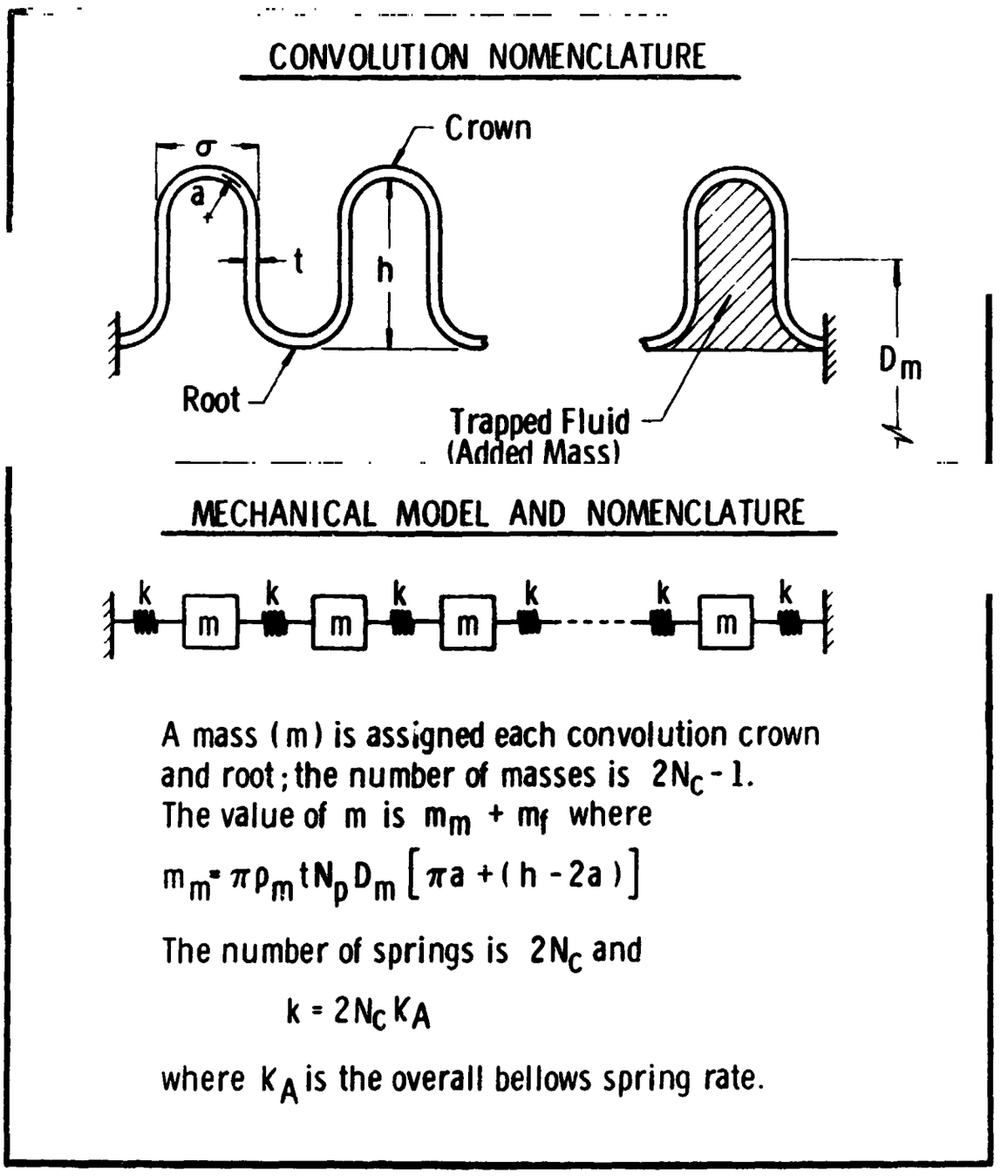

Figure 9. Convolution nomenclature and lumped spring-mass mechanical model.

B. Spring Rate

Presently, no spring rate calculation procedure exists which is accurate enough for general use in bellows mode frequency prediction. Rough estimates of spring rate may be made through use of the equation

$$K_a \approx D_m E \frac{N_P}{N_C} \left(\frac{t}{h}\right)^3 \tag{5}$$

where E is Young's modulus for the bellows material. The Salzmann method [3,4] is a refinement of the above simple form for bellows spring rate but in our experience does not improve the accuracy. Until an accurate method is available, the user is advised to employ experimental K_a values where possible. Section VI.B and Appendix C of this report compares experimental spring rate values with predictions by the simplified and Salzmann method.

C. Modal Frequency Calculations

The mechanical model shown in Figure 9 represents a $2N_c$-1 degree of freedom representation of a metal bellows. Therefore, solution of the equations of motion for this system will predice $2N_c$-1 distinct mode frequencies. The letter N will be used to denote mode number. The general solution of the mechanical model dynamic equations results in the following equations for the modal frequencies:

$$f(N) = \frac{1}{2\pi} \left\{ \frac{2k}{m} \left[1 + \cos\left(\frac{\pi(2\,N_c - N)}{2N_c}\right)\right] \right\}^{1/2}$$

$$= \frac{1}{2\pi} \sqrt{\frac{k}{m}}\; B_N \qquad \text{where } N = 1, 2, 3, \ldots, 2N_c-1 \tag{6}$$

Values of B_N for a limited number of N_c values are shown in Table 1.

D. Fluid Added Mass

There appear to be two types of fluid added mass loading on the vibrating convolutes, as illustrated in Figure 10. When vibrating in the first longitudinal mode, all of the convolutes are moving in-phase back and forth, but not necessarily with the same amplitude. The fluid, or some portion thereof, which is trapped or contained between adjacent convolutes is accelerated back and forth longitudinally, as illustrated in Figure 10a. This fluid contributes a mass loading which is additive to the metal mass. The ideal value of this fluid mass is given by

TABLE 1. DIMENSIONLESS FREQUENCY FACTORS B_N

MODE NUMBER

N_c	1	2	3	4	5	6	7	8	9	10	11	12	13	14	15	16	17	18	19	20	21	22	23	24	25
1	1.414																								
2	0.765	1.414	1.845																						
3	0.520	1.000	1.414	1.732	1.930																				
4	0.390	0.765	1.111	1.414	1.663	1.848	1.962																		
5	0.314	0.618	0.908	1.176	1.414	1.618	1.782	1.902	1.975																
6	0.264	0.518	0.765	1.000	1.217	1.414	1.587	1.732	1.848	1.932	1.983														
7	0.226	0.445	0.661	0.868	1.064	1.247	1.414	1.563	1.693	1.802	1.888	1.950	1.987												
8	0.199	0.390	0.583	0.765	0.942	1.111	1.269	1.414	1.546	1.663	1.764	1.848	1.913	1.962	1.990										
9	0.174	0.347	0.518	0.684	0.845	1.000	1.147	1.285	1.414	1.532	1.638	1.732	1.812	1.879	1.931	1.969	1.992								
10	0.157	0.313	0.467	0.618	0.765	0.908	1.044	1.175	1.298	1.414	1.520	1.618	1.705	1.782	1.847	1.902	1.944	1.975	1.993						
11	0.142	0.285	0.425	0.563	0.699	0.831	0.958	1.081	1.198	1.309	1.414	1.511	1.601	1.682	1.755	1.819	1.873	1.918	1.954	1.979	1.994				
12	0.131	0.262	0.390	0.518	0.643	0.765	0.885	1.000	1.111	1.217	1.318	1.414	1.503	1.586	1.662	1.732	1.793	1.847	1.893	1.931	1.961	1.982	1.995		
13	0.121	0.241	0.361	0.479	0.595	0.709	0.821	0.929	1.034	1.136	1.233	1.326	1.414	1.497	1.574	1.645	1.711	1.770	1.823	1.870	1.909	1.941	1.967	1.985	1.996

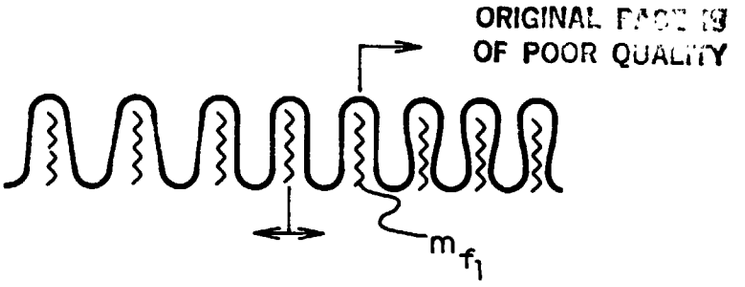

a. FLUID CARRIED LONGITUDINALLY BACK AND FORTH

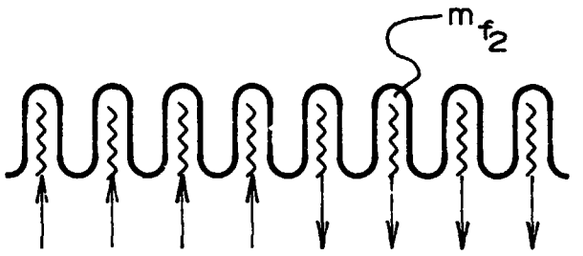

b. FLUID MOVING IN AND OUT OF CONVOLUTES BECAUSE OF RELATIVE TIP DISPLACEMENT

Figure 10. Fluid added masses.

$$m_{f_1} = \frac{\pi}{2} \rho_f D_m h (2a - t N_p) \tag{7}$$

The fluid which is "squeezed" in and out of the space between convolutes, as illustrated in Figure 10b, also contributes an apparent mass loading whose ideal value is proportional to

$$m_{f_2} = \frac{D_m \rho_f h^3}{\delta} \tag{8}$$

The contribution of m_{f_2} increases as mode number increases while the contribution of m_{f_1} is constant or may decrease as N increases. The currently used general model for m_f is

$$m_f = C_1 m_{f_1} + C_2 m_{f_2} \left(\frac{N}{N_c}\right) \tag{9}$$

The above equation represents a departure from the form previously published in SwRI reports and used, which was

$$m_f = m_{f_1}\left(\frac{2N_c-1-N}{2N_c-2}\right) + m_{f_2}\left(\frac{N-1}{2N_c-2}\right) \qquad \text{OLD EQUATION}$$

Figure 11 shows a plot of experimentally determined normalized fluid added mass given by

$$m_{f_e}{}^* = \frac{m_{f_e}}{D_m \rho_f \frac{h^3}{\delta}} \tag{10}$$

plotted versus N/N_c. Note the rather tight grouping of data and linear relationship with N/N_c. The results of Figure 11 indicate the validity of the current fluid added mass model.

E. Strouhal Number and Frequency Prediction

For a given bellows, having some particular convolute geometry and structural mode frequencies, there are certain optimum fluid velocities which result in a maximum amplitude of bellows excitation for each mode.

It is at these velocities that the vortex shedding process is best able to feed energy from the fluid stream into the vibration process. In other words, the vibration frequency and fluid velocity conditions are "optimum" from a vortex shedding standpoint. It has been found that the use of a Strouhal number is an excellent means of correlating the vibration frequency, fluid velocity and bellows geometry under these optimum conditions, as is true for any vibration phenomena involving vortex shedding.

In general terms, a Strouhal number is a dimensionless quantity of the form

$$S = \frac{f\ell}{V} \tag{1}$$

where f is a frequency, ℓ is a length quantity, and V is a fluid velocity. For the case of bellows flow-induced vibrations, the only problem in using this correlation parameter was in selecting a satisfactory length quantity.

In early studies where only limited test data was available the Strouhal correlation shown in Figure 12 was adopted. Based on more recent test results, this model is now considered obsolete and the current Strouhal correlation is:

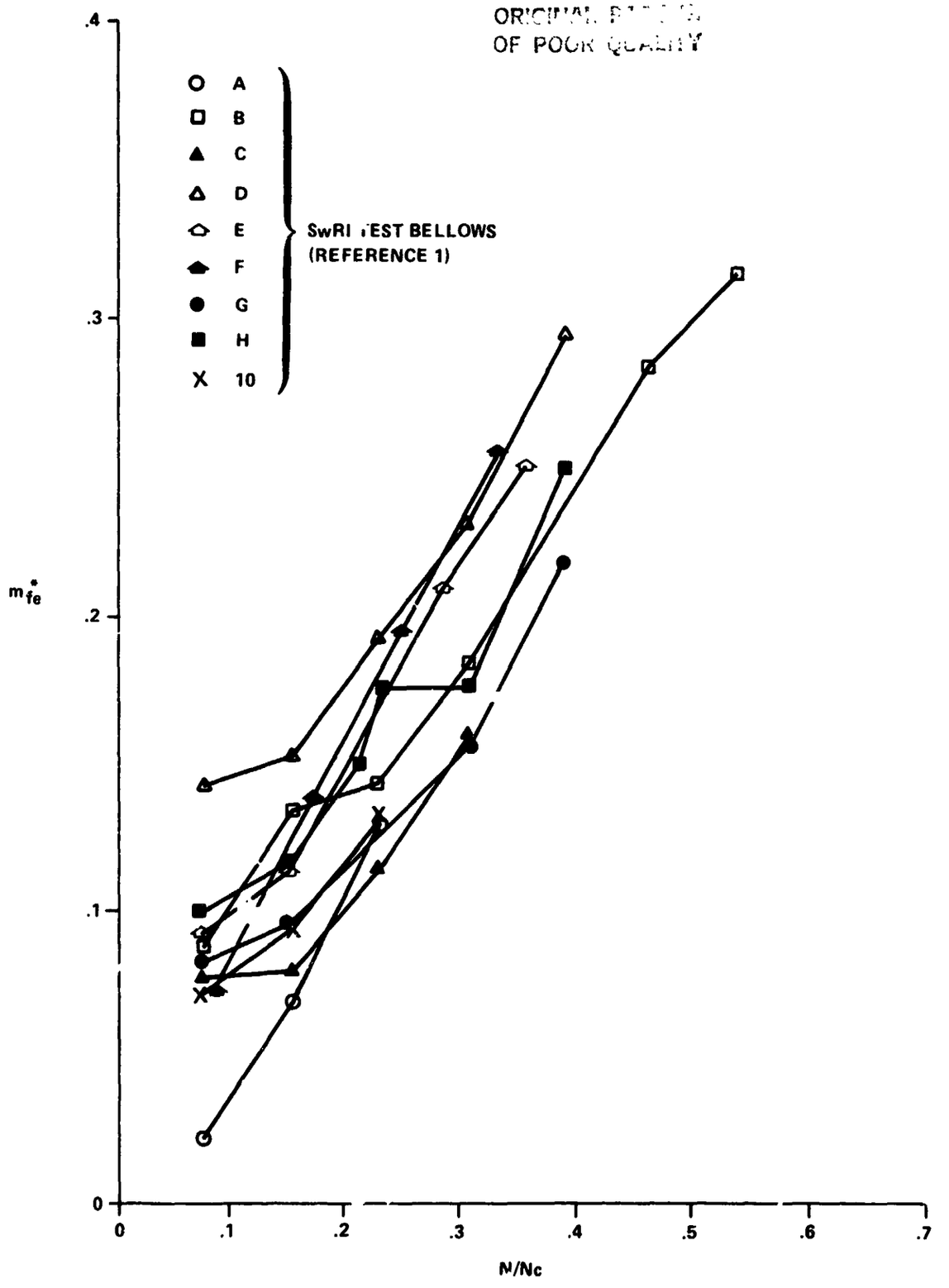

Figure 11. Normalized fluid added mass as function of N/N_c for SwRI test bellows.

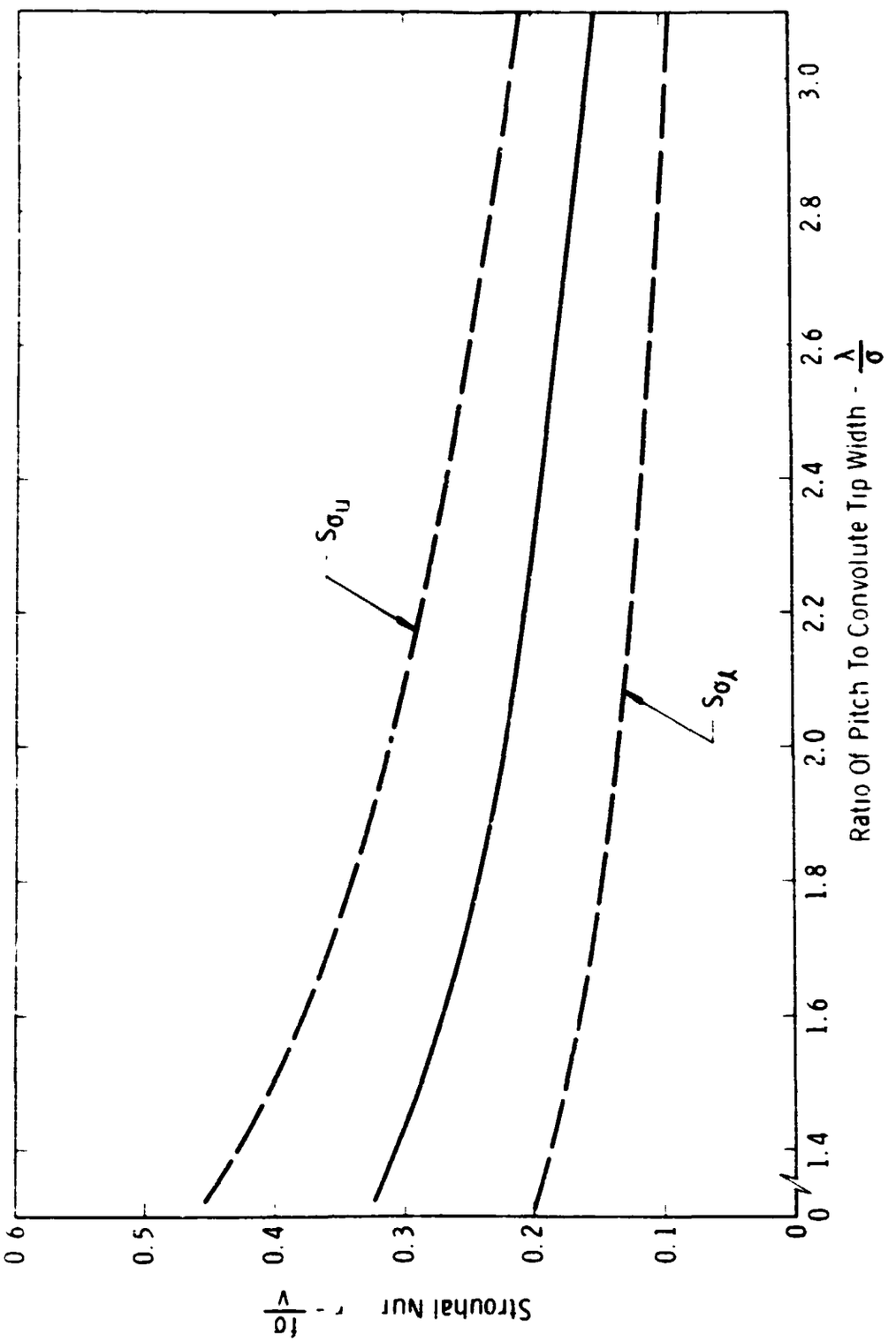

Figure 12. Composite of all SwRI Strouhal number correlation data — now obsolete.

$S_{\sigma\ell}$ = lower Strouhal limit = 0.1

$S_{\sigma c}$ = critical Strouhal value = 0.2

$S_{\sigma u}$ = upper Strouhal limit = 0.3

For a given bellows mode defined by frequency f, flow excitation may occur over a velocity range (called the lock-in range) and given by

$$\frac{f\sigma}{S_{\sigma u}} \leqslant V \leqslant \frac{f\sigma}{S_{\sigma\ell}} \tag{11}$$

Figure 13 shows a plot of frequency versus fluid velocity illustrating the lock-in region.

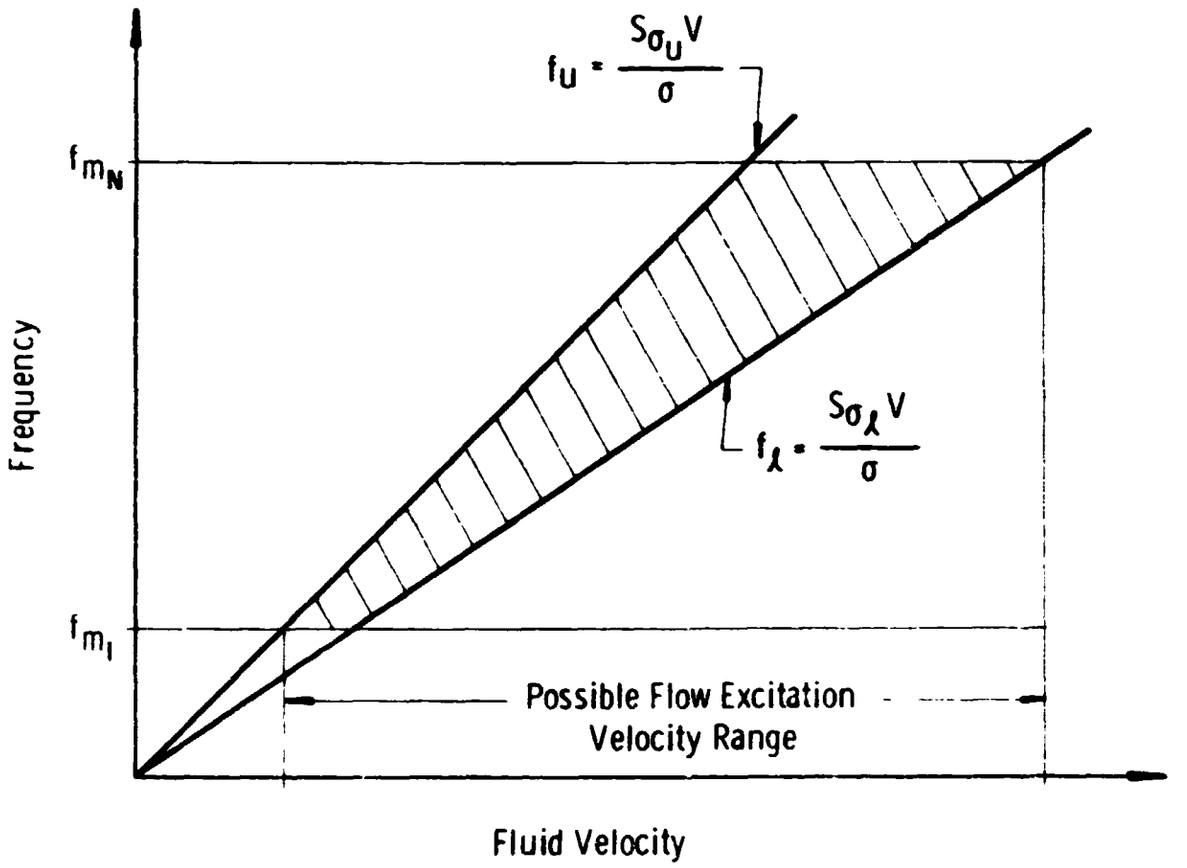

Figure 13. Frequency versus velocity plot to illustrate bellows flow excitation region.

The range of possible bellows flow excitation may be predicted as follows:

1) Calculate the lowest and highest bellows mode frequencies, f_{m1} and f_{mn} as summarized in Section III.C of this report.

2) Calculate the limits of fluid velocity corresponding to these two frequencies. This calculation is done with equation (11) and with the values of the Strouhal numbers $S_{\sigma\ell}$ and $S_{\sigma u}$ given above.

3) Compare this flow excitation fluid velocity range with the known operating range of the bellows. If an overlap of these ranges exists, then excitation may occur.

IV. STRESS MODEL

A. Basis

The basis for calculation of bellows flow-induced stress is illustrated in Figure 14. Motion of the bellows convolutes results in periodic formation and shedding of vortices from the convolute tips. This vortex activity is assumed to produce an alternating force acting on each convolute whose magnitude is

$$F = C_F C_E A_P \left(\frac{1}{2} \rho V^2\right) \quad . \tag{12}$$

where C_F is a vortex force coefficient (roughly analogous to a wing lift coefficient), C_E is an elbow effect factor, A_P is some projected area over which the vortex force acts, and $1/2\ \rho V^2$ is the fluid free stream dynamic pressure (P_d). It has been determined by comparison of theory and experiment that the most proper projected area to use in the model is the total projected convolute area given by

$$A_P = \pi D_m h \tag{13}$$

When flow-induced vibration exists, a relative convolute dynamic displacement x results which is assumed to be of the form

$$x = \frac{C_m F Q}{K_a} \tag{14}$$

Where C_m is a vibration mode factor and Q is a dynamic amplification factor reflecting the systems effective damping (coupled fluid-structure damping).

Finally, the relative displacement x is assumed to produce a convolute stress given by

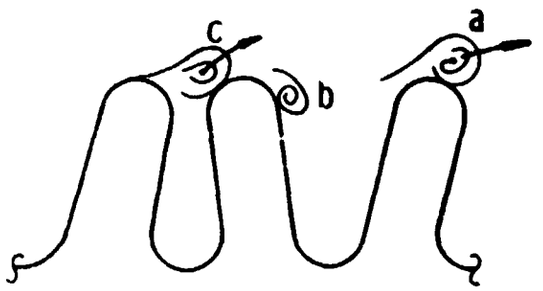

Vortex Shedding From Convolutions

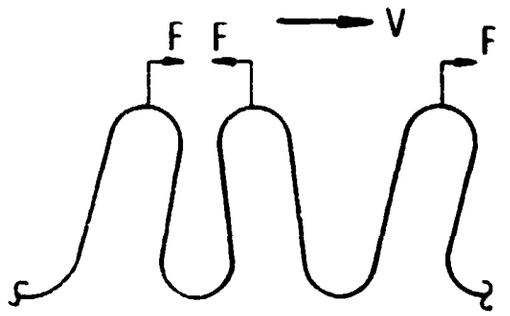

Vortex Force

$$F = C_F C_E A_p \left(\frac{1}{2} \rho V^2 \right)$$

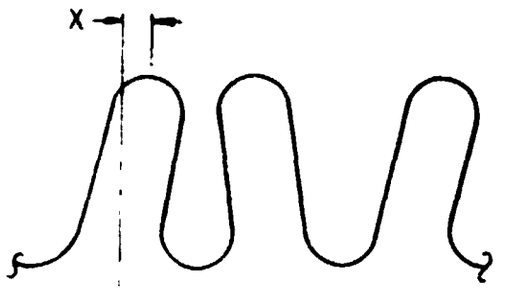

Convolution Displacement

$$x = \frac{C_m F Q}{K_A}$$

The resultant stress is

$$\text{Stress} = \frac{C_S E t x}{h^2}$$

In the above equations

C_F = vortex force coefficient
C_E = elbow factor
C_m = vibration mode factor
Q = dynamic amplification (damping)
C_S = geometric stress factor

Figure 14. Illustration of stress resulting from vortex force.

$$\text{Stress} = \frac{C_S\, E\, t\, x}{h^2} \tag{15}$$

where C_S is a geometric stress factor.

B. Stress Indicator Approach

In previous studies the above equations were combined, a simplified form for K_a, given by equation (5), was substituted, C_S was assumed constant, and C_m was approximated by

$$C_m \approx \frac{1}{4N_c} \tag{16}$$

This produced an equation for stress given by

$$\text{Stress} \approx \pi\, C_S \left(\frac{C_F\, C_E\, Q}{N_P}\right)\left(\frac{h}{t}\right)^2\left(\frac{1}{2}\rho\, V^2\right) \tag{17}$$

and from which a quantity called "stress indicator" was defined by

$$\text{Stress Indicator} = \left(\frac{C_F\, C_E\, Q}{N_P}\right)\left(\frac{h}{t}\right)^2\left(\frac{1}{2}\rho\, V^2\right) \tag{18}$$

Graphs were developed presenting models of C_F, based on experimental tests of bellows, and of Q, based primarily on shaker tests of fluid filled bellows. To accompany this model, a plot of stress indicator versus cycles to failure was developed representing an accumulation of known bellows failures to that time. In equation (18), a value of 2.0 was used for C_E if an elbow was present upstream of the bellows. If no elbow was present, a value of 1.0 was used for C_E. Subsequently, a more extensive experimental program was undertaken to validate the stress indicator failure prediction approach and those results are shown in Figure 15. Note that these initial results showed the original failure plot to be incorrectly shaped and conservative by a factor of 2 to 3. Further, the vertical data scatter was unsatisfactory for the accurate fatigue life prediction desired (this has been a long time objective of the program). Clearly refinements of the stress model were needed.

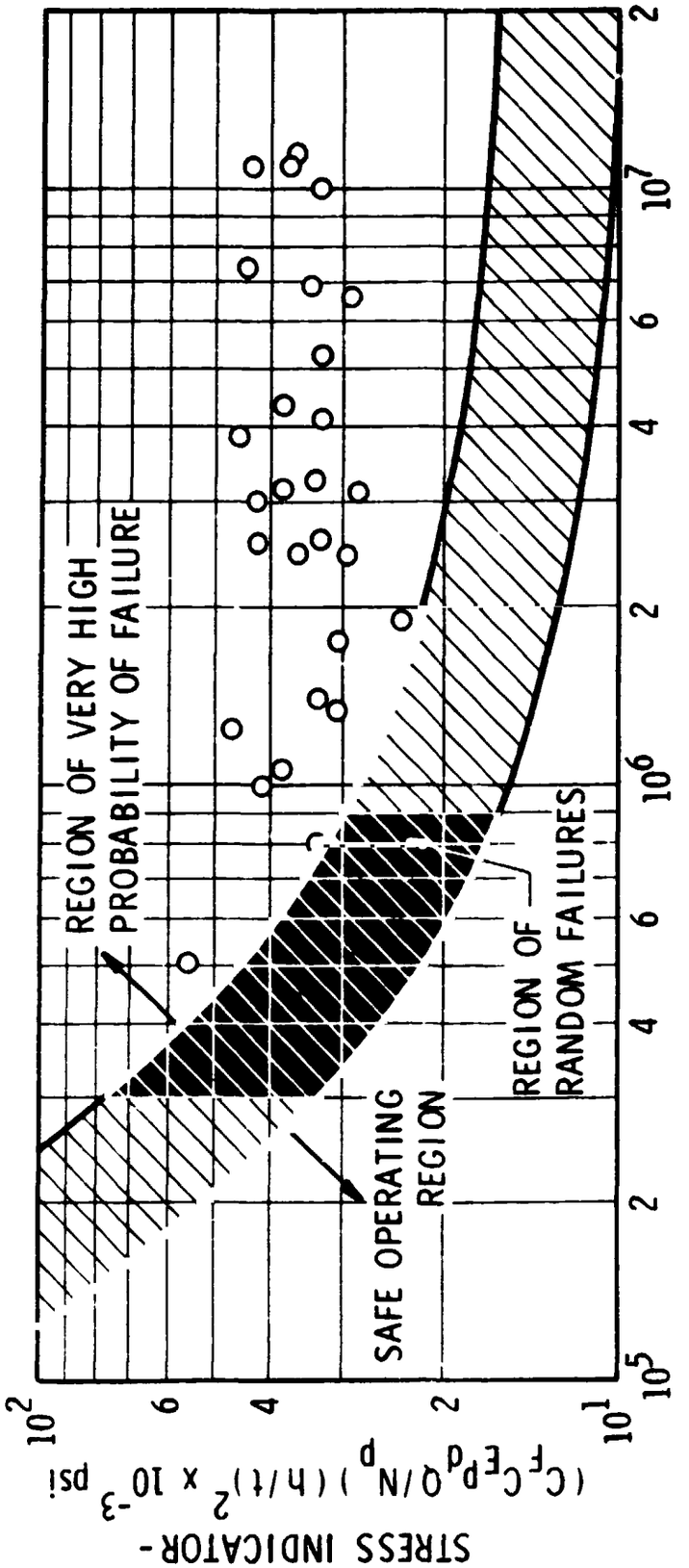

Figure 15. Bellows fatigue life data using stress indicator approach.

C. C_FQ Approach

The rationale of the C_FQ approach was based on the data shown in Figures 16, 17, and 18, and led to the definition of the parameter

$$C_F^* = C_F\, Q \left(\frac{N}{N_c}\right) \quad . \tag{19}$$

Figures 16 through 18 show plots of the force coefficient parameter (C_F^*) for representative samplings of the total data base. The effect of changes on the force coefficient parameter C_F^* is illustrated in Figure 16. Here, a single bellows was tested at various pitch values, and the peak response of the first longitudinal mode (N=1) was noted.

The reduced data shown in Figure 17 clearly illustrates the effect of vortex reinforcement and vortex retardation on the flow-induced response of the bellows.

A vortex reinforcement occurs when the vortex shedding from an upstream convolute arrives at the adjacent downstream convolute at the right moment to aid in the formation of the vortex forming at that adjacent convolute. Vortex retardation has the opposite effect. The vortex shed from an upstream convolute arrives at the adjacent downstream convolute at the right moment to detract from the formation at that adjacent convolute.

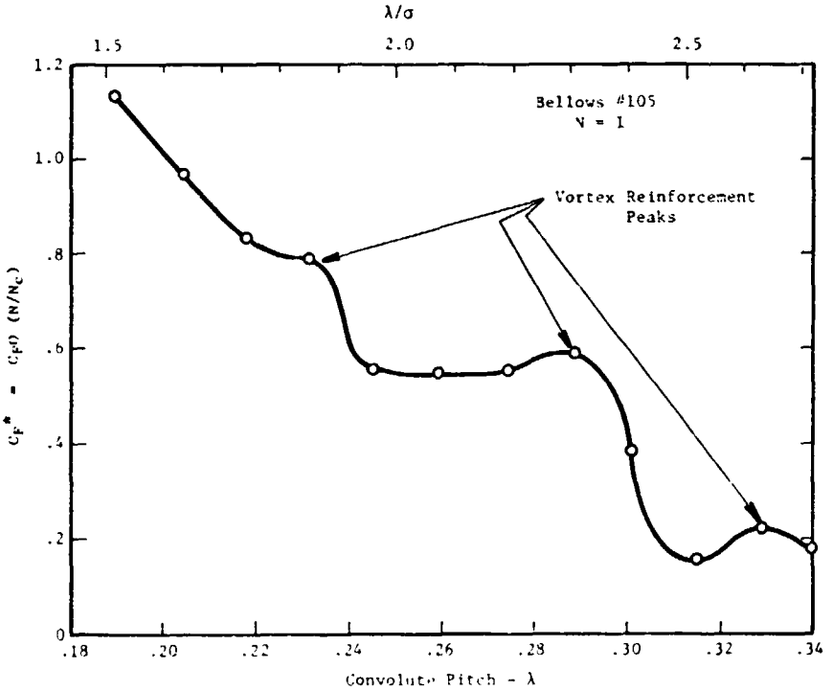

Figure 16. Vortex force coefficient C_F^* versus pitch for the first mode of SwRI bellows 105.

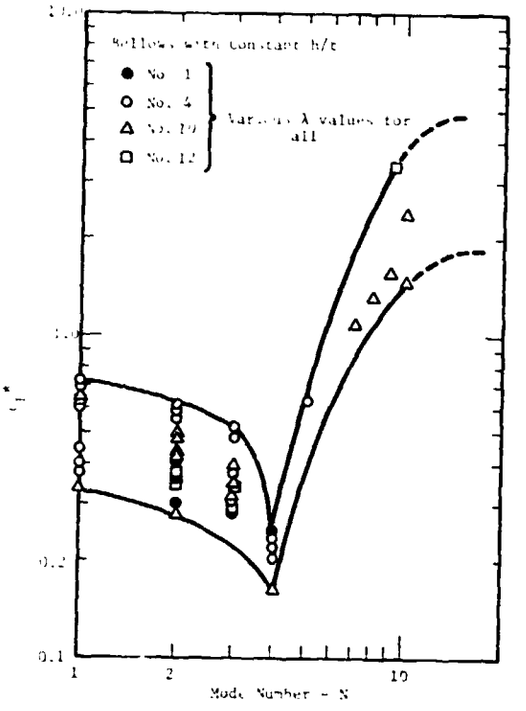

Figure 17. Vortex force coefficient C_F^* as a function of mode number for SwRI bellows with constant (h/t).

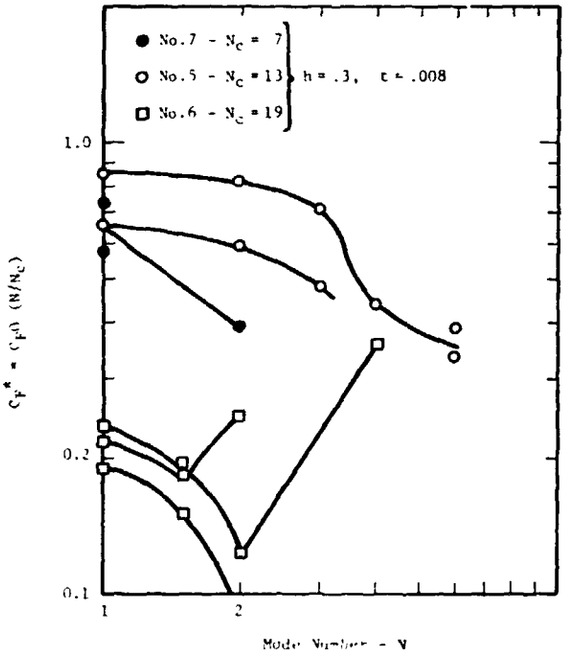

Figure 18. Vortex force coefficient C_F^* as a function of mode number for SwRI bellows with different N_c.

Figure 17 presents a plot of C_F* versus the mode number N for four SwRI test bellows that have constant values of the parameter (h/t) but having h values ranging from 0.2 to 0.5. Since spring rate is proportional to (h/t), this family had similar modal frequencies, so that convolute height h was the primary variable. Also, however, each of the four bellows were tested for three or four values of λ achieved by stretching. Note that there is a spread of the combined C_F* values for these four bellows for each mode number or N value. This spread is caused by a combination of two factors. First, it represents the influence of the effect of changing λ as illustrated previously in Figure 16. Secondly, it reflects the normal variation expected in flow-induced vibration experiments of bellows where slight changes in alignment, clamping of the ducting, etc., cause changes in the peak response point.

From Figure 17, at the time of development of the C_FQ approach, we concluded the following:

1) Other than specimen No. 1, which had h = 0.2 or a very short convolute, the effect of h was not apparent between the bellows. Specimen No. 1 had lower C_F* values than the other bellows, probably because short convolutes do not couple so well as taller convolutes. After all, the limiting case is h = 0 which represents a straight pipe which has no response of the type under consideration.

2) The vertical spread of C_F* for each mode is primarily caused by vortex reinforcement or vortex cancellation.

3) The pronounced minimum of C_F* is a result of an optimum vortex cancellation effect for this mode number range.

4) The rapid rise of C_F* for the higher longitudinal modes is a result of a predominance of vortex reinforcement for these modes.

5) Many of the higher modes simply never appear because other modes close to them predominate and prevent their occurrence.

Figure 18 presents C_F* as a function of mode number N for three SwRI bellows having similar convolute geometry but different number of convolutes. Bellows No. 6 illustrates yet another phenomena. Note that the C_F* values for this bellows are quite low for the first two longitudinal modes. Also note the strong presence of the first cocking mode plotted for N = 1.5. For this bellows, the cocking mode was stronger than normal so it suppressed the first and second longitudinal modes causing their C_F* values to be abnormally low.

The primary intent of the C_F* relation was to mathematically collapse all of the experimentally generated Q surfaces into one relationship that applies to all ranges of the bellows operational parameters, hence, the stress indicator was computed from

$$\text{S.I.} = \frac{C_F^* \, N_C}{N \, N_P} \left(\frac{h}{t}\right)^2 \left(\frac{1}{2} \rho \, V_C^2\right) \tag{20}$$

For the C_FQ model, the parameter C_F* was obtained from Figure 19 which was a somewhat conservative curve that enveloped all previously generated experimental bellows data. This curve was assumed to contain all inherent information relating to C_F and Q that was available at the time.

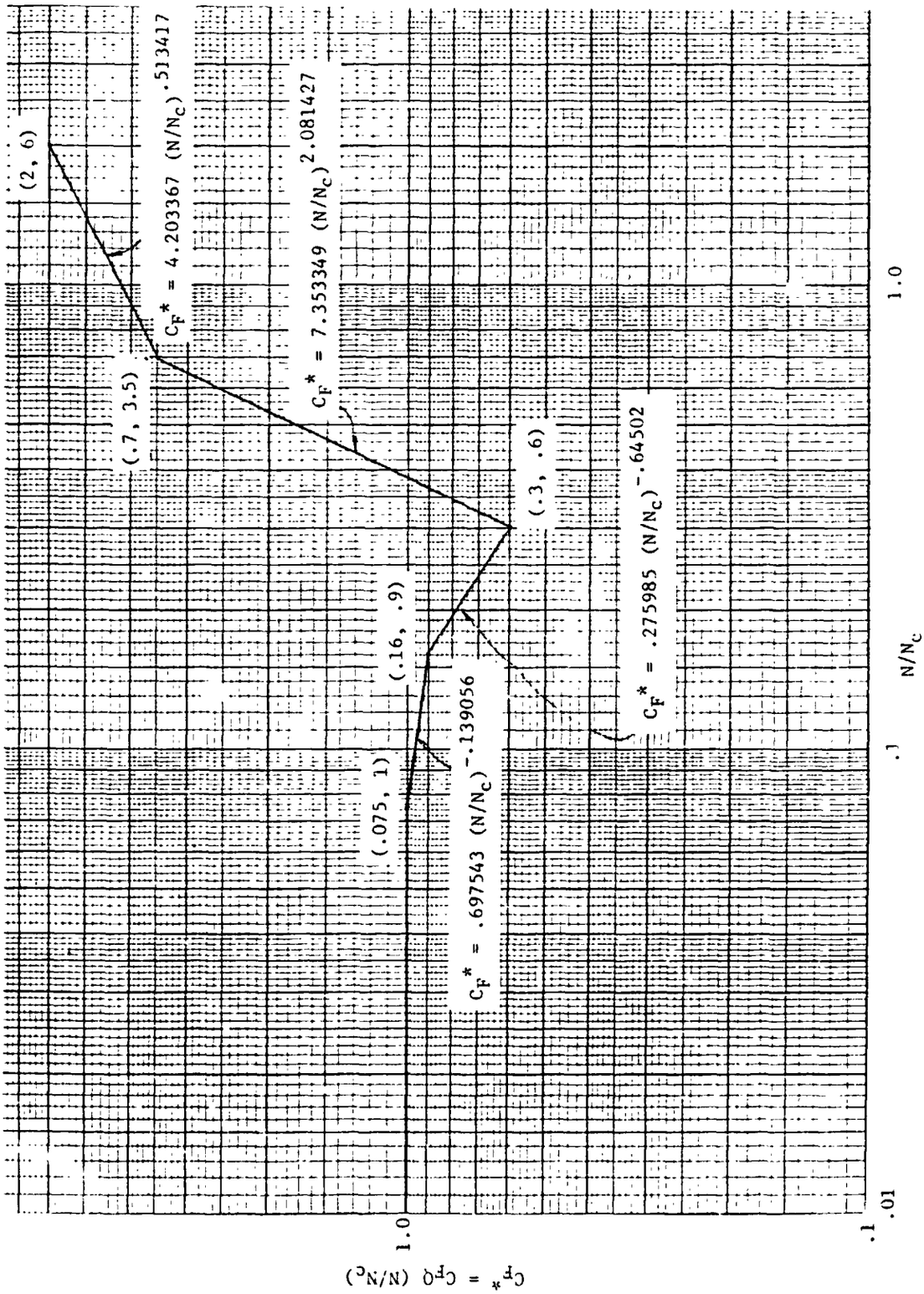

Figure 19. Envelope curve for C_F^* correlation.

D. Stress Model Critique

The primary problem with the stress indicator approach summarized earlier was that mode number effect was not recognized or addressed. On the other hand, the $C_F Q$ approach addresses the mode number effect but neglects the nonlinear behavior of Q as a function of the Bellows Operational Parameter (BOP). Clearly both effects must be incorporated if an accurate model is to be achieved. Before discussing such a model, a better or updated understanding of the force coefficient C_F, dynamic amplification factor Q, and mode number effect will now be presented.

Figure 20 illustrates the vortex formation and shedding processes, and their interaction with fluid pumping in and out of the convolutes. Energy for the vortex activity is basically derived from the fluid free stream which is flowing at velocity V. Convolute motion or vibration will produce dynamic pumping of fluid in and out of the convolutes at a velocity amplitude v. This pumped fluid will enhance or retard the vortex strength, depending on the phase relationship between vortex and convolute motions; this is a nonlinear effect since the fluid force is now amplitude dependent.

The fluid pumped in and out of the convolutes will also produce virtual mass and velocity dependent retarding forces (damping). The virtual or added mass effect was discussed and treated in Section III. Note that the pumped fluid amplitude will also be a function of convolute height h and gap δ. Clearly the force coefficient C_F and dynamic amplification factor Q should exhibit nonlinear behavior and be amplitude dependent.

Figure 21 shows the original model of Q as a function of a BOP. Basically BOP is proportional to convolute displacement divided by Q and therefore this model incorporates a displacement dependence of Q. The accuracy of this model, however, is not satisfactory. Table 2 gives application information for use with Q value data.

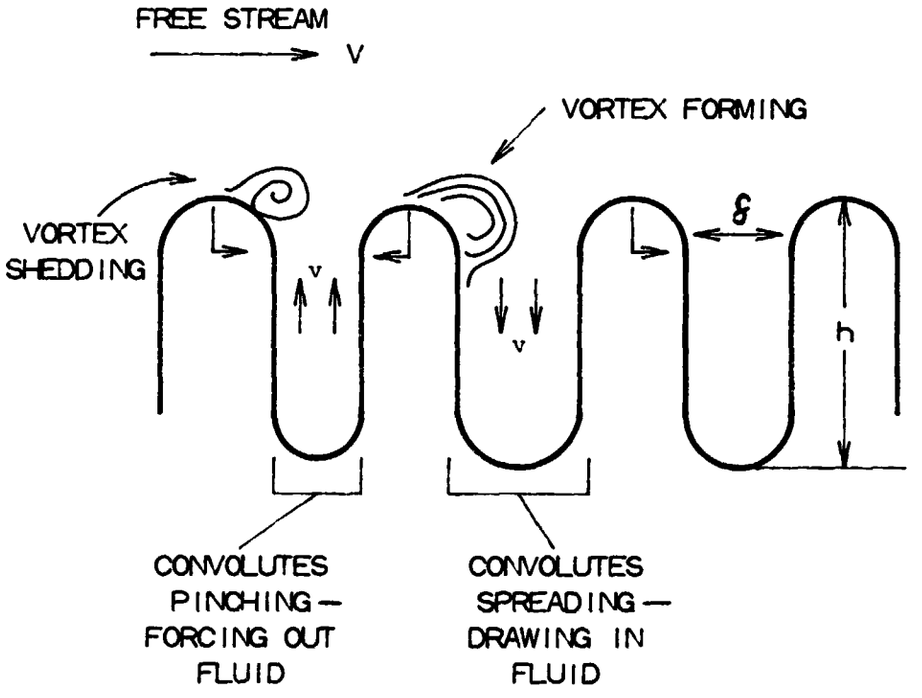

Figure 20. Illustration of fluid pumped between vibrating convolutes.

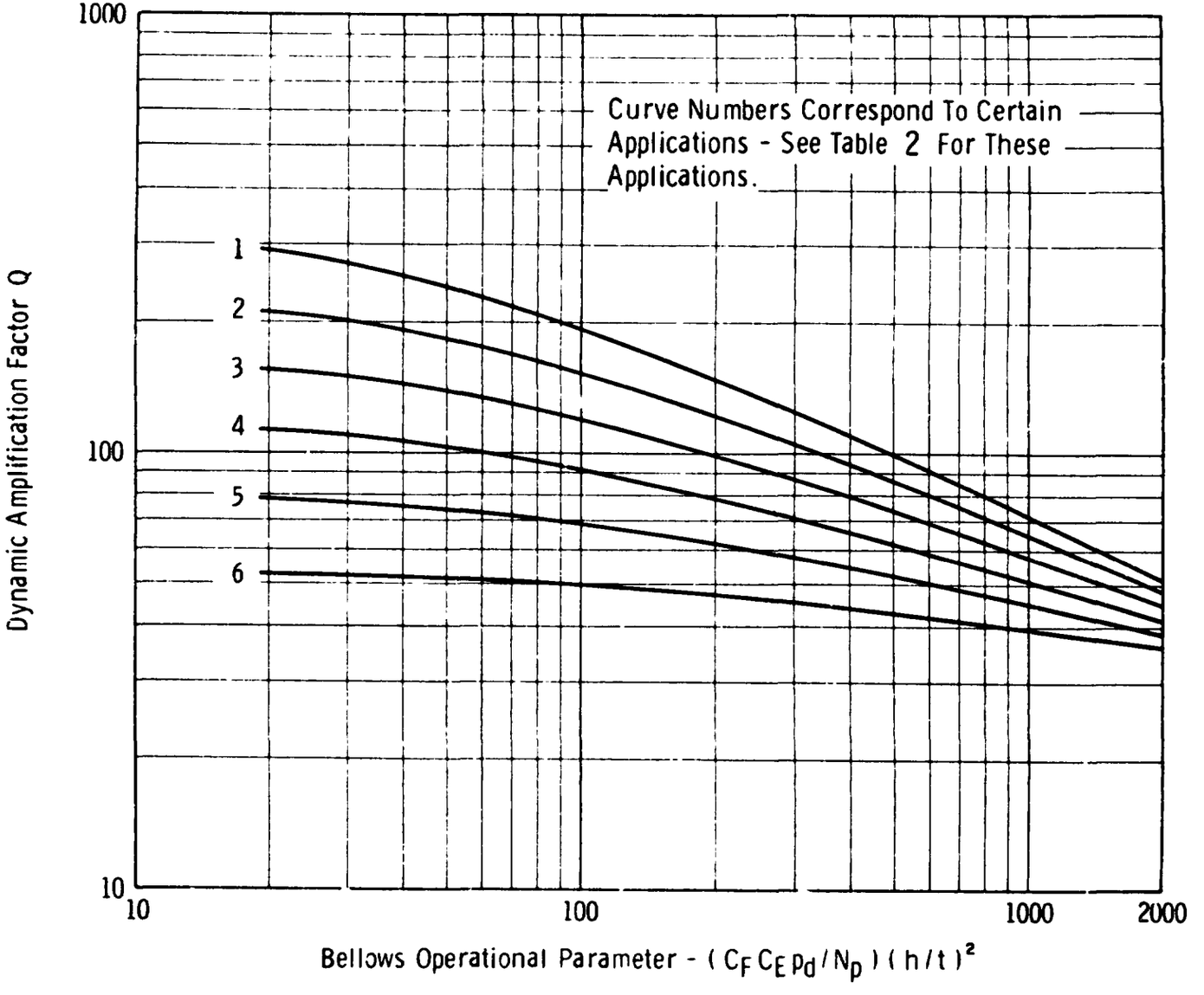

Figure 21. Previous SwRI dynamic amplification factors for various bellows applications.

TABLE 2. APPLICATION INFORMATION FOR USE WITH Q VALUE DATA IN FIGURE 21.

Specific Spring Rate (see Note 1)	Number of Plies	Internal Media (see Note 2)	Curve No.
all ranges	1	low pressure gases	1
over 2000 lb/in^2	1	high pressure gases, light liquids	1
over 2000	1	water, dense liquids	2
under 2000	1	high pressure gases, light liquids	2
under 2000	1	water, dense liquids	3
over 3000	2	all	3
2000-3000	2	all pressure gases	4
under 2000	2	all pressure gases	5
2000-3000	2	all liquids	5
under 2000	2	all liquids	6
over 3000	3	all	4
2000-3000	3	all	5
under 2000	3	all pressure gases	5
under 2000	3	all liquids	6

Use of Table - The table was used by first calculating the bellows specific spring rate (S.S.R.), and then looking up the application curve number corresponding to the S.S.R., number of plies, and internal media.

Note 1: The specific spring rate here is defined as

$$S.S.R. = \frac{K_a N_c}{D_m N_p} \qquad (21)$$

or is the spring rate per convolute, per ply, per unit of diameter.

Note 2: Low pressure gases are defined here as those gases below 150 psia. Light liquids are defined as having a density, relative to water, of less than 0.2.

E. Final Flow-Induced Stress Model

The final flow-induced stress model is based on a slightly different approach from the two methods (now considered obsolete) which were discussed above. As before, we use the same starting equation, i.e.,

$$\text{Stress} = \frac{C_S\, E\, t\, x}{h^2} \tag{15}$$

where

$$x = \frac{C_m\, C_F\, \pi\, D_m\, h\, P_d\, Q}{K_a} \tag{22}$$

and

$$C_m \approx \frac{1}{4\, N_c} \tag{16}$$

Combining, we have

$$\text{Stress} = \frac{\pi}{4}\, C_S\, C_F\, Q\, E\, P_d \left(\frac{t}{h}\right)\left(\frac{D_m}{N_c\, K_a}\right)$$

or

$$\text{Stress} = \frac{\pi}{4}\, C_S\, C_F\, Q\, E\, P_d \left(\frac{t}{h}\right)\left(\frac{1}{N_p \cdot \text{SSR}}\right) \tag{23}$$

Based on correlation with all available experimental strain and failure data (Section IV.D), the term $\pi/4\, C_S\, C_F\, Q$ has been empirically modeled in the form

$$\frac{\pi}{4}\, C_S\, C_F\, Q = C^*\, C_{NP}\, C_E \left[1 + 0.1\left(\frac{400}{\text{SSR}}\right)^2\right]\left(\frac{h}{\delta}\right)\left(\frac{V_c}{V}\right) \tag{24}$$

where V_c is the critical velocity for mode $N = N_c$ and C^* is a force and damping coefficient given by

$$C^* = \frac{C_1}{C_2 + V'^2} + \frac{C_3 \left|\sin (180\ V')\right|}{C_4 + V'^2} + C_5 \tag{25}$$

where $V' = V/V_c$. The coefficients C_1, C_2, C_3, C_4, and C_5 are constants and will be defined later in Section VI.D. The coefficient C_{NP} is a damping modifier coefficient for multi-ply bellows given by

$$C_{NP} = 1.0 \qquad \text{for } N_P = 1$$

$$C_{NP} = 1.0 - \frac{C_6 \left(\frac{\sigma}{h}\right)}{1 + C_7\ V'^2} \qquad \text{for } N_P = 2, 3, \ldots \tag{26}$$

The coefficients C_6 and C_7 are constants and will be defined later in Section VI.D. The coefficient C_E is an elbow factor for application where an elbow is present immediately upstream of the bellows. This elbow factor will be defined later in Section VI.E.

The equation for peak flow-induced stress may now be written as

$$\text{Stress} = C^*\, C_{NP}\, C_E \left[1 + 0.1 \left(\frac{400}{SSR}\right)^2\right] \left(\frac{h}{\delta}\right) \left(\frac{V_c}{V}\right) \left(\frac{t}{h}\right) E \frac{P_d}{SSR \cdot N_P} \tag{27}$$

Figure 22 shows C^* as a function of $V' = V/V_c$. Note that this curve reflects a vortex reinforcement and cancellation variation. Figure 23 shows a plot of C_{NP} as a function of V' and σ/h, and represents the added damping influence of multi-ply bellows. Figure 24 shows a preliminary model of C_E, however, the user of this data is cautioned that the data base for this curve is from tests of a small number of bellows.

Appendix H lists a computer code which calculates flow-induced stress (FIS) based on the above model for each of the bellows modes, or optionally, calculates flow-induced stress at arbitrary velocities fed into the computer. Also included is an example of the input data deck for the computer code.

V. EXPERIMENTAL PROGRAM

As originally conceived, the MSFC test program was fairly broad in scope. It included such effects as static pressure on the susceptibility of flow-induced vibrations, the effect of upstream bends, the effect of ball-strut assemblies internal to the bellows, characterization of two commonly used bellows

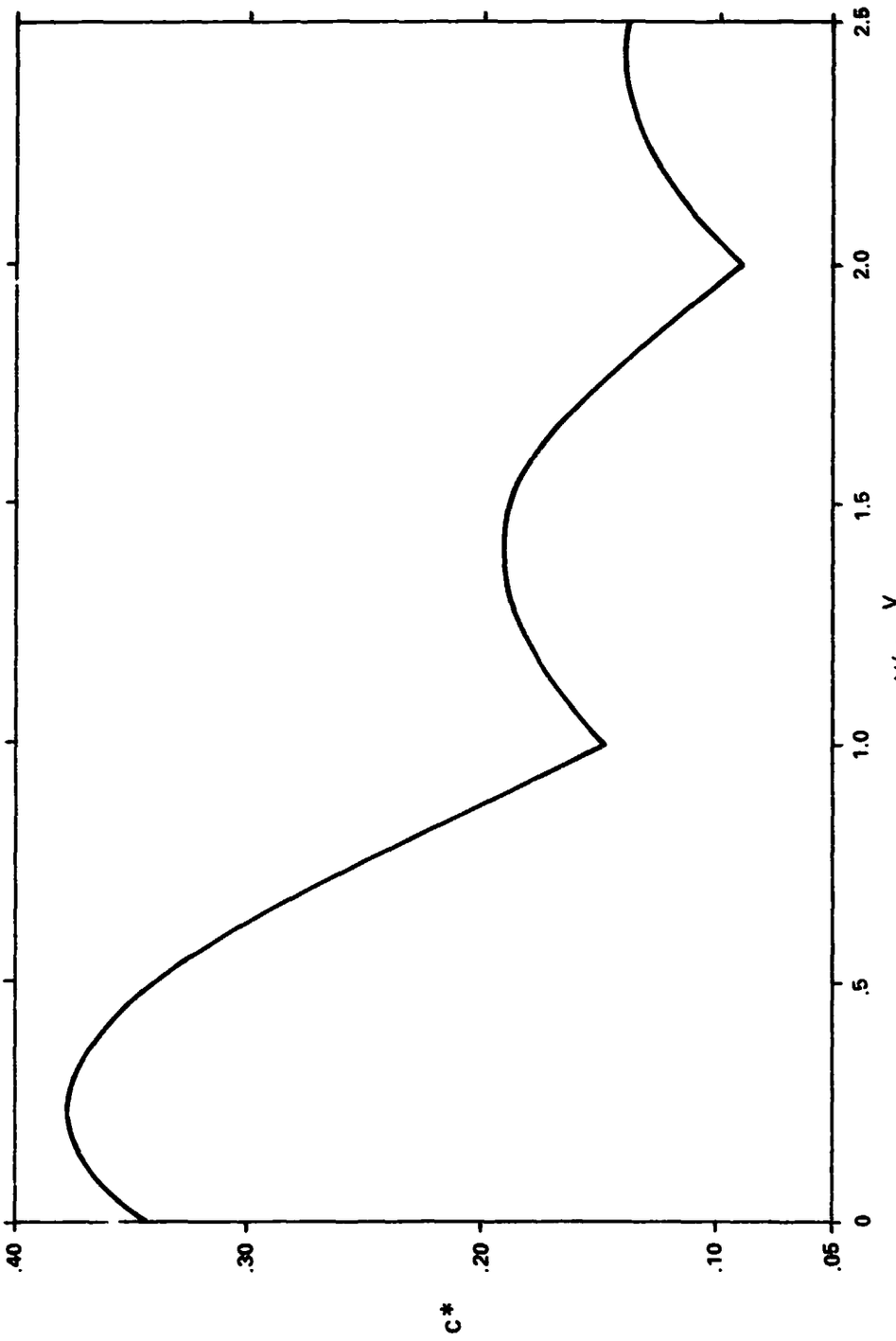

Figure 22. Dimensionless force-damping coefficient C* as a function of V'.

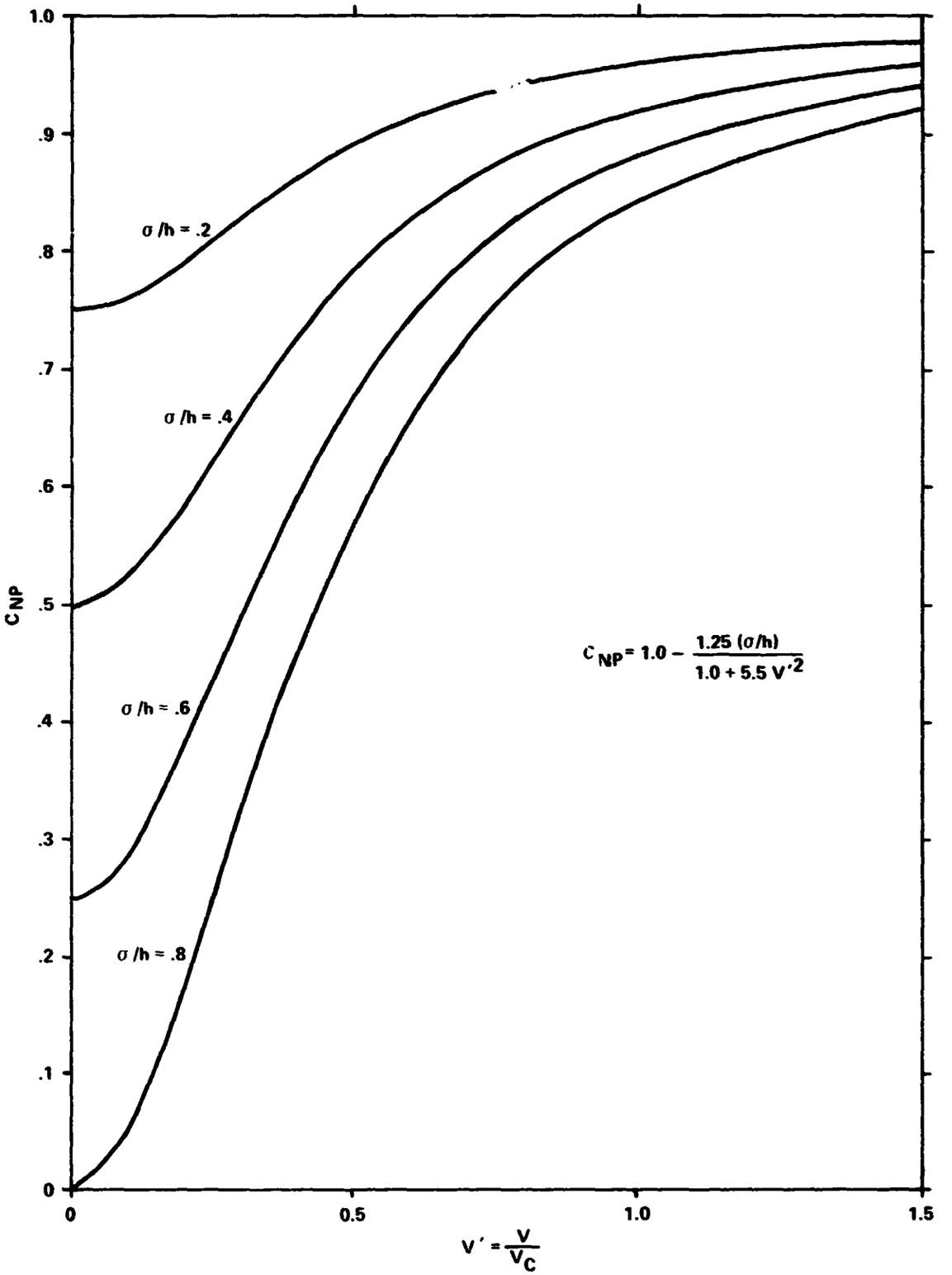

Figure 23. Multi-ply bellows stress multiplier C_{NP} as a function of V' and σ/h.

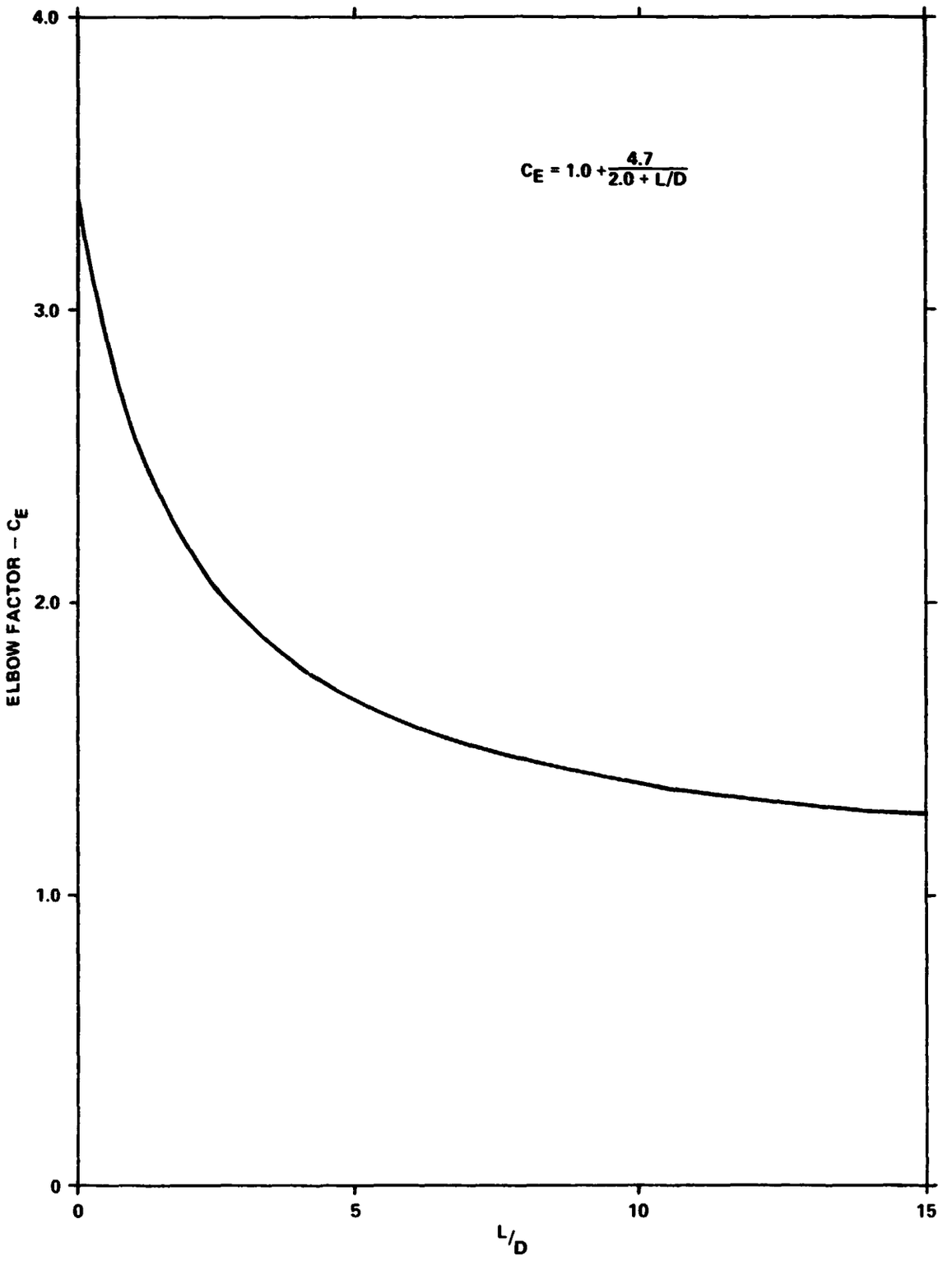

Figure 24. Elbow factor as a function of downstream length to diameter ratio.

materials, 21-6-9 alloy and 321 stainless steel, and the effects of manufacturing variations. Limited resources prevented the full scope of the program from being accomplished. Of the original 100 planned specimens of 15 different configurations, only 56 specimens of 10 different configurations were actually tested (Appendix A).

A. Test Facility Description

Bellows of the MSFC program were tested at two different test facilities, Marshall Space Flight Center and Wyle Laboratories. The majority of the bellows were tested at position No. 300 of Marshall Space Flight Center's Test Laboratory, shown schematically in Figure 25 and the photo in Figure 26. Water was supplied to the facility from a pumping station with a maximum discharge head and flow of 170 psig and 3400 gpm. Since the test position was a considerable distance from the pumping station, the maximum available pressure at the facility was 140 psig. The flow was routed through a hand operated 8-in. Pacific Globe valve, following which the duct diameter was immediately reduced to 6 in. and the flow was channeled through a straight section approximately 62 ft in length. A secondary 6-in. butterfly valve preceded an elbow section immediately above the bellows test section. After passing through the test specimen, the flow exited through a variable position 6-in. Annin valve and into a drainage ditch.

With the set-up shown in Figure 25, the maximum flow was limited to 2600 gpm, which was insufficient to resonate some bellows configurations. The flow fixture was also intended to allow the bellows test specimen to be placed at a varying distance from the upstream elbow to measure the effect of the turbulence, created by the upstream elbow, on flow-induced vibrations. Also the facility would allow the bellows to angulate so as to ascertain this effect on the vortex generation. The bellows angulation method proved less than satisfactory. The bellows pivot was shifted axially from the center of the bellows, introducing squirm and undesirable loading. A feasible solution could not be found so it was then necessary to modify the facility to that shown in Figure . 7. This would eliminate virtually all piping located downstream of the bellows.

The piping containing the elbows and the Annin valve located downstream of the test specimen was eliminated and a spool piece with an orifice for back pressure was installed. The bellows specimens were fixtured with threaded rods to prevent squirm and facilitate alignment.

Testing in the modified facility was performed by opening the 6-in. Hadley valve and manually controlling flow with the 8-in. Pacific valve. Failure of the bellows was determined usually by the test engineer.

Due to other priorities at the Marshall test facility, it was necessary to move the test program to Wyle Laboratories for completion of the bellows testing. The test facility at Wyle Laboratories featured a closed loop flow facility. A schematic of the facility is shown in Figure 28.

The water was pumped from a storage tank by a Worthington two-stage impeller type pump. The maximum flow was limited to 4400 gpm with a corresponding head of 670 ft. The flow was routed through a hand-operated 10-in. gate valve and then around two 90 deg bends. After the second bend, duct diameter was immediately reduced to 6 in., followed by a straight section approximately 22 ft in length. The duct was then reduced to 4 in. approximately 2 ft before the bellows test section. After passing through the bellows test specimen, the flow was then routed back to the water storage tank. With this facility the flow rate could not be as finely tuned as in the MSFC test facility. Since this facility was a closed loop, a great deal of mechanical vibration was noticed in the system. Failure of the bellows was determined usually by the test engineer.

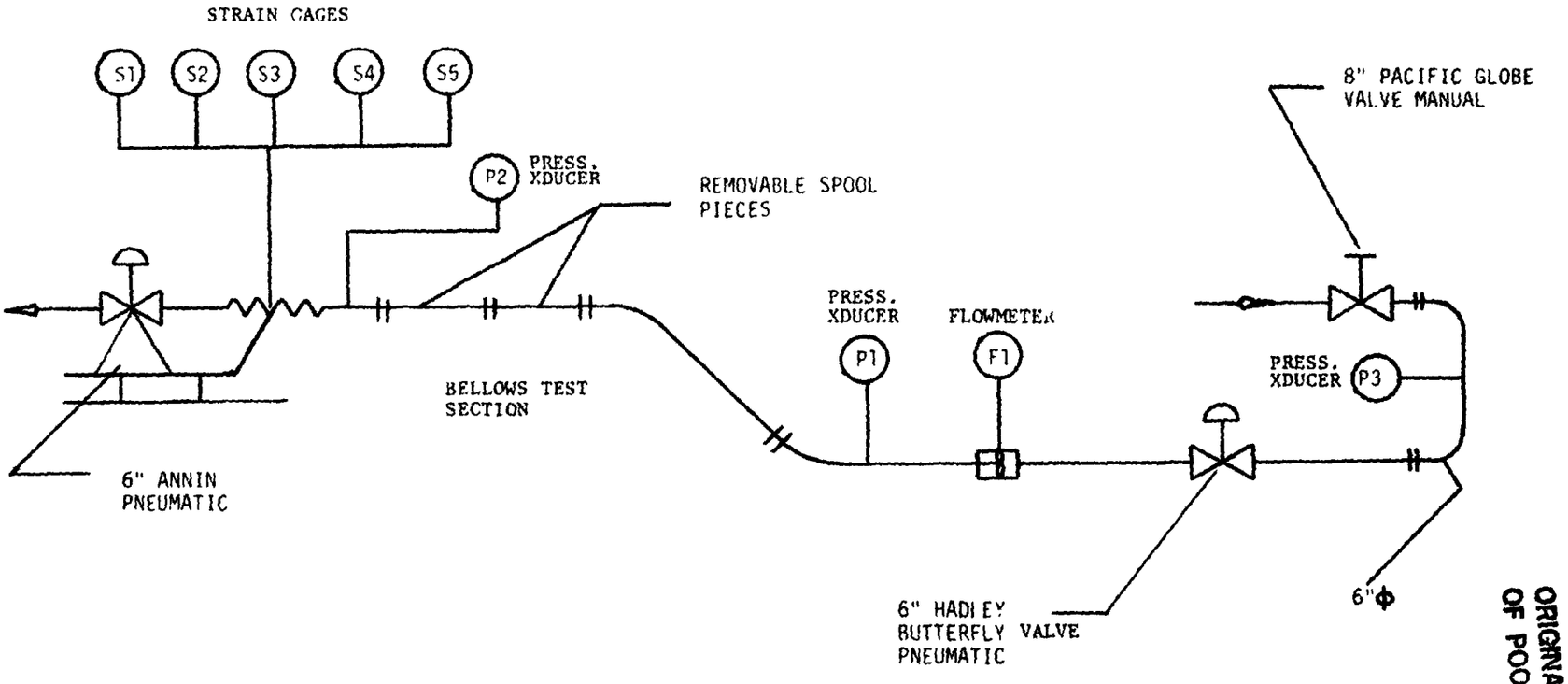

Figure 25. Schematic of original MSFC test facility.

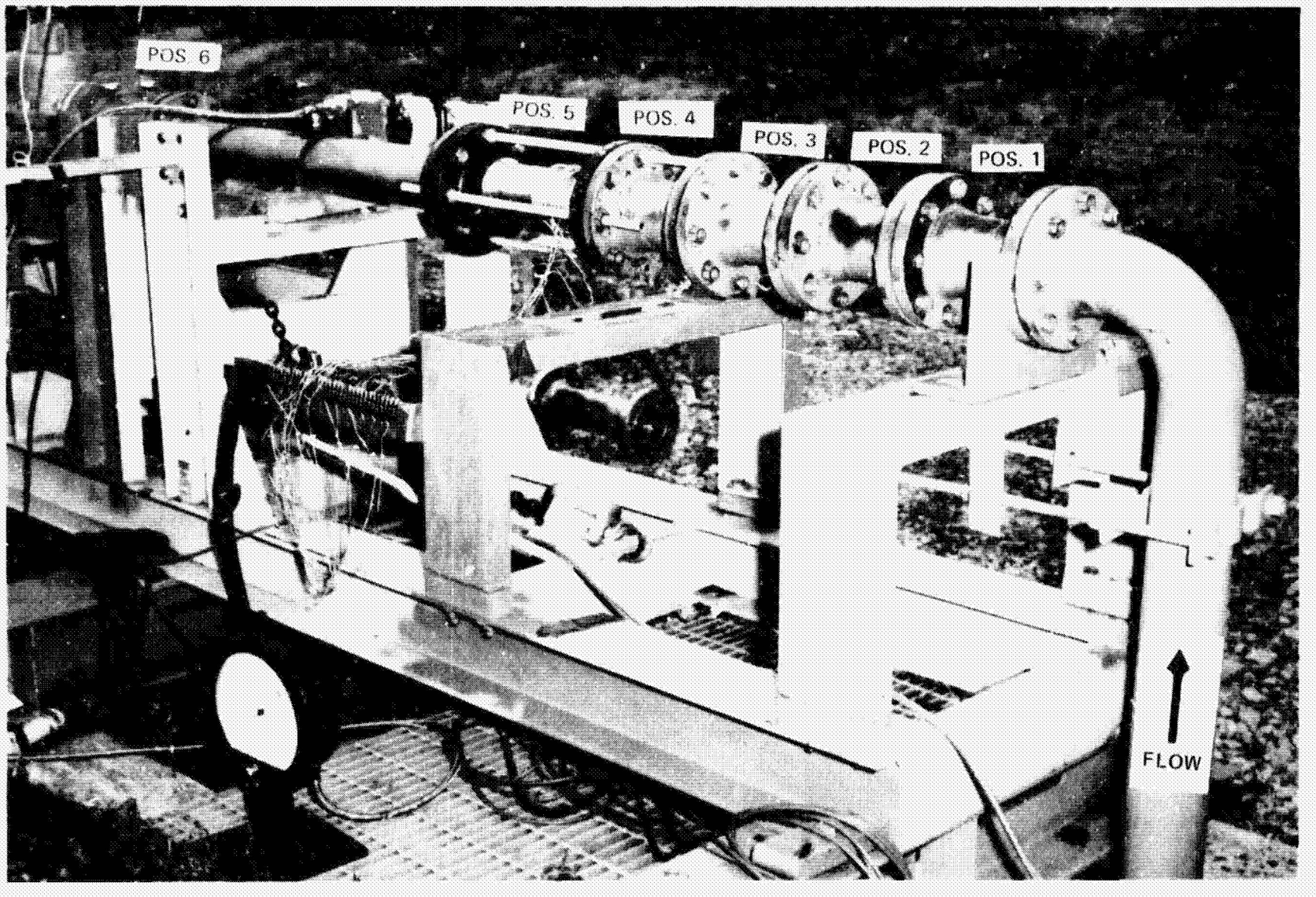

Figure 26. Photo of original MSFC flow test facility.

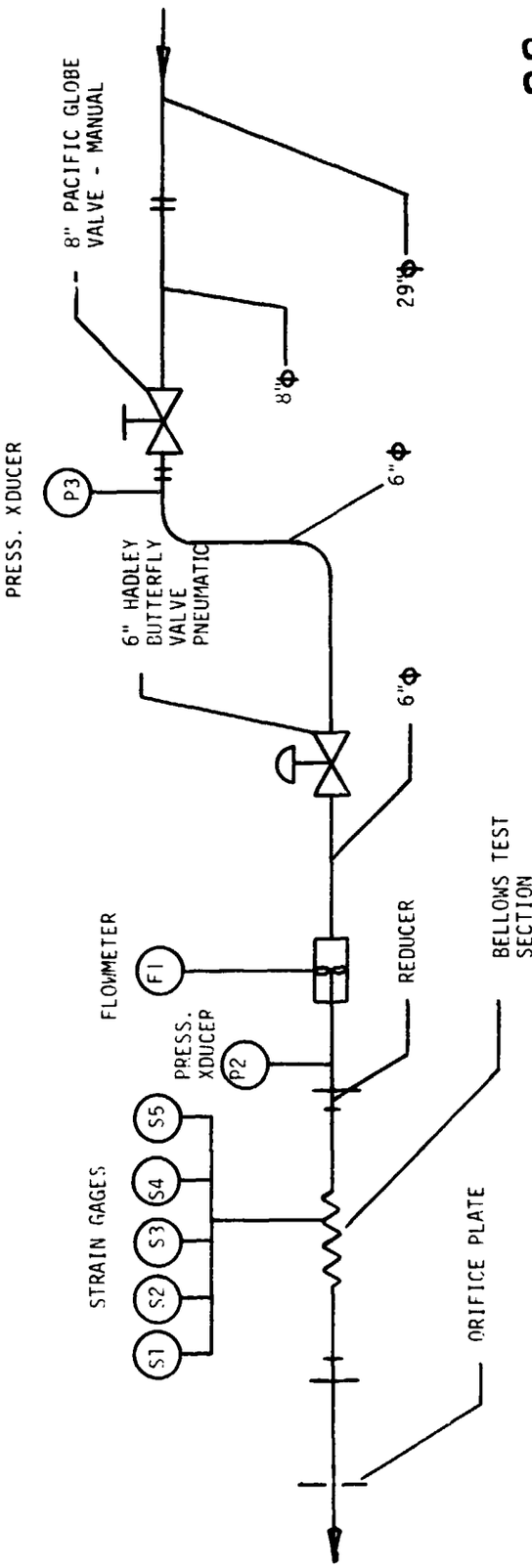

ORIGINAL PAGE IS
OF POOR QUALITY

Figure 27. Schematic of MSFC modified test facility.

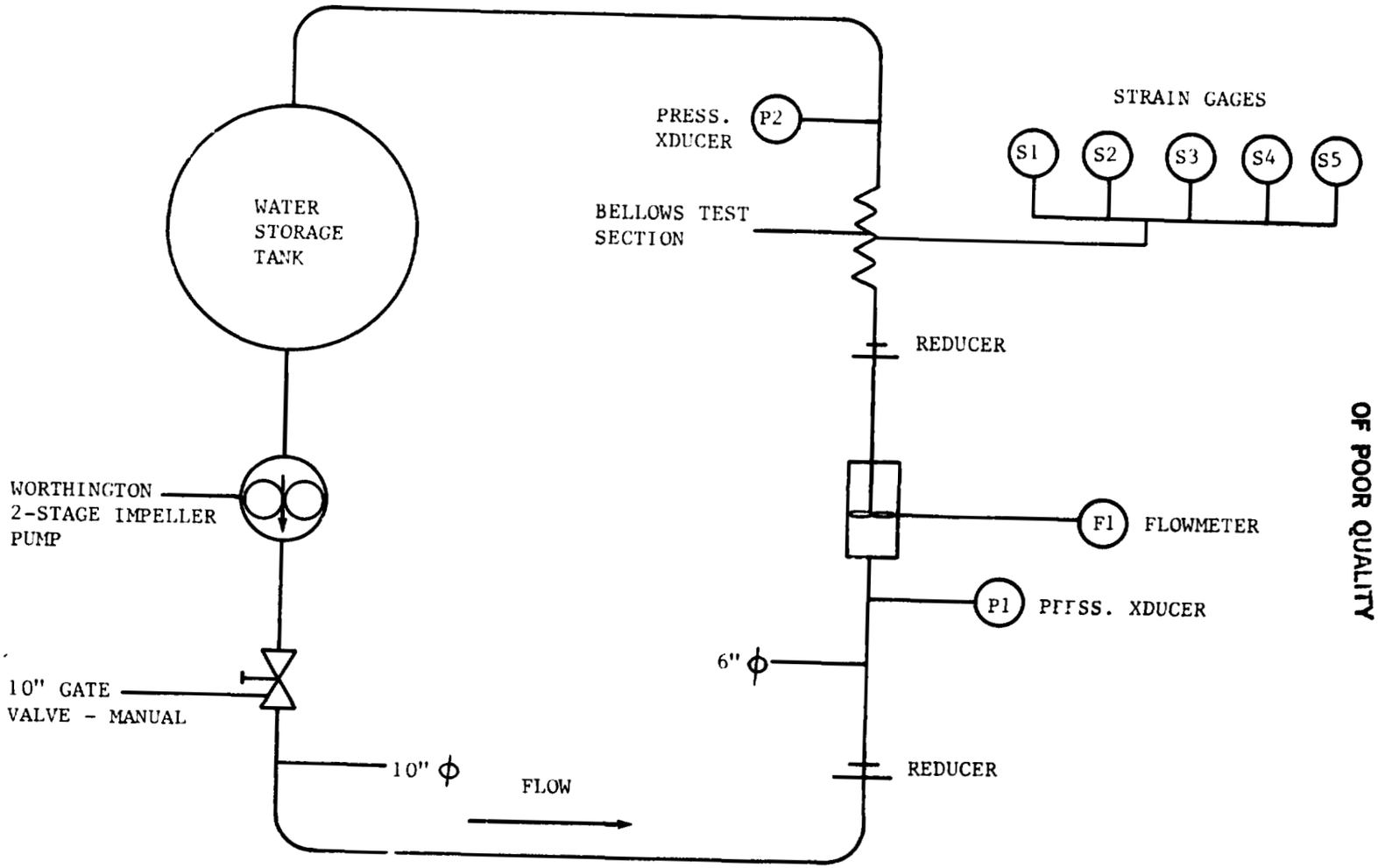

Figure 28. Schematic of Wyle Laboratories test facility (closed loop flow facility).

B. Test Procedure

Prior to the installation into the flow facility, all bellows specimens had strain gages applied to specific convolute crowns. A spring rate test was then performed and strains were measured at loads of 20, 40, and 60 lb except where such a load would cause permanent deformation. Subsequent to bench testing, the bellows were installed in the flow facility and pressurized to 0, 50, 100, 150, and 0 psig at zero flow to record baseline strain data.

The procedure for the initial test setup shown in Figure 25 was to open the 8-in. Pacific valve to the full open position and then open the by-pass line around the 6-in. Hadley to allow the line to fill. Flow was then controlled with the variable position 6-in. Annin globe valve. This valve was setup to automatically match a given transient condition of 0 to 100 percent open and back to 0. Oscillographs of the strain gage data were then examined to determine at what flow the bellows resonated. The valve was then reset to maintain this flow until the bellows failed.

Generally, one specimen of each type bellows was subjected to an initial sweep test, ramping flow velocity slowly up to some maximum then back to zero as illustrated in Figure 29. The strain data recorded for this ramp test was then analyzed to produce an RMS strain amplitude versus time plot such as that illustrated in Figure 30. From the strain-time history and velocity-time plots, a velocity was chosen for the subsequent dwell test. The purpose of the dwell tests was to induce a fatigue failure if possible. Some bellows were subjected to several dwell tests but never failed. A few bellows were tested in the original facility with an elbow located at one of six distances upstream (Fig. 26). Most bellows were tested in the MSFC modified facility or at the Wyle Laboratories facility.

C. Summary of Results

The appendices of this report include a significant amount of raw test data so that, as required, it may be used in subsequent model correlation efforts in those areas not adequately pursued herein or not pursued at all.

Geometric data for each test bellows is given in Appendix A, including the range of non-standard pitch (λ') values for those bellows tested in a stretched or compressed condition. A listing of all tests, bench or flow, conducted is summarized in Appendix B along with a table defining those bellows tested with an upstream elbow. Relative position of the upstream elbow is also defined in Appendix B. Results of the bench spring rate tests is presented in Appendix C along with corresponding theoretical calculations. Strain versus force and strain versus pressure bench test results for a typical bellows configuration are given in Appendix I. Appendix D gives bar graphs of velocity for all flow tests conducted and indicates whether the bellows failed or passed. Appendix E gives corresponding velocity versus time plots for each flow test conducted on each bellows.

Appendix F contains graphs of frequency versus velocity for those tests where resonance occurred and data was available. For comparison, the theoretical and observed frequencies were plotted on the same graph, and the bellows corresponding geometry were indicated. Also included in Appendix F are some corresponding power-spectral-density plots.

A table summarizing failure velocity (V_F), time to failure (TTF), cycles to failure (CTF), and failure stress level is given in Appendix G. The S-N curves from which the failure stress levels were derived are also given in Appendix G.

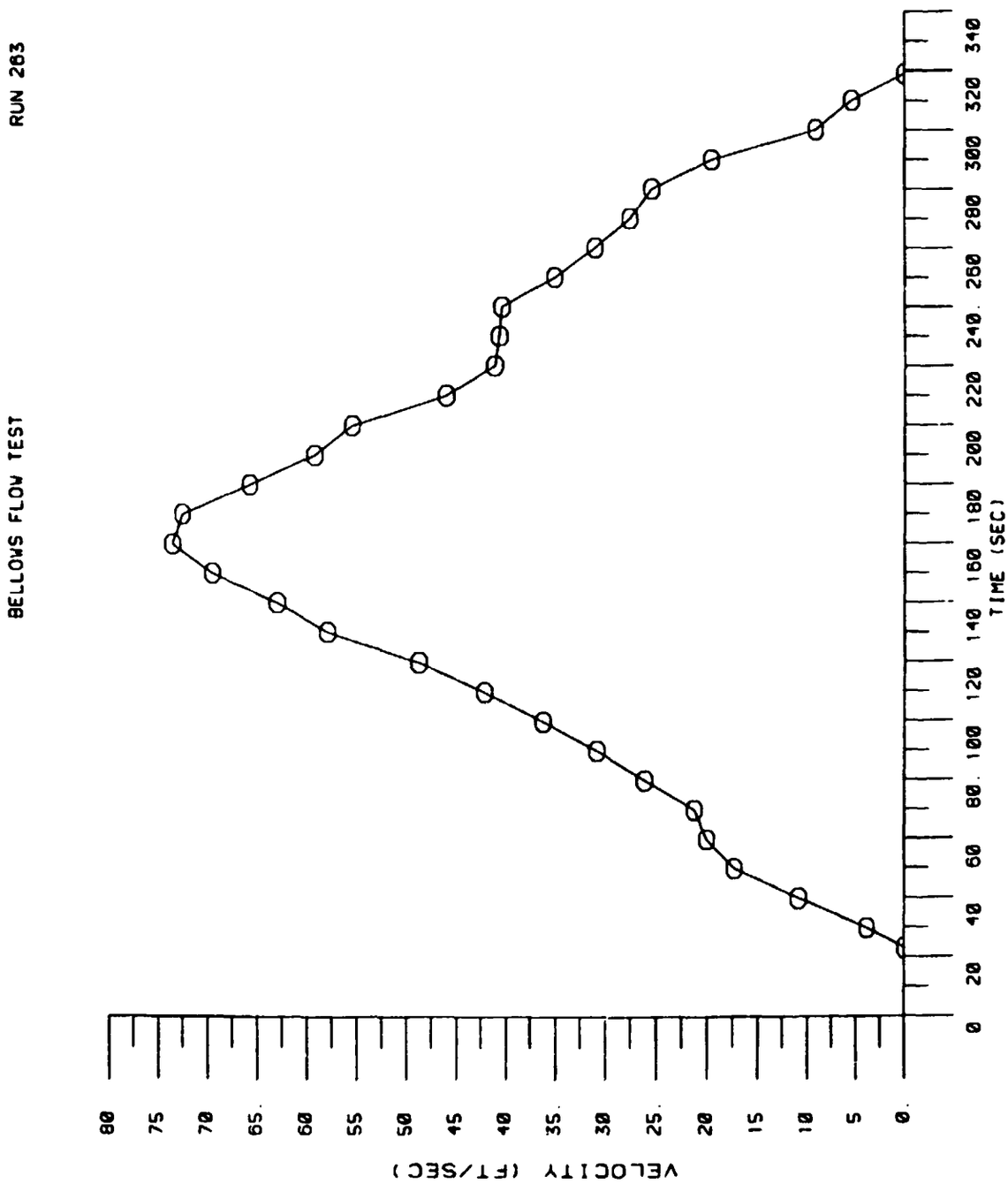

Figure 29. Sweep test of bellows 5002-3 (Test No. 263).

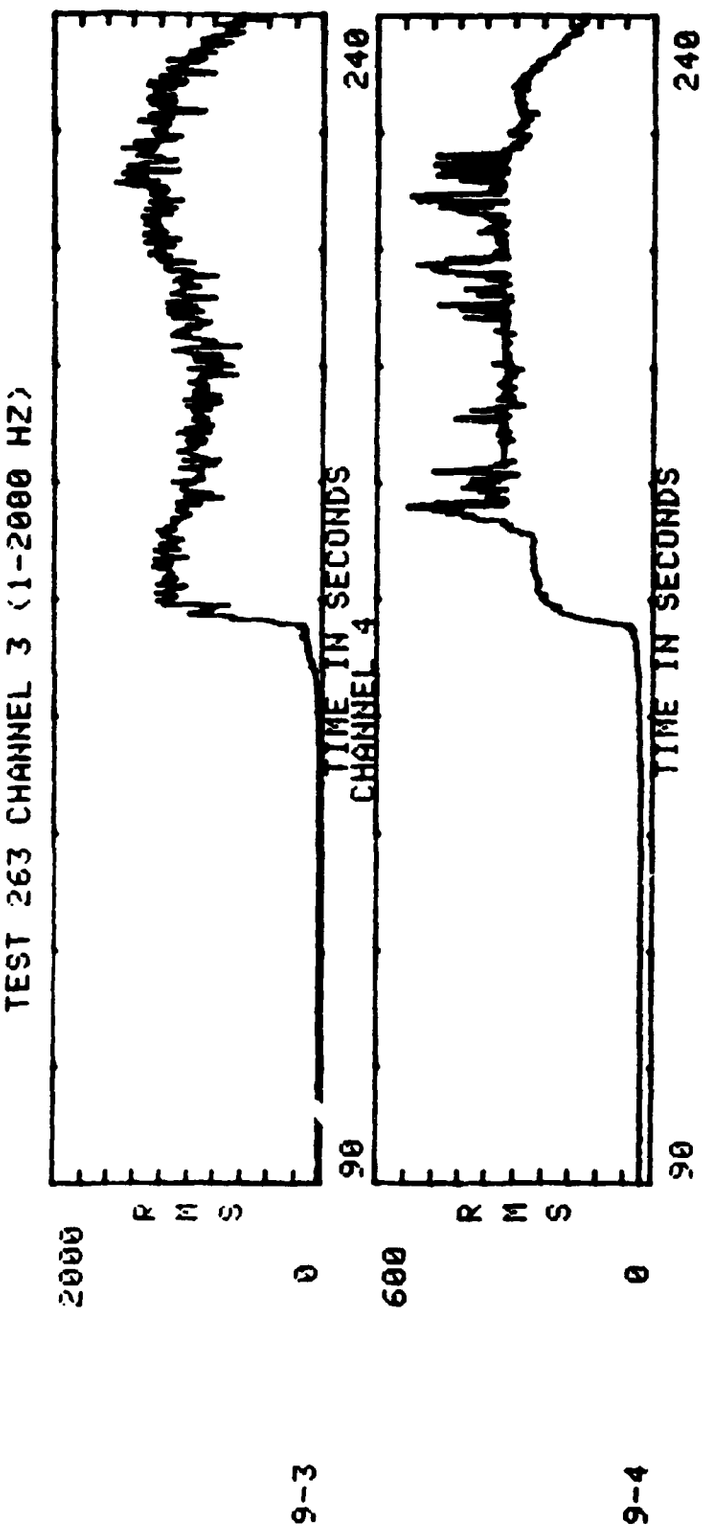

Figure 30. RMS strain versus time for bellows 5002-3 (Test No. 263).

VI. COMPARISON OF THEORY AND EXPERIMENT

A. General

Results of the MSFC bench and flow tests, plus results of previous SwRI tests, have been used as a basis for correlation and correction of the analytical models described earlier in this report. These correlations are divided into three separate areas, namely, spring rate model, frequency prediction model, and flow-induced stress model. An original objective of this program was to examine and model the effect of static pressure induced stress, however, limited time prevented completion of this aspect.

B. Spring Rate

Appendix C presents a tabulation of measured and calculated spring rates for all test bellows. Both simplified and refined Salzmann method calculations are included. As may be seen, the Salzmann method offers no advantage over the simplified method and in fact results in greater error in most cases. Originally, the calculated spring rate was based on blueprint or vendor supplied geometry. Subsequently, significant differences were found between vendor and actual geometry. Spring rate was therefore calculated based on measured or actual geometry. Appendix C also gives percent error between measured and calculated values for vendor and actual geometry. Figure 31 shows calculated (by the simplified method) versus measured spring rate for both geometries. Clearly, there are significant errors (up to 52 percent) in the calculated spring rate based on vendor geometry. Use of measured geometry reduces the maximum average error for the test specimens to about 14 percent. We concluded that measured spring rate should be used in the calculation of mode frequencies and flow-induced stress where accurate results are required. Where calculated spring rate is to be used, the simplified method is preferred over the Salzmann method. Note the difference between vendor quoted and actual spring rates.

C. Frequency Prediction

Appendix F contains plots of frequency versus velocity for all MSFC bellows tested. Each plot includes the calculated values for the $2N_c$-1 longitudinal modes and the test data. For these calculations, a constant value of Strouhal number (0.2) was used. While some bellows show significant variation of test versus theory, a constant value of 0.2 appears to be a good compromise and is currently used. A more accurate model of Strouhal number must include as variables, for example, λ/σ and V/V_c or N/N_c.

In prior SwRI tests, most bellows showed significant response in successive modes, starting with the first, as velocity was increased from zero. However, the SwRI flow facility operator was standing next to the test bellows and able to maintain fine control of fluid velocity. In the MSFC tests, the operator was not standing near the bellows and fine flow control was not possible. Examination of the results in Appendix F show that many of the MSFC tested bellows did not show response in many lower order modes and there are two possible explanations. First, these modes may simply have been missed because of the rather rapid flow velocity changes used in sweeps. Secondly, the possible mode response level may have been too low to permit the fluid-structural instability to exist because of, for example, extra damping of multiple plies.

Appendix J shows comparison of theoretical and experimental frequency versus velocity for typical SwRI bellows tests. This rather good agreement gives credence to the frequency prediction method.

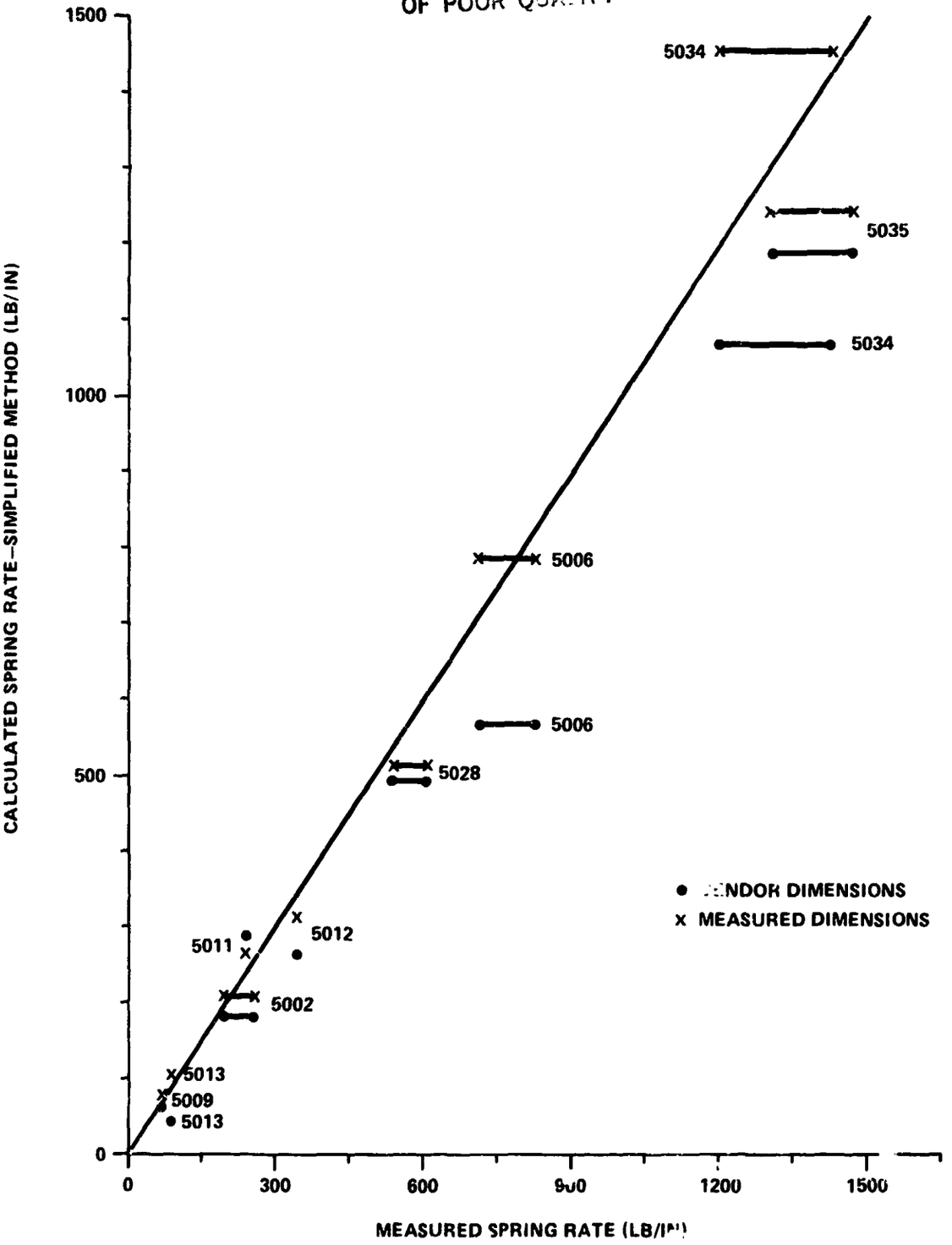

Figure 31. Calculated versus measured spring rate for both the vendor geometry and measured geometry.

In summary, tests conducted at MSFC represented more nearly a "real world" situation of flow and flow-induced vibration in a bellows, while the SwRI tests more typically represented strict laboratory results. In both cases, the Strouhal and frequency prediction method works, however, actual modes excited are difficult to determine for most of the MSFC test data. This really is of little concern however, since proper prediction of flow-induced stress levels is the main goal.

D. Flow-Induced Stress

In Section IV.E, a model of flow-induced stress was analytically developed in the form

$$\text{Stress} = \frac{\pi}{4} C_S C_F Q E P_d \left(\frac{t}{h}\right) \left(\frac{1}{N_P \cdot SSR}\right) \tag{23}$$

the term $\pi/4\ C_S\ C_F\ Q \equiv CSFQ$ was acknowledged as a function of geometric and flow variables to be empirically derived from the experimental results. We will now briefly discuss how this was accomplished.

All failure test results were initially grouped into three major categories:

I All bellows, including the SwRI tests, where no elbow effect was in evidence, and no static or initial stress was induced.

II Bellows tested with an elbow present at some variable distance upstream.

III Bellows tested in a state of initial compression or extension.

Group I results were treated in the most detail and form the basis for the final stress model correlation. The data given in Appendix G – failure velocity, time to failure and cycles to failure – were used to identify from an S-N curve for the bellows material (321 or 21-6-9) a failure stress level. In other words, we accepted a published S-N diagram (Appendix G) for these materials and used this to determine an "experimental" stress level for each failed bellows, since the cycles to failure were known. Next, we used this stress value to calculate experimental CSFQ since from the model

$$CSFQ \equiv \frac{\pi}{4} C_S C_F Q = \frac{\text{Stress}}{\dfrac{E P_d}{N_P \cdot SSR} \left(\dfrac{t}{h}\right)} \tag{28}$$

Next, the experimental CSFQ data base was subjected to a correlation study to produce a preliminary empirical analytical model. It was determined that CSFQ could be approximately expressed in the form

$$CSFQ \approx C^* \left(\frac{h}{\delta}\right) \left(\frac{V_c}{V}\right) \tag{29}$$

where

$$C^* = \frac{C_1}{C_2 + V'^2} + \frac{C_3 \left|\sin (180\ V')\right|}{C_4 + V'^2} + C_5 \quad . \tag{25}$$

An initial set of coefficients were chosen and computer runs were made to calculate flow-induced stress which was then compared with the experimental values. This comparison showed that corrections were needed to account for the added damping effect of multiple ply bellows and for a noticeable increase in stress for bellows having low specific spring rate (SSR) values.

It should be noted that early attempts to find a model correlation were met with considerable frustration, caused by excessive data scatter. This excessive data scatter was later traced primarily to significant differences between vendor supplied and actual bellows geometry. See Appendix A which shows vendor geometry and measured geometry.

Based on the above, a new or improved correlation of CSFQ (with no elbow effect) was developed as

$$CSFQ = C^* C_{NP} \left[1 + 0.1\left(\frac{400}{SSR}\right)^2\right]\left(\frac{h}{\delta}\right)\left(\frac{V_c}{V}\right) \tag{30}$$

where

$$C_{NP} = 1.0 - \frac{C_6\left(\frac{\sigma}{h}\right)}{1.0 + C_7 V'^2} \qquad \text{for } N_p = 2, 3, \ldots \tag{26}$$

Computer runs were made to allow selection of a final set of coefficients which were

$C_1 = 0.13$
$C_2 = 0.462$
$C_3 = 1.0$
$C_4 = 10.0$
$C_5 = 0.06$
$C_6 = 1.25$
$C_7 = 5.5$

Using this model, final computer runs were made for the Group I bellows and the calculated results compared with actual data. Results of this comparison (both SwRI and MSFC bellows) are given in Table 3 and Table 4 for the Group I category bellows. In general, note the following:

TABLE 3. COMPARISON OF ACTUAL AND PREDICTED STRESS FOR SwRI TEST BELLOWS WITH NO ELBOW EFFECT AND NO INITIAL STRESS INDUCED (GROUP I BELLOWS)

BELLOWS NO.	V_F (FPS)	CYCLES TO FAILURE ($\times 10^6$)	MATERIAL	ACTUAL STRESS (PSI)	PREDICTED STRESS (PSI)	ACT. STRESS / PRED. STRESS
1A	55.5	2.6	321	27,600	58,300	.473
2A	55.5	10.0	321	26,500	58,300	.455
3A	57.0	6.9	321	26,900	59,870	.449
4A	55.5	4.1	321	27,400	58,300	.470
1B	41.5	1.05	321	28,700	34,520	.831
2B	38.0	0.7	321	29,000	33,060	.877
3B	55.5	0.5	321	29,400	35,770	.822
4B	38.0	1.4	321	28,200	33,060	.853
5B	58.5	1.2	321	28,400	35,070	.810
6B	48.0	11.0	321	26,500	36,040	.735
7B	55.5	10.5	321	26,500	35,770	.741
1C	58.5	1.2	321	28,400	34,710	.818
2C	48.0	11.0	321	26,500	31,070	.853
3C	55.5	10.5	321	26,500	33,860	.783
4C	46.0	3.1	321	27,500	30,160	.912
1D	35.0	1.3	321	28,300	34,040	.831
2D	29.0	1.9	321	27,900	31,360	.890
3D	35.0	1.7	321	28,000	34,920	.802
E	33.0	5.3	321	27,000	33,040	.817
F	33.0	3.1	321	27,500	33,470	.822
1C	52.5	3.1	321	27,500	31,070	.885
2G	52.5	4.4	321	27,300	31,750	.860
3G	43.0	6.5	321	26,900	28,470	.945
4G	50.0	2.4	321	27,800	30,930	.899
5G	43.5	2.4	321	27,800	28,680	.969
1H	45.0	2.5	321	27,700	33,740	.821
2H	45.5	3.0	321	27,500	32,410	.849
3H	45.0	11.0	321	26,500	33,100	.801

TABLE 4. COMPARISON OF ACTUAL AND PREDICTED STRESS FOR MSFC TEST BELLOWS WITH NO ELBOW EFFECT AND NO INITIAL STRESS INDUCED (GROUP I BELLOWS)

BELLOWS NO.	V_F (FPS)	MATERIAL	ACTUAL STRESS (PSI)	PREDICTED STRESS (PSI)	ACT. STRESS / PRED. STRESS
5005-1	33.2	321	28,200	31,760	.888
5006-10	77.7	321	27,900	50,930	.548
5009-1	40.5	321	27,900	28,390	.983
5011-1	49.4	321	27,600	27,620	.999
5013-2	50	321	28,000	29,140	.961
5013-2	45	321	28,800	32,990	.873
5034-2	84	21-6-9	31,200	37,250	.838
5034-8	85.8	21-6-9	31,900	38,640	.826
5034-10	70.9	21-6-9	31,000	31,880	.972
5034-13	79.5	21-6-9	31,200	33,890	.921
5034-15	69	21-6-9	31,000	31,540	.983
5035-1	113	21-6-9	31,000	36,630	.846
5035-2	110	21-6-9	31,800	37,000	.859

1) Predicted FIS values are always greater than actual values, hence, the model is conservative.

2) Model accuracy is best for single ply bellows.

3) Bellows of different materials (321 and 21-6-9) are treated.

Three antigeyser bellows, having internal ball and strut assemblies, were tested along with the Group I category bellows. These three bellows were obtained from the LO_2 antigeyser line of the External Tank.

Using the same stress model as for the other Group I bellows, computer runs were made and the calculated results and actual data are compared in Table 5. Because of very limited data and lack of time, the effect of the internal ball and strut assembly is not incorporated in the stress model. Therefore, the predicted stress values in Table 5 are not a true description of the actual stress.

TABLE 5. COMPARISON OF ACTUAL AND PREDICTED STRESS FOR MSFC TEST BELLOWS WITH INTERNAL BALL AND STRUT ASSEMBLY, NO ELBOW EFFECT AND NO INITIAL STRESS INDUCED (GROUP I BELLOWS)

BELLOWS NO.	V_F (FPS)	MATERIAL	ACTUAL STRESS (PSI)	PREDICTED STRESS (PSI)	ACT. STRESS / PRED. STRESS
AG#1	57.8	21-6-9	31,400	24,150	1.30
AG#2	74.8	21-6-9	----	31,980	----
AG#3	80.5	21-6-9	----	34,020	----

E. Elbow Effect

Failure tests of bellows with an upstream elbow have produced a limited data base, hence, the resultant elbow factor should be considered preliminary. In referring back to Figure 6, which shows results from a single bellows tested at SwRI the following is noted. First, the velocity range over which a given mode is excited is shifted downward. Secondly, the flow-induced stress level for a given velocity is increased by the presence of the elbow. Therefore, a proper model of the elbow effect should include a velocity shift phenomena and a stress amplifier effect. The present model, based on our limited data base reflects only a stress amplifier effect and is given by a C_E multiplier as

$$C_E = 1.0 \qquad \text{with no elbow present}$$

$$C_E = 1.0 + \frac{4.7}{2.0 + L/D} \qquad \text{with elbow present} \qquad (31)$$

where L/D is the ratio of L, the distance from the bellows first convolute to the elbow termination, divided by the pipe internal diameter D. Table 6 compares experimental and predicted stress for those bellows tested with an upstream elbow and had failed. For low V′ values, eg. V′ < 1.0, the simple C_E model given here seems to be quite accurate for the limited data base. The results in Figure 6 (SwRI elbow test) were at low V′ values and the model predicts $C_E \approx 2.0$ which would provide proper adjustment of the strain level for V ~ 35 ft/sec. However, for high V′ values and small L/D the stress is over predicted by a considerable margin.

F. Effect of Prestress

Several of the MSFC 5034 configuration bellows were tested in a state of initial prestress induced by stretching or compressing the bellows from their manufactured length prior to test. The stretch or compress process was accomplished by adjusting the relative position of the spool end pieces with threaded fasteners. Subsequent calculations have shown that all bellows tested in this manner were in yield at the test condition, which was not accounted for in predicting effective stress. Lack of time has prevented further examination of these bellows. Table 7 compares experimental and predicted stress (with no prestress effect incorporated in the stress model) for those failed bellows with an initial state of prestress.

G. General Comments of Tests

Virtually all bellows tested at SwRI showed response of successive longitudinal modes, starting with mode number one. Some modes were suppressed because of the "vigor" of the preceding and following modes. Strain output was monitored through the use of an AC output coupled resistance bridge of high sensitivity and low noise. A standard carrier wave or AC excited strain gage bridge unit proved unsatisfactory. Velocity sweeps were performed with manual adjustments and the operator stood next to the test bellows in order to best detect resonance.

For the MSFC tests, the sweeps were preprogrammed and the operator did not stand next to the bellows. Further, the instrumentation was not believed to be as sensitive as that employed at SwRI. In general, excitation of the first few longitudinal modes was not observed in the MSFC tests. Either speed of the sweeps or background noise (electronic and flow) prevented their occurrence and/or detection. In a practical sense these same modes did not occur in the MSFC tests although they might have been observed in a slower paced laboratory environment. These modes were of primarily academic value anyway since the response levels would have been too low to cause failure.

VII. DISCUSSION AND CONCLUSIONS

The MSFC tests greatly extended the data base compared with the fatigue results obtained at SwRI. First, all SwRI failures were for single ply bellows constructed of 321 S.S. The majority of the MSFC bellows were multiple ply, some 321 S.S. and some 21-6-9 alloy. Secondly, while limited in scope, the elbow effect results obtained at MSFC represent a significant increase in knowledge. Thirdly, tests on two bellows configurations (5002 and 5005) were conducted at a much higher normalized velocity V′ than any prior tests. These particular tests showed, for the first time, that excitation of the bellows longitudinal modes continues indefinitely as velocity increases, even though the prior theory predicted that excitation would cease once the lock-in range of the highest longitudinal mode was exceeded.

TABLE 6. COMPARISON OF ACTUAL AND PREDICTED STRESS FOR MSFC TEST BELLOWS WITH UPSTREAM ELBOW PRESENT (GROUP II BELLOWS)

BELLOWS NO.	V_F (FPS)	V	MATERIAL	ACTUAL STRESS (PSI)	PREDICTED STRESS (PSI)	ACT. STRESS / PRED. STRESS	L/D	C_E
5002-1	62	1.65	321	29,800	43,480	.685	8.17	1.462
5002-2	72	1.86	321	28,300	27,900	1.01	28.3	1.155
5002-3	48	1.38	321	29,000	33,290	.871	28.3	1.155
5002-4	56	1.56	321	27,800	65,400	.425	2.17	2.127
5002-5	70	1.91	321	26,500	26,680	.993	28.3	1.155
5002-6	70	1.81	321	28,100	30,020	.936	28.3	1.155
5005-2	65.2	3.23	321	~33,000	45,740	~.722	20.45	1.209
5028-1	65.8	.60	21-6-9	~33,000	33,190	~.994	3.81	1.809
5028-2	66.6	.57	21-6-9	37,000	38,840	.953	1.813	2.233

TABLE 7. COMPARISON OF ACTUAL AND PREDICTED STRESS FOR MSFC TEST BELLOWS WITH INITIAL COMPRESSION OR EXTENSION (GROUP III BELLOWS)

BELLOWS NO.	V_F (FPS)	MATERIAL	ACTUAL STRESS (PSI)	PREDICTED STRESS (PSI)	ACT. STRESS / PRED. STRESS	COMPRESSION OR EXTENSION
5034-1	82.5	21-6-9	31,200	41,850	.746	48% COMPRESSION
5034-3	84.2	21-6-9	31,000	33,770	.918	30% COMPRESSION
5034-4	84.4	21-6-9	31,000	29,510	1.05	17% COMPRESSION
5034-5	65.5	21-6-9	34,000	17,510	1.94	11% EXTENSION
5034-6	85.5	21-6-9	34,200	21,160	1.62	26% EXTENSION
5034-7	85	21-6-9	31,000	90,730	.342	71% COMPRESSION
5035-3	94	21-6-9	31,000	41,750	.743	38% COMPRESSION

NOTE: The predicted stress includes only the dynamic component. The mean stress is not accounted for.

The range of bellows sizes and geometries tested in the MSFC and prior SwRI programs were quite diverse. Internal diameters of test bellows ranged from about 3 in. to 14 in. Bellows having as few as 5 convolutes and as many as 20 convolutes were tested to failure. Bellows of 1, 2, and 3 plies were included, and both 321 S.S. and 21-6-9 alloy materials were employed.

The results of this program suggest that the calculation of flow-induced stress as a function of velocity should be the main goal of a bellows analysis. The consideration of what modes are excited and at what frequency they occur is de-emphasized in this report.

The procedure for calculating flow-induced stress as presented herein is believed conservative when applied to a bellows with or without an upstream elbow, but not conservative where a high mean stress is present because of internal pressure or other prestress means. Use of a seven ordinate stress-fatigue life plot would be useful in accounting for the effect of prestress and this should be one subject of further study.

Conclusions

The following conclusions have been made regarding this study:

1) Bellows flow-induced vibration (FIV) is caused by a nonlinear coupling of the bellows elastic structure and a fluid vortex formation and shedding process, i.e., a fluid-structure instability.

2) A dimensionless velocity defined by $V' = V/V_c$ is an important parameter in modeling bellows FIV. Here V is an arbitrary velocity and V_c is the critical velocity for the mode $N = N_c$.

3) Up to $V' = 1.0$ the bellows excitation frequency and fluid velocity may be calculated from the Strouhal number $f\sigma/V = 0.2$.

4) The mode $N = N_c$ seems to be the highest mode normally excited with liquid flows. With gaseous flows the local convolute bending mode may be the highest one excited when acoustic resonance occurs.

5) For fluid velocities exceeding $V = V_c$, the bellows tends to respond in a subharmonic manner.

6) Contrary to prior theory, bellows response appears to continue indefinitely as the velocity is increased beyond $V = V_c$ with subharmonic response (1/2, 1/3, etc.) of the higher modes ($N \sim N_c$) sustained.

7) A good correlation of frequency and velocity where $V > V_c$ does not presently exist.

8) The magnitude of flow-induced stress may be conservatively calculated by the method presented in this report for bellows, including those with an upstream elbow, in all velocity ranges where prestress is negligible.

9) Calculation of stress versus velocity by this method allows a conservative evaluation of a bellows design and application.

10) Static stresses induced by pressure or other means should be considered in the evaluation of a bellows design. No means for accomplishing this was discussed in this report as this remains an area for future study.

11) Present spring rate and probably also pressure-stress calculation methods are inadequate.

REFERENCES

1. Gerlach, C. R., Schroeder, E. C., Bass, R. L., III, a Holster, J. L.: Bellows Flow-Induced Vibrations and Pressure Loss. Contract No. NAS8-21133, Southwest Research Institute, April 1973.

2. Johnson, J. E., Deffenbaugh, D. M., Astleford, W. J., and Gerlach, C. R.: Bellows Flow-Induced Vibrations. Contract No. NAS8-31994, Southwest Research Institute, October 1979.

3. Salzmann, F.: Ueber die Nachgiebigkeit von Wellrohrexpansionen. Schweiz. Bauztg., Band 127, Nr. 11, March 1946, pp. 127-130.

4. Aerospace Recommended Practice (ARP) No. 735, Society of Automotive Engineers Publication, 1966.

APPENDIX A

GEOMETRIC DATA FOR MSFC BELLOWS

BELLOWS SPECIFICATIONS

BELLOWS	NO. TESTED	D_i	D_o	N_c	N_p	σ	σ_i	σ_o	λ	h	h_i	t	L.L.	MAT'L
5002	6	3.0	3.65	16	3	.076	.095	.076	.113	.325	.312	.007	1.80	321
5028	2	4.0	4.748	9	3	.158	.158	.174	.310	.350	.346	.008	2.83	21-6-9
5005	2	4.0	5.0	19	1	.111	.130	.145	.205	.500	.475	.008	3.90	321
5006	10	4.47	5.26	8	2	.170	.225	.170	.300	.395	.355	.010	2.40	321
5011	1	4.54	5.53	14	1	.169	.175	.170	.309	.495	.510	.015	4.32	321
5013	3	4.87	6.0	20	1	.141	.170	.140	.261	.565	.425	.010	5.26	321
5009	1	5.0	5.75	16	1	.132	.132	.125	.250	.375	.350	.007	4.00	321
5012	3	5.28	6.08	15	3	.158	.200	.158	.300	.400	.376	.008	4.50	321
5035	10	2.93	3.60	9	2	.111	.125	.125	.174	.311	.306	.012	1.56	21-6-9
*5034	18	4.00	4.76	5	2	.150	.165	.145	.260	.360	.325	.010	1.30	21-6-9

SYMBOLS:
- D_i - inside diameter (inches)
- D_o - outside diameter (inches)
- N_c - number of convolutes
- N_p - number of plies
- σ - convolute width (inches)
- σ_i - measured inside convolute width (inches)
- σ_o - measured outside convolute width (inches)
- λ - convolute pitch (inches)
- h - mean disc height (inches)
- h_i - measured inside disc height (inches)
- t - ply thickness (inches)
- L.L.-live length (inches)

Material Properties: For 321 S.S. the density is taken to be 0.286 lb/cu in and a Young's modulus of 0.290×10^8 psi. For 21-6-9 the density is taken to be 0.282 lb/cu in and a Young's modulus of 0.285×10^8 psi.

*Three of the 5034 configuration were antigeyser lines with ball struts. They will be referred to in the data as AG #1, AG #2, and AG #3.

DIMENSIONAL DATA FOR COMPRESSED AND EXTENDED BELLOWS

BELLOWS	TEST NO.	L	L'	λ'	δ	δ'	COMPRESSION OR EXTENSION
5006-1	367	2.50	1.95	.254	.163	.084	48% COMPRESSION
	368	2.50	1.67	.214	.163	.044	73% COMPRESSION
5012-1	426	4.50	4.003	.275	.152	.117	23% COMPRESSION
	427	4.50	3.506	.239	.152	.081	47% COMPRESSION
	428	4.50	3.01	.204	.152	.046	70% COMPRESSION
5034-1	331	1.46	1.34	.299	.184	.154	16% COMPRESSION
	332	1.46	1.22	.269	.183	.123	33% COMPRESSION
	333	1.46	1.11	.241	.184	.096	48% COMPRESSION
	334	1.46	1.11	.241	.184	.096	48% COMPRESSION
5034-3	354	1.47	1.25	.276	.186	.131	30% COMPRESSION
	355	1.47	1.25	.276	.186	.131	30% COMPRESSION
5034-4	365	1.47	1.34	.299	.186	.154	17% COMPRESSION
5034-5	390	1.47	1.55	.351	.186	.206	11% EXTENSION
5034-6	400	1.47	1.66	.379	.186	.234	26% EXTENSION
5034-7	411	1.19	1.297	.288	.116	.147	23% EXTENSION
	412	1.19	1.41	.316	.116	.171	47% EXTENSION
	413	1.19	1.08	.234	.116	.089	24% COMPRESSION
	414	1.19	.97	.206	.116	.061	47% COMPRESSION
	415	1.19	.86	.179	.116	.034	71% COMPRESSION
5034-9	535	1.19	1.30	.289	.116	.144	24% EXTENSION
	537	1.19	1.30	.289	.116	.144	24% EXTENSION
5035-3	454	1.570	1.401	.160	.056	.035	38% COMPRESSION
	455	1.570	1.401	.160	.056	.035	38% COMPRESSION
5035-5	511	1.570	1.401	.160	.056	.035	38% COMPRESSION
	512	1.570	1.401	.160	.056	.035	38% COMPRESSION
	513	1.570	1.401	.160	.056	.035	38% COMPRESSION
	514	1.570	1.401	.160	.056	.035	38% COMPRESSION

NOTE: PRIME MARK INDICATES DIMENSION AFTER THE BELLOW WAS COMPRESSED OR EXTENDED.

APPENDIX B

A LISTING OF ALL BENCH AND FLOW TESTS CONDUCTED ON MSFC BELLOWS AND THE FLOW FACILITY ON WHICH THEY WERE TESTED

BELLOW	TEST NO.	TEST
5002-1	265	BENCH SPRING RATE ZERO
5002-1	266	BENCH SPR. RATE 10#
5002-1	267	BENCH SPR. RATE 20#
5002-1	268	BENCH SPR. RATE 40#
5002-1	269	BENCH ZERO
5002-1	270	BENCH 50 psig
5002-1	271	BENCH 100 psig
5002-1	272	BENCH 150 psig
5002-1	273	BENCH ZERO
5002-1	274	SWEEP FLOW
5002-1	275	SWEEP FLOW
5002-1	276	SWEEP FLOW
5002-1	277	SWEEP FLOW
5002-1	278	SWEEP FLOW - FAILURE
5002-2	239	BENCH SPR. RATE ZERO
5002-2	240	BENCH SPR. RATE 10#
5002-2	241	BENCH SPR. RATE 20#
5002-2	242	BENCH SPR. RATE 40#
5002-2	243	BENCH ZERO
5002-2	244	BENCH 50 psig
5002-2	245	BENCH 100 psig
5002-2	246	BENCH 150 psig
5002-2	247	BENCH ZERO
5002-2	248	SWEEP FLOW
5002-2	249	SWEEP FLOW
5002-2	250	SWEEP FLOW
5002-2	251	SWEEP FLOW
5002-2	252	SWEEP FLOW
5002-2	253	STEADY FLOW - FAILURE
5002-3	254	BENCH SPR. RATE ZERO
5002-3	255	BENCH SPR. RATE 10#
5002-3	256	BENCH SPR. RATE 20#
5002-3	257	BENCH SPR. RATE 40#
5002-3	258	BENCH ZERO
5002-3	259	BENCH 50 psig
5002-3	260	BENCH 100 psig
5002-3	261	BENCH 150 psig
5002-3	262	BENCH ZERO
5002-3	263	SWEEP FLOW
5002-3	264	STEADY FLOW - FAILURE

BELLOW	TEST NO.	TEST
5002-4	279	BENCH SPR. RATE ZERO
5002-4	280	BENCH SPR. RATE 10#
5002-4	281	BENCH SPR. RATE 20#
5002-4	282	BENCH SPR. RATE 40#
5002-4	283	BENCH ZERO
5002-4	284	BENCH 50 psig
5002-4	285	BENCH 100 psig
5002-4	286	BENCH 150 psig
5002-4	287	BENCH ZERO
5002-4	288	SWEEP FLOW
5002-4	289	STEADY FLOW
5002-4	290	STEADY FLOW - FAILURE
5002-5	291	BENCH SPR. RATE ZERO
5002-5	292	BENCH SPR. RATE 10#
5002-5	293	BENCH SPR. RATE 20#
5002-5	294	BENCH SPR. RATE 40#
5002-5	295	BENCH ZERO
5002-5	296	BENCH 50 psig
5002-5	297	BENCH 100 psig
5002-5	298	BENCH 150 psig
5002-5	299	BENCH ZERO
5002-5	300	STEADY FLOW
5002-5	301	STEADY FLOW
5002-5	312	STEADY FLOW - FAILURE
5002-6	302	BENCH SPR. RATE ZERO
5002-6	303	BENCH SPR. RATE 10#
5002-6	304	BENCH SPR. RATE 20#
5002-6	305	BENCH SPR. RATE 40#
5002-6	306	BENCH ZERO
5002-6	307	BENCH 50 psig
5002-6	308	BENCH 100 psig
5002-6	309	BENCH 150 psig
5002-6	310	BENCH ZERO
5002-6	311	STEADY FLOW - FAILURE

BELLOW	TEST NO.	TEST
5005-1	001	BENCH ZERO
5005-1	002	BENCH COMPRESSION .11"
5005-1	003	BENCH COMPRESSION .22"
5005-1	004	BENCH ZERO
5005-1	070	BENCH 2° ANGULATION
5005-1	071	BENCH 4° ANGULATION
5005-1	072	BENCH 6° ANGULATION
5005-1	073	BENCH 8° ANGULATION
5005-1	074	BENCH ZERO
5005-1	559	BENCH ZERO
5005-1	560	BENCH 25 psig
5005-1	561	BENCH 50 psig
5005-1	562	BENCH 75 psig
5005-1	563	BENCH ZERO
5005-1	564	STEADY FLOW
5005-1	565	STEADY FLOW - FAILURE
5005-2	005	BENCH ZERO
5005-2	006	BENCH COMPRESSION .11"
5005-2	007	BENCH COMPRESSION .22"
5005-2	008	BENCH ZERO
5005-2	033	BENCH 50 psig
5005-2	034	BENCH 100 psig
5005-2	035	BENCH 150 psig
5005-2	036	BENCH ZERO
5005-2	065	BENCH 2° ANGULATION
5005-2	066	BENCH 4° ANGULATION
5005-2	067	BENCH 6° ANGULATION
5005-2	068	BENCH 8° ANGULATION
5005-2	069	BENCH ZERO
5005-2	075	RERUN OF BFT-0065
5005-2	076	RERUN OF BFT-0066
5005-2	077	RERUN OF BFT-0067
5005-2	078	RERUN OF BFT-0068
5005-2	079	RERUN OF BFT-0069
5005-2	104	BENCH ZERO
5005-2	105	BENCH 50 psig
5005-2	106	BENCH 100 psig
5005-2	107	BENCH 150 psig
5005-2	108	BENCH ZERO
5005-2	109	BENCH 2° ANGULATION
5005-2	110	BENCH 4° ANGULATION
5005-2	111	BENCH 6° ANGULATION
5005-2	112	BENCH 8° ANGULATION
5005-2	113	BENCH ZERO
5005-2	114	BENCH DEFLECTION .11"
5005-2	115	BENCH DEFLECTION .22"
5005-2	116	BENCH ZERO
5005-2	117	SWEEP FLOW - FAILURE

BELLOW	TEST NO.	TEST
5006-1	029	BENCH ZERO
5006-1	030	BENCH COMPRESSION .08"
5006-1	031	BENCH COMPRESSION .12"
5006-1	032	BENCH ZERO
5006-1	037	BENCH 50 psig
5006-1	038	BENCH 100 psig
5006-1	039	BENCH 150 psig
5006-1	040	BENCH ZERO
5006-1	080	BENCH 1° ANGULATION
5006-1	081	BENCH 2° ANGULATION
5006-1	082	BENCH 3° ANGULATION
5006-1	083	BENCH ZERO
5006-1	118	BENCH SPR. RATE ZERO
5006-1	119	BENCH SPR. RATE 60#
5006-1	120	BENCH ZERO
5006-1	121	BENCH 50 psig
5006-1	122	BENCH 100 psig
5006-1	123	BENCH 150 psig
5006-1	124	BENCH ZERO
5006-1	125	SWEEP FLOW
5006-1	126	SWEEP FLOW
5006-1	366	STEADY FLOW
5006-1	367	SWEEP FLOW COMPRESSED 48%
5006-1	368	SWEEP FLOW COMPRESSED 73%
5006-2	021	BENCH ZERO
5006-2	022	BENCH COMPRESSION .08"
5006-2	023	BENCH COMPRESSION .12"
5006-2	024	BENCH ZERO
5006-2	041	BENCH 50 psig
5006-2	042	BENCH 100 psig
5006-2	043	BENCH 150 psig
5006-2	044	BENCH ZERO
5006-2	084	BENCH 1° ANGULATION
5006-2	085	BENCH 2° ANGULATION
5006-2	086	BENCH 3° ANGULATION
5006-2	087	BENCH ZERO
5006-2	127	BENCH SPR. R ZERO
5006-2	128	BENCH SPR. R 60#
5006-2	129	BENCH ZERO
5006-2	130	BENCH 50 psig
5006-2	131	BENCH 100 psig
5006-2	132	BENCH 150 psig
5006-2	133	BENCH ZERO
5006-2	134	SWEEP FLOW
5006-2	135	SWEEP FLOW

BELLOW	TEST NO	TEST
5006-3	025	BENCH ZERO
5006-3	026	BENCH COMPRESSION .08"
5006-3	027	BENCH COMPRESSION .12"
5006-3	028	BENCH ZERO
5006-3	045	BENCH 50 psig
5006-3	046	BENCH 100 psig
5006-3	047	BENCH 150 psig
5006-3	048	BENCH ZERO
5006-3	088	BENCH 1^{o} ANGULATION
5006-3	089	BENCH 2^{o} ANGULATION
5006-3	090	BENCH 3^{o} ANGULATION
5006-3	091	BENCH ZERO
5006-3	136	BENCH SPR. RATE ZERO
5006-3	137	BENCH SPR. RATE 20#
5006-3	138	BENCH SPR. RATE 40#
5006-3	139	BENCH SPR. RATE 60#
5006-3	140	BENCH ZERO
5006-3	141	BENCH 50 psig
5006-3	142	BENCH 100 psig
5006-3	143	BENCH 150 psig
5006-3	144	BENCH ZERO
5006-3	183	SWEEP FLOW
5006-3	184	SWEEP FLOW
5006-4	013	BENCH ZERO
5006-4	014	BENCH COMPRESSION .08"
5006-4	015	BENCH COMPRESSION .12"
5006-4	016	BENCH ZERO
5006-4	185	BENCH SPR. RATE ZERO
5006-4	186	BENCH SPR. RATE 20#
5006-4	187	BENCH SPR. RATE 40#
5006-4	188	BENCH SPR. RATE 60#
5006-4	189	BENCH ZERO
5006-4	190	BENCH 50 psig
5006-4	191	BENCH 100 psig
5006-4	192	BENCH 150 psig
5006-4	193	BENCH ZERO
5006-4	194	SWEEP FLOW

BELLOW	TEST NO.	TEST
5006-5	009	BENCH ZERO
5006-5	010	BENCH COMPRESSION .08"
5006-5	011	BENCH COMPRESSION .12"
5006-5	012	BENCH ZERO
5006-5	049	BENCH 50 psig
5006-5	050	BENCH 100 psig
5006-5	051	BENCH 150 psig
5006-5	052	BENCH ZERO
5006-5	092	BENCH 1° ANGULATION
5006-5	093	BENCH 2° ANGULATION
5006-5	094	BENCH 3° ANGULATION
5006-5	095	BENCH ZERO
5006-5	145	BENCH SPR. RATE ZERO
5006-5	146	BENCH SPR. RATE 60#
5006-5	147	BENCH ZERO
5006-5	148	BENCH 50 psig
5006-5	149	BENCH 100 psig
5006-5	150	BENCH 150 psig
5006-5	151	BENCH ZERO
5006-5	152	SWEEP FLOW
5006-6	017	BENCH ZERO
5006-6	018	BENCH COMPRESSION .08"
5006-6	019	BENCH COMPRESSION .12"
5006-6	020	BENCH ZERO
5006-6	053	BENCH 50 psig
5006-6	054	BENCH 100 psig
5006-6	055	BENCH 150 psig
5006-6	056	BENCH ZERO
5006-6	096	BENCH 1° ANGULATION
5006-6	097	BENCH 2° ANGULATION
5006-6	098	BENCH 3° ANGULATION
5006-6	099	BENCH ZERO
5006-6	153	BENCH SPR. RATE ZERO
5006-6	154	BENCH SPR. RATE 20#
5006-6	155	BENCH SPR. RATE 40#
5006-6	156	BENCH SPR. RATE 60#
5006-6	157	BENCH ZERO
5006-6	158	BENCH 50 psig
5006-6	159	BENCH 100 psig
5006-6	160	BENCH 150 psig
5006-6	161	BENCH ZERO
5006-6	162	SWEEP FLOW

BELLOW	TEST NO.	TEST
5006-7	057	BENCH ZERO
5006-7	058	BENCH COMPRESSION .08"
5006-7	059	BENCH COMPRESSION .12"
5006-7	060	BENCH ZERO
5006-7	061	BENCH 50 psig
5006-7	062	BENCH 100 psig
5006-7	063	BENCH 150 psig
5006-7	064	BENCH ZERO
5006-7	100	BENCH 1^{o} ANGULATION
5006-7	101	BENCH 2^{o} ANGULATION
5006-7	102	BENCH 3^{o} ANGULATION
5006-7	103	BENCH ZERO
5006-7	163	BENCH SPR. RATE ZERO
5006-7	164	BENCH SPR. RATE 20#
5006-7	165	BENCH SPR. RATE 40#
5006-7	166	BENCH SPR. RATE 60#
5006-7	167	BENCH ZERO
5006-7	168	BENCH 50 psig
5006-7	169	BENCH 100 psig
5006-7	170	BENCH 150 psig
5006-7	171	BENCH ZERO
5006-7	172	SWEEP FLOW
5006-8	173	BENCH SPR. RATE ZERO
5006-8	174	BENCH SPR. RATE 20#
5006-8	175	BENCH SPR. RATE 40#
5006-8	176	BENCH SPR. RATE 60#
5006-8	177	BENCH ZERO
5006-8	178	BENCH 50 psig
5006-8	179	BENCH 100 psig
5006-8	180	BENCH 150 psig
5006-8	181	BENCH ZERO
5006-8	182	SWEEP FLOW
5006-8	645	BENCH SPRING RATE ZERO
5006-8	646	BENCH SPRING RATE 20#
5006-8	647	BENCH SPRING RATE 40#
5006-8	648	BENCH SPRING RATE 60#
5006-8	649 (RUN #13)	SWEEP FLOW
5006-8	650 (RUN #14)	SWEEP FLOW
5006-9	195	BENCH SPR. RATE ZERO
5006-9	196	BENCH SPR. RATE 20#
5006-9	197	BENCH SPR. RATE 40#
5006-9	198	BENCH SPR. RATE 60#
5006-9	199	BENCH ZERO
5006-9	200	BENCH 50 psig
5006-9	201	BENCH 100 psig
5006-9	202	BENCH 150 psig
5006-9	203	BENCH ZERO
5006-9	204	SWEEP FLOW
5006-9	651 (RUN #26)	SWEEP FLOW

BELLOW	TEST NO.	TEST
5006-10	205	BENCH SPR. RATE ZERO
5006-10	206	BENCH SPR. RATE 20#
5006-10	207	BENCH SPR. RATE 40#
5006-10	208	BENCH SPR. RATE 60#
5006-10	209	BENCH ZERO
5006-10	210	BENCH 50 psig
5006-10	211	BENCH 100 psig
5006-10	212	BENCH 150 psig
5006-10	213	BENCH ZERO
5006-10	214	SWEEP FLOW
5006-10	652 (RUN #25)	SWEEP FLOW
5006-10	653 (RUN #25)	STEADY FLOW - FAILURE
5009-1	481	BENCH SPR. RATE ZERO
5009-1	482	BENCH SPR. RATE 10#
5009-1	483	BENCH SPR. RATE 20#
5009-1	484	BENCH ZERO
5009-1	485	BENCH 20 psig
5009-1	486	BENCH 40 psig
5009-1	487	BENCH ZERO
5009-1	488	SWEEP FLOW
5009-1	489	STEADY FLOW - FAILURE
5011-1	490	BENCH SPR. RATE ZERO
5011-1	491	BENCH SPR. RATE 10#
5011-1	492	BENCH SPR. RATE 20#
5011-1	493	BENCH SPR. RATE 40#
5011-1	494	BENCH ZERO
5011-1	495	BENCH 30 psig
5011-1	496	BENCH 60 psig
5011-1	497	BENCH ZERO
5011-1	498	SWEEP FLOW
5011-1	499	STEADY FLOW - FAILURE
5012-1	416	BENCH SPR. RATE ZERO
5012-1	417	BENCH SPR. RATE 20#
5012-1	418	BENCH SPR. RATE 40#
5012-1	419	BENCH SPR. RATE 60#
5012-1	420	BENCH ZERO
5012-1	421	BENCH 50 psig
5012-1	422	BENCH 100 psig
5012-1	423	BENCH 150 psig
5012-1	424	BENCH ZERO
5012-1	425	SWEEP FLOW
5012-1	426	SWEEP FLOW COMPRESSED 23%
5012-1	427	SWEEP FLOW COMPRESSED 47%
5012-1	428	SWEEP FLOW COMPRESSED 70%
5012-1	429	SWEEP FLOW FACILITY CHECK-OUT
5012-1	456	SWEEP FLOW FACILITY CHECK-OUT

BELLOW	TEST NO.	TEST
5012-2	654	BENCH SPR. RATE ZERO
5012-2	655	BENCH SPR. RATE 20.3#
5012-2	656	BENCH SPR. RATE 40.3#
5012-2	657	BENCH SPR. RATE 60.3#
5012-2	658 (RUN #28)	SWEEP FLOW
5012-3	659	BENCH SPR. RATE ZERO
5012-3	660	BENCH SPR. RATE 20.3#
5012-3	661	BENCH SPR. RATE 40.3#
5012-3	662	BENCH SPR. RATE 60.3#
5012-3	663 (RUN #27)	SWEEP FLOW
5013-1	457	BENCH SPR. RATE ZERO
5013-1	458	BENCH SPR. RATE 10#
5013-1	459	BENCH SPR. RATE 20#
5013-1	460	BENCH TEST ZERO
5013-1	461	BENCH TEST 50 psig
5013-1	462	BENCH TEST 100 psig
5013-1	463	BENCH TEST 150 psig - FAILURE
5013-2	464	BENCH SPR. RATE ZERO
5013-2	465	BENCH SPR. RATE 10#
5013-2	466	BENCH SPR. RATE 20#
5013-2	467	BENCH ZERO
5013-2	468	BENCH 20 psig
5013-2	469	BENCH 40 psig
5013-2	470	BENCH ZERO
5013-2	471	SWEEP FLOW
5013-2	472	STEADY FLOW - FAILURE
5013-3	473	BENCH SPR. RATE ZERO
5013-3	474	BENCH SPR. RATE 10#
5013-3	475	BENCH SPR. RATE 20#
5013-3	476	BENCH ZERO
5013-3	477	BENCH 20 psig
5013-3	478	BENCH 40 psig
5013-3	379	BENCH ZERO
5013-3	480	STEADY FLOW - FAILURE

BELLOW	TEST NO.	TEST
5028-1	215	BENCH SPR. RATE ZERO
5028-1	216	BENCH SPR. RATE 20#
5028-1	217	BENCH SPR. RATE 40#
5028-1	218	BENCH SPR. RATE 60#
5028-1	219	BENCH ZERO
5028-1	220	BENCH 50 psig
5028-1	221	BENCH 100 psig
5028-1	222	BENCH 150 psig
5028-1	223	BENCH ZERO
5028-1	224	SWEEP FLOW
5028-1	225	SWEEP FLOW
5028-1	226	SWEEP FLOW
5028-1	227	STEADY FLOW - FAILURE
5028-2	228	BENCH SPR. RATE ZERO
5028-2	229	BENCH SPR. RATE 20#
5028-2	230	BENCH SPR. RATE 40#
5028-2	231	BENCH SPR. RATE 60#
5028-2	232	BENCH ZERO
5028-2	233	BENCH 50 psig
5028-2	234	BENCH 100 psig
5028-2	235	BENCH 150 psig
5028-2	236	BENCH ZERO
5028-2	237	SWEEP FLOW
5028-2	238	STEADY FLOW - FAILURE
5034-1	316	BENCH SPR. RATE ZERO
5034-1	317	BENCH SPR. RATE 20#
5034-1	318	BENCH SPR. RATE 40#
5034-1	319	BENCH SPR. RATE 60#
5034-1	325	BENCH ZERO
5034-1	326	BENCH 50 psig
5034-1	327	BENCH 100 psig
5034-1	328	BENCH 150 psig
5034-1	329	BENCH ZERO
5034-1	330	SWEEP FLOW
5034-1	331	SWEEP FLOW COMPRESSED 16%
5034-1	332	SWEEP FLOW COMPRESSED 33%
5034-1	333	SWEEP FLOW COMPRESSED 48%
5034-1	334	STEADY FLOW COMPRESSED 48% - FAILURE

BELLOW	TEST NO.	TEST
5034-2	335	BENCH SPR. RATE ZERO
5034-2	336	BENCH SPR. RATE 20#
5034-2	337	BENCH SPR. RATE 40#
5034-2	338	BENCH SPR. RATE 60#
5034-2	339	BENCH ZERO
5034-2	340	BENCH 50 psig
5034-2	341	BENCH 100 psig
5034-2	342	BENCH 150 psig
5034-2	343	BENCH ZERO
5034-2	344	STEADY FLOW - FAILURE
5034-3	345	BENCH SPR. RATE ZERO
5034-3	346	BENCH SPR. RATE 20#
5034-3	347	BENCH SPR. RATE 40#
5034-3	348	BENCH SPR. RATE 60#
5034-3	349	BENCH ZERO
5034-3	350	BENCH 50 psig
5034-3	351	BENCH 100 psig
5034-3	352	BENCH 150 psig
5034-3	353	BENCH ZERO
5034-3	354	STEADY FLOW COMPRESSED 30%
5034-3	355	STEADY FLOW COMPRESSED 30% - FAILURE
5034-4	356	BENCH SPR. RATE ZERO
5034-4	357	BENCH SPR. RATE 20#
5034-4	358	BENCH SPR. RATE 40#
5034-4	359	BENCH SPR. RATE 60#
5034-4	360	BENCH ZERO
5034-4	361	BENCH 50 psig
5034-4	362	BENCH 100 psig
5034-4	363	BENCH 150 psig
5034-4	364	BENCH ZERO
5034-4	365	STEADY FLOW COMPRESSED 17%
5034-5	381	BENCH SPR. RATE ZERO
5034-5	382	BENCH SPR. RATE 20#
5034-5	383	BENCH SPR. RATE 40#
5034-5	384	BENCH SPR. RATE 60#
5034-5	385	BENCH ZERO
5034-5	386	BENCH 50 psig
5034-5	387	BENCH 100 psig
5034-5	388	BENCH 150 psig
5034-5	389	BENCH ZERO
5034-5	390	STEADY FLOW EXTENDED 11% - FAILURE

BELLOW	TEST NO.	TEST
5034-6	391	BENCH SPR. RATE ZERO
5034-6	392	BENCH SPR. RATE 20#
5034-6	393	BENCH SPR. RATE 40#
5034-6	394	BENCH SPR. RATE 60#
5034-6	395	BENCH ZERO
5034-6	396	BENCH 50 psig
5034-6	397	BENCH 100 psig
5034-6	398	BENCH 150 psig
5034-6	399	BENCH ZERO
5034-6	400	STEADY FLOW EXTENDED 26% - FAILURE
5034-7	401	BENCH SPR. RATE ZERO
5034-7	402	BENCH SPR. RATE 20#
5034-7	403	BENCH SPR. RATE 40#
5034-7	404	BENCH SPR. RATE 60#
5034-7	405	BENCH ZERO
5034-7	406	BENCH 50 psig
5034-7	407	BENCH 100 psig
5034-7	408	BENCH 150 psig
5034-7	409	BENCH ZERO
5034-7	410	SWEEP FLOW
5034-7	411	SWEEP FLOW EXTENDED 23%
5034-7	412	SWEEP FLOW EXTENDED 47%
5034-7	413	SWEEP FLOW COMPRESSED 24%
5034-7	414	SWEEP FLOW COMPRESSED 47%
5034-7	415	STEADY FLOW COMPRESSED 71% - FAILURE
5034-8	515	BENCH SPR. RATE ZERO
5034-8	516	BENCH SPR. RATE 20#
5034-8	517	BENCH SPR. RATE 40#
5034-8	518	BENCH SPR. RATE 60#
5034-8	519	BENCH ZERO
5034-8	520	BENCH 50 psig
5034-8	521	BENCH 100 psig
5034-8	522	BENCH 150 psig
5034-8	523	BENCH ZERO
5034-8	524	STEADY FLOW - FAILURE
5034-9	525	BENCH SPR. RATE ZERO
5034-9	526	BENCH SPR. RATE 20#
5034-9	527	BENCH SPR. RATE 40#
5034-9	528	BENCH SPR. RATE 60#
5034-9	529	BENCH ZERO
5034-9	530	BENCH 50 psig
5034-9	531	BENCH 100 psig
5034-9	532	BENCH 150 psig
5034-9	533	BENCH ZERO
5034-9	534	SWEEP FLOW
5034-9	535	SWEEP FLOW EXTENDED 24%
5034-9	536	SWEEP FLOW
5034-9	537	SWEEP FLOW EXTENDED 24%

BELLOW	TEST NO.	TEST
5034-10	608	BENCH SPR. RATE ZERO
5034-10	609	BENCH SPR. RATE 20#
5034-10	610	BENCH SPR. RATE 40#
5034-10	611	BENCH SPR. RATE 60#
5034-10	612 (RUN #23)	SWEEP FLOW
5034-10	613 (RUN #23A)	STEADY FLOW - FAILURE
5034-11	614	BENCH SPR. RATE ZERO
5034-11	615	BENCH SPR. RATE 20#
5034-11	616	BENCH SPR. RATE 40#
5034-11	617	BENCH SPR. RATE 60#
5034-11	618 (RUN #22)	SWEEP FLOW
5034-11	619 (RUN #22A)	STEADY FLOW
5034-12	620	BENCH SPR. RATE ZERO
5034-12	621	BENCH SPR. RATE 20#
5034-12	622	BENCH SPR. RATE 40#
5034-12	623	BENCH SPR. RATE 60#
5034-12	624 (RUN #18)	SWEEP FLOW
5034-12	625 (RUN #19)	STEADY FLOW
5034-13	626	BENCH SPR. RATE ZERO
5034-13	627	BENCH SPR. RATE 20#
5034-13	628	BENCH SPR. RATE 40#
5034-13	629	BENCH SPR. RATE 60#
5034-13	630 (RUN #15)	SWEEP FLOW
5034-13	631 (RUN #16)	STEADY FLOW
5034-13	632 (RUN #17)	STEADY FLOW - FAILURE
5034-14	633	BENCH SPR. RATE ZERO
5034-14	634	BENCH SPR. RATE 20#
5034-14	635	BENCH SPR. RATE 40#
5034-14	636	BENCH SPR. RATE 60#
5034-14	637 (RUN #20)	SWEEP FLOW
5034-14	638 (RUN #21)	STEADY FLOW
5034-15	639	BENCH SPR. RATE ZERO
5034-15	640	BENCH SPR. RATE 20#
5034-15	641	BENCH SPR. RATE 40#
5034-15	642	BENCH SPR. RATE 60#
5034-15	643 (RUN #24)	SWEEP FLOW
5034-15	644 (RUN #24)	STEADY FLOW - FAILURE

BELLOW	TEST NO.	TEST
ANTI-GEYSER #1	538	BENCH ZERO
ANTI-GEYSER #1	539	BENCH 50 psig
ANTI-GEYSER #1	540	BENCH 100 psig
ANTI-GEYSER #1	541	BENCH 150 psig
ANTI-GEYSER #1	542	BENCH ZERO
ANTI-GEYSER #1	543	STEADY FLOW - FAILURE
ANTI-GEYSER #2	544	BENCH ZERO
ANTI-GEYSER #2	545	BENCH 50 psig
ANTI-GEYSER #2	546	BENCH 100 psig
ANTI-GEYSER #2	547	BENCH 150 psig
ANTI-GEYSER #2	548	BENCH ZERO
ANTI-GEYSER #2	549	STEADY FLOW
ANTI-GEYSER #2	550	STEADY FLOW
ANTI-GEYSER #2	551	STEADY FLOW - FAILURE
ANTI-GEYSER #3	552	BENCH ZERO
ANTI-GEYSER #3	553	BENCH 50 psig
ANTI-GEYSER #3	554	BENCH 100 psig
ANTI-GEYSER #3	555	BENCH 150 psig
ANTI-GEYSER #3	556	BENCH ZERO
ANTI-GEYSER #3	557	STEADY FLOW
ANTI-GEYSER #3	558	STEADY FLOW - FAILURE
5035-1	369	BENCH SPR. RATE ZERO
5035-1	370	BENCH SPR. RATE 10#
5035-1	371	BENCH SPR. RATE 20#
5035-1	372	BENCH SPR. RATE 40#
5035-1	373	BENCH SPR. RATE 60#
5035-1	374	BENCH SPR. RATE 70#
5035-1	375	BENCH ZERO
5035-1	376	BENCH 50 psig
5035-1	377	BENCH 100 psig
5035-1	378	BENCH 150 psig
5035-1	379	BENCH ZERO
5035-1	380	STEADY FLOW - FAILURE

BELLOW	TEST NO.	TEST
5035-2	430	BENCH SPR. RATE ZERO
5035-2	431	BENCH SPR. RATE 20#
5035-2	432	BENCH SPR. RATE 40#
5035-2	433	BENCH SPR. RATE 60#
5035-2	434	BENCH SPR. RATE 70#
5035-2	435	BENCH ZERO
5035-2	436	BENCH 50 psig
5035-2	437	BENCH 100 psig
5035-2	438	BENCH 150 psig
5035-2	439	BENCH ZERO
5035-2	440	SWEEP FLOW
5035-2	441	STEADY FLOW
5035-2	442	STEADY FLOW - FAILURE
5035-3	443	BENCH SPR. RATE ZERO
5035-3	444	BENCH SPR. RATE 20#
5035-3	445	BENCH SPR. RATE 40#
5035-3	446	BENCH SPR. RATE 60#
5035-3	447	BENCH SPR. RATE 70#
5035-3	448	BENCH ZERO
5035-3	449	BENCH 50 psig
5035-3	450	BENCH 100 psig
5035-3	451	BENCH 150 psig
5035-3	452	BENCH ZERO
5035-3	453	SWEEP FLOW
5035-3	454	STEADY FLOW COMPRESSED 38%
5035-3	455	STEADY FLOW COMPRESSED 38%
5035-4	566	BENCH SPR. RATE ZERO
5035-4	567	BENCH SPR. RATE 20#
5035-4	568	BENCH SPR. RATE 40#
5035-4	569	BENCH SPR. RATE 60#
5035-4	570	BENCH SPR. RATE 70#
5035-4	571 (RUN #3)	SWEEP FLOW
5035-4	572 (RUN #4)	STEADY FLOW
5035-5	500	BENCH SPR. RATE ZERO
5035-5	501	BENCH SPR. RATE 20#
5035-5	502	BENCH SPR. RATE 40#
5035-5	503	BENCH SRR. RATE 60#
5035-5	504	BENCH SPR. RATE 70#
5035-5	505	BENCH ZERO
5035-5	506	BENCH 50 psig
5035-5	507	BENCH 100 psig
5035-5	508	BENCH 150 psig
5035-5	509	BENCH ZERO
5035-5	510	SWEEP FLOW
5035-5	511	STEADY FLOW COMPRESSED 38%
5035-5	512	STEADY FLOW COMPRESSED 38%
5035-5	513	STEADY FLOW COMPRESSED 38%
5035-5	514	STEADY FLOW COMPRESSED 38%

BELLOW	TEST NO.	TEST
5035-6	573	BENCH SPR. RATE ZERO
5035-6	574	BENCH SPR. RATE 20#
5035-6	575	BENCH SPR. RATE 40#
5035-6	576	BENCH SPR. RATE 60#
5035-6	577	BENCH SPR. RATE 70#
5035-6	578 (RUN #1)	SWEEP FLOW
5035-6	579 (RUN #2)	STEADY FLOW
5035-7	580	BENCH SPR. RATE ZERO
5035-7	581	BENCH SPR. RATE 20#
5035-7	582	BENCH SPR. RATE 40#
5035-7	583	BENCH SPR. RATE 60#
5035-7	584	BENCH SPR. RATE 70#
5035-7	585 (RUN #7)	SWEEP FLOW
5035-7	586 (RUN #8)	STEADY FLOW
5035-8	587	BENCH SPR. RATE ZERO
5035-8	588	BENCH SPR. RATE 20#
5035-8	589	BENCH SPR. RATE 40#
5035-8	590	BENCH SPR. RATE 60#
5035-8	591	BENCH SPR. RATE 70#
5035-8	592 (RUN #5)	SWEEP FLOW
5035-8	593 (RUN #6)	STEADY FLOW
5035-9	594	BENCH SPR. RATE ZERO
5035-9	595	BENCH SPR. RATE 20#
5035-9	596	BENCH SPR. RATE 40#
5035-9	597	BENCH SPR. RATE 60#
5035-9	598	BENCH SPR. RATE 70#
5035-9	599 (RUN #11)	SWEEP FLOW
5035-9	600 (RUN #12)	SWEEP FLOW
5035-10	601	BENCH SPR. RATE ZERO
5035-10	602	BENCH SPR. RATE 20#
5035-10	603	BENCH SPR. RATE 40#
5035-10	604	BENCH SPR. RATE 60#
5035-10	605	BENCH SPR. RATE 70#
5035-10	606(RUN #9)	SWEEP FLOW
5035-10	607(RUN #10)	STEADY FLOW

BELLOW FLOW TESTS CONDUCTED ON THE
ORIGINAL MSFC TEST FACILITY (FIGURE 25)

BELLOW	TEST NO.	POSITION NO.	L/D	ELBOW UPSTREAM
5002-1	274	5	10.17	90°
	275	5	10.17	90°
	276	4	8.17	90°
	277	4	8.17	90°
	278	4	8.17	90°
5002-2	248	6	28.3	90°
	249	6	28.3	90°
	250	6	28.3	90°
	251	6	28.3	90°
	252	6	28.3	90°
	253	6	28.3	90°
5002-3	263	6	28.3	90°
	264	6	28.3	90°
5002-4	288	3	6.17	90°
	289	3	6.17	90°
	290	1	2.17	90°
5002-5	300	1	2.17	90°
	301	1	2.17	90°
	312	6	28.3	90°
5002-6	311	6	28.3	90°
5005-2	117	6	20.45	90°
5006-1	125	6	20.45	90°
	126	1	1.5	90°
5006-2	134	1	1.5	90°
	135	1	1.5	90°
5006-3	183	1	1.5	90°
	184	1	1.5	90°
5006-4	194	1	1.5	90°
5006-5	152	1	1.5	90°
5006-6	162	1	1.5	90°
5006-7	172	1	1.5	90°
5006-8	182	1	1.5	90°
5006-9	204	1	1.5	90°
5006-10	214	1	1.5	90°
5028-1	224	1	1.813	90°
	225	2	3.81	90°
	226	5	9.81	90°
	227	2	3.81	90°
5028-2	237	2	3.81	90°
	238	1	1.813	90°

BELLOW FLOW TESTS CONDUCTED ON THE
MODIFIED MSFC TEST FACILITY (FIG. 27)

BELLOWS	TEST NO.
5005-1	564
	565
5006-1	366
	367
	368
5009-1	488
	489
5011-1	498
	499
5012-1	425
	426
	427
	428
5013-2	471
	472
5013-3	480

BELLOWS	TEST NO.
5034-1	330
	331
	332
	333
	334
5034-2	344
5034-3	354
	355
5034-4	365
5034-5	390
5034-6	400
5034-7	410
	411
	412
	413
	414
	415
5034-8	524

BELLOWS	TEST NO.
5034-9	534
	535
	536
	537
AG#1	543
AG#2	549
	550
	551
AG#3	557
	558
5035-1	380
5035-2	440
	441
	442
5035-3	454
	455
5035-5	510
	511
	512
	513
	514

BELLOW FLOW TESTS CONDUCTED AT THE WYLE LABORATORY
TEST FACILITY (FIGURE 28)

BELLOWS	TEST NO.
5006-8	649
	650
5006-9	651
5006-10	652
	653
5012-2	658
5012-3	663
5034-10	612
	613

BELLOWS	TEST NO.
5034-11	618
	619
5034-12	624
	625
5034-13	630
	631
	632
5034-14	637
	638
5034-15	643
	644

BELLOWS	TEST NO.
5035-4	571
	572
5035-6	578
	579
5035-7	585
	586
5035-8	592
	593
5035-9	599
	600
5035-10	606
	607

APPENDIX C

SPRING RATE DATA

BELLOWS NO.	VENDOR K_a (LB/IN)	TEST K_a (LB/IN)	THEO. K_{a1} VENDOR GEOM. (LB/IN)	% ERROR	THEC. K_{a1} MEAS. GEOM. (LB/IN)	% ERROR	THEO. K_{a2} MEAS. GEOM. (LB/IN)	% ERROR
5002-1	167	230	181	21.3	204	11.3	267	16.1
5002-2	167	243	181	25.5	204	16.0	267	9.9
5002-3	167	198	181	8.6	204	3.0	267	34.9
5002-4	167	212	181	14.6	204	3.8	267	25.9
5002-5	167	220	181	17.7	204	7.3	267	21.3
5002-6	167	244	181	25.8	204	16.4	267	9.4
5005-1	50-80	-	28.1	-	32.8	-	42.9	-
5005-2	50-80	-	28.1	-	32.8	-	42.9	-
5006-1	560	773	572	26.0	788	1.9	898	16.2
5006-2	560	786	572	27.2	788	.3	898	14.2
5006-3	560	759	572	24.6	788	3.8	898	18.3
5006-4	560	822	572	30.4	788	4.1	898	9.2
5006-5	560	717	572	20.2	788	9.9	898	25.2
5006-6	560	774	572	26.1	788	1.8	898	16.0
5006-7	560	829	572	31.0	788	4.9	898	8.3
5006-8	560	747	572	23.4	788	5.5	898	20.2
5006-9	560	775	572	26.2	788	1.7	898	15.9
5006-10	560	804	572	28.9	788	2.0	898	11.7
5009-1	63	72.5	63.4	12.6	77.9	7.4	92.4	27.4
5011-1	290	239	290	21.3	265	10.9	314	31.4
5012-1	310	342	264	22.8	317	7.3	368	7.6
5012-2	310	380	264	30.5	317	16.6	368	3.2
5012-3	310	366	264	27.9	317	13.4	368	.5
5013-1	140	90.6	43.7	51.8	103	13.7	122	34.7
5013-2	140	91	43.7	52.0	103	13.2	122	34.1
5013-3	140	88.7	43.7	50.7	103	16.1	122	37.5
5028-1	344-464	540	496	8.2	514	4.8	610	13.0
5028-2	344-464	605	496	18.0	514	15.0	610	.8

THEORETICAL $K_{a1} \approx D_m E \frac{N_p}{N_c} \left(\frac{t}{h}\right)^3$ (Simplified Method) (5)

THEORETICAL $K_{a2} = \frac{.5754}{\zeta_{zv}} D_m E \frac{N_p}{N_c} \left(\frac{t}{h}\right)^3$ (Salzmann Method)

BELLOWS NO.	VENDOR K_a (LB/IN)	TEST K_a (LB/IN)	THEO. K_{a1} VENDOR GEOM. (LB/IN)	% ERROR	THEO. K_{a1} MEAS. GEOM. (LB/IN)	% ERROR	THEO. K_{a2} MEAS. GEOM. (LB/IN)	% ERROR
5034–1	1120–1680	1201	1070	10.9	1455	21.1	1642	36.7
5034–2	1120–1680	1221	1070	12.4	1455	19.2	1642	34.5
5034–3	1120–1680	1239	1070	13.6	1455	17.4	1642	32.5
5034–4	1120–1680	1272	1070	15.9	1455	14.4	1642	29.1
5034–5	1120–1680	1298	1070	17.6	1455	12.1	1642	26.5
5034–6	1120–1680	1246	1070	14.1	1455	16.8	1642	31.8
5034–7	1120–1680	1339	1070	20.1	1455	8.7	1642	22.6
5034–8	1120–1680	1084	1070	1.3	1455	34.2	1642	51.5
5034–9	1120–1680	1297	1070	17.5	1455	12.2	1642	26.6
5034–10	1120–1680	1329	1070	19.5	1455	9.5	1642	23.6
5034–11	1120–1680	1342	1070	20.3	1455	8.4	1642	22.4
5034–12	1120–1680	1355	1070	21.0	1455	7.4	1642	21.2
5034–13	1120–1680	1435	070	25.4	1455	1.4	1642	14.4
5034–14	1120–1680	1272	1070	15.9	1455	14.4	1642	26.6
5034–15	1120–1680	1292	1070	17.2	1455	12.6	1642	27.1
AG #1	1120–1680	–	1070	–	1455	–	1642	–
AG #2	1120–1680	–	1070	–	1455	–	1642	–
AG #3	1120–1680	–	1070	–	1455	–	1642	–
5035–1	1004	1325	1188	10.3	1247	5.9	1464	10.4
5035–2	1004	1307	1188	9.1	1247	4.6	1464	12.0
5035–3	1004	1323	1188	10.2	1247	5.7	1464	10.7
5034–4	1004	1376	1188	13.7	1247	9.4	1464	6.3
5035–5	1004	1375	1188	13.6	1247	9.3	1464	6.5
5035–6	1004	1419	1188	16.3	1247	12.1	1464	3.2
5035–7	1004	1469	1188	19.1	1247	15.1	1464	.3
5035–8	1004	1353	1188	12.2	1247	7.8	1464	8.2
5035–9	1004	1389	1188	14.5	1247	10.2	1464	5.4
5035–10	1004	1329	1188	10.6	1247	6.0	1464	10.2

THEORETICAL $K_{a1} \approx D_m E \frac{N_p}{N_c} \left(\frac{t}{h}\right)^3$ (Simplified Method) (5)

THEORETICAL $K_{a2} = \frac{.5754}{\zeta_{IV}} D_m E \frac{N_p}{N_c} \left(\frac{t}{h}\right)^3$ (Salzmann Method)

APPENDIX D

VELOCITY BAR GRAPHS FOR MSFC BELLOWS FLOW TESTS

● ACTUAL 1ST RESONANCE

▷ MAXIMUM FLOW (NO RESONANCE)

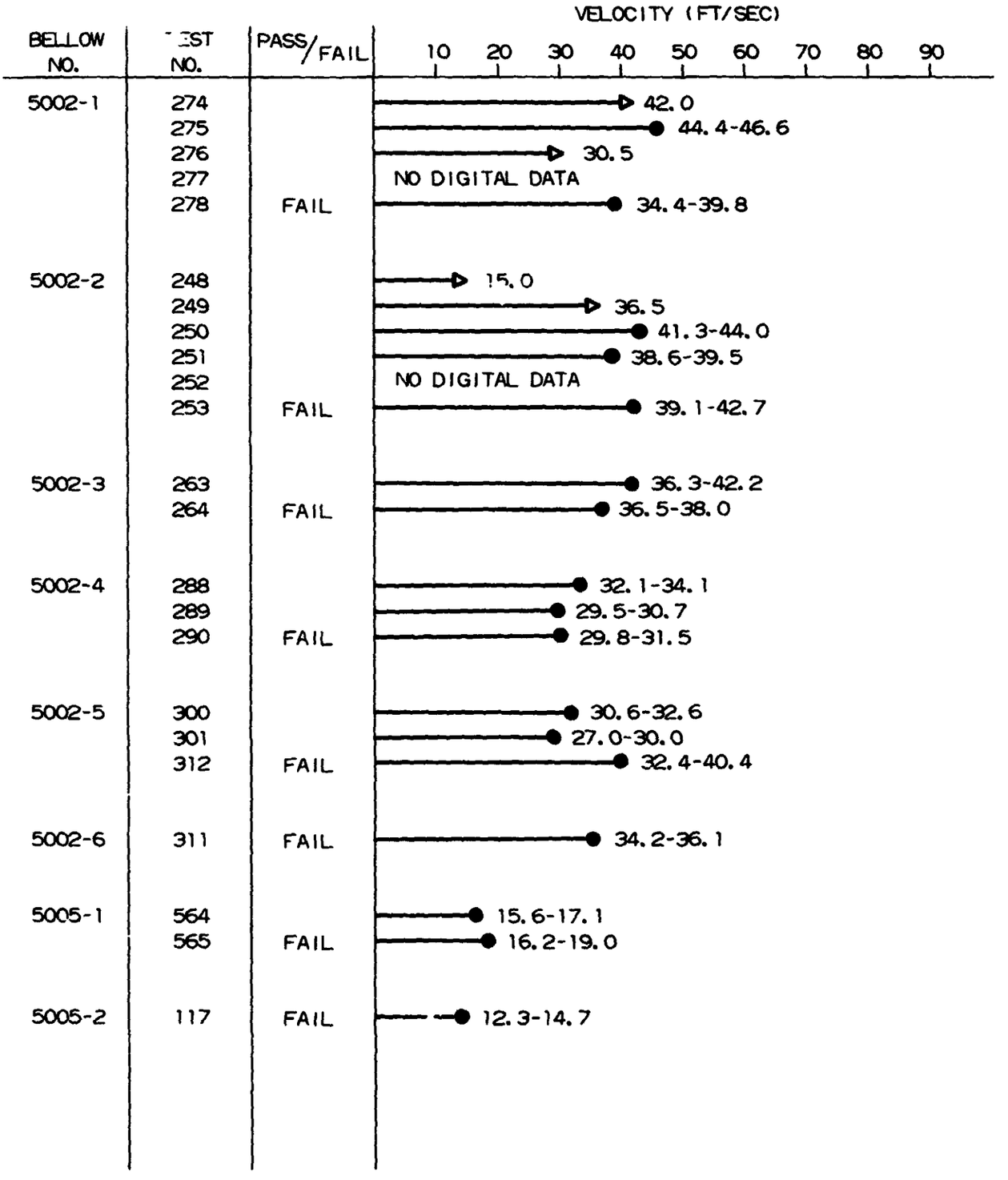

BELLOW NO.	TEST NO.	PASS/FAIL	
5002-1	274		42.0
	275		44.4-46.6
	276		30.5
	277		NO DIGITAL DATA
	278	FAIL	34.4-39.8
5002-2	248		15.0
	249		36.5
	250		41.3-44.0
	251		38.6-39.5
	252		NO DIGITAL DATA
	253	FAIL	39.1-42.7
5002-3	263		36.3-42.2
	264	FAIL	36.5-38.0
5002-4	288		32.1-34.1
	289		29.5-30.7
	290	FAIL	29.8-31.5
5002-5	300		30.6-32.6
	301		27.0-30.0
	312	FAIL	32.4-40.4
5002-6	311	FAIL	34.2-36.1
5005-1	564		15.6-17.1
	565	FAIL	16.2-19.0
5005-2	117	FAIL	12.3-14.7

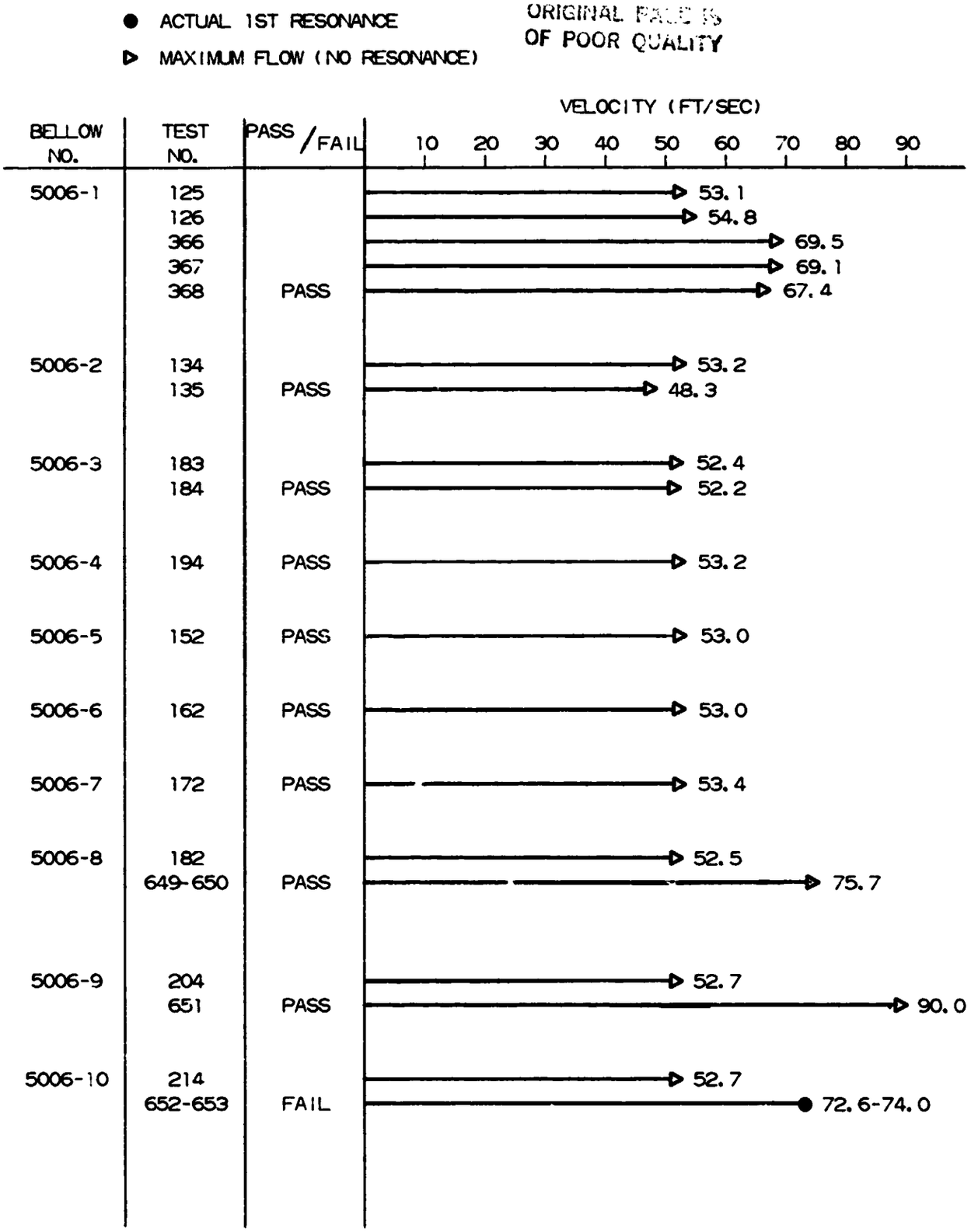

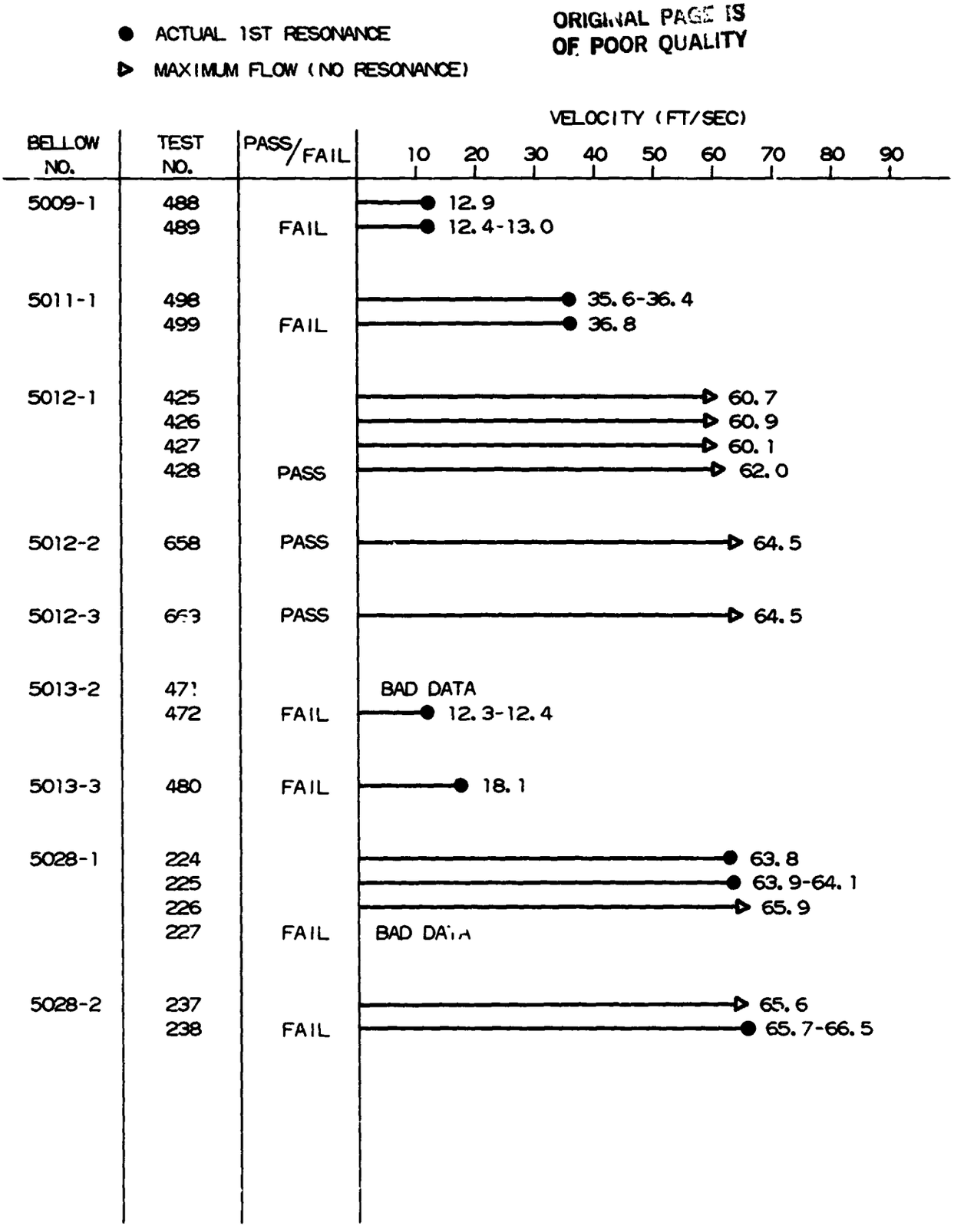

● ACTUAL 1ST RESONANCE

▷ MAXIMUM FLOW (NO RESONANCE)

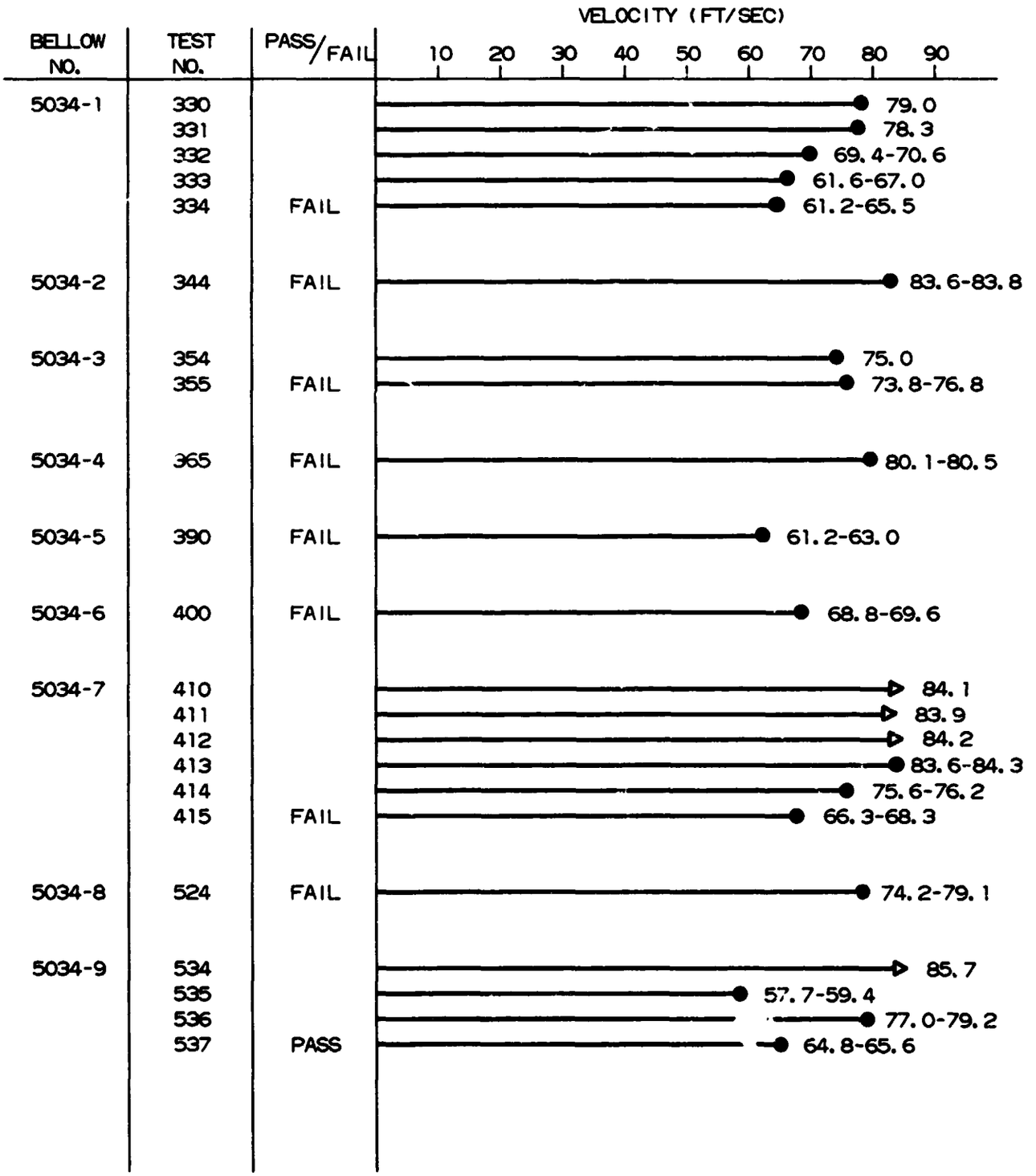

● ACTUAL 1ST RESONANCE

▷ MAXIMUM FLOW (NO RESONANCE)

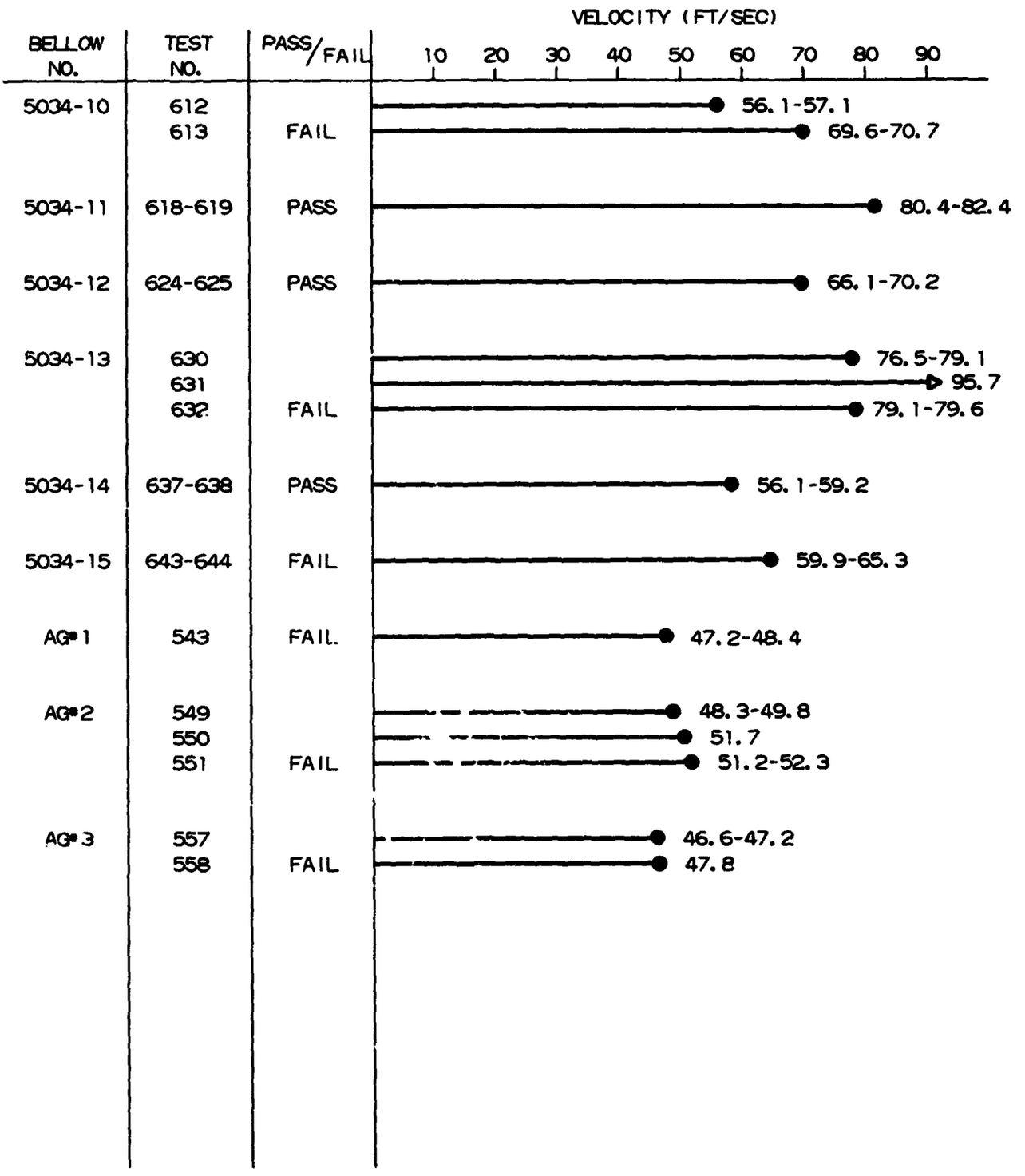

● ACTUAL 1ST RESONANCE

▷ MAXIMUM FLOW (NO RESONANCE)

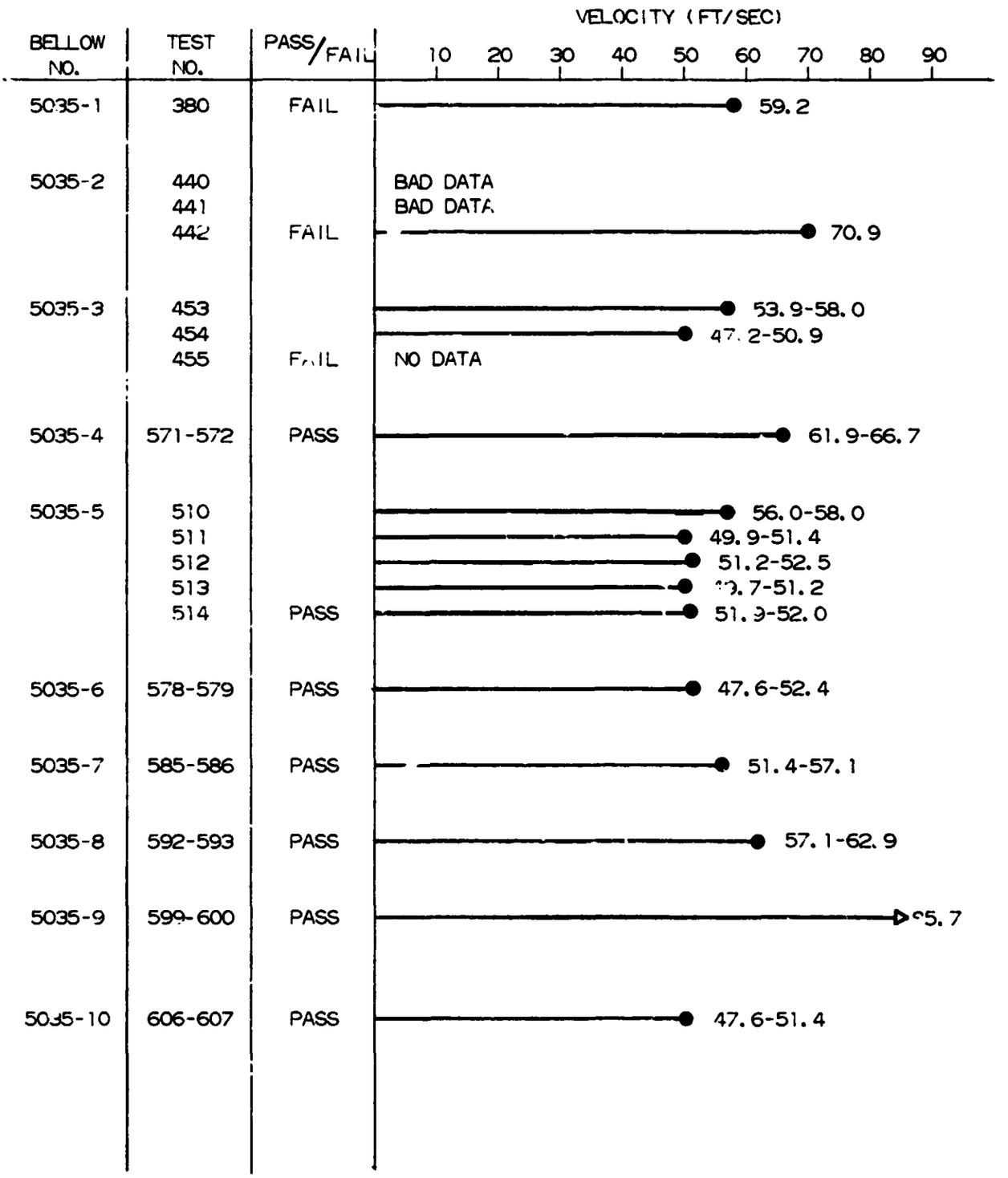

BELLOW NO.	TEST NO.	PASS/FAIL	
5035-1	380	FAIL	59.2
5035-2	440		BAD DATA
	441		BAD DATA
	442	FAIL	70.9
5035-3	453		53.9-58.0
	454		47.2-50.9
	455	FAIL	NO DATA
5035-4	571-572	PASS	61.9-66.7
5035-5	510		56.0-58.0
	511		49.9-51.4
	512		51.2-52.5
	513		49.7-51.2
	514	PASS	51.9-52.0
5035-6	578-579	PASS	47.6-52.4
5035-7	585-586	PASS	51.4-57.1
5035-8	592-593	PASS	57.1-62.9
5035-9	599-600	PASS	▷95.7
5035-10	606-607	PASS	47.6-51.4

APPENDIX E

VELOCITY VERSUS TIME PLOTS FOR MSFC BELLOWS FLOW TESTS

ORIGINAL PAGE IS
OF POOR QUALITY

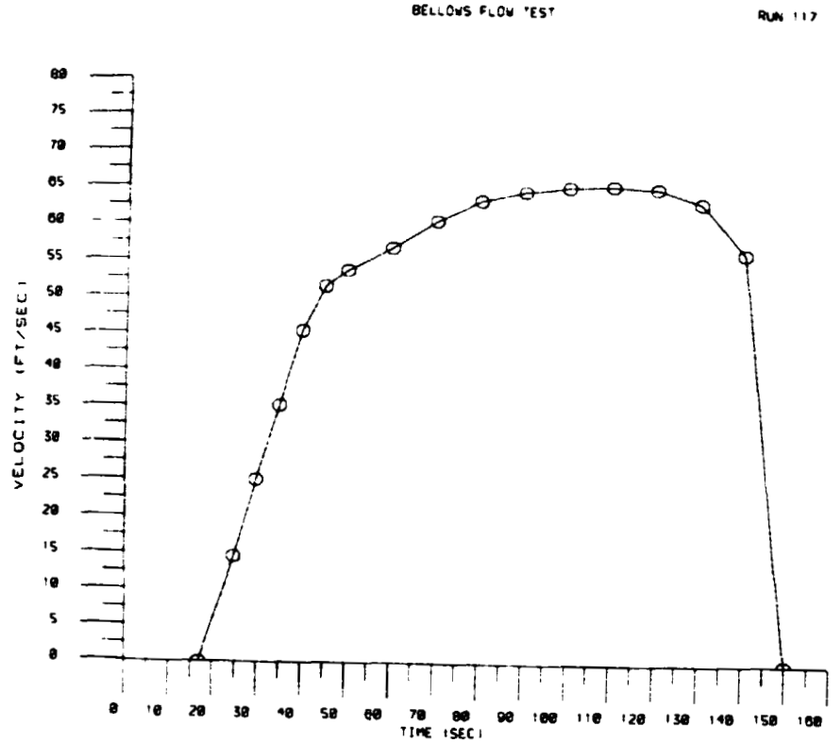

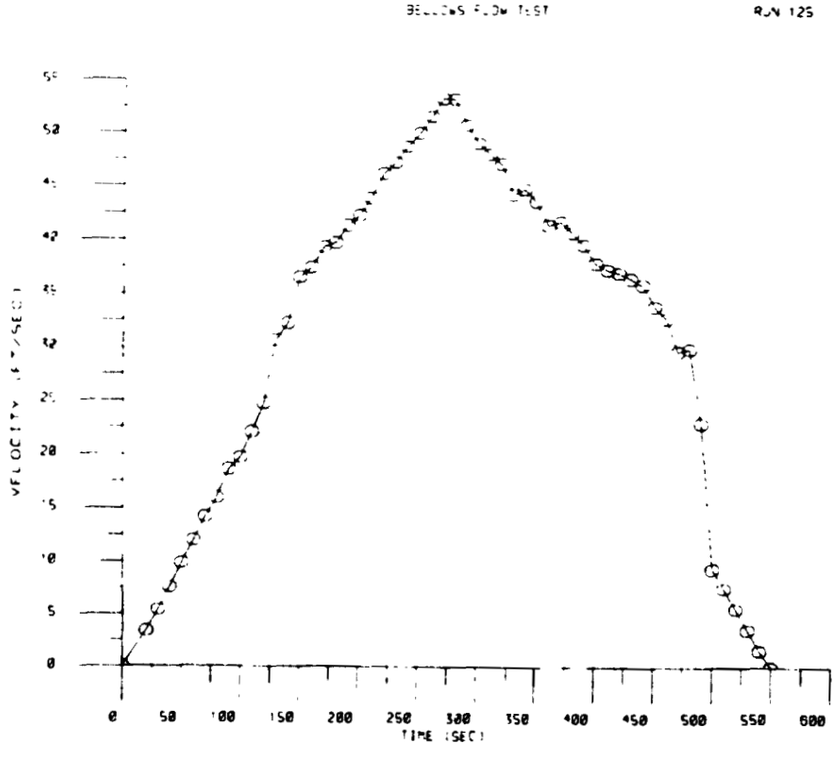

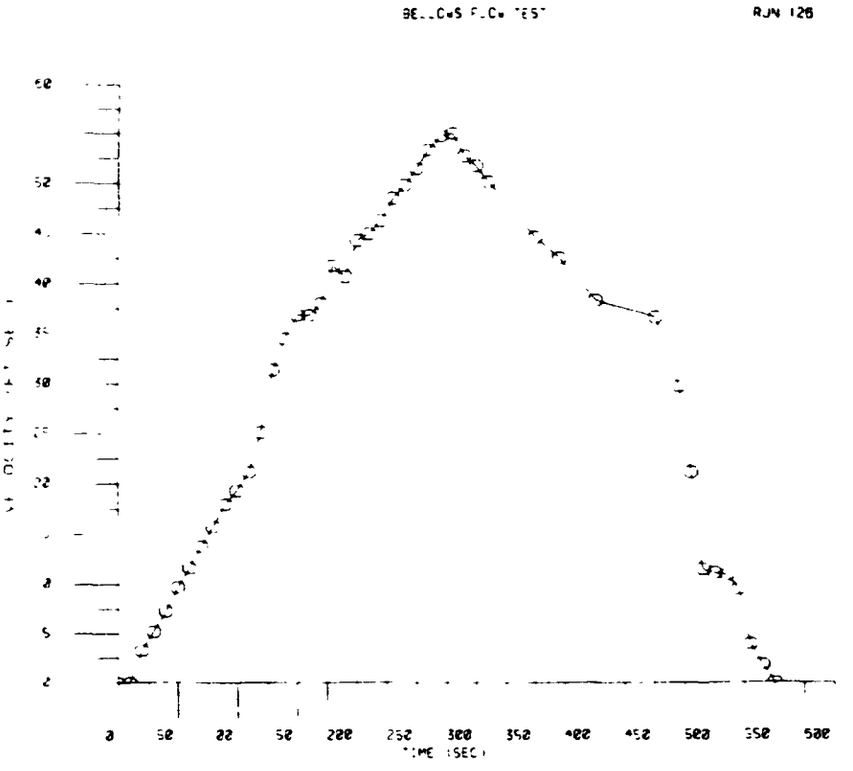

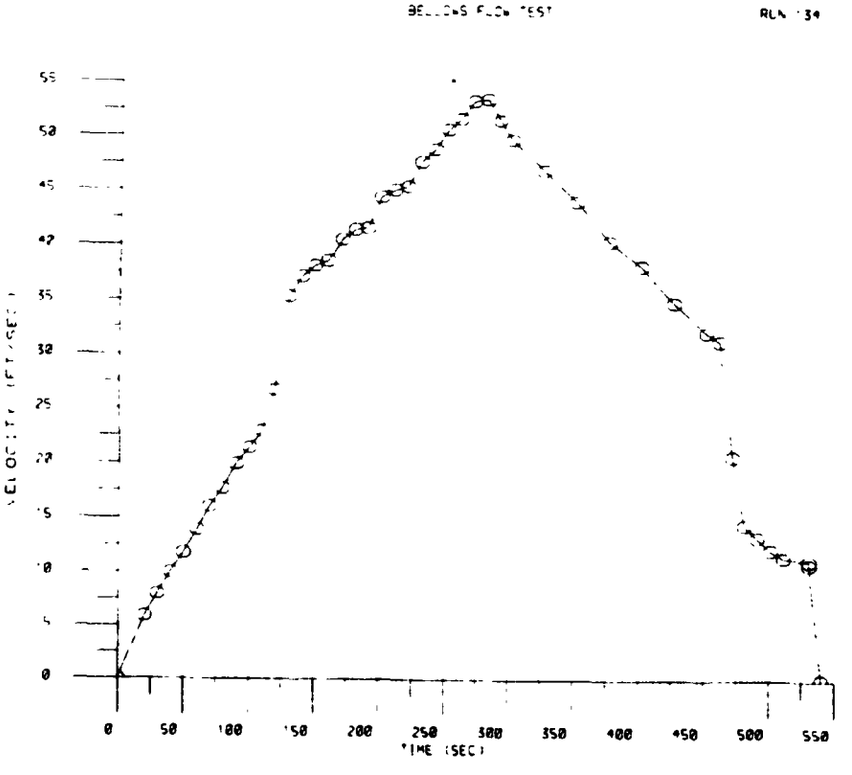

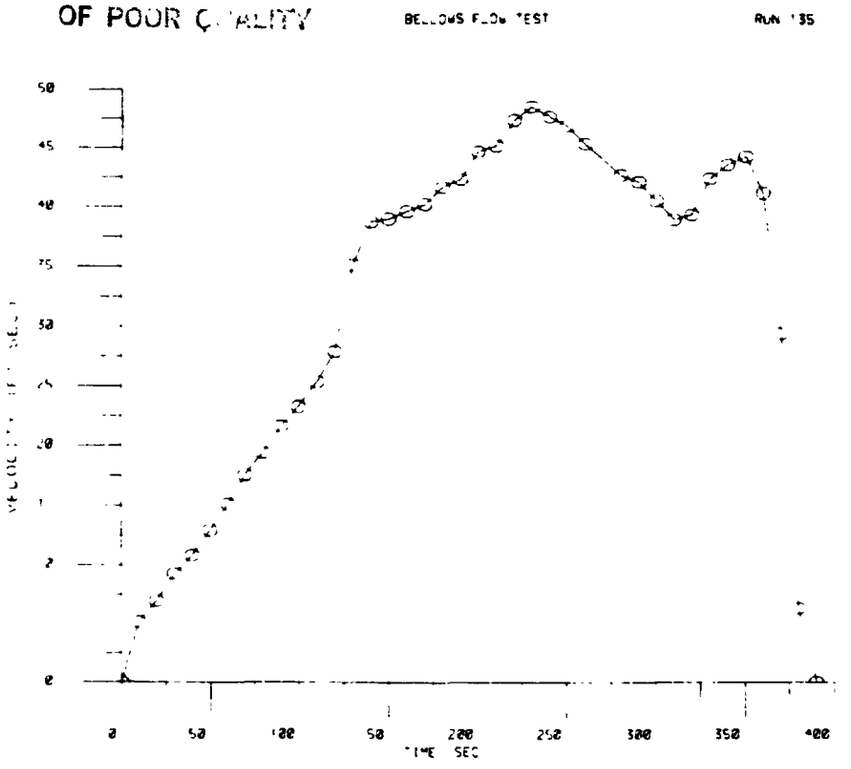

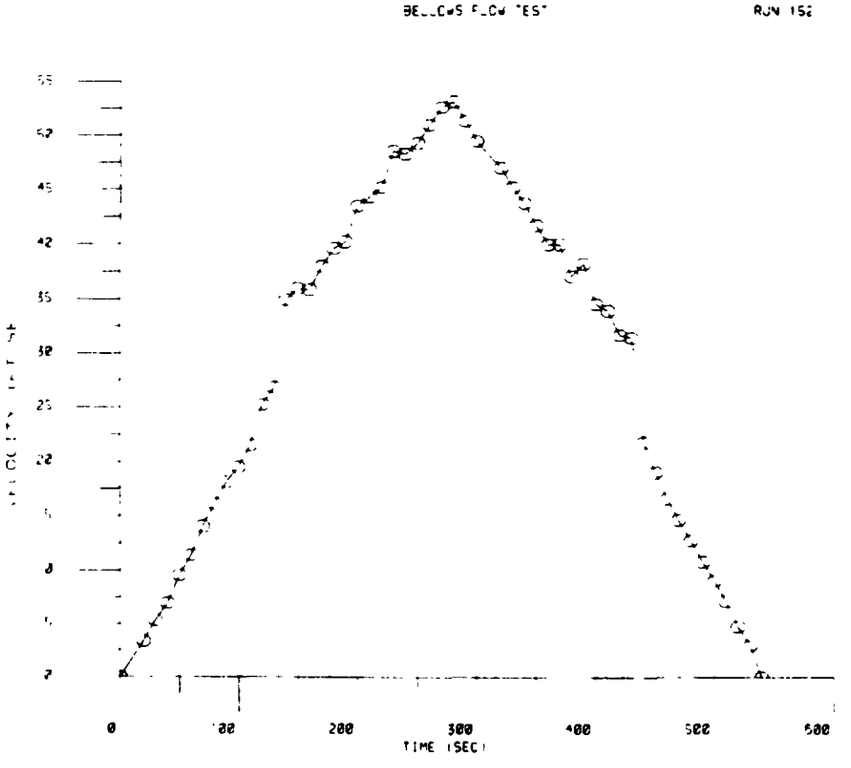

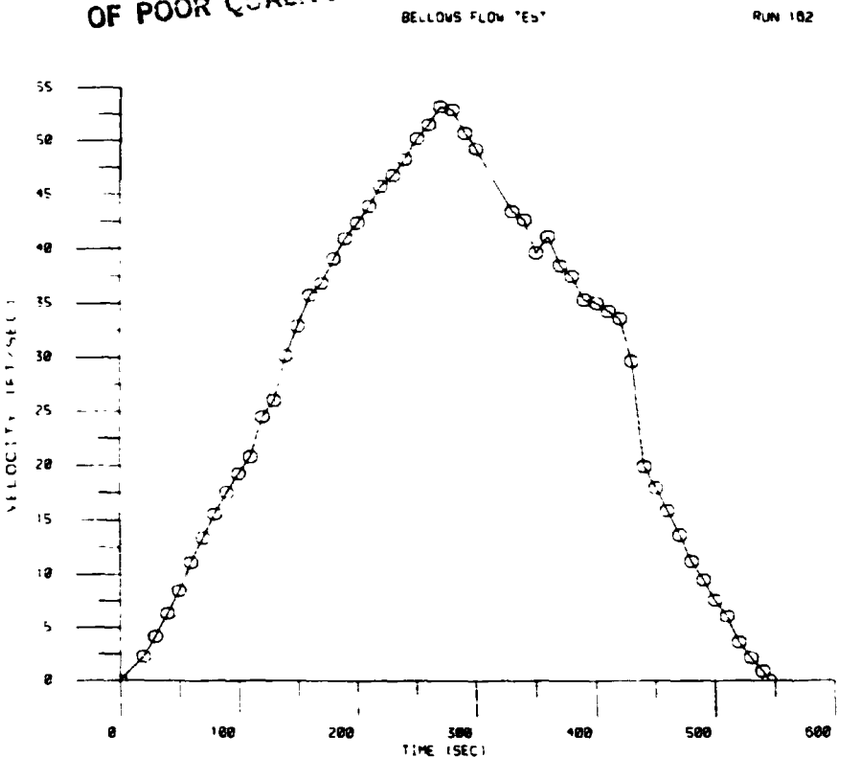

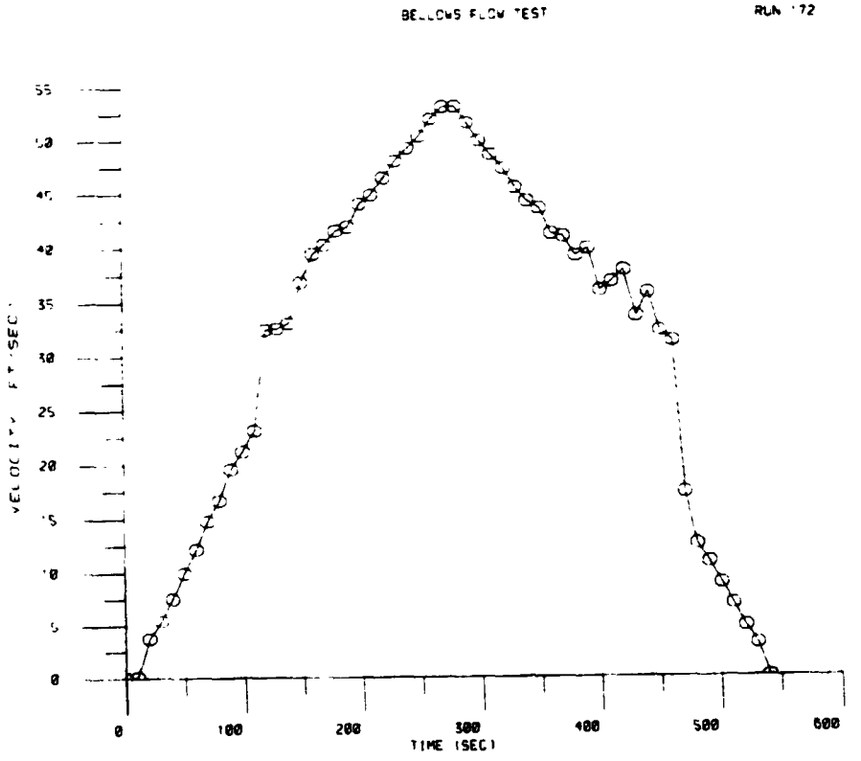

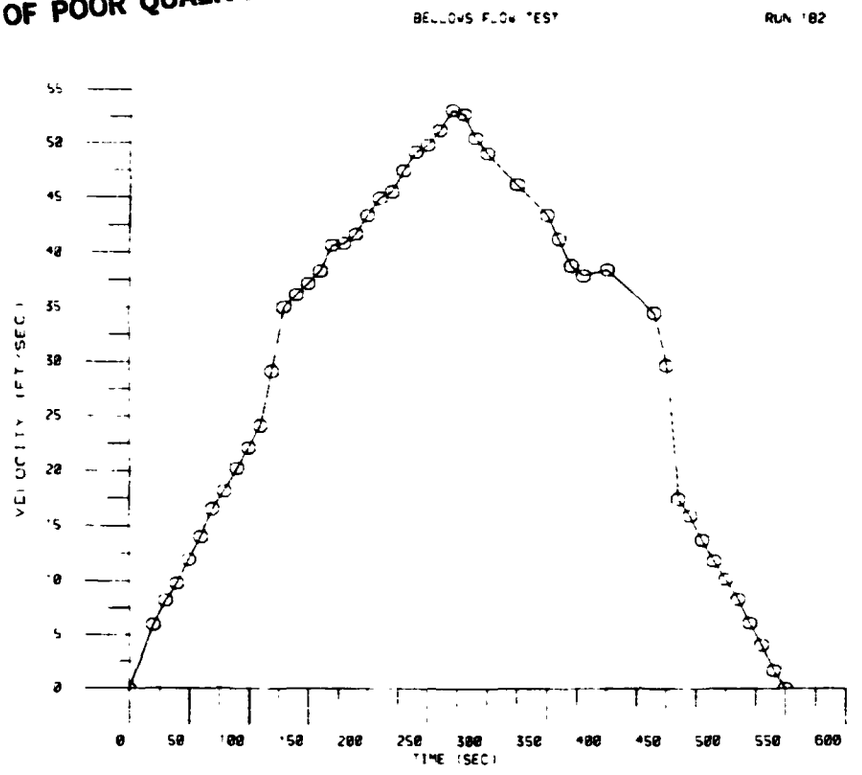

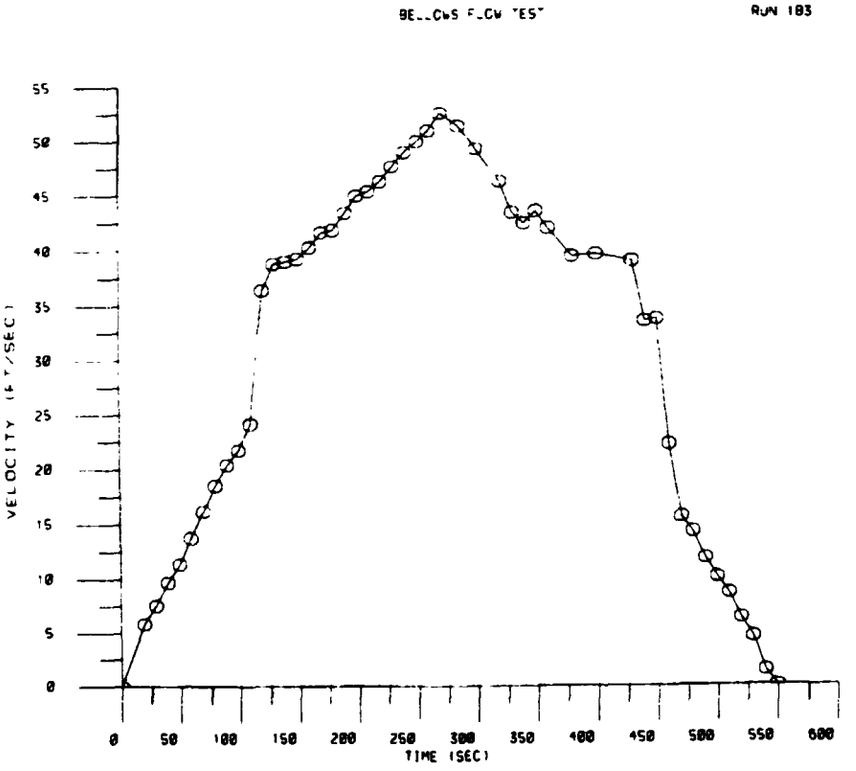

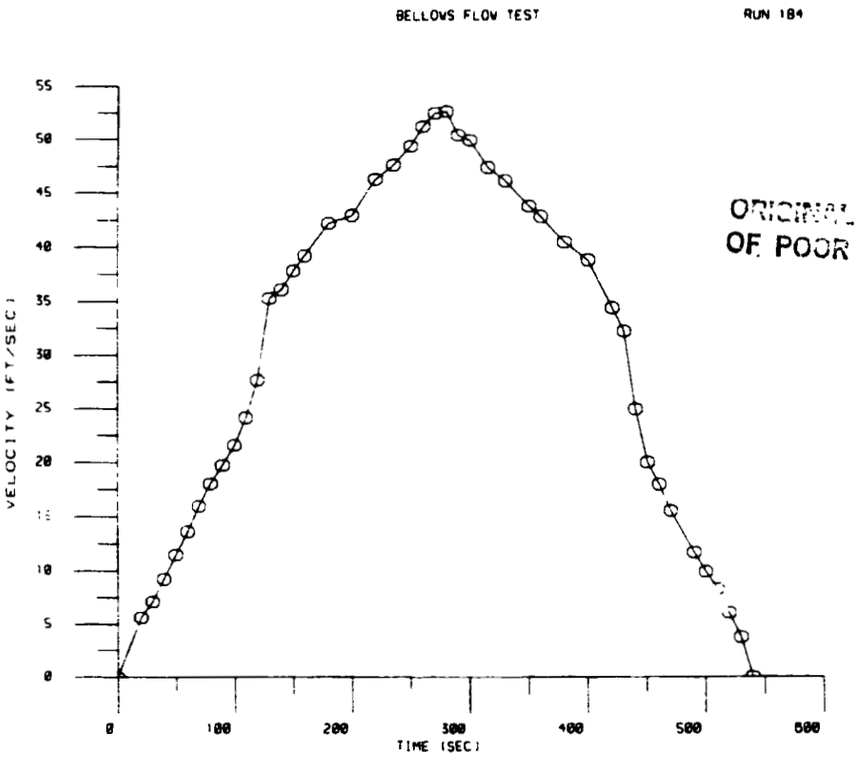

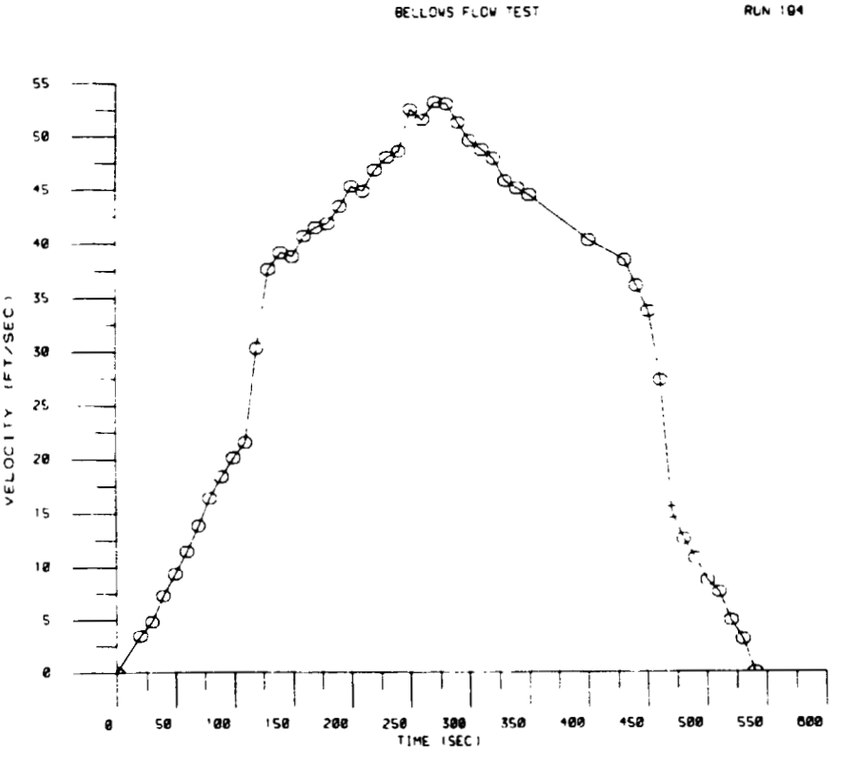

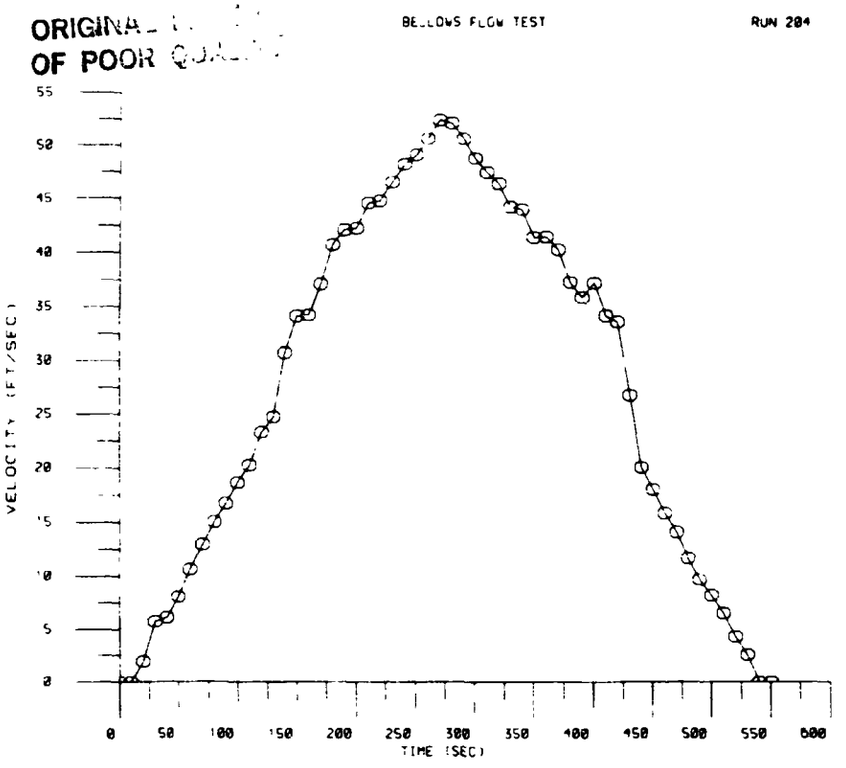

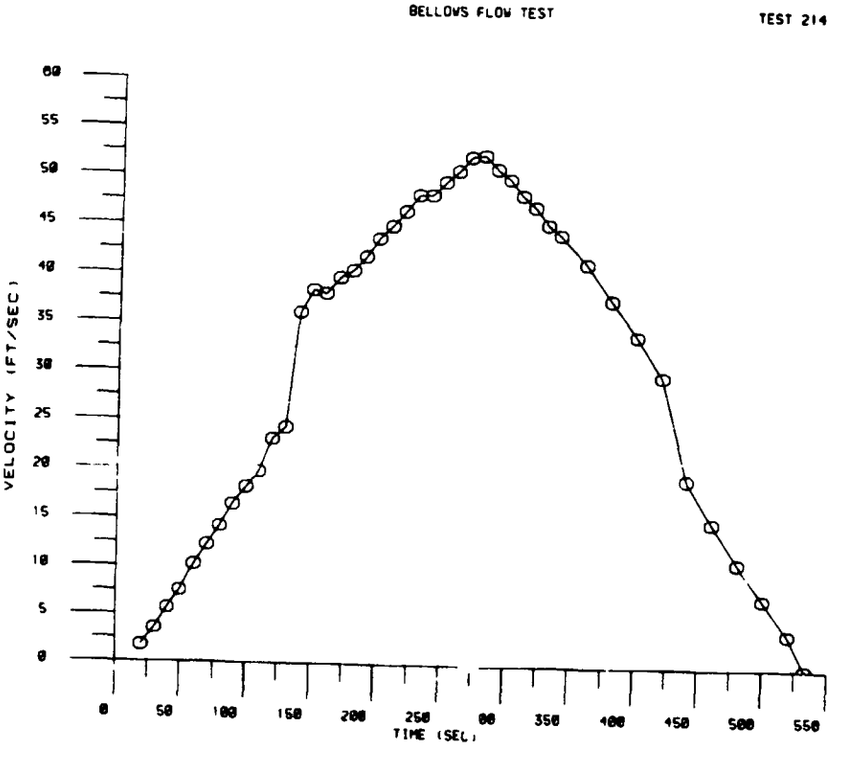

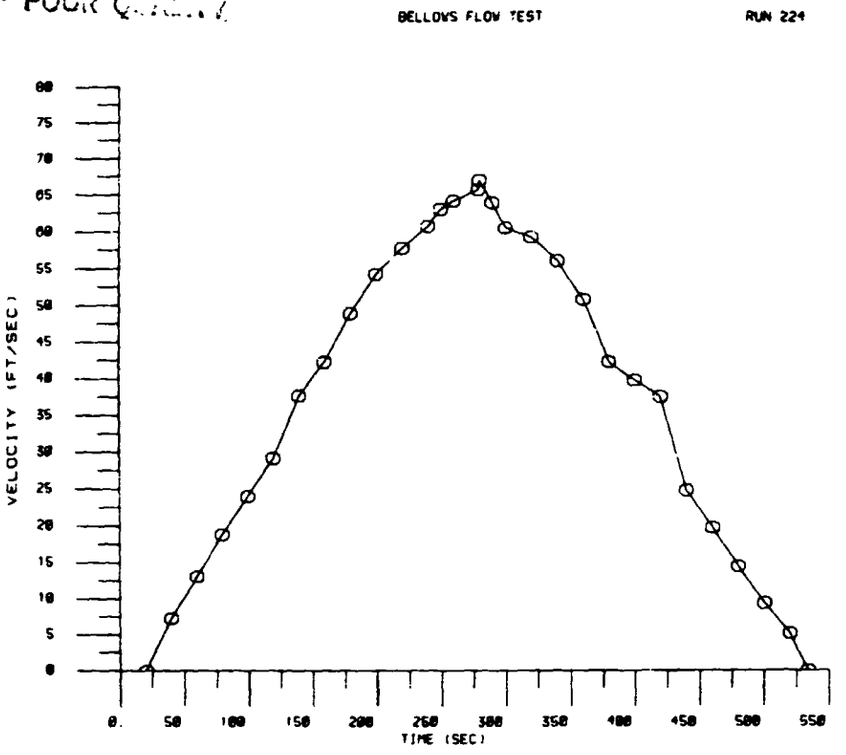

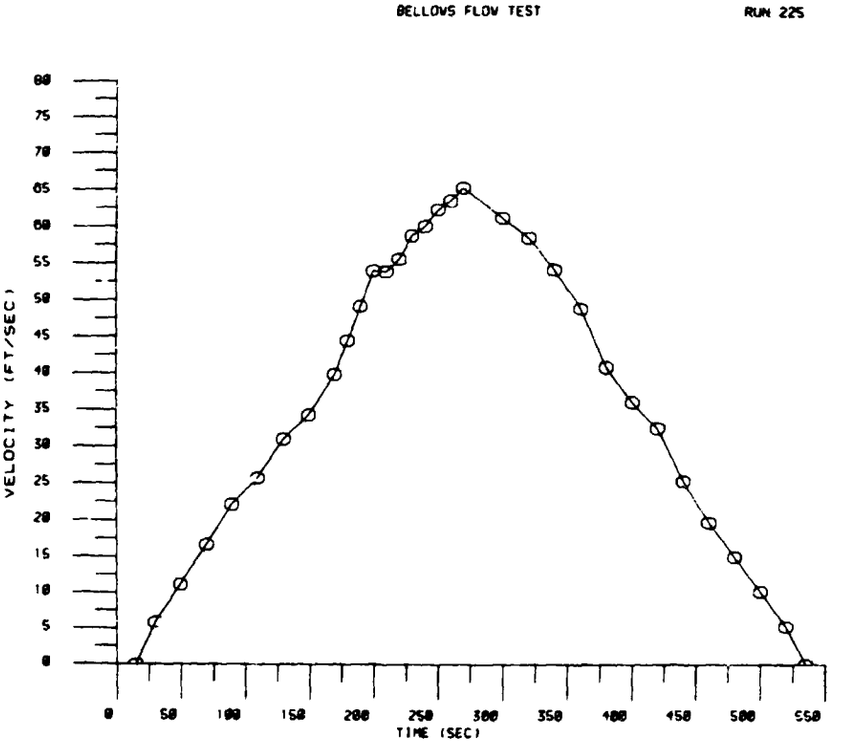

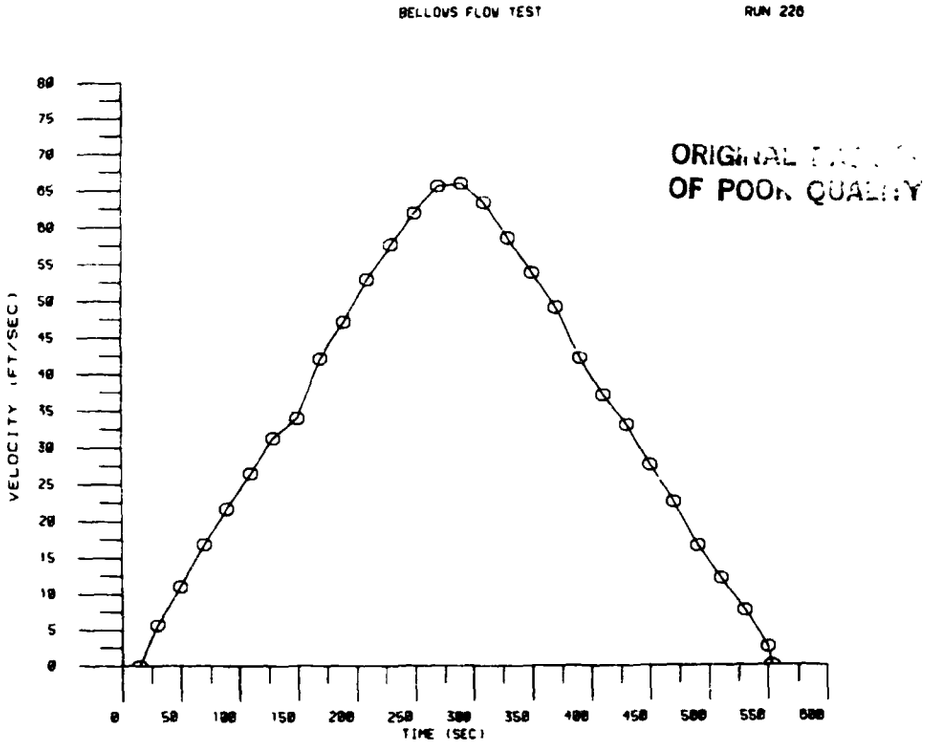

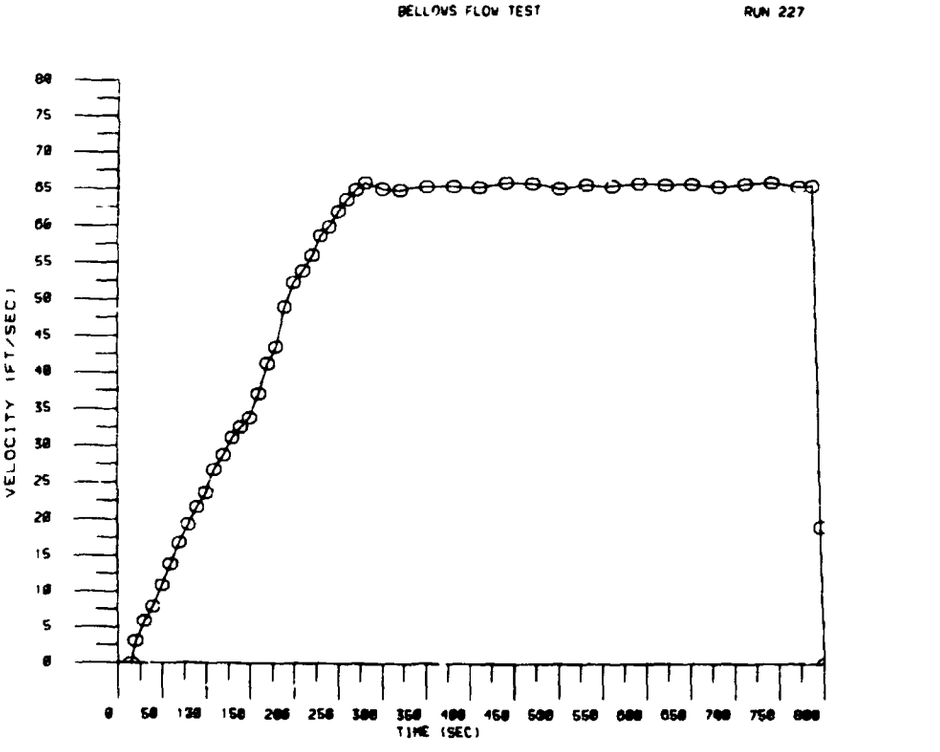

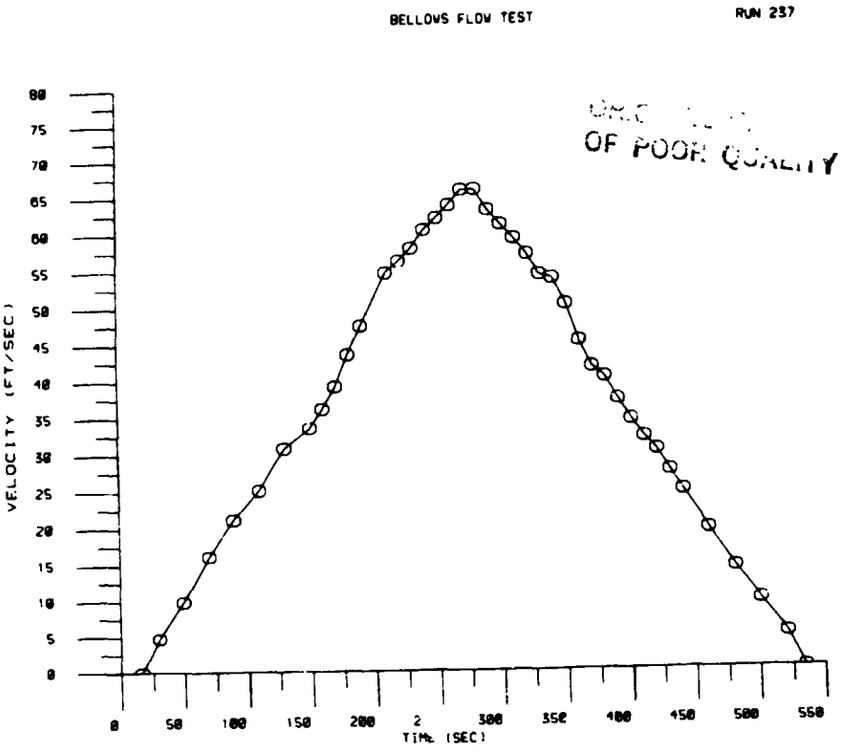

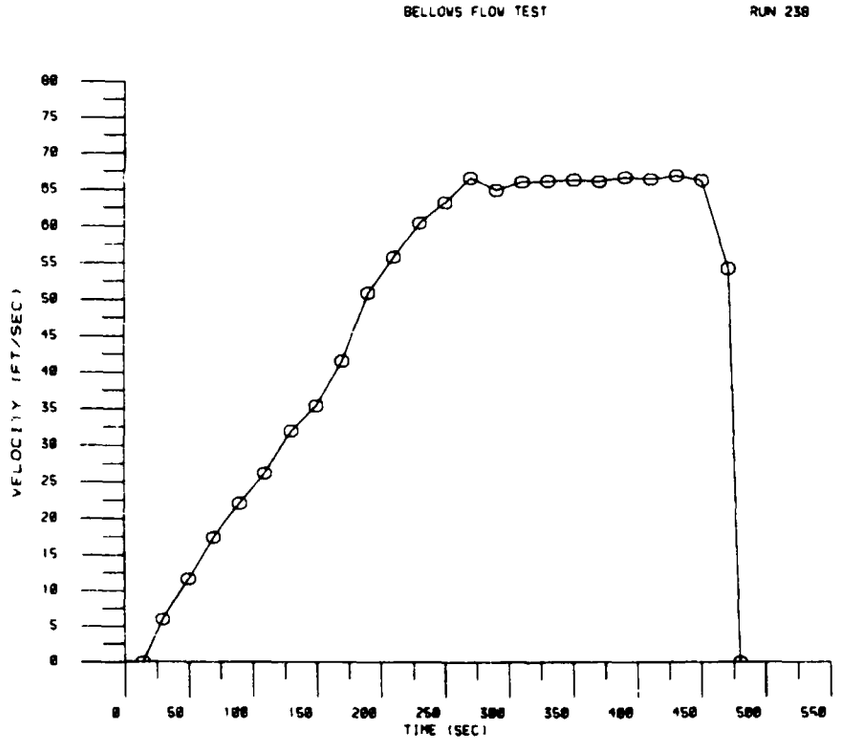

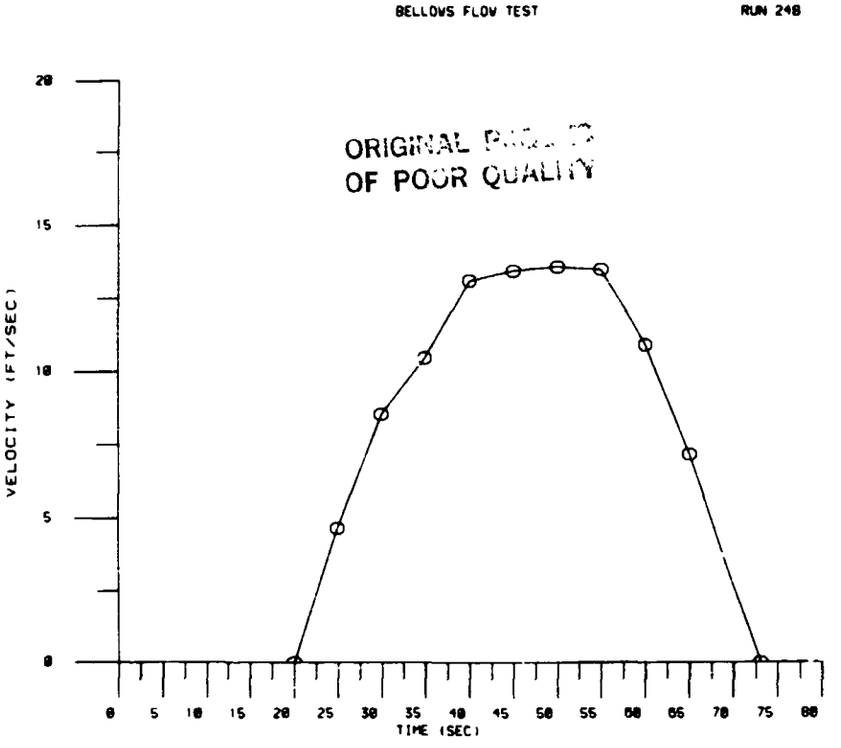
BELLOWS FLOW TEST
RUN 248
ORIGINAL PAGE IS
OF POOR QUALITY
VELOCITY (FT/SEC)
0
5
10
15
20
0
5
10
15
20
25
30
35
40
45
50
55
60
65
70
75
80
TIME (SEC)

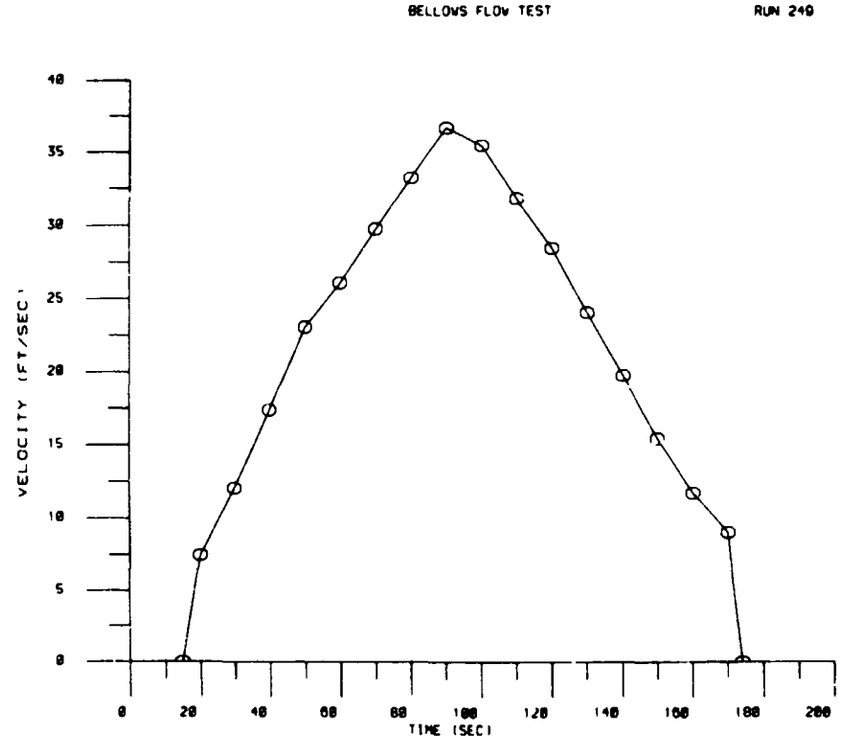
BELLOWS FLOW TEST
RUN 249
VELOCITY (FT/SEC)
0
5
10
15
20
25
30
35
40
0
20
40
60
80
100
120
140
160
180
200
TIME (SEC)

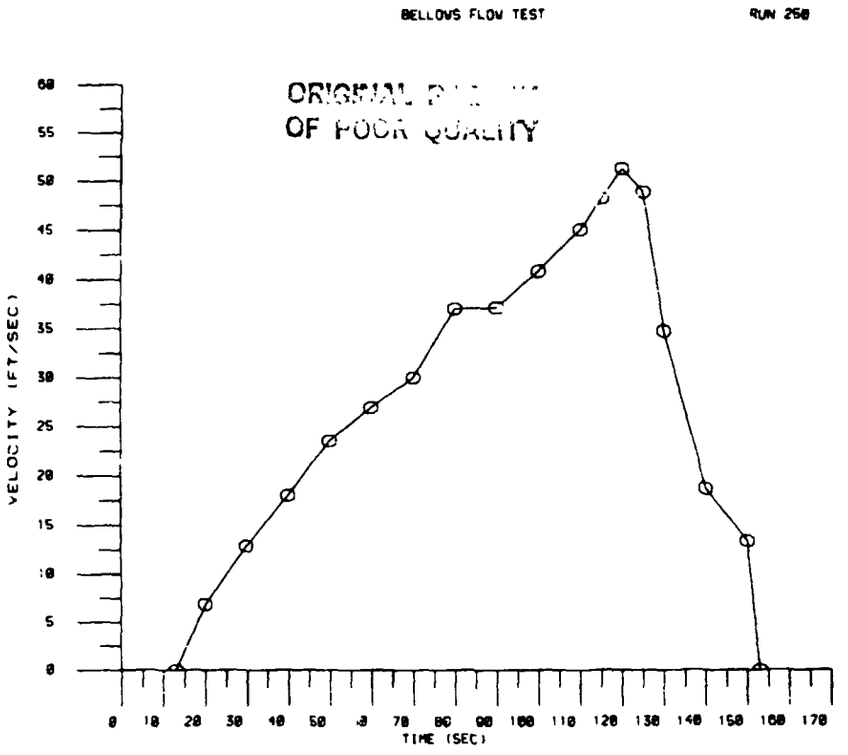
BELLOWS FLOW TEST
RUN 250
ORIGINAL PAGE IS
OF POOR QUALITY
VELOCITY (FT/SEC)
0
5
10
15
20
25
30
35
40
45
50
55
60
0 10 20 30 40 50 60 70 80 90 100 110 120 130 140 150 160 170
TIME (SEC)

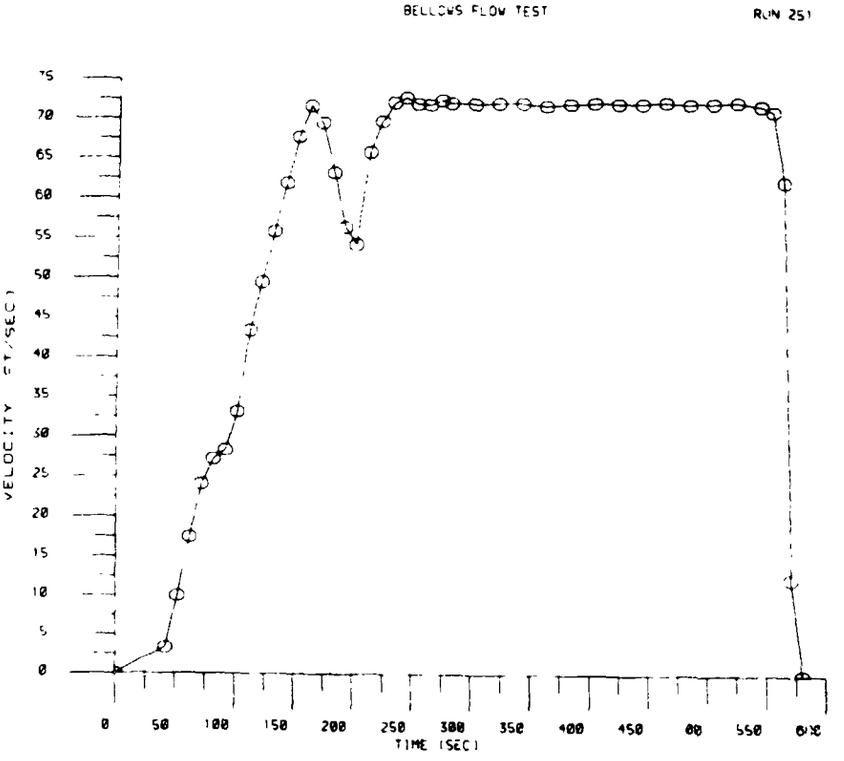
BELLOWS FLOW TEST
RUN 251
VELOCITY (FT/SEC)
0
5
10
15
20
25
30
35
40
45
50
55
60
65
70
75
0 50 100 150 200 250 300 350 400 450 500 550
TIME (SEC)

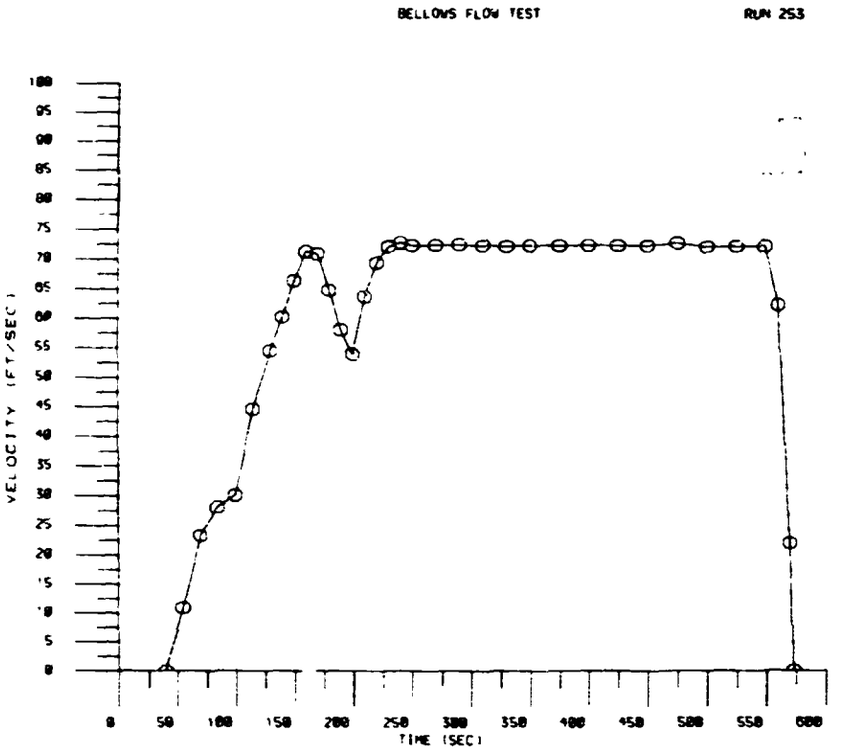
BELLOWS FLOW TEST
RUN 253
VELOCITY (FT/SEC)
TIME (SEC)

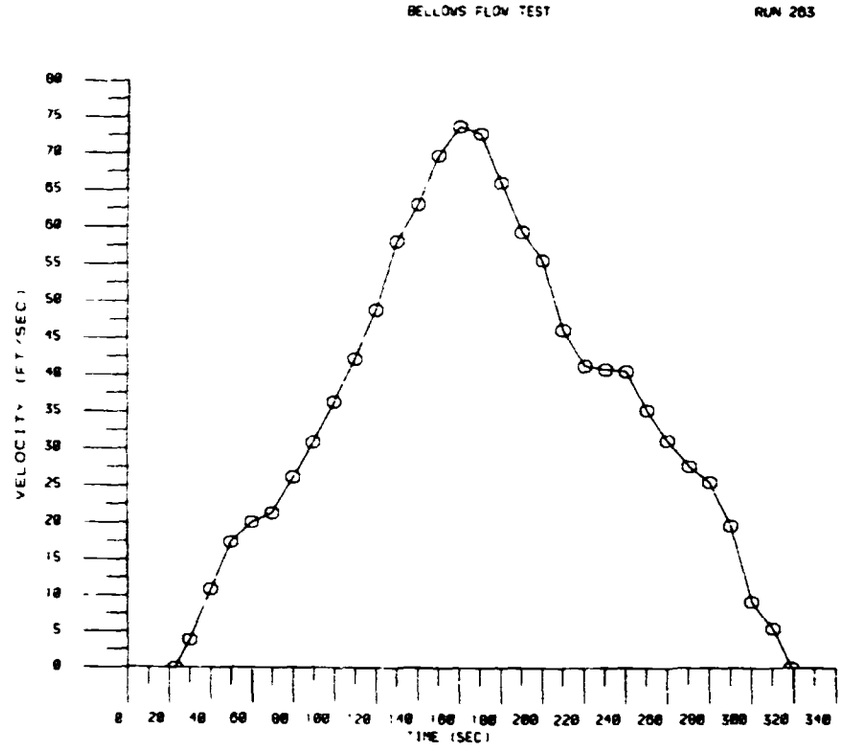
BELLOWS FLOW TEST
RUN 203
VELOCITY (FT/SEC)
TIME (SEC)

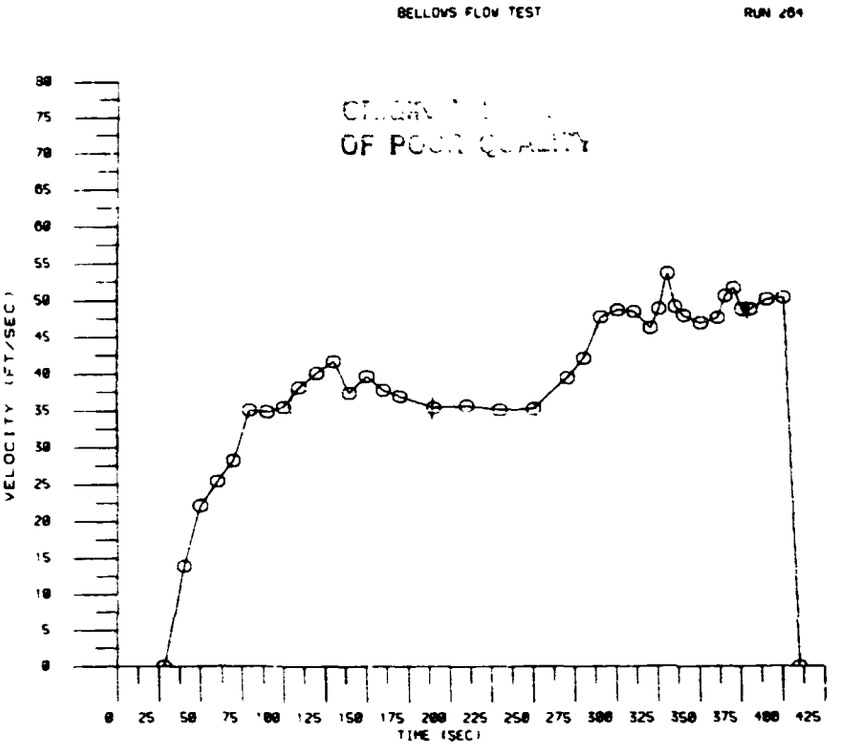
BELLOWS FLOW TEST
RUN 284
VELOCITY (FT/SEC)
TIME (SEC)

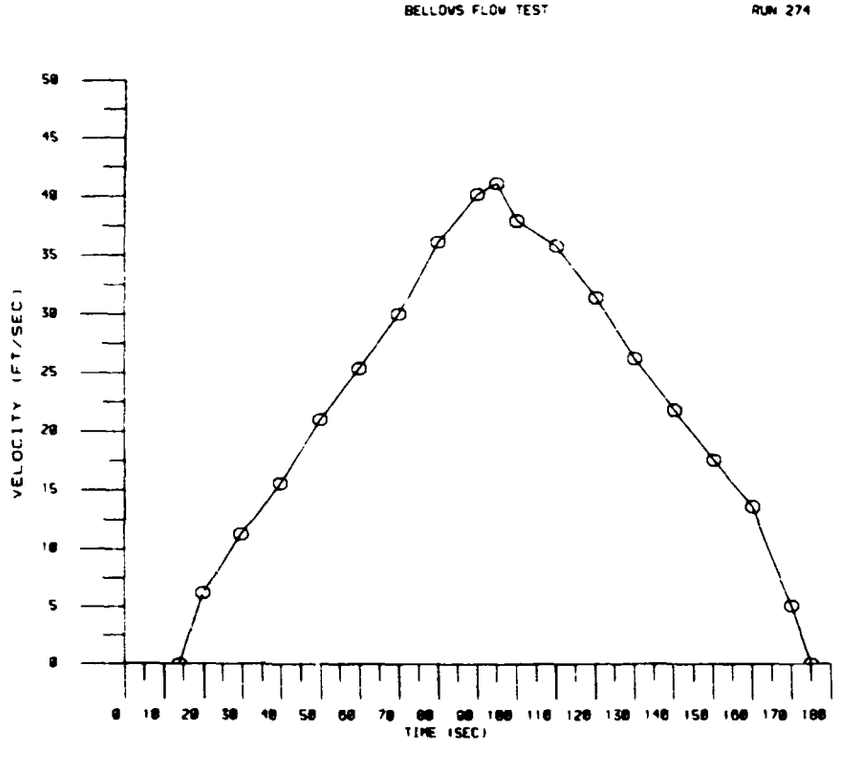
BELLOWS FLOW TEST
RUN 274
VELOCITY (FT/SEC)
TIME (SEC)

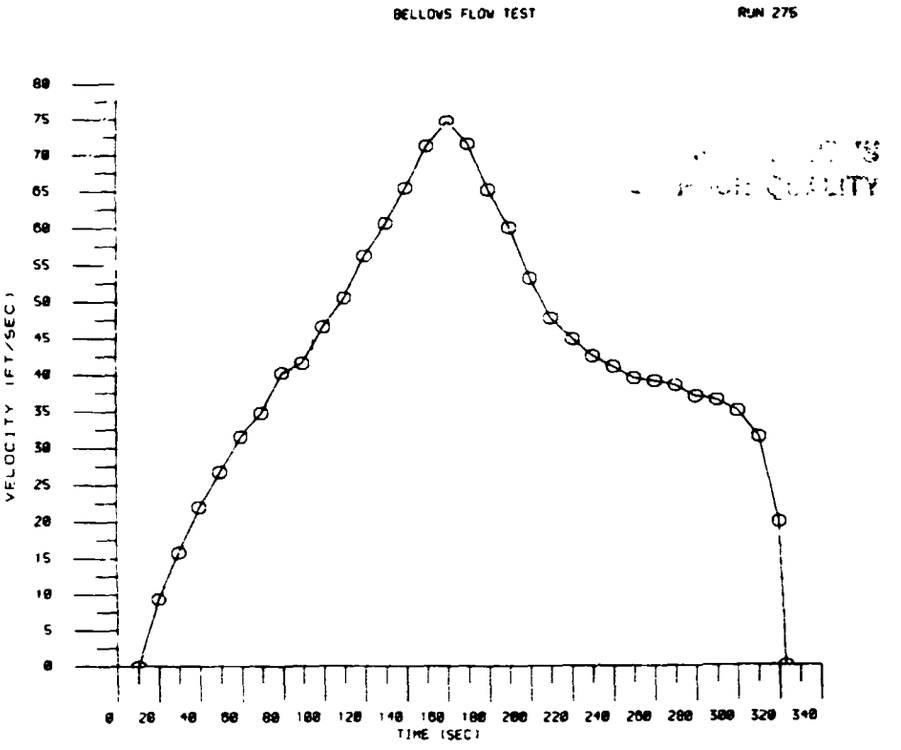
BELLOWS FLOW TEST
RUN 275
VELOCITY (FT/SEC)
0 5 10 15 20 25 30 35 40 45 50 55 60 65 70 75 80
0 20 40 60 80 100 120 140 160 180 200 220 240 260 280 300 320 340
TIME (SEC)

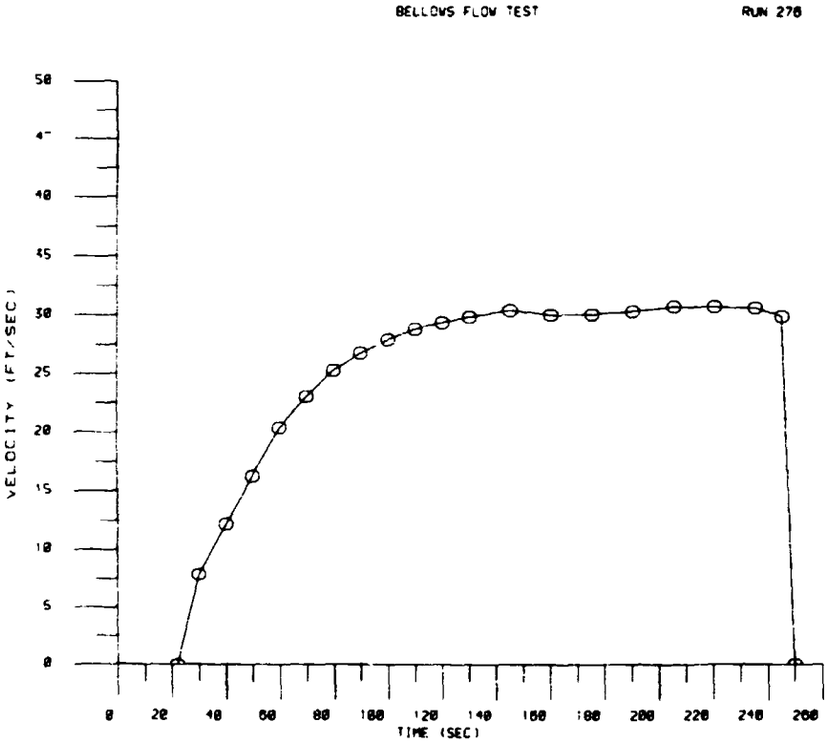
BELLOWS FLOW TEST
RUN 276
VELOCITY (FT/SEC)
0 5 10 15 20 25 30 35 40 45 50
0 20 40 60 80 100 120 140 160 180 200 220 240 260
TIME (SEC)

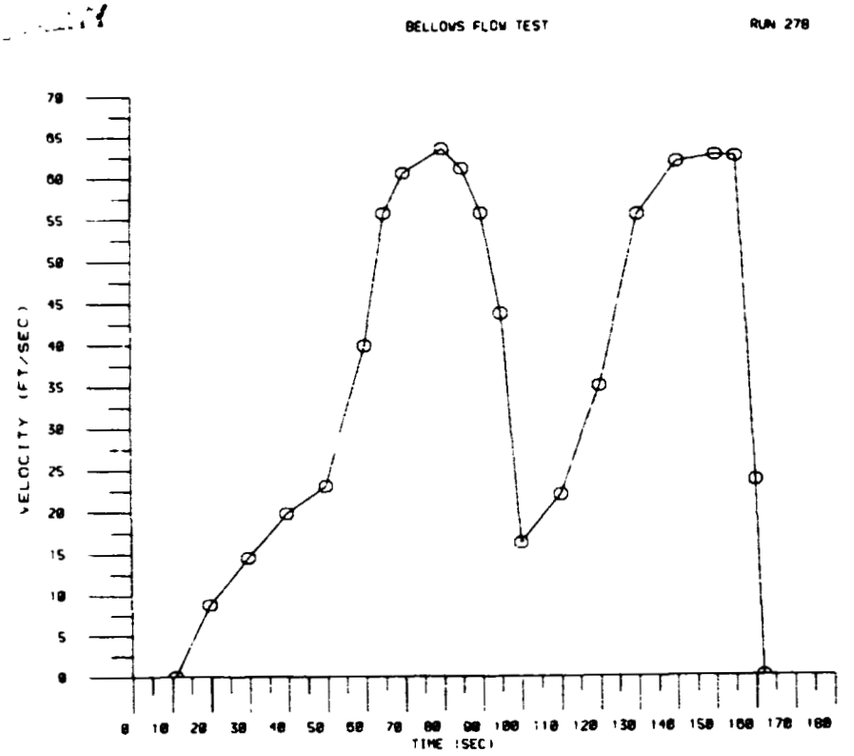
BELLOWS FLOW TEST
RUN 27B
VELOCITY (FT/SEC)
0 5 10 15 20 25 30 35 40 45 50 55 60 65 70
0 10 20 30 40 50 60 70 80 90 100 110 120 130 140 150 160 170 180
TIME (SEC)

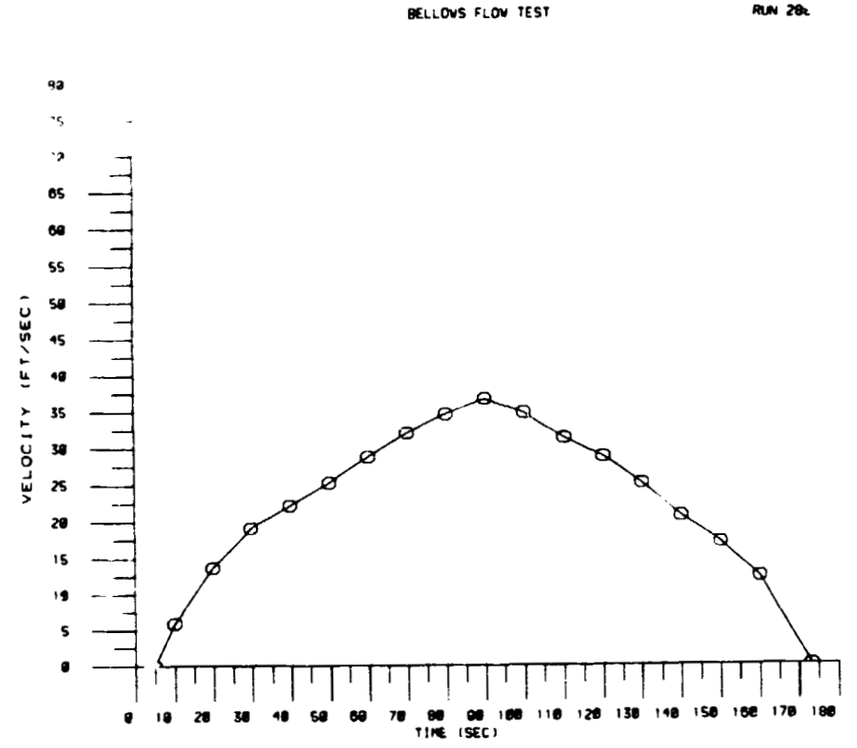
BELLOWS FLOW TEST
RUN 28
VELOCITY (FT/SEC)
0 5 10 15 20 25 30 35 40 45 50 55 60 65
0 10 20 30 40 50 60 70 80 90 100 110 120 130 140 150 160 170 180
TIME (SEC)

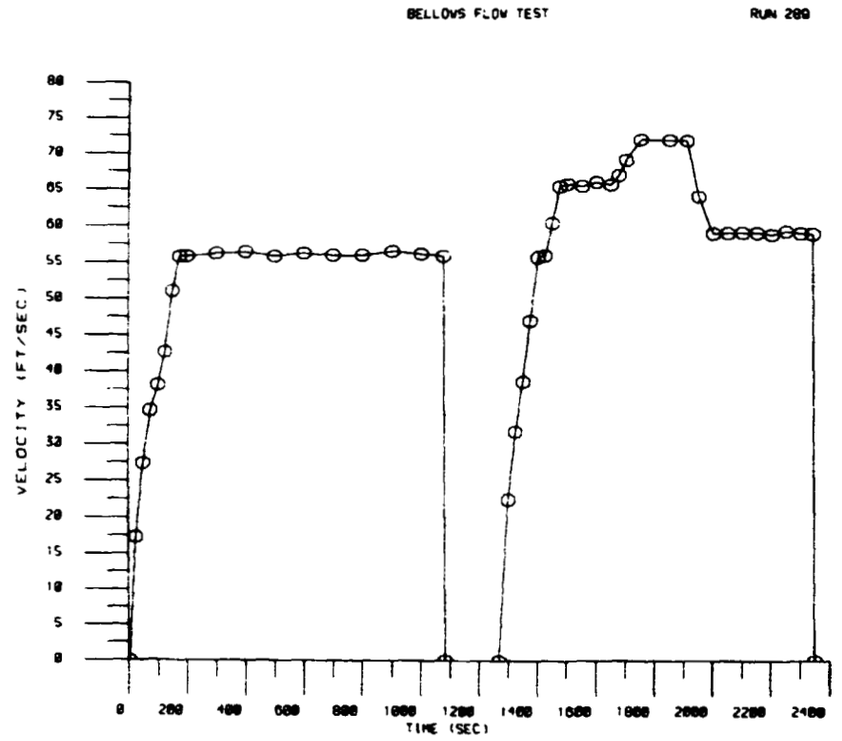
BELLOWS FLOW TEST
RUN 209
VELOCITY (FT/SEC)
TIME (SEC)

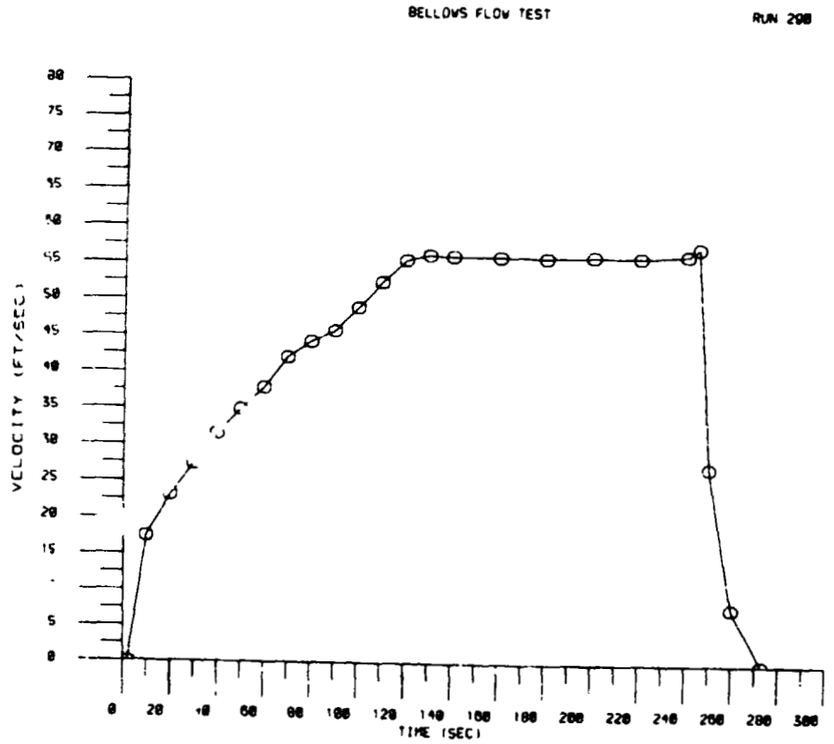
BELLOWS FLOW TEST
RUN 208
VELOCITY (FT/SEC)
TIME (SEC)

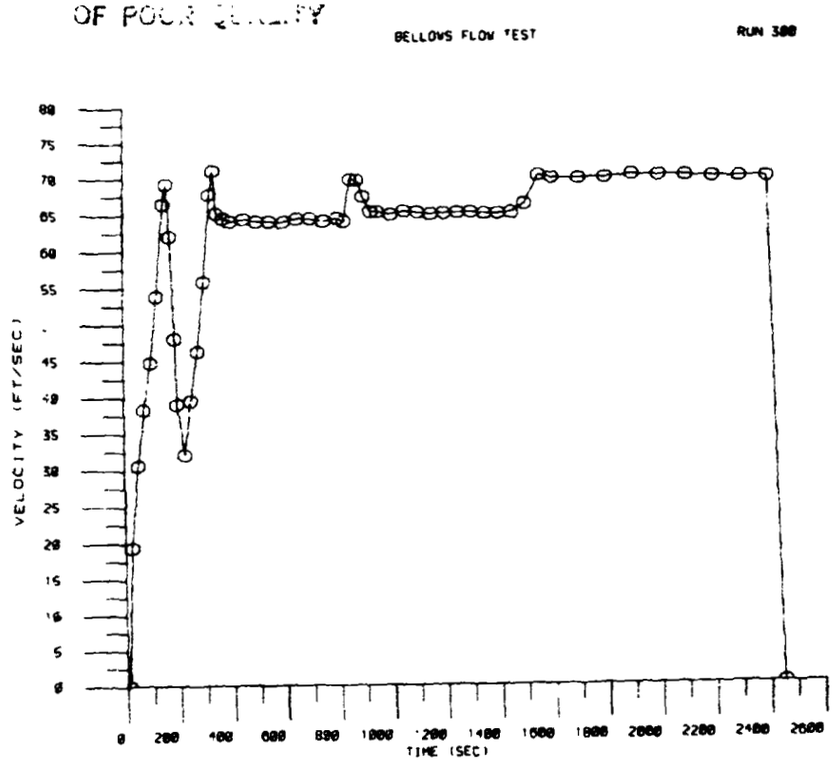

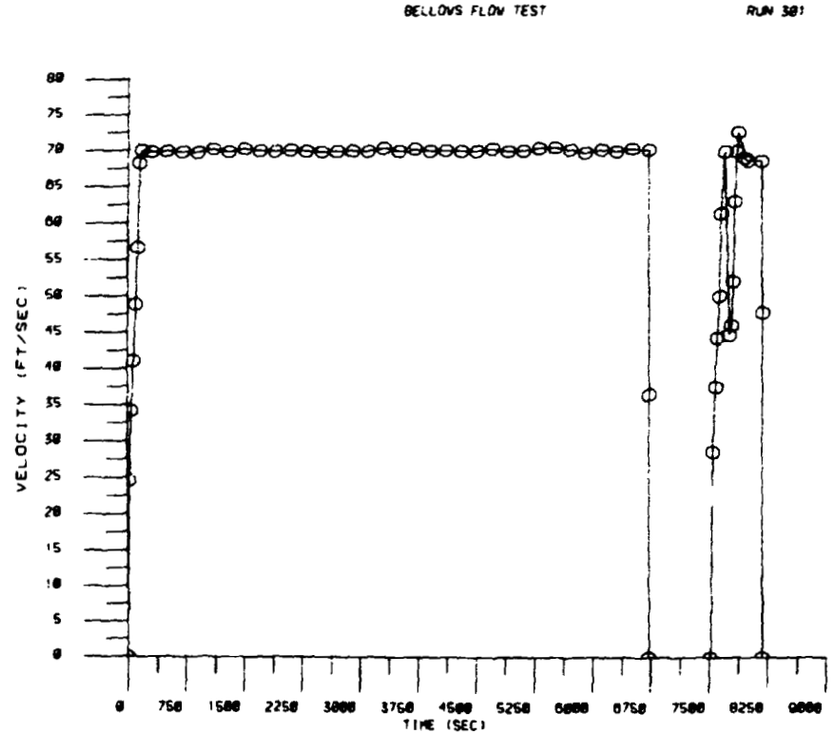

BELLOWS FLOW TEST RUN 311

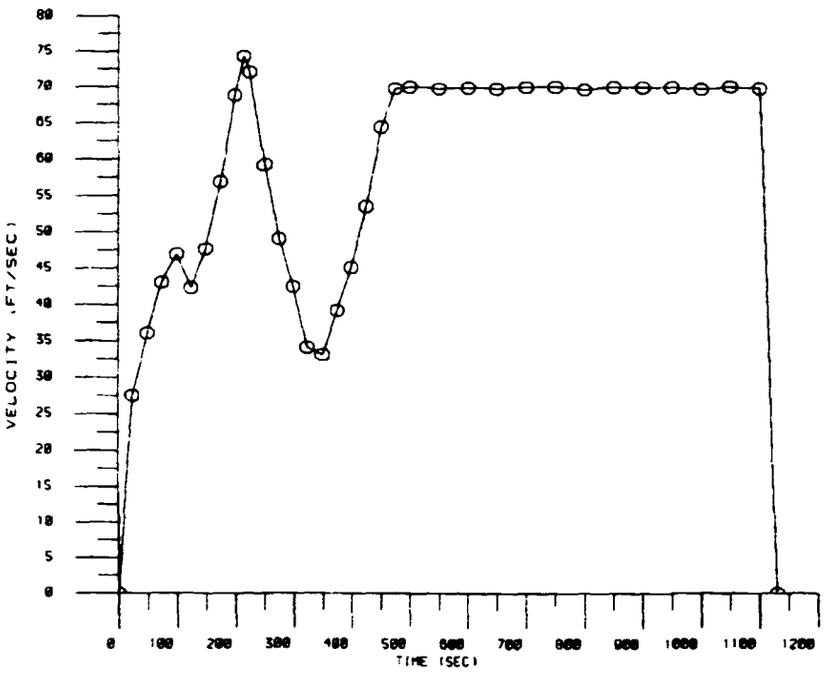

BELLOWS FLOW TEST RUN 312

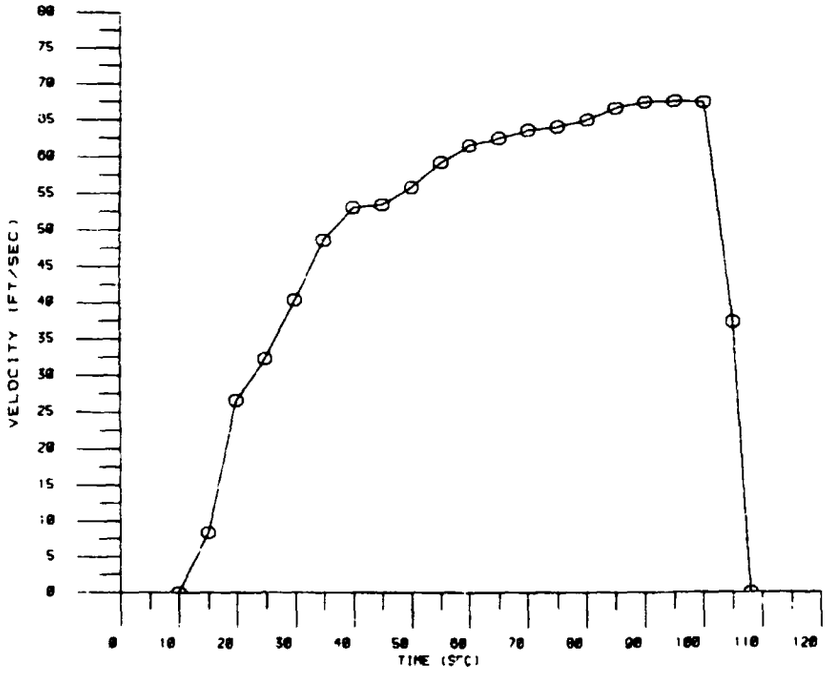

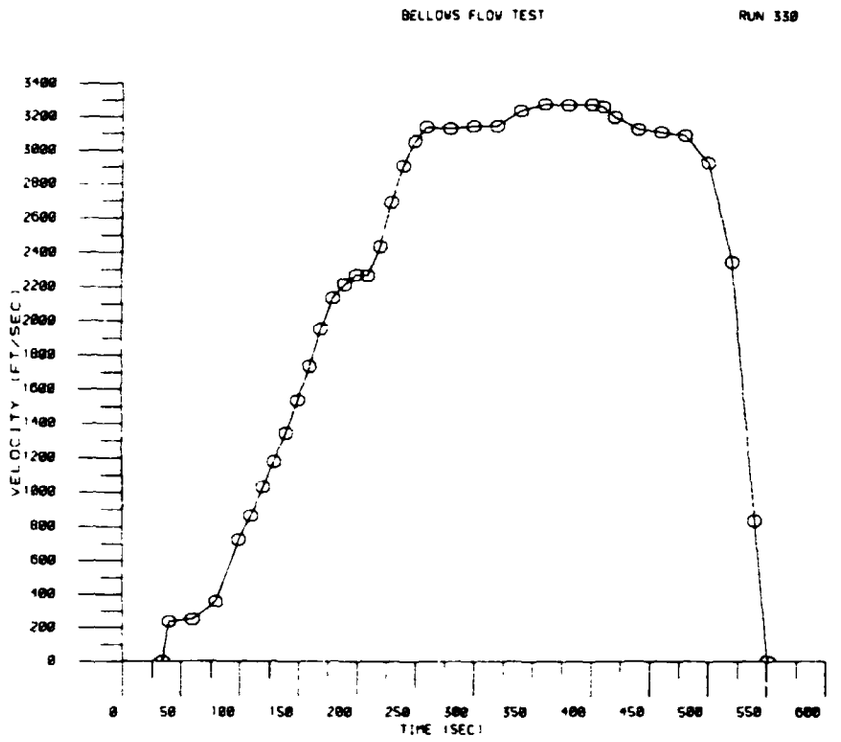

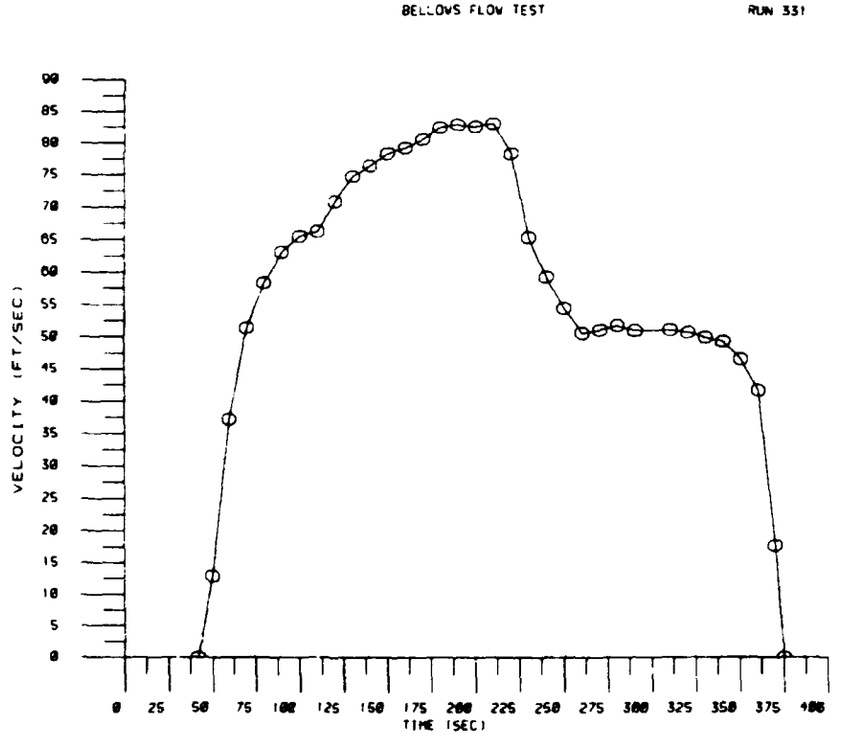

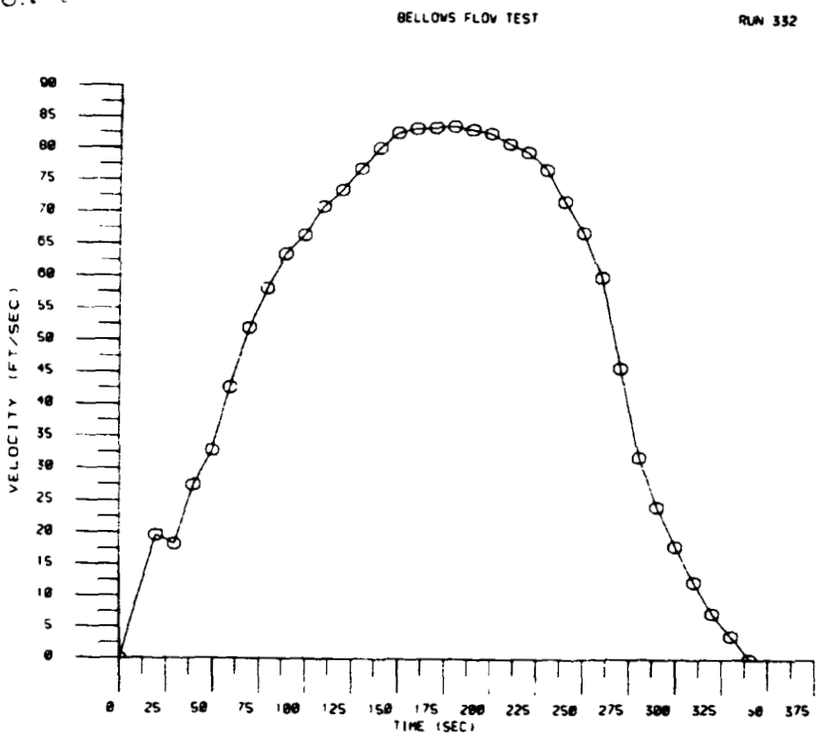

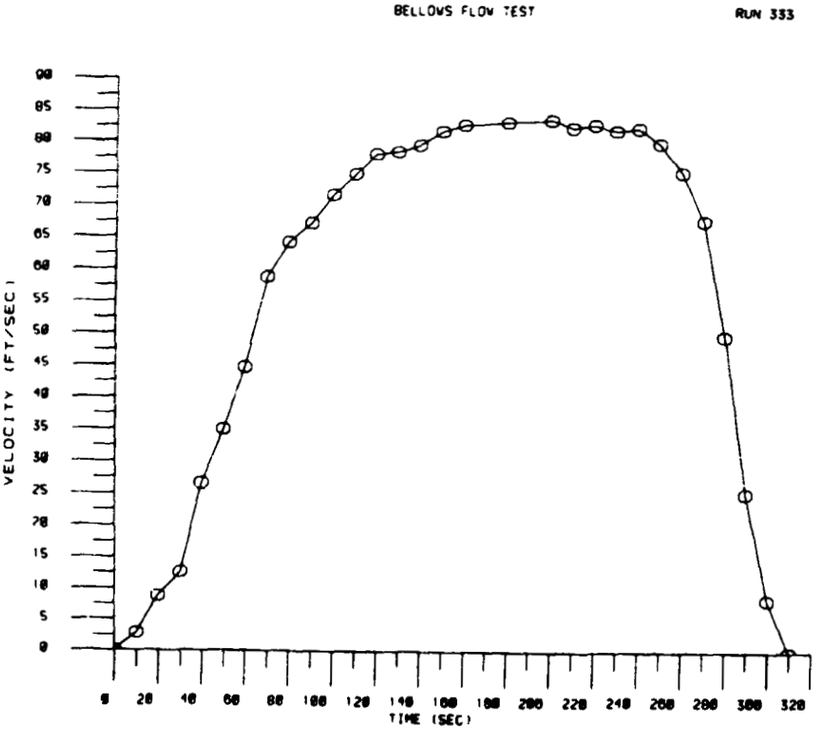

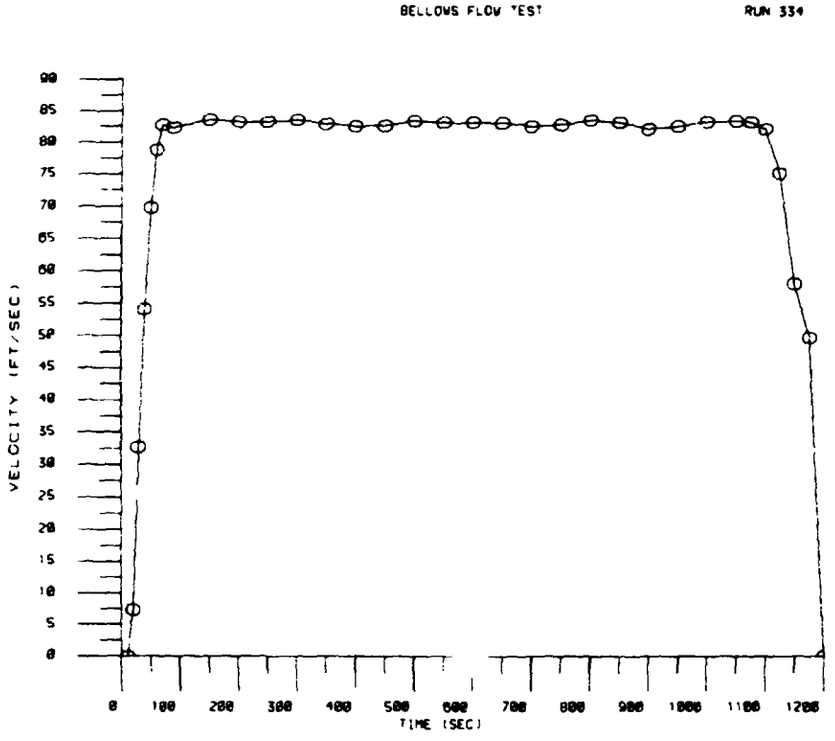
BELLOWS FLOW TEST
RUN 334
VELOCITY (FT/SEC)
TIME (SEC)

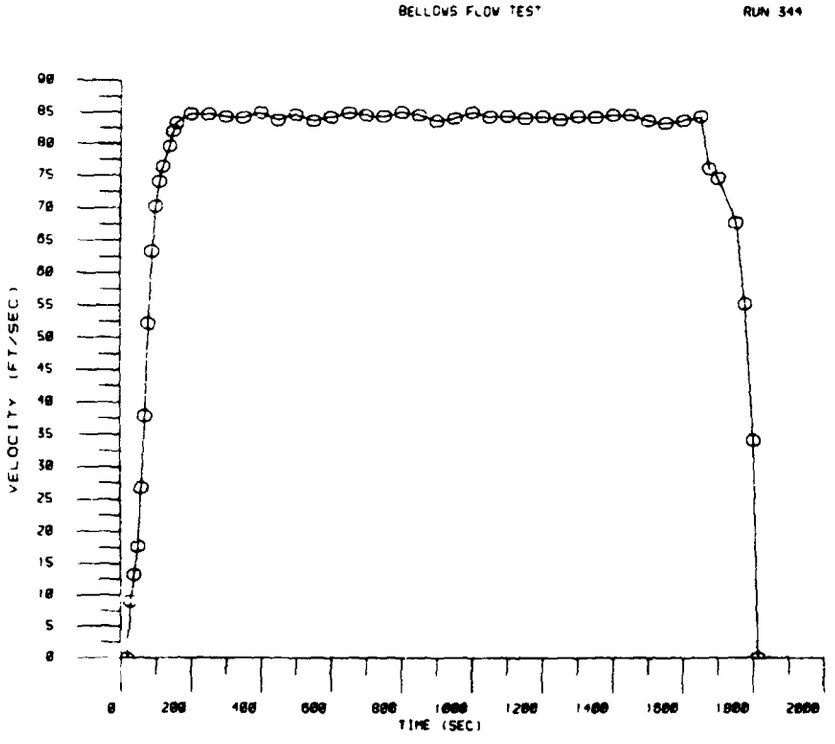
BELLOWS FLOW TEST
RUN 344
VELOCITY (FT/SEC)
TIME (SEC)

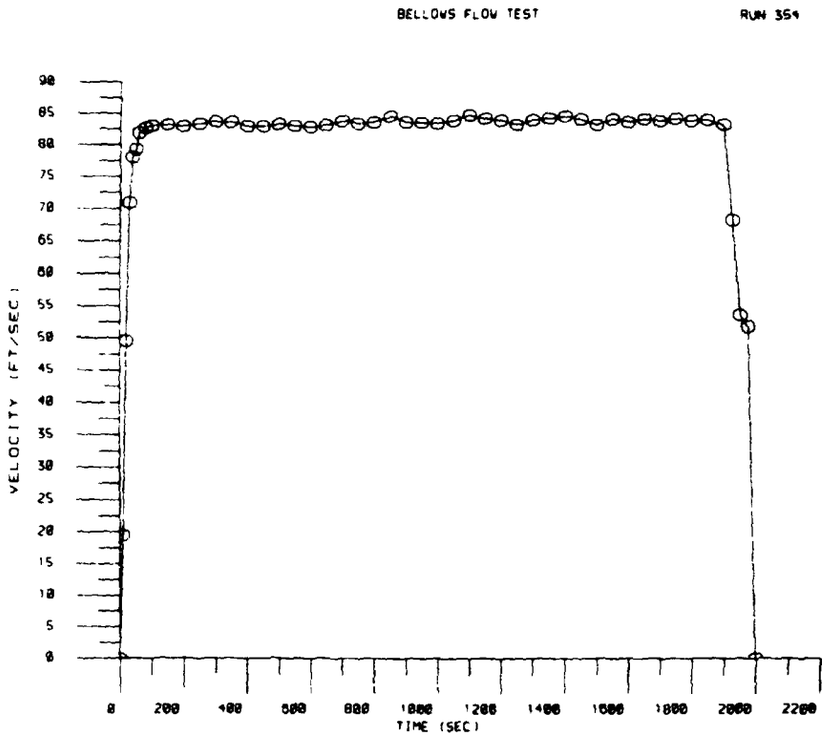
BELLOWS FLOW TEST
RUN 354
VELOCITY (FT/SEC)
TIME (SEC)

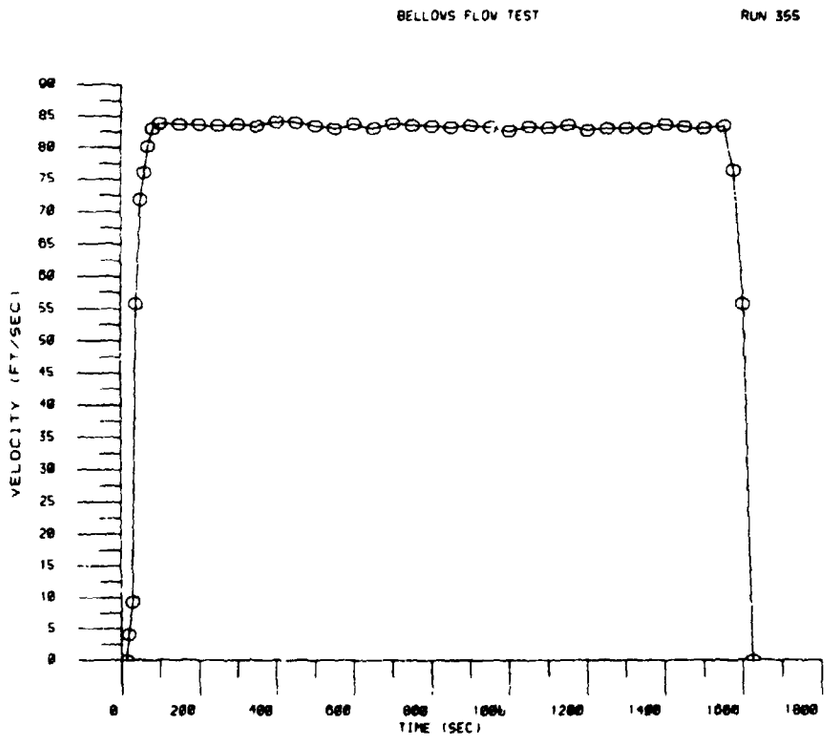
BELLOWS FLOW TEST
RUN 355
VELOCITY (FT/SEC)
TIME (SEC)

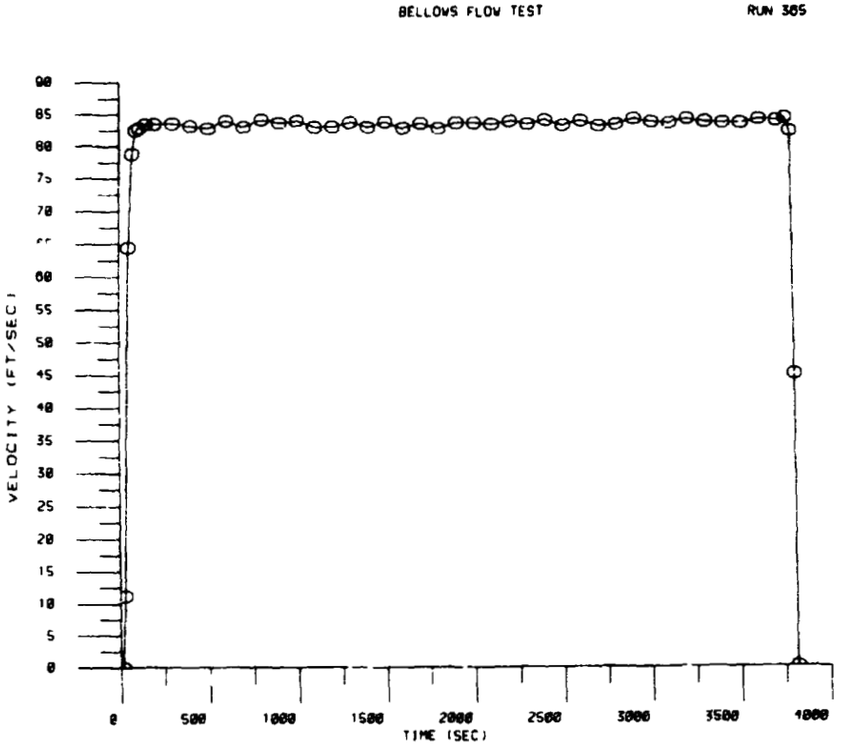

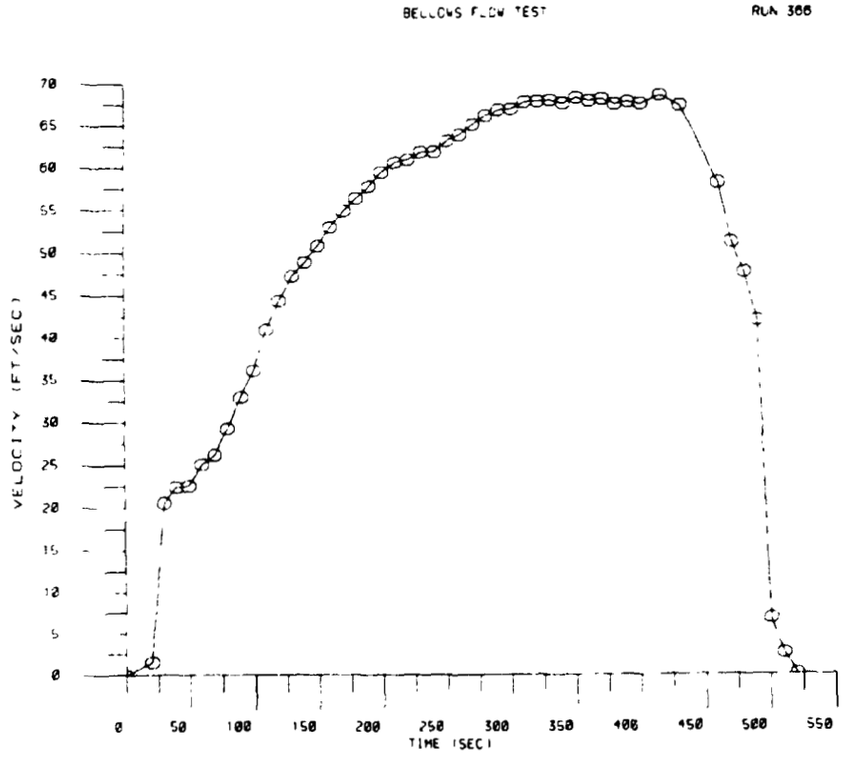

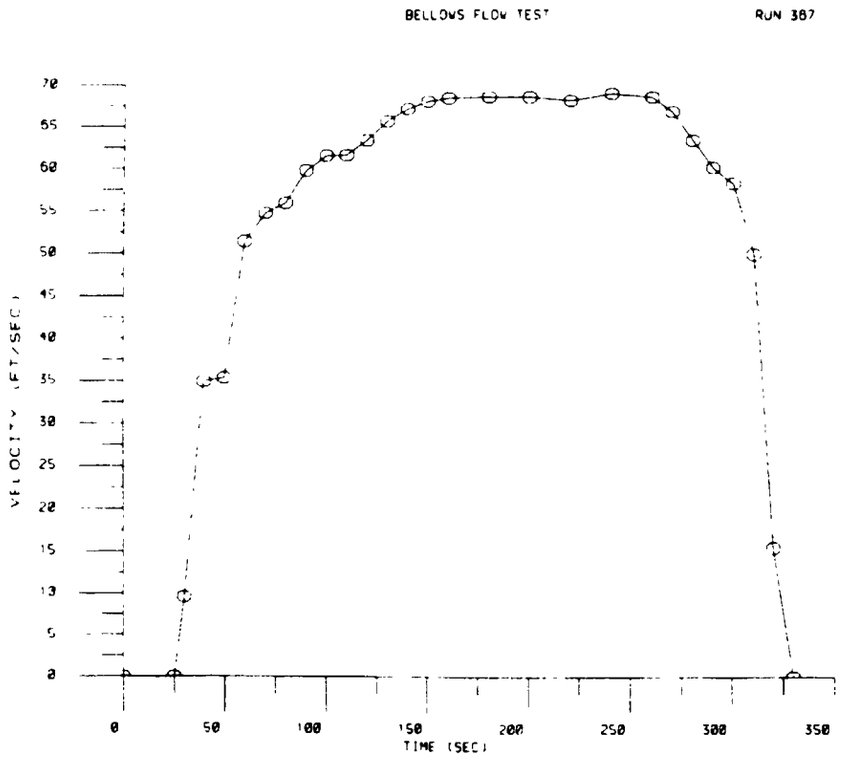
BELLOWS FLOW TEST
RUN 387
VELOCITY (FT/SEC)
70
65
60
55
50
45
40
35
30
25
20
15
10
5
0
0
50
100
150
200
250
300
350
TIME (SEC)

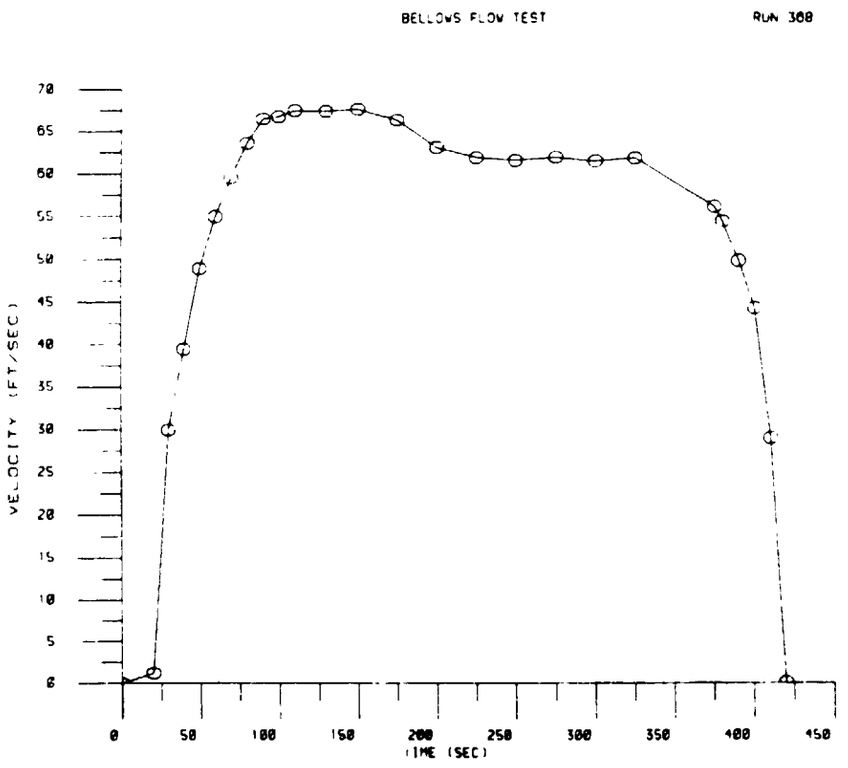
BELLOWS FLOW TEST
RUN 388
VELOCITY (FT/SEC)
70
65
60
55
50
45
40
35
30
25
20
15
10
5
0
0
50
100
150
200
250
300
350
400
450
TIME (SEC)

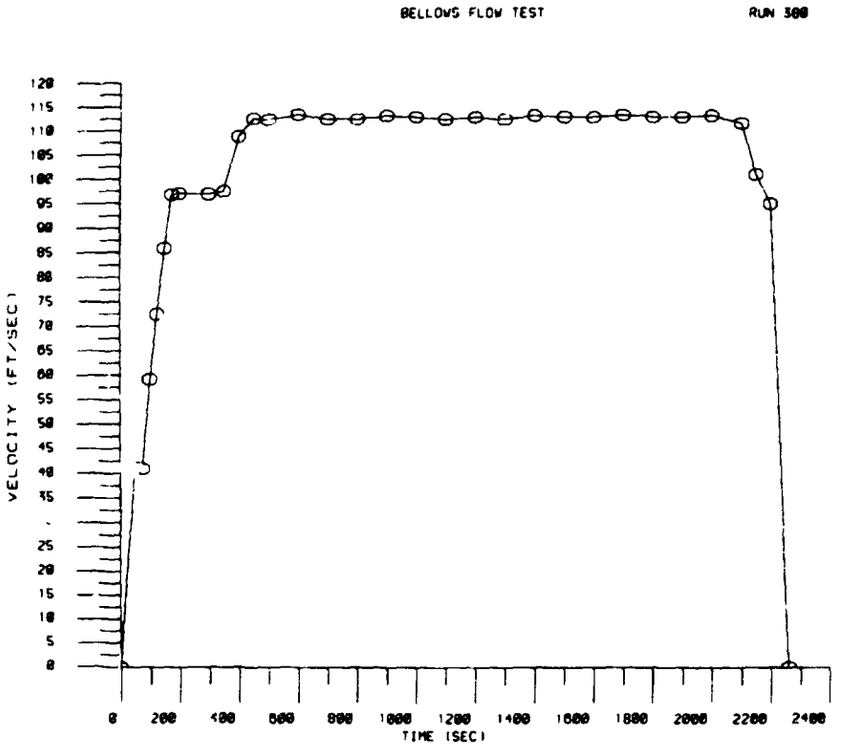

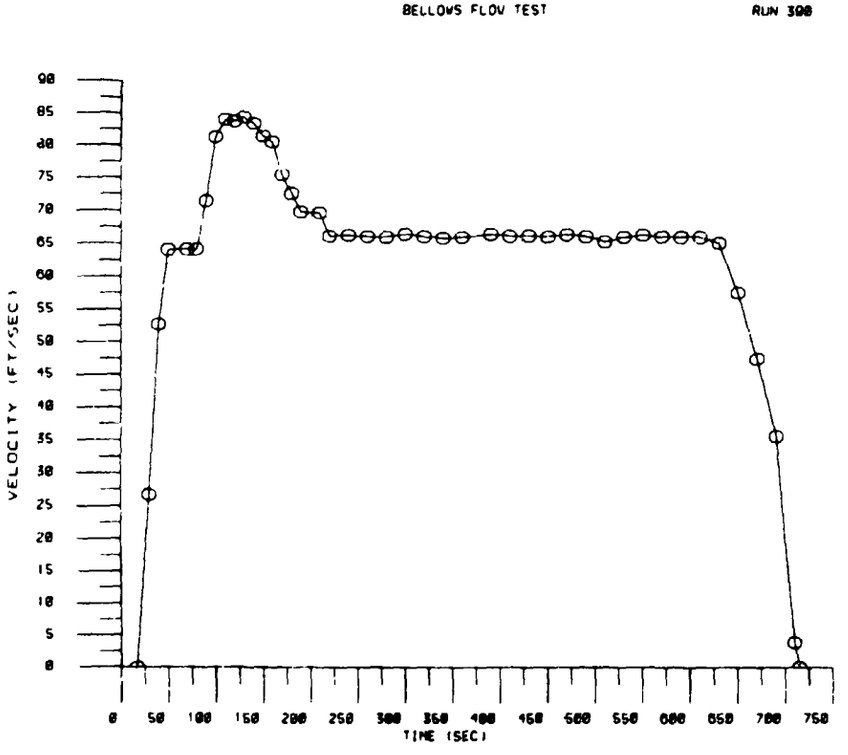

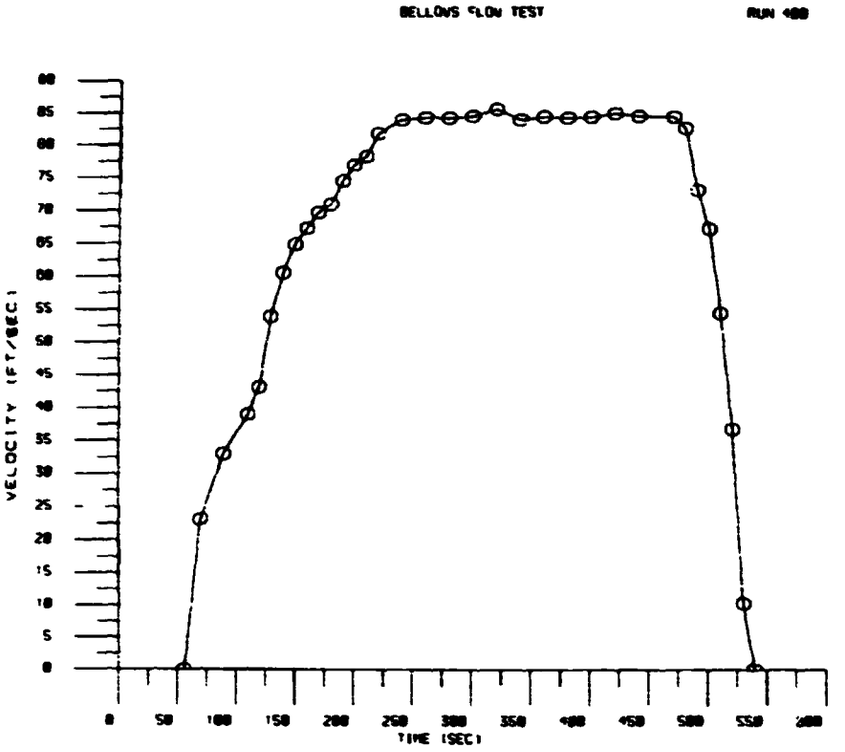

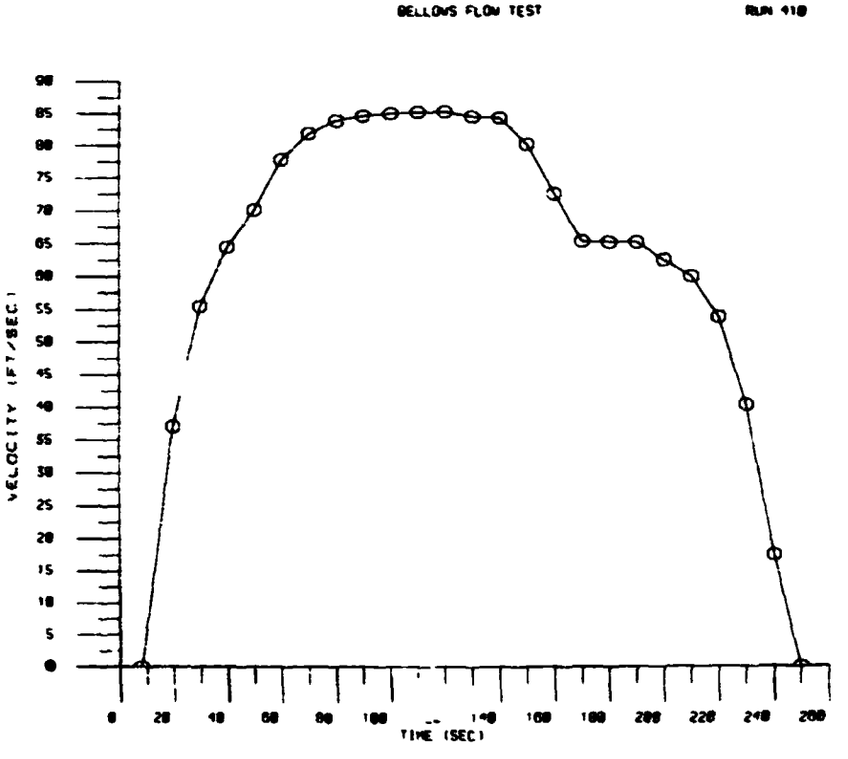

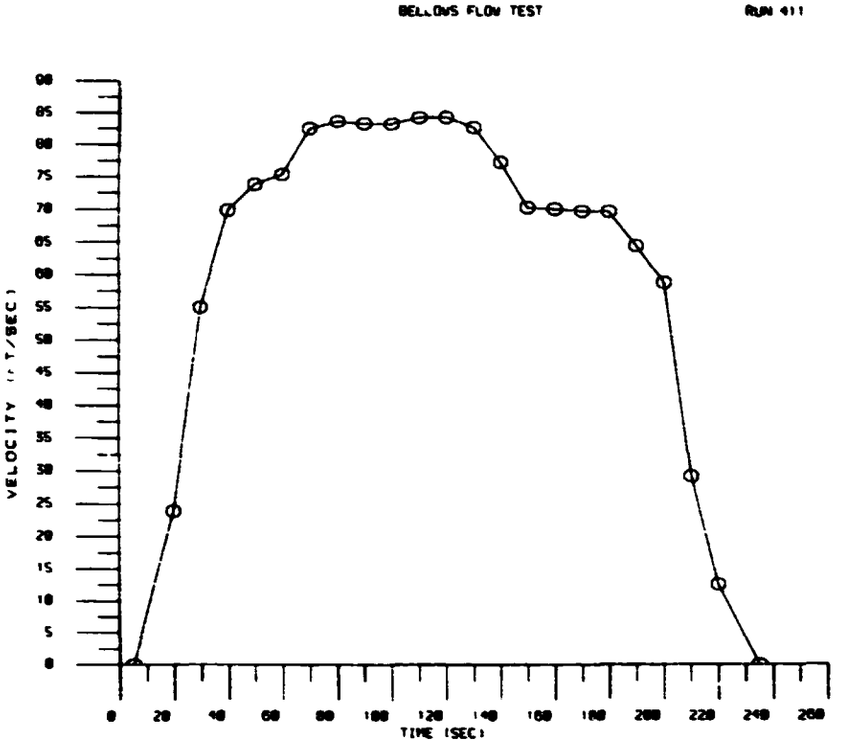

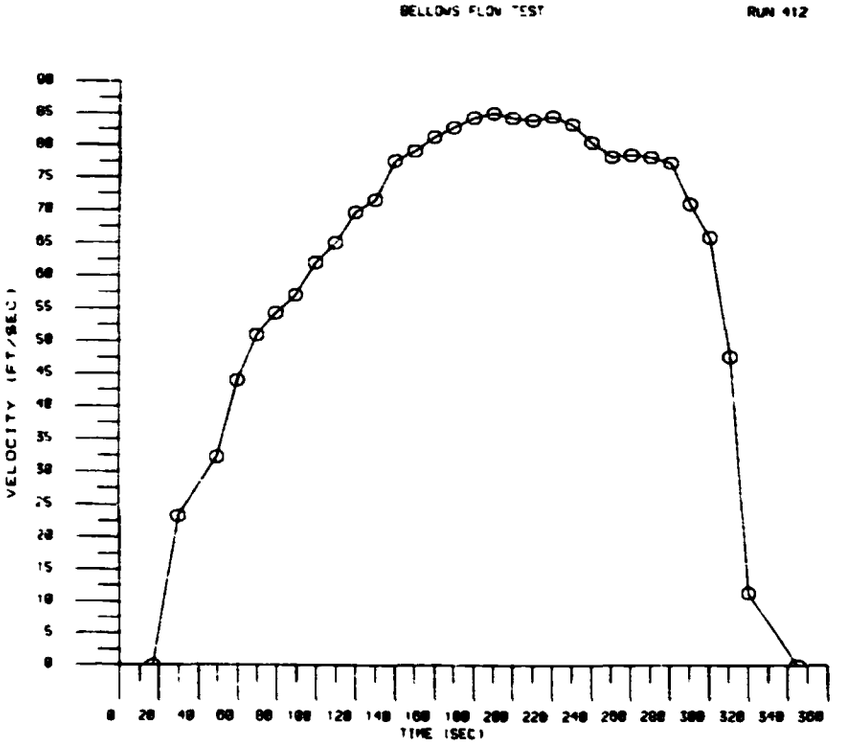

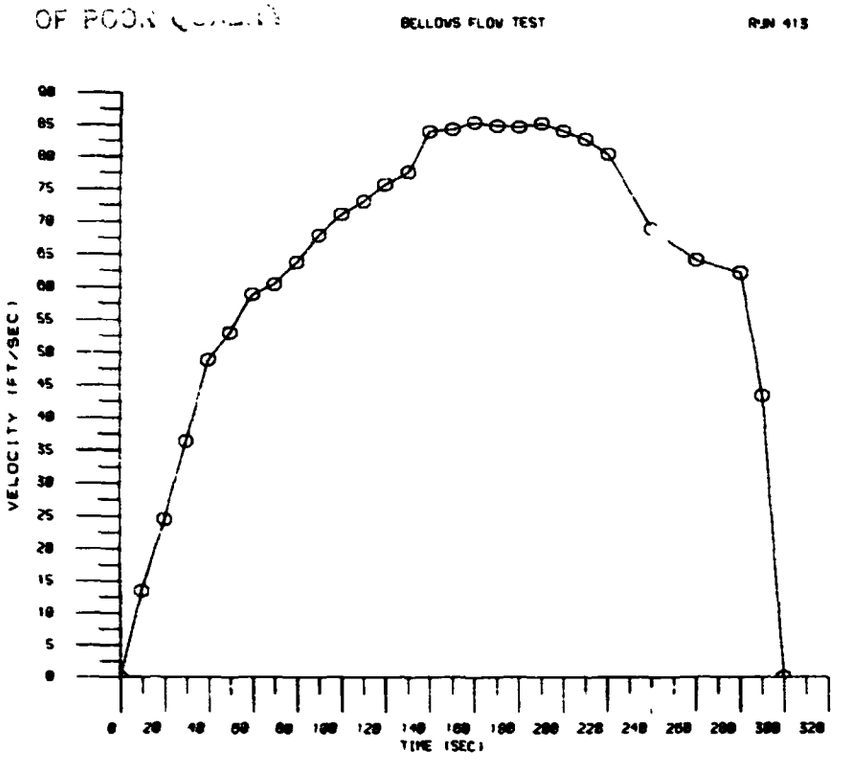

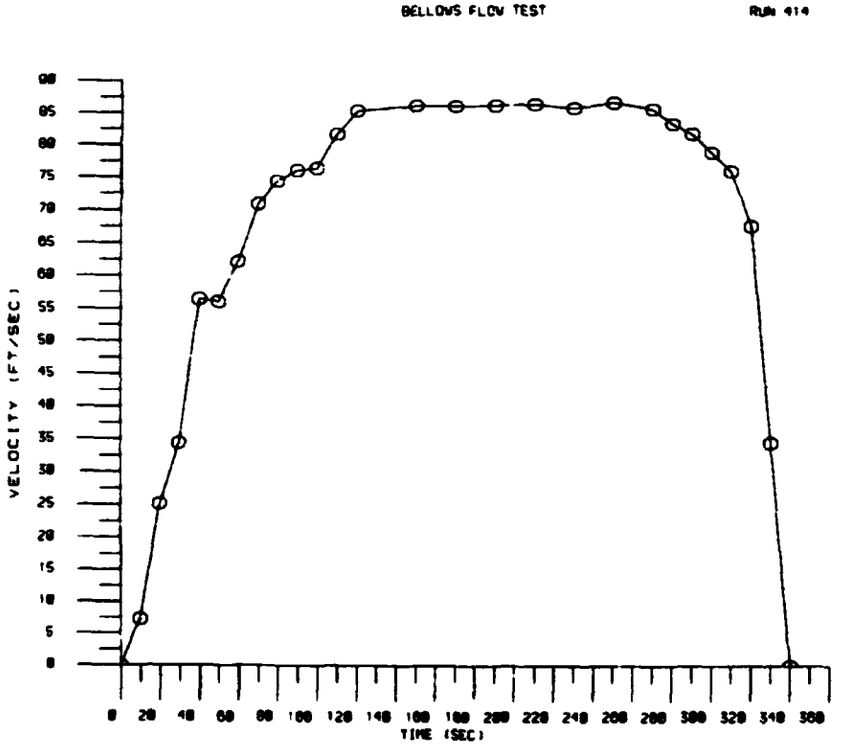

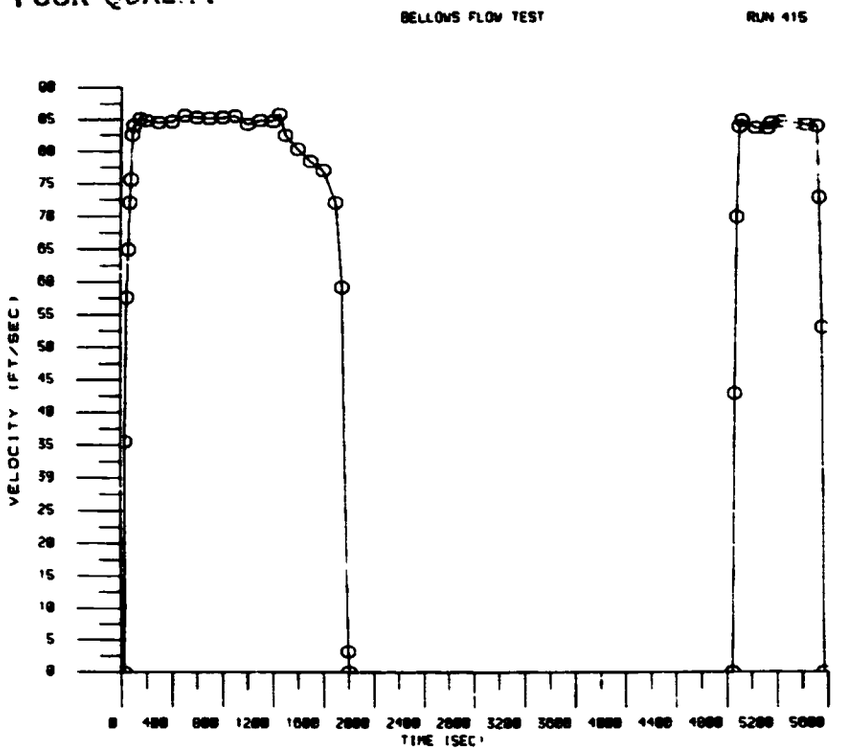

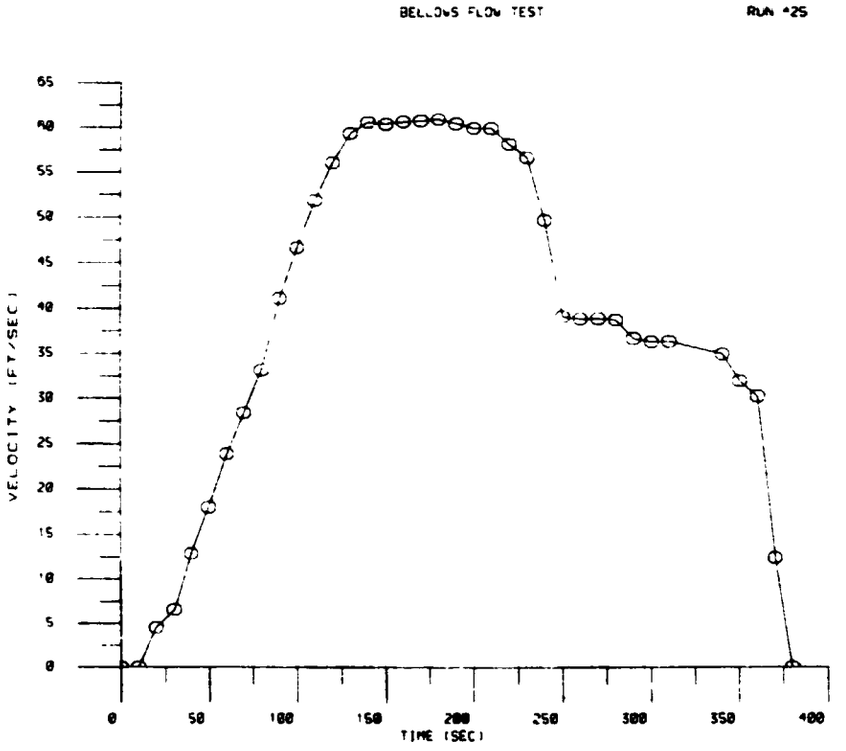

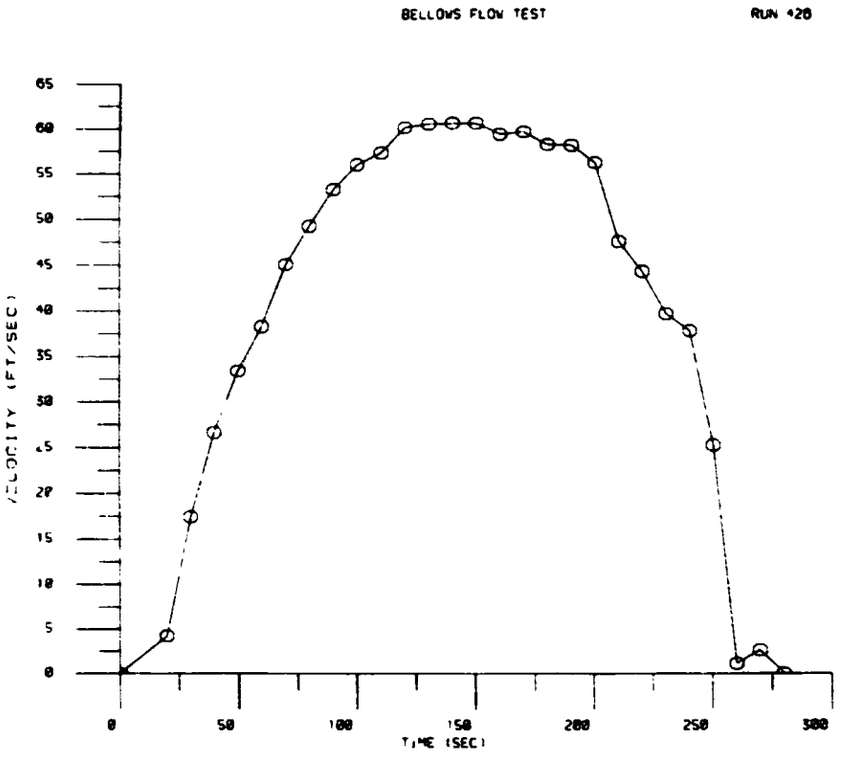

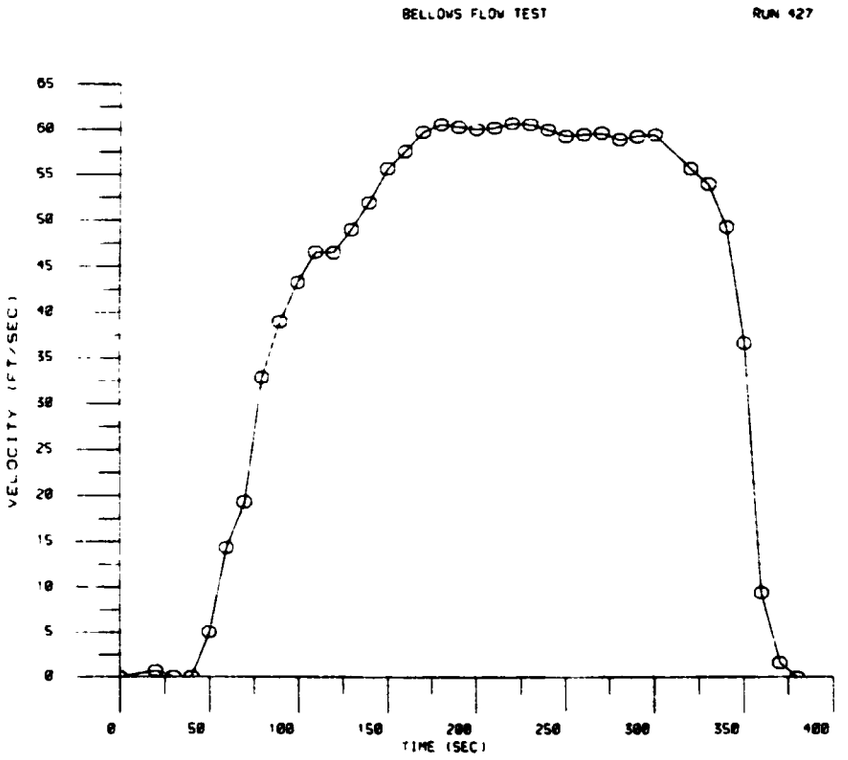

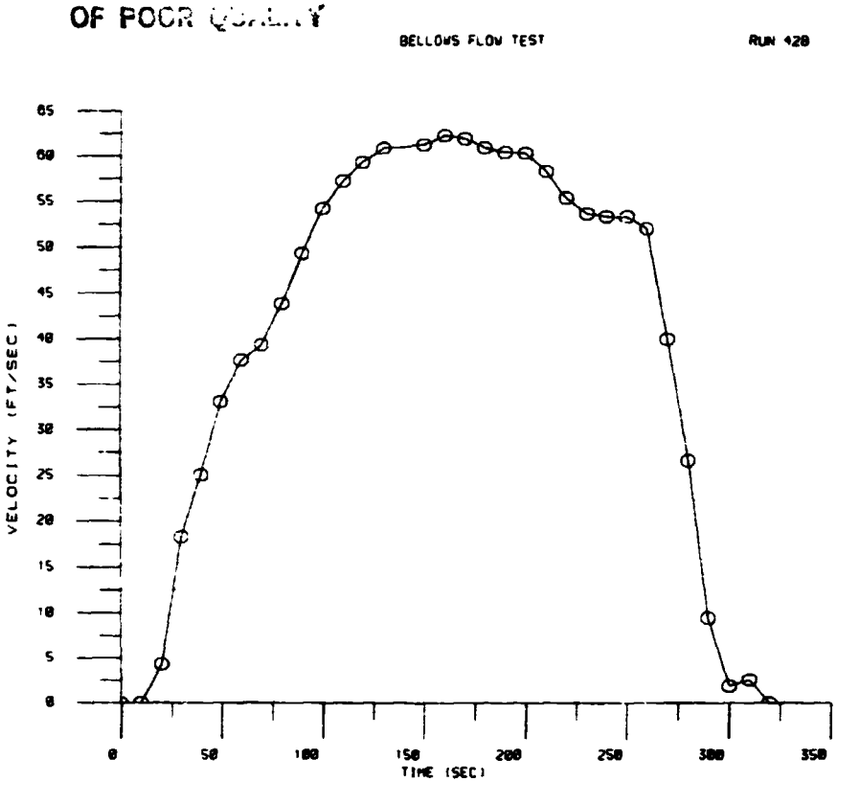

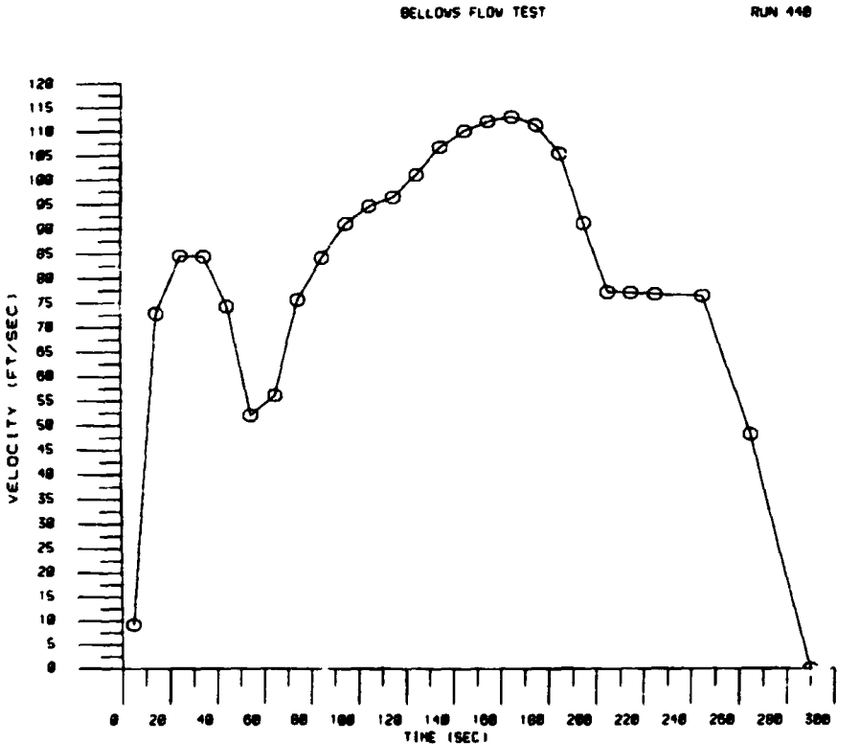

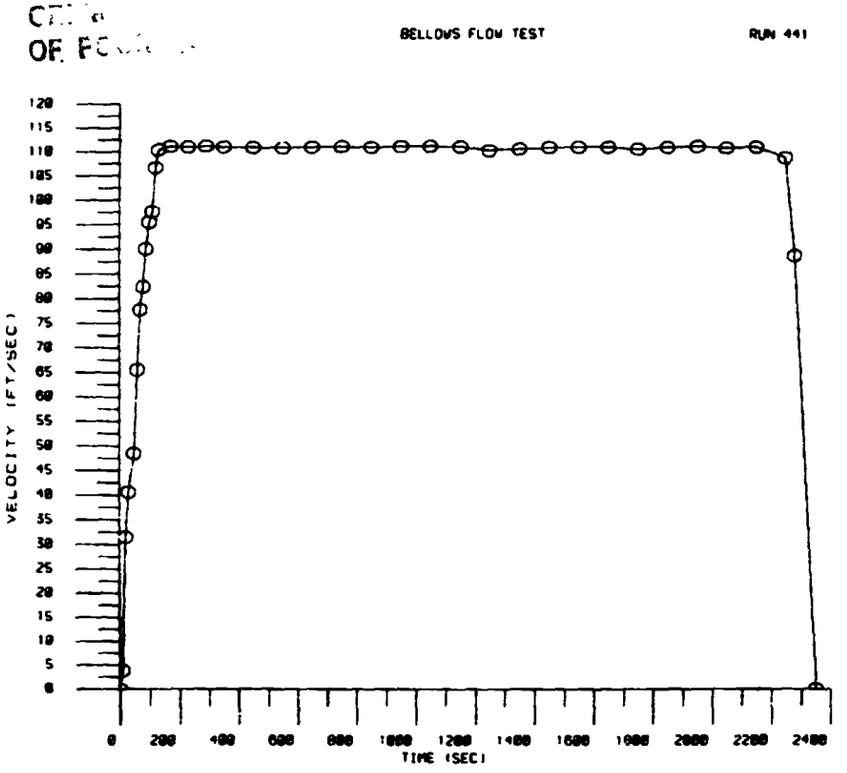
BELLOWS FLOW TEST
RUN 441
VELOCITY (FT/SEC)
TIME (SEC)

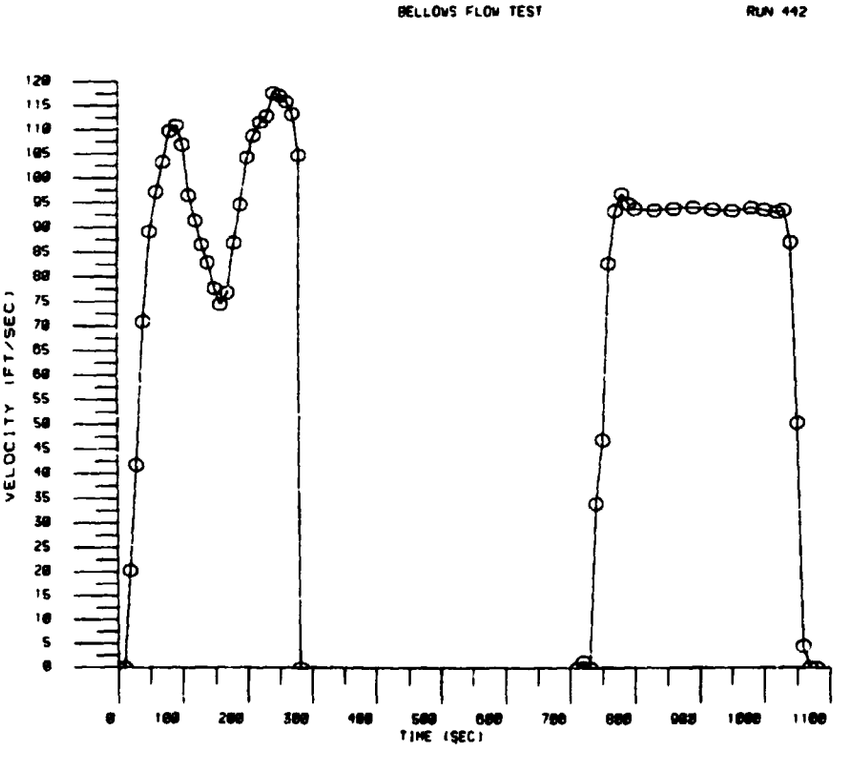
BELLOWS FLOW TEST
RUN 442
VELOCITY (FT/SEC)
TIME (SEC)

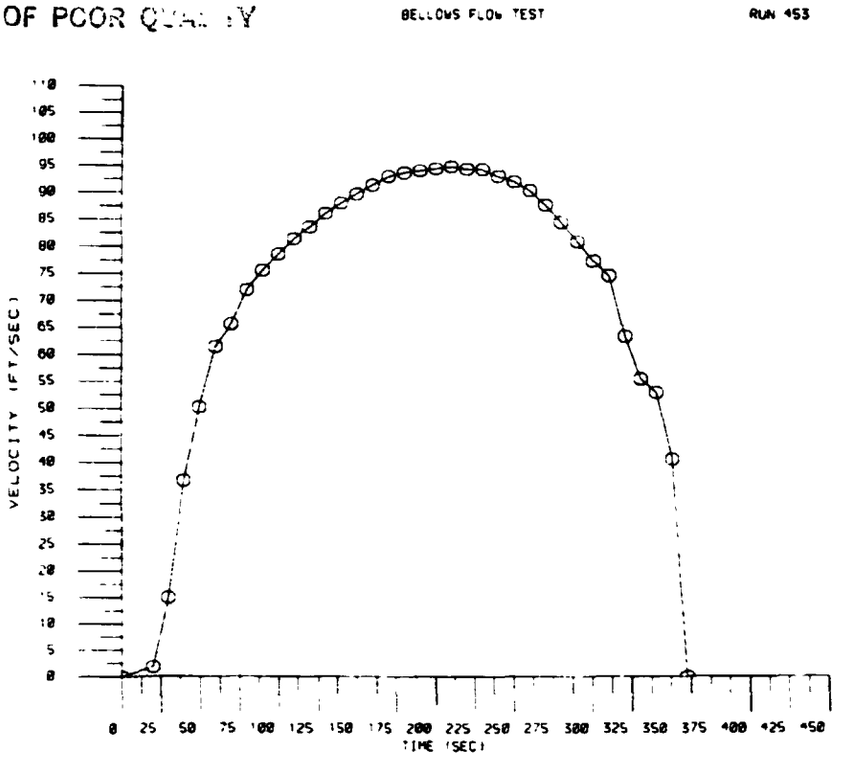

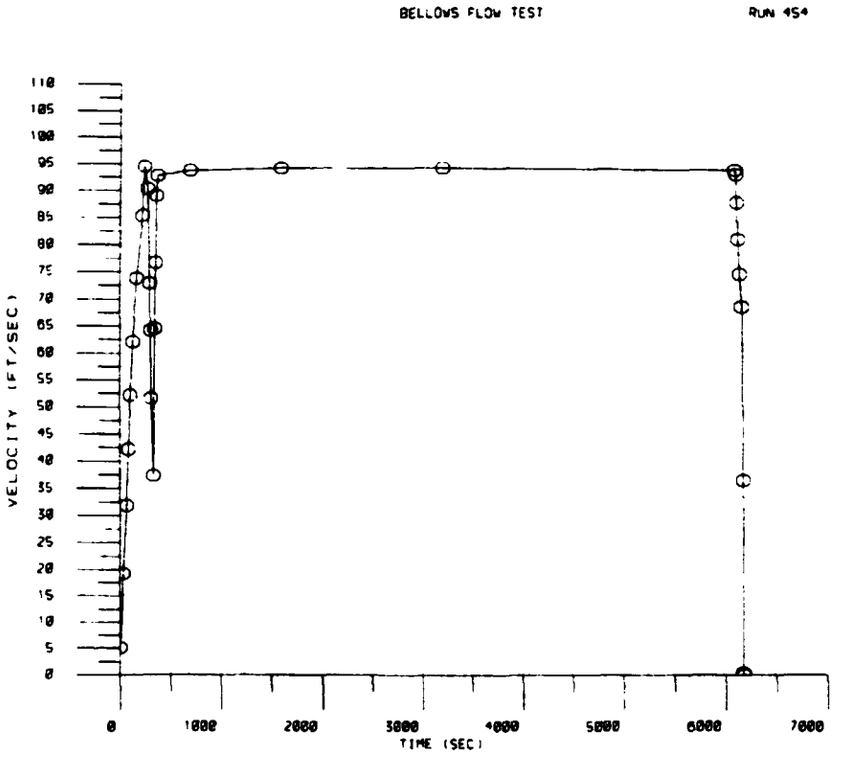

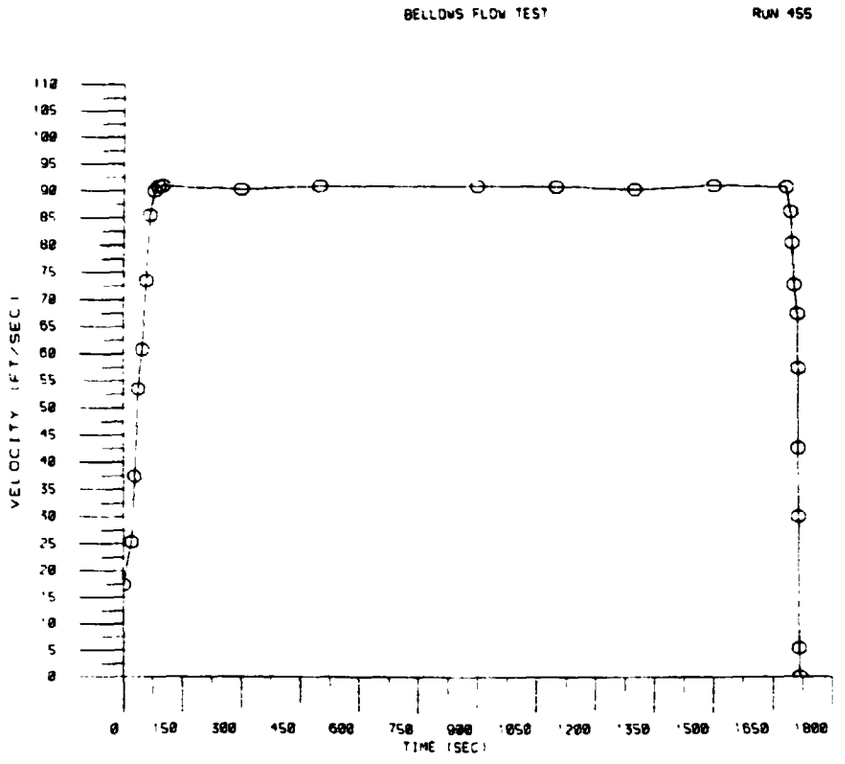
BELLOWS FLOW TEST
RUN 455
VELOCITY (FT/SEC)
TIME (SEC)

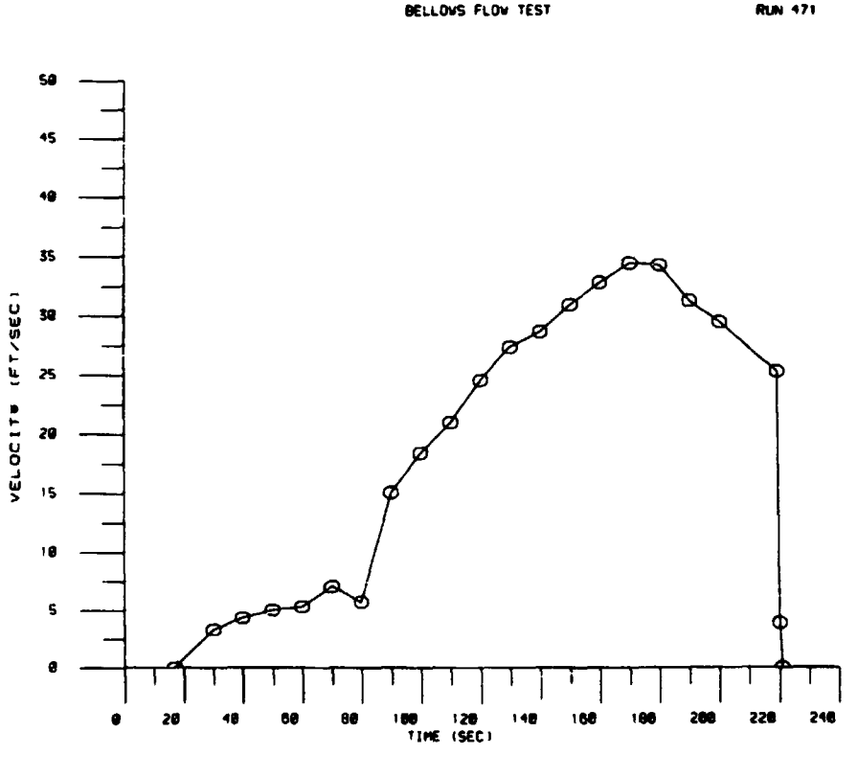
BELLOWS FLOW TEST
RUN 471
VELOCITY (FT/SEC)
TIME (SEC)

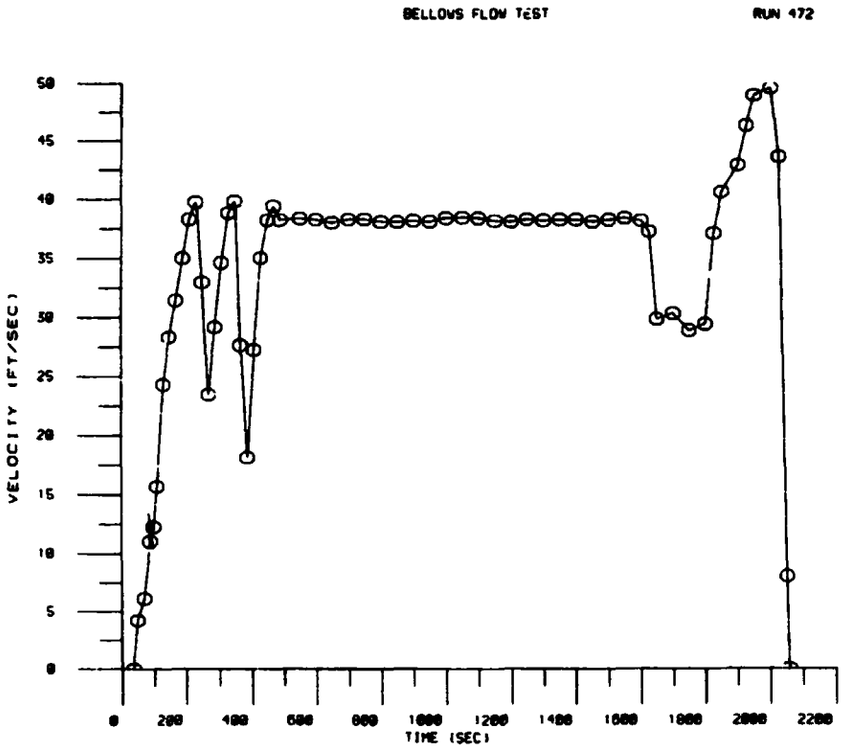

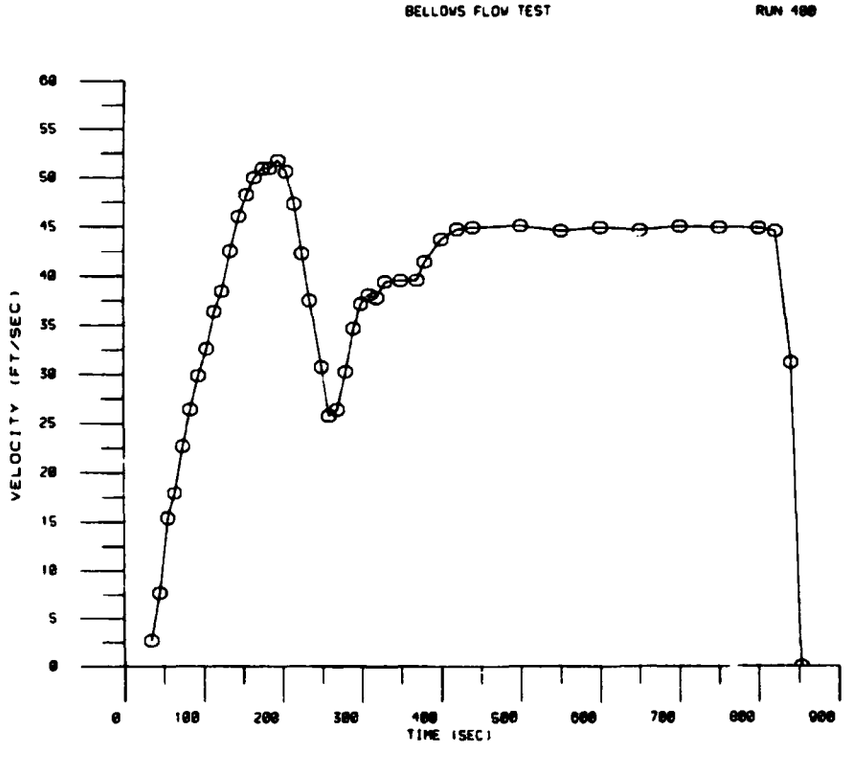

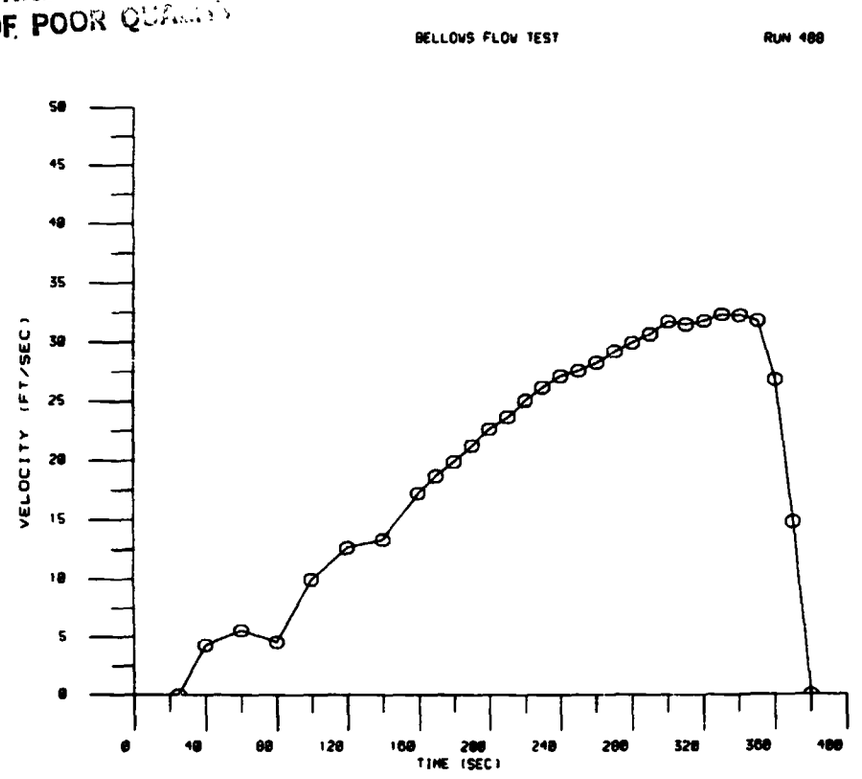

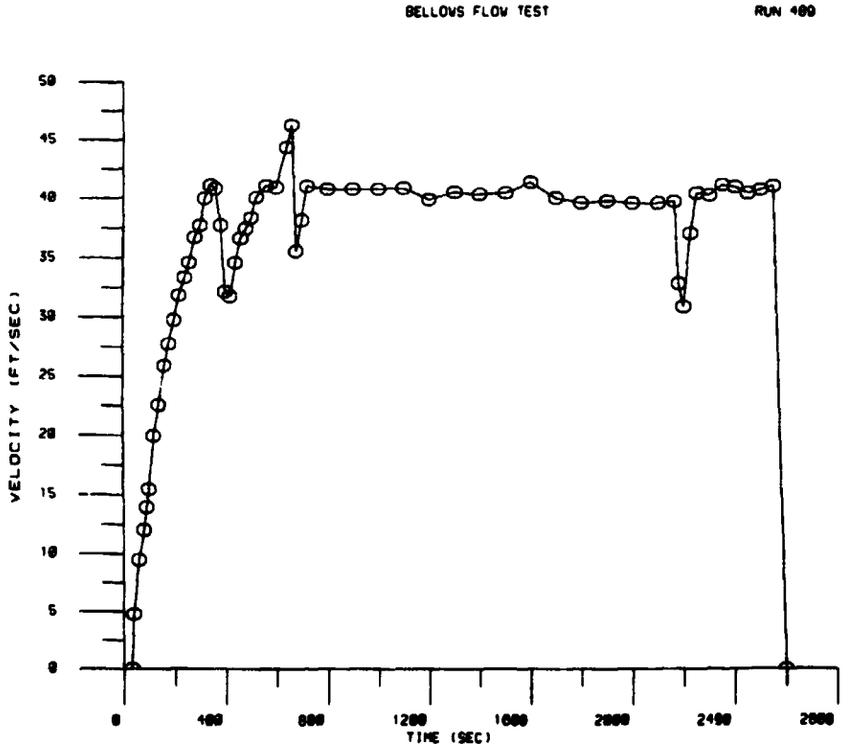

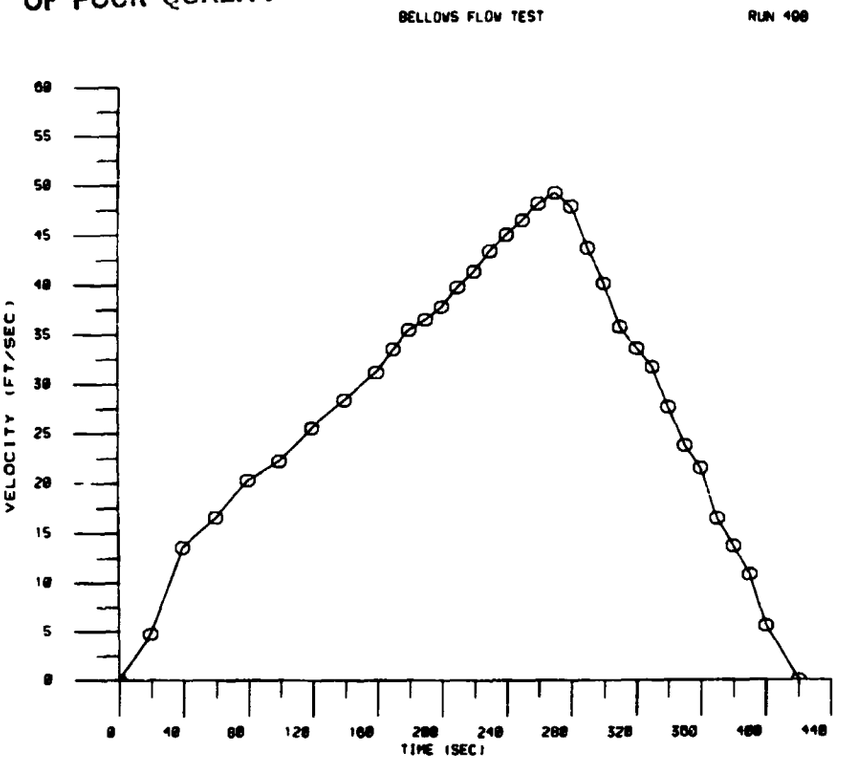

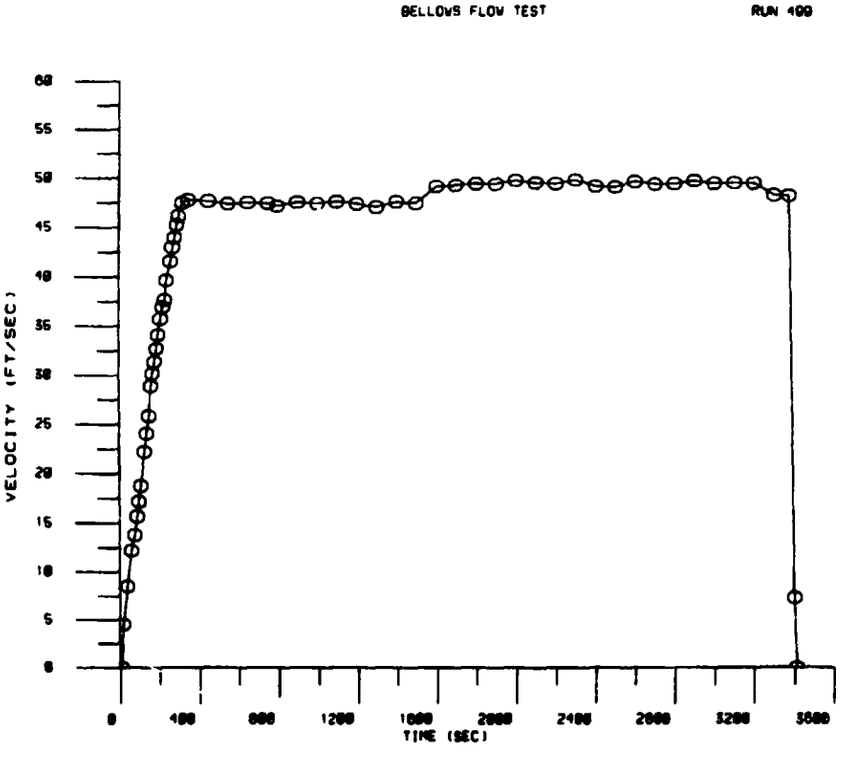

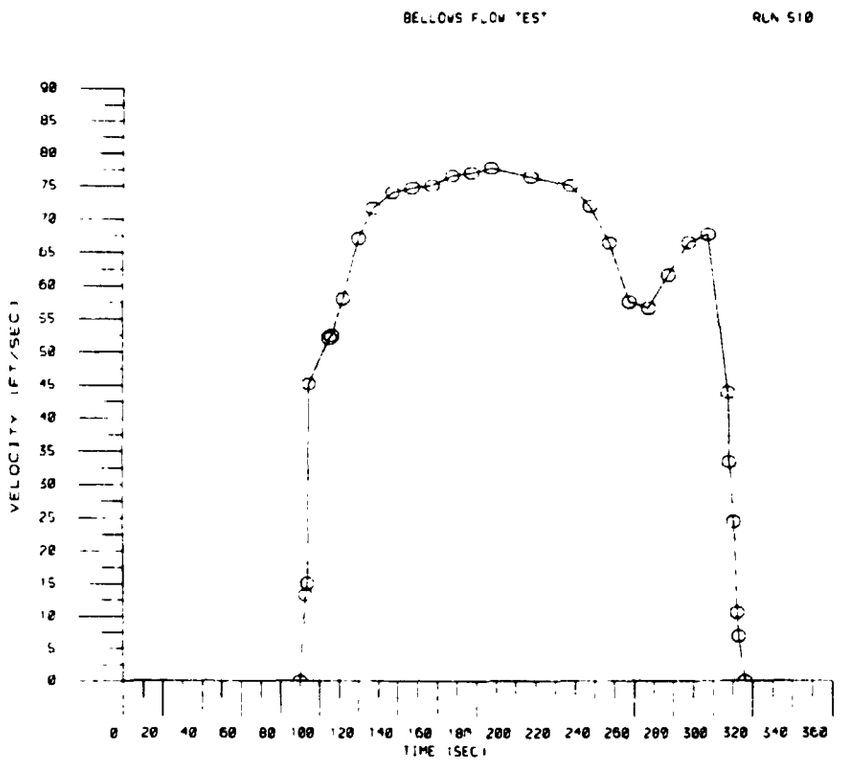
BELLOWS FLOW TEST
RUN S10
VELOCITY (FT/SEC)
TIME (SEC)

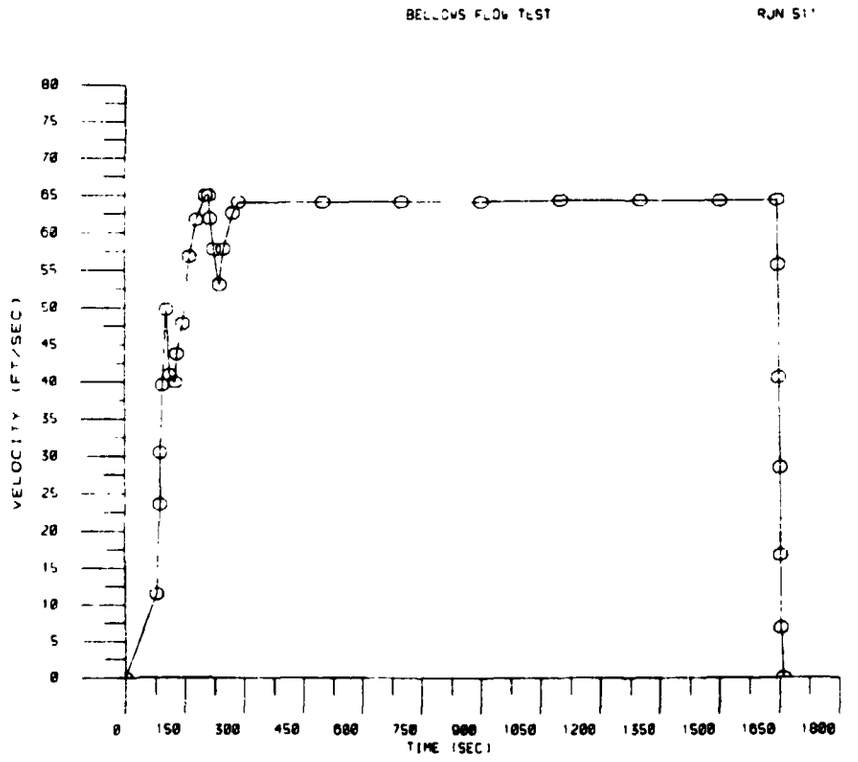
BELLOWS FLOW TEST
RUN S11
VELOCITY (FT/SEC)
TIME (SEC)

ORIGINAL PAGE IS
OF POOR QUALITY

BELLOWS FLOW TEST RUN 512

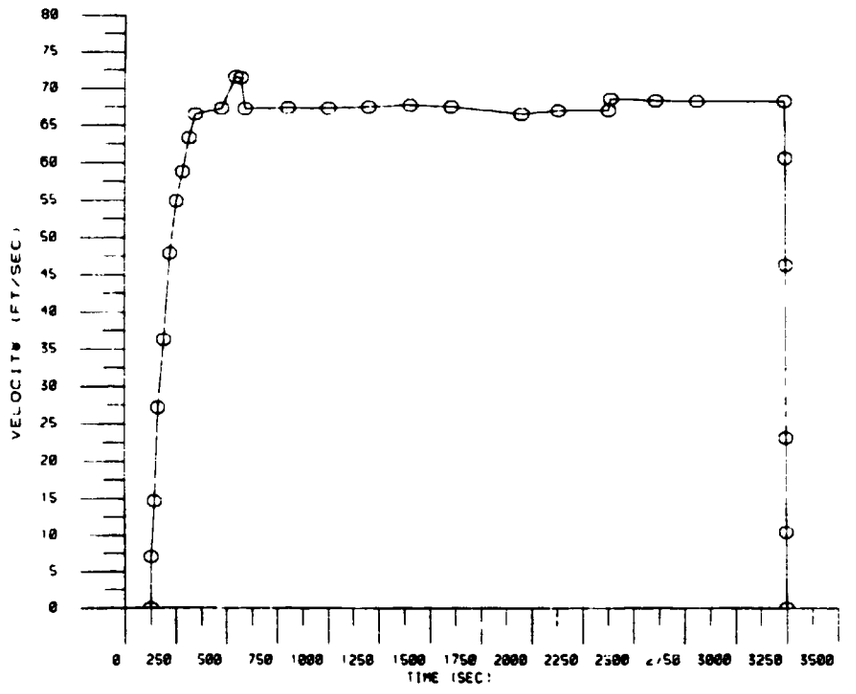

BELLOWS FLOW TEST RUN 513

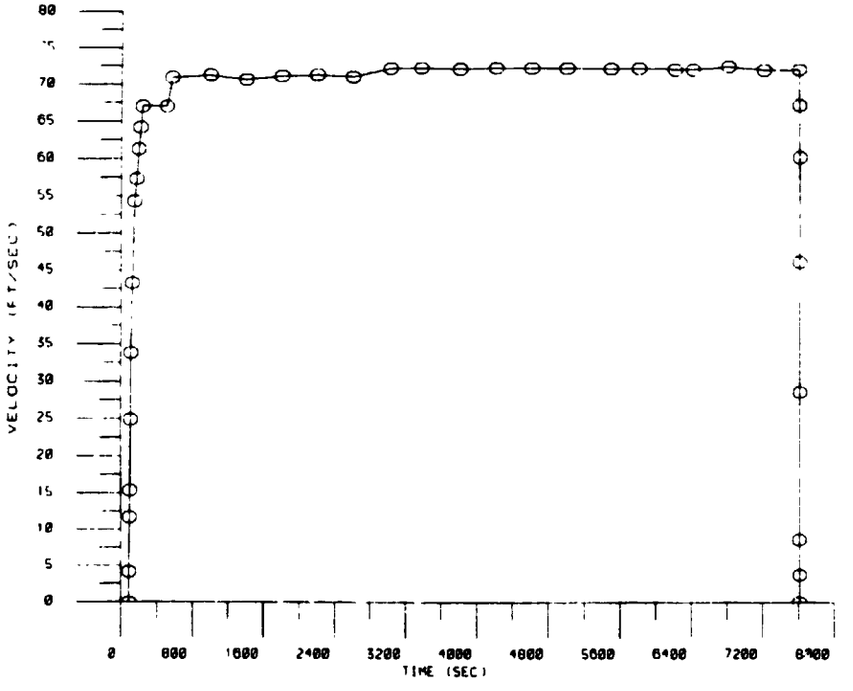

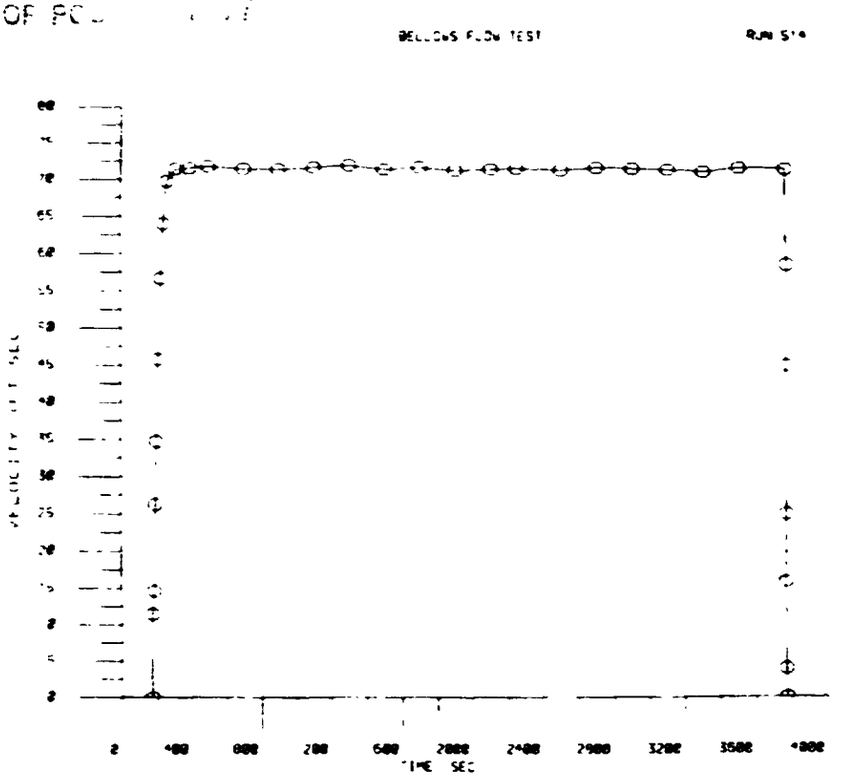
BELLOWS FLOW TEST
RUN S24
TIME SEC

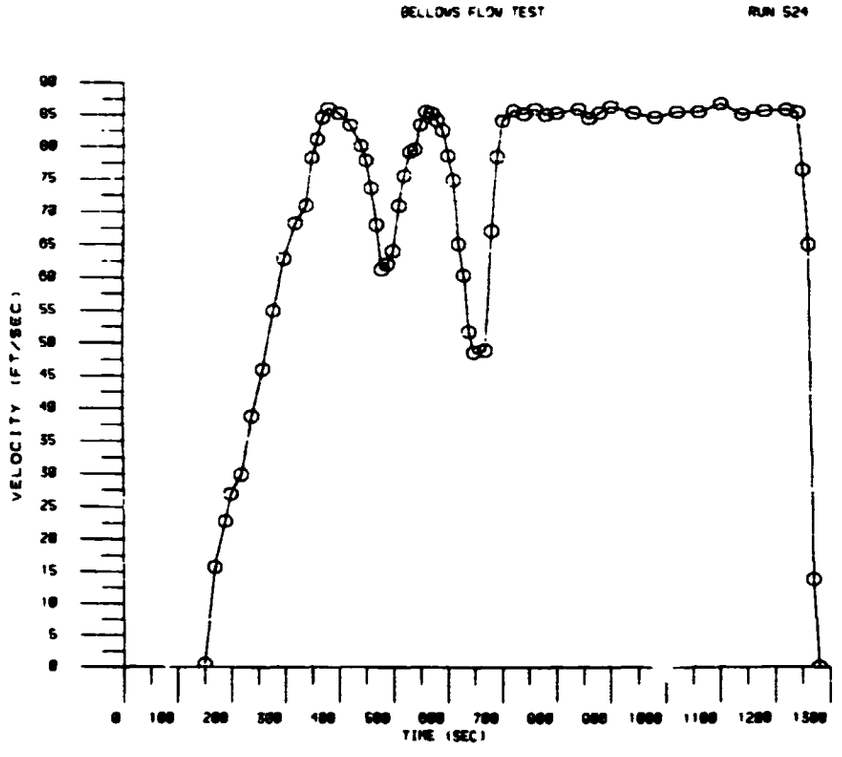
BELLOWS FLOW TEST
RUN S24
VELOCITY (FT/SEC)
TIME (SEC)

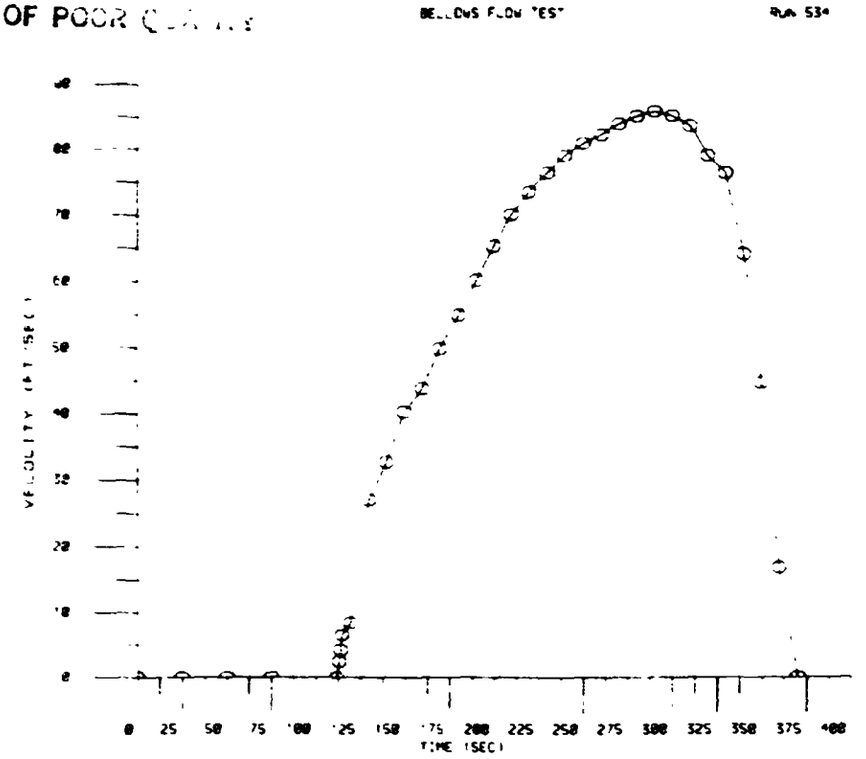

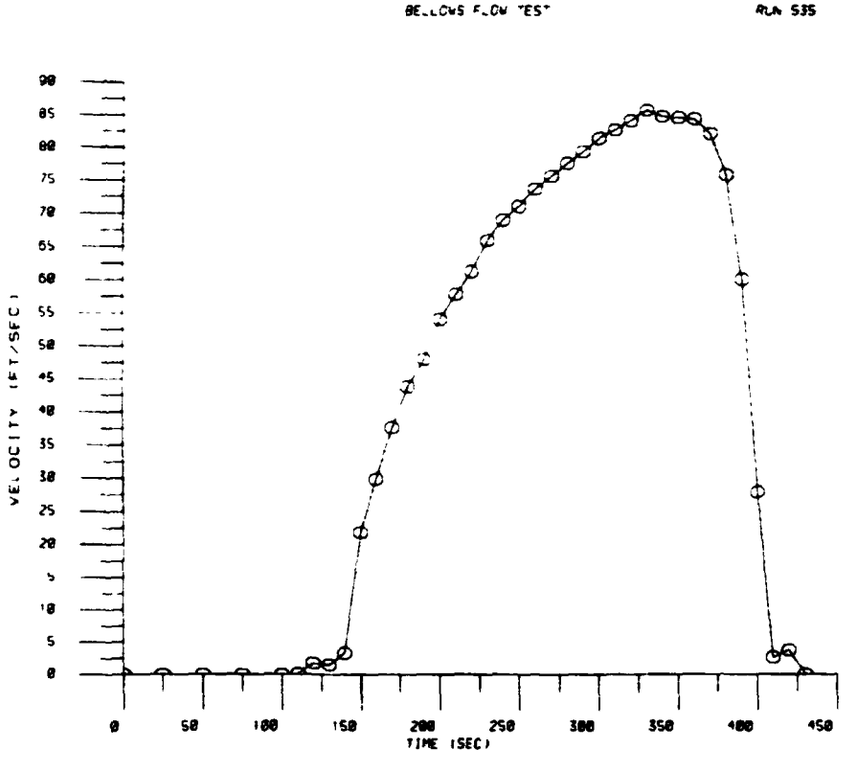

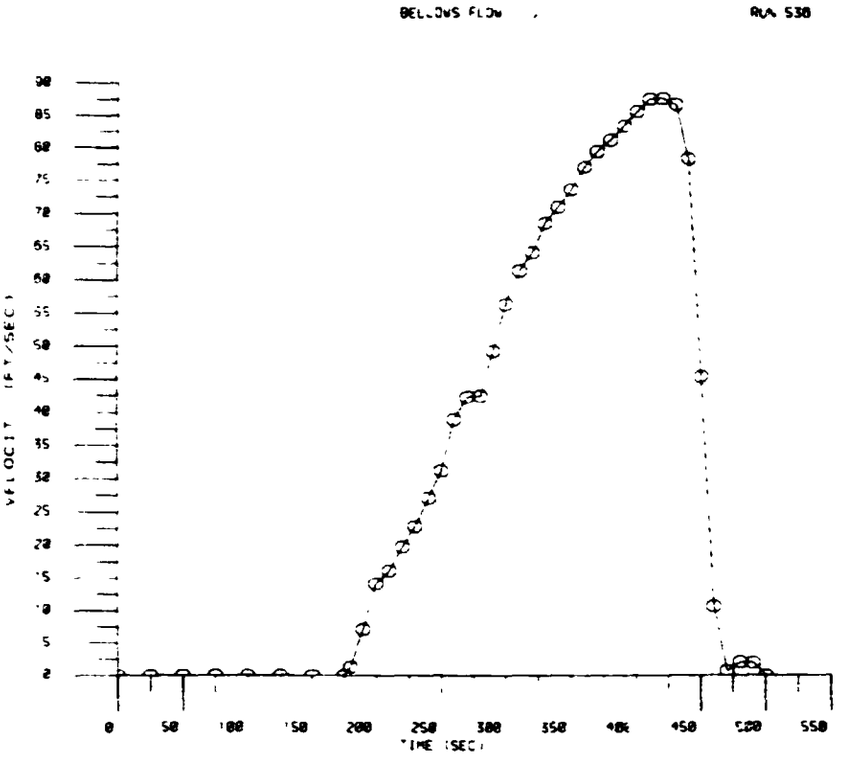
BELLOWS FLOW
RUN 530
VELOCITY (FT/SEC)
0
5
10
15
20
25
30
35
40
45
50
55
60
65
70
75
80
85
90
0
50
100
150
200
250
300
350
400
450
500
550
TIME (SEC)

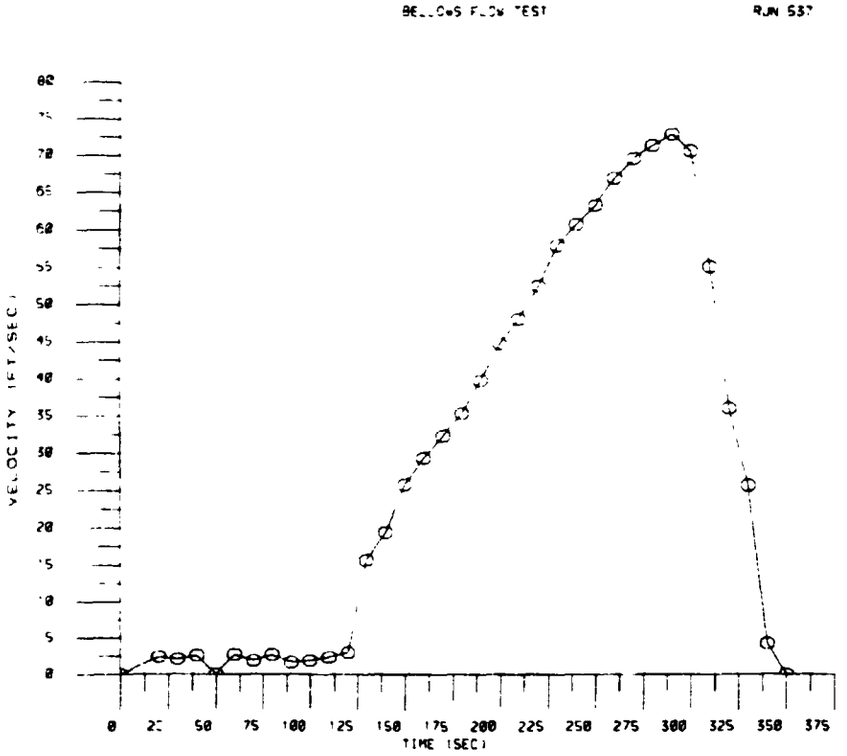
BELLOWS FLOW TEST
RUN 537
VELOCITY (FT/SEC)
0
5
10
15
20
25
30
35
40
45
50
55
60
65
70
75
80
0
25
50
75
100
125
150
175
200
225
250
275
300
325
350
375
TIME (SEC)

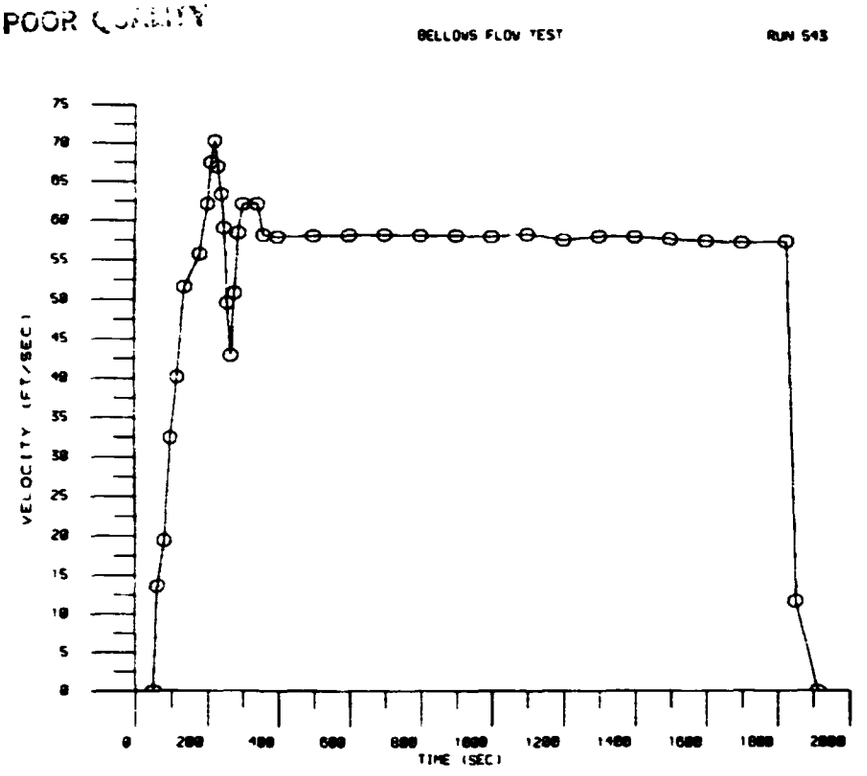

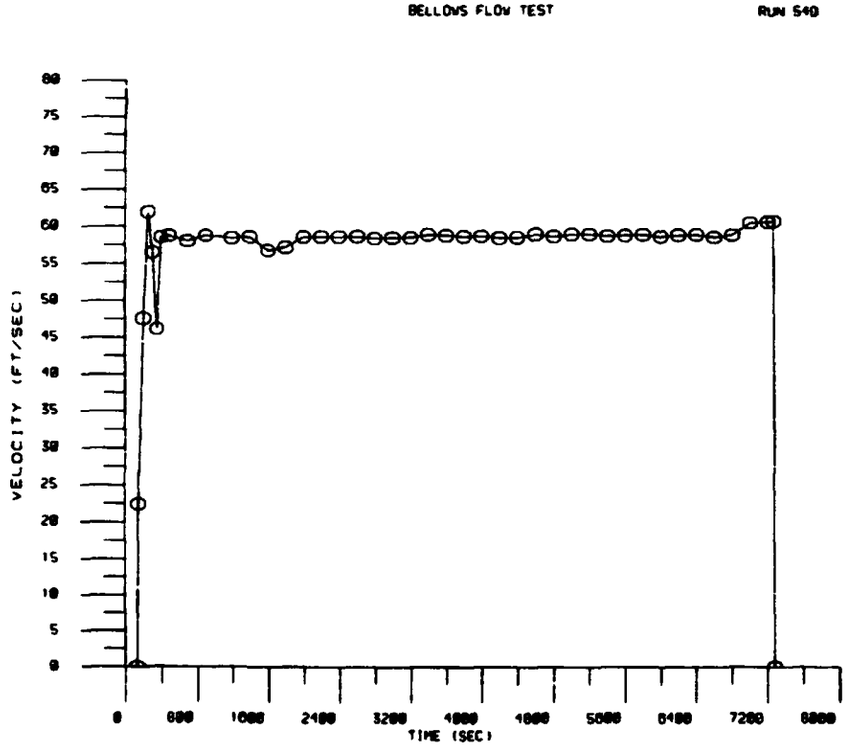

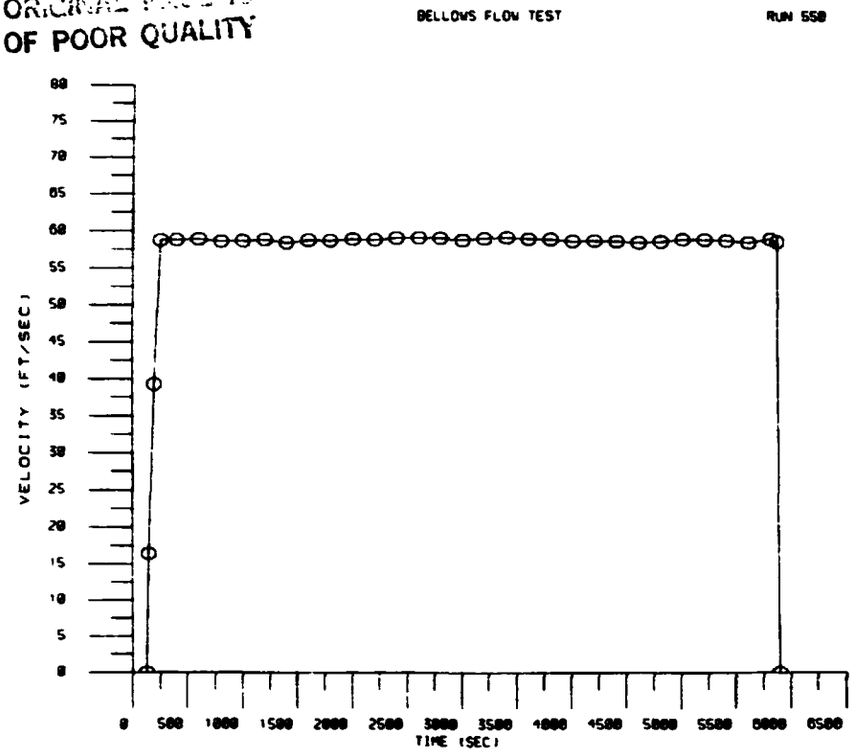

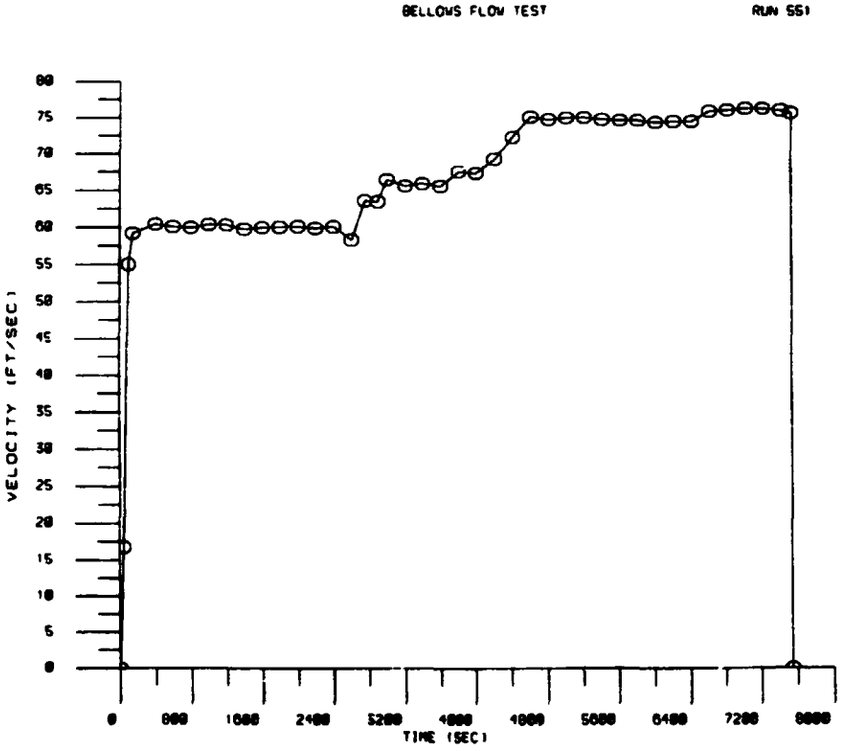

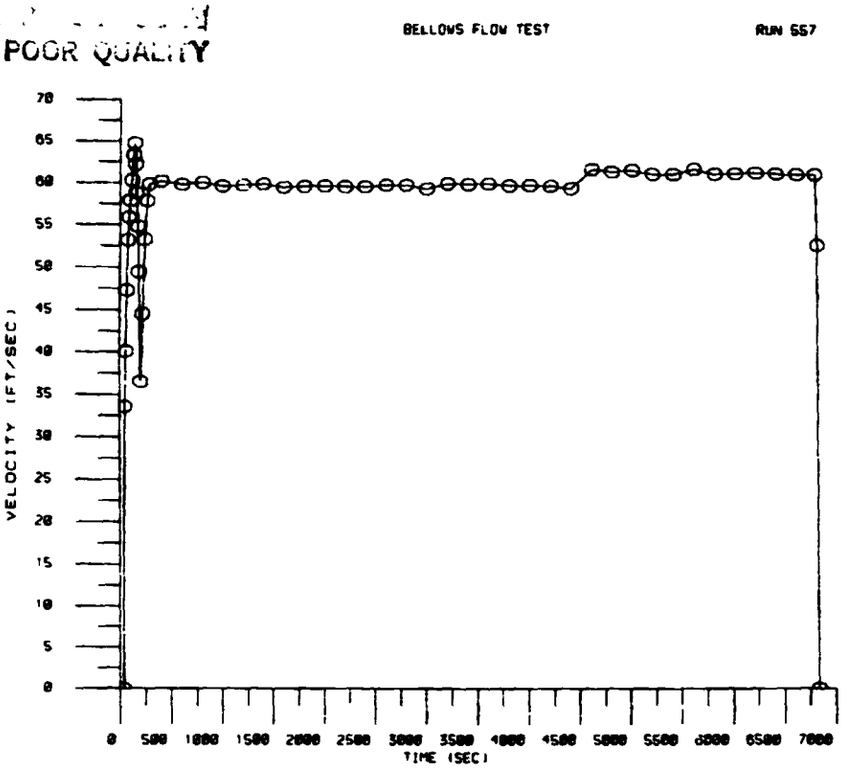

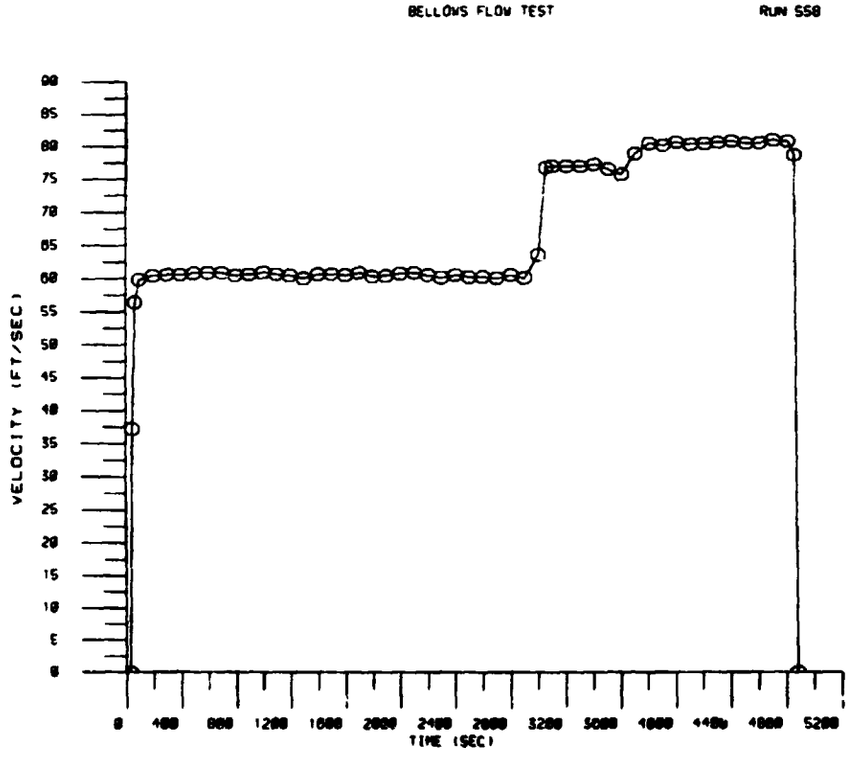

BELLOWS FLOW TEST RUN 584

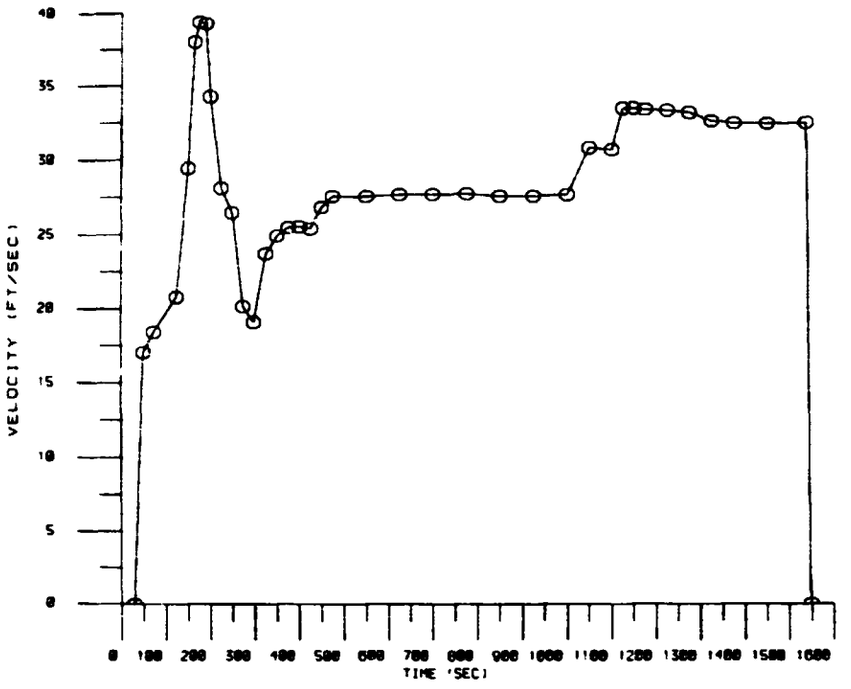

BELLOWS FLOW TEST RUN 585

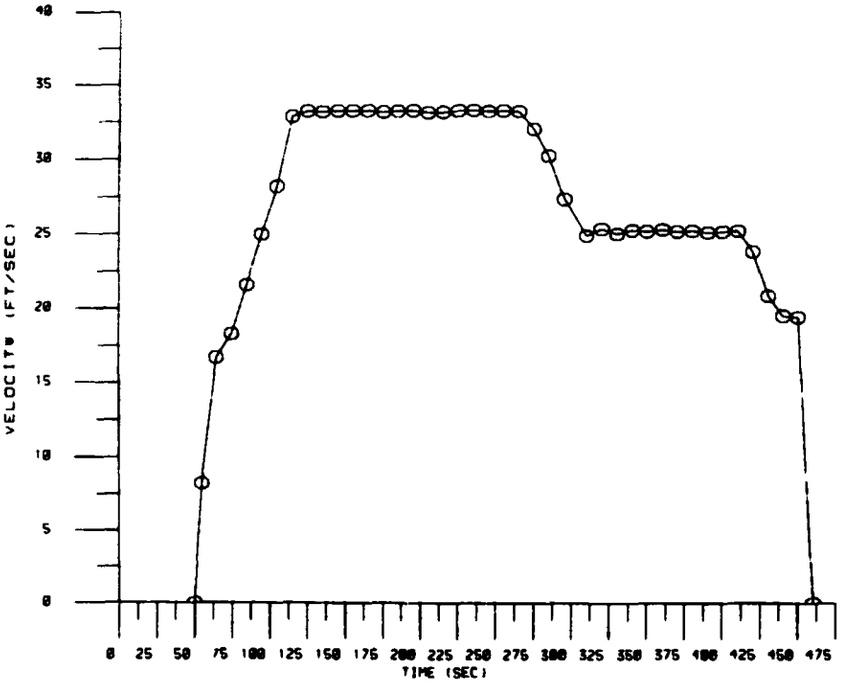

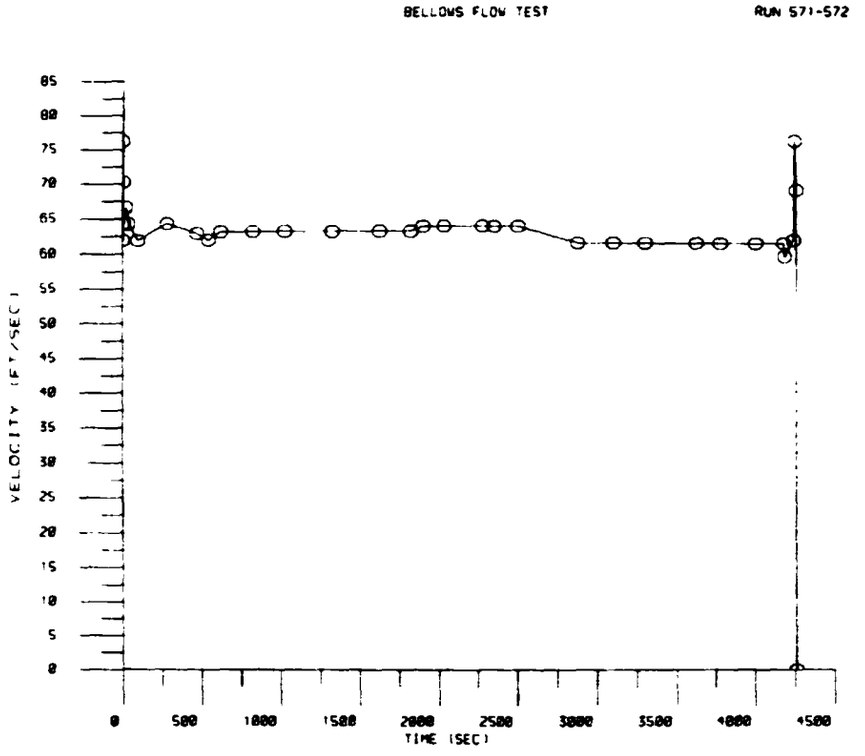

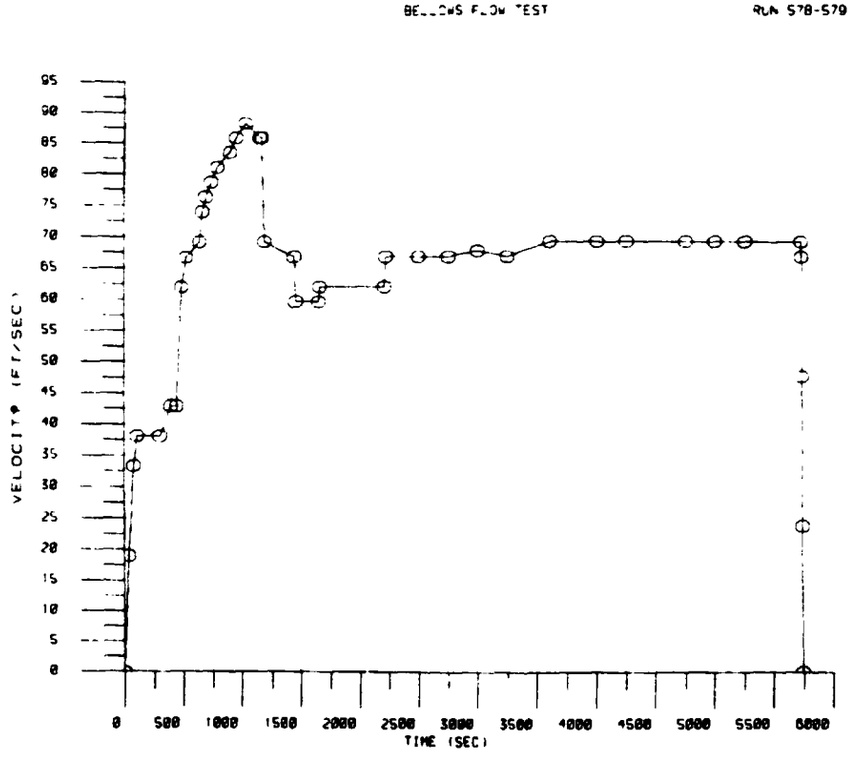

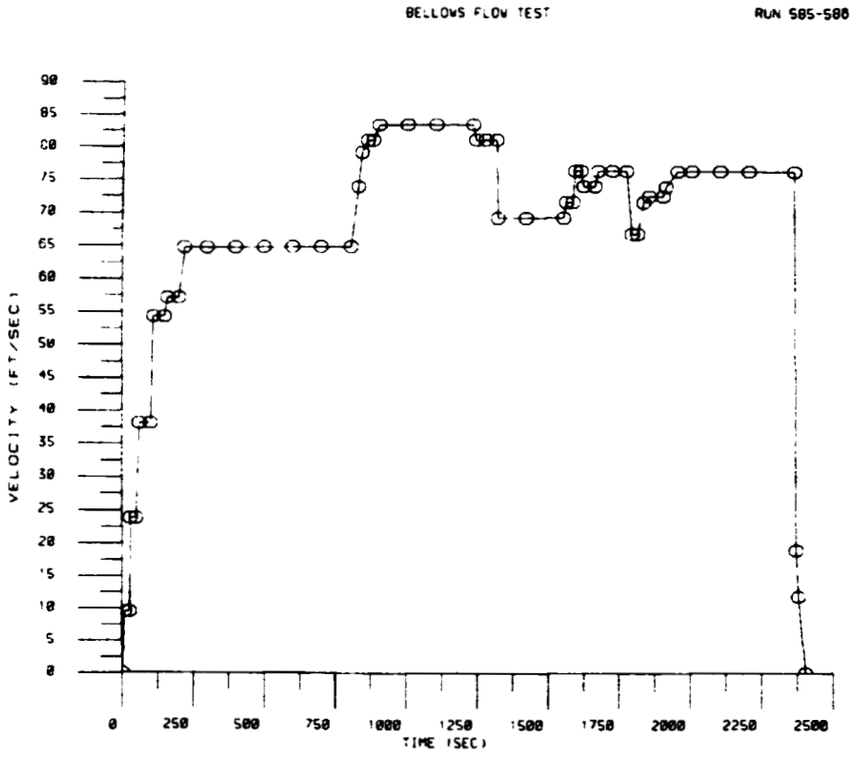

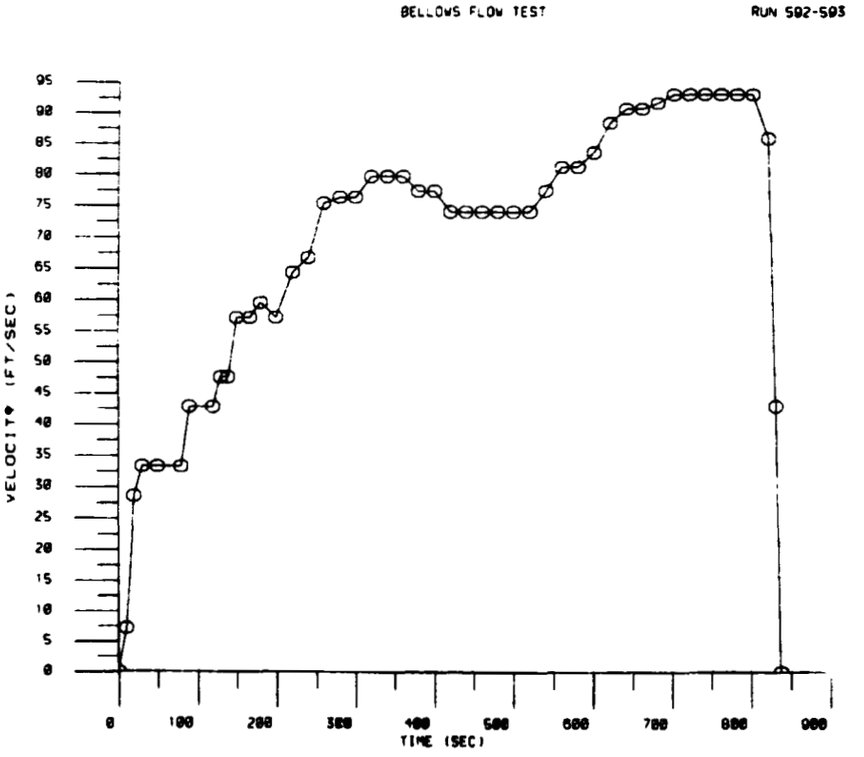

BELLOWS FLOW TEST RUN 590-600

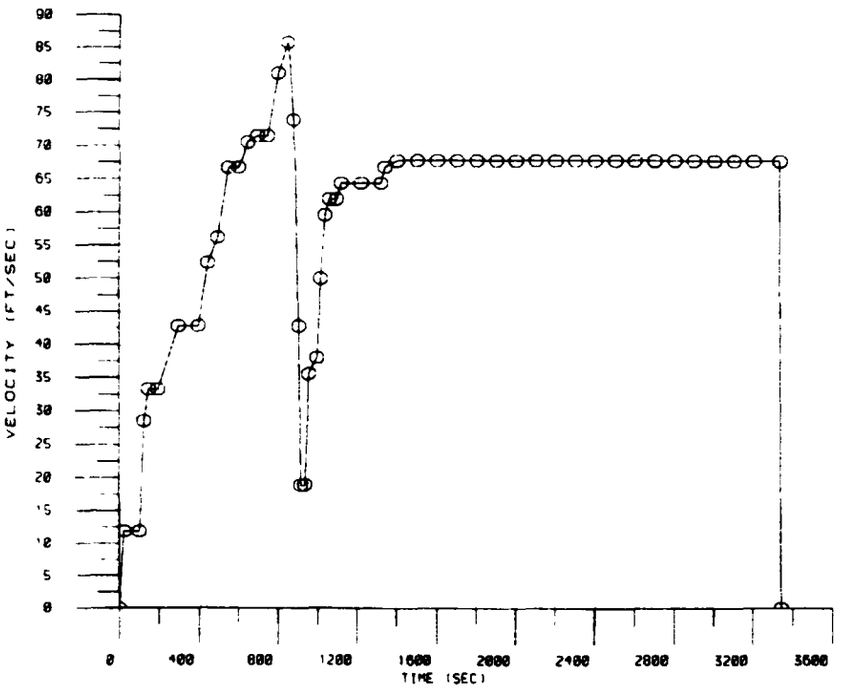

BELLOWS FLOW TEST RUN 600-607

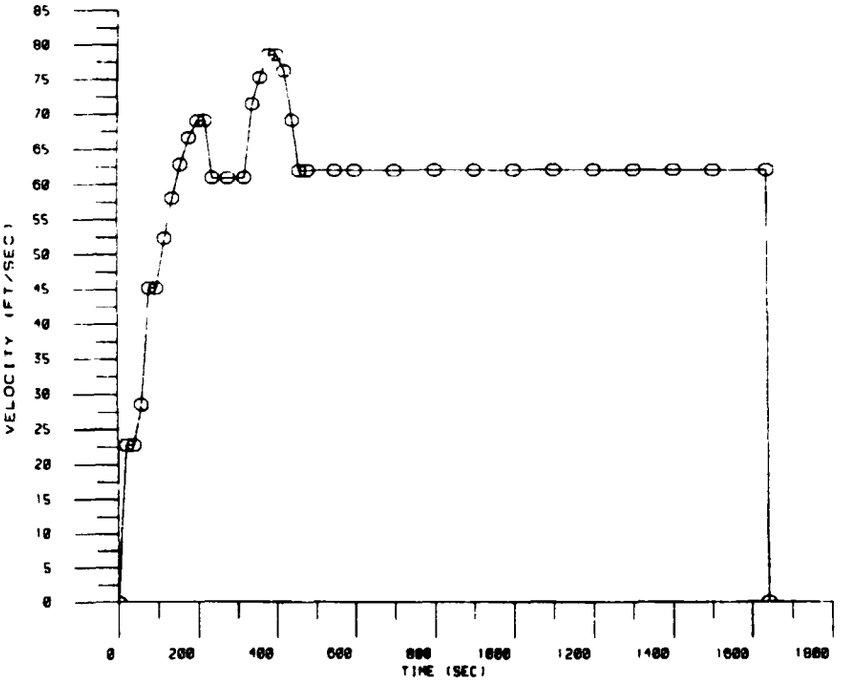

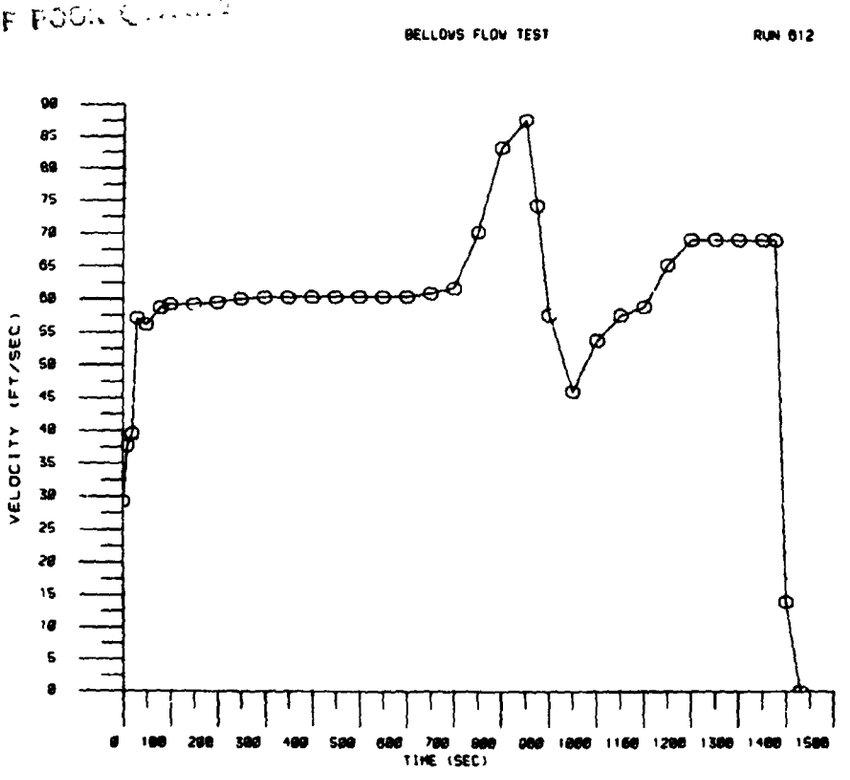
BELLOWS FLOW TEST
RUN 012
VELOCITY (FT/SEC)
TIME (SEC)

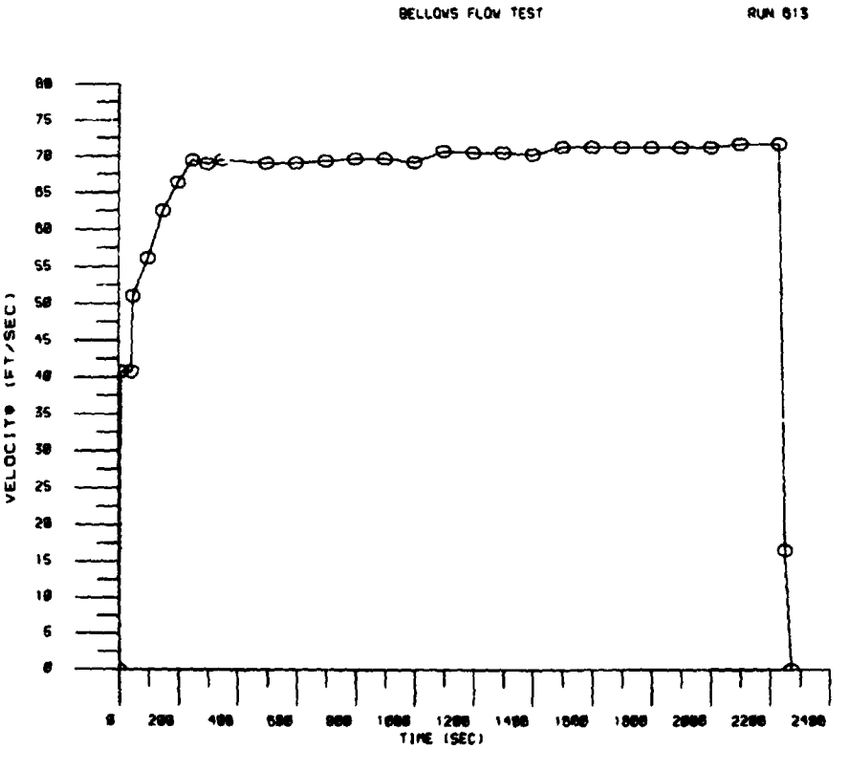
BELLOWS FLOW TEST
RUN 013
VELOCITY (FT/SEC)
TIME (SEC)

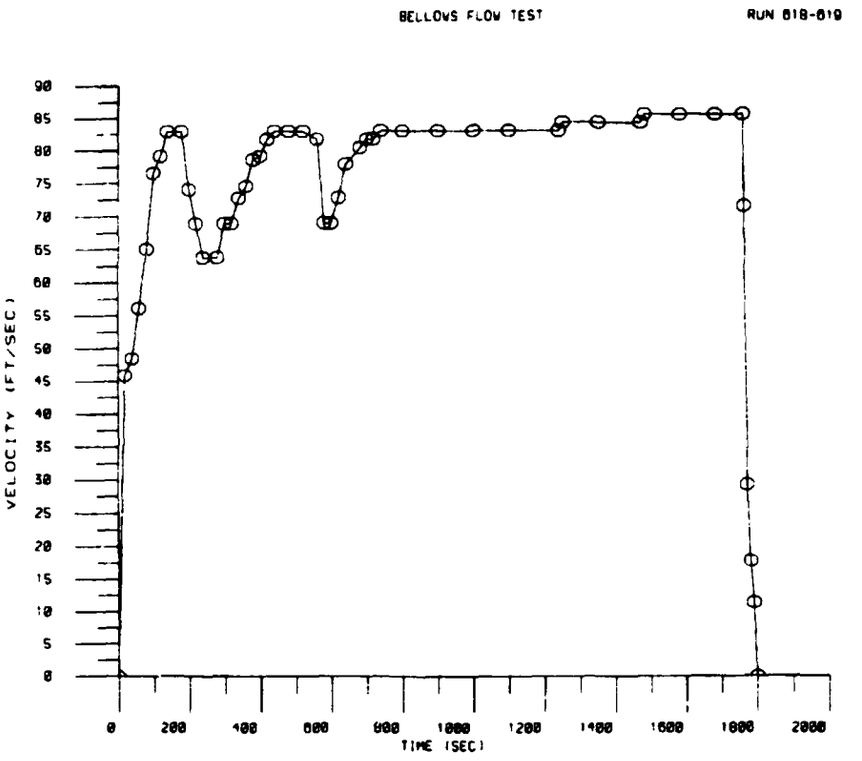

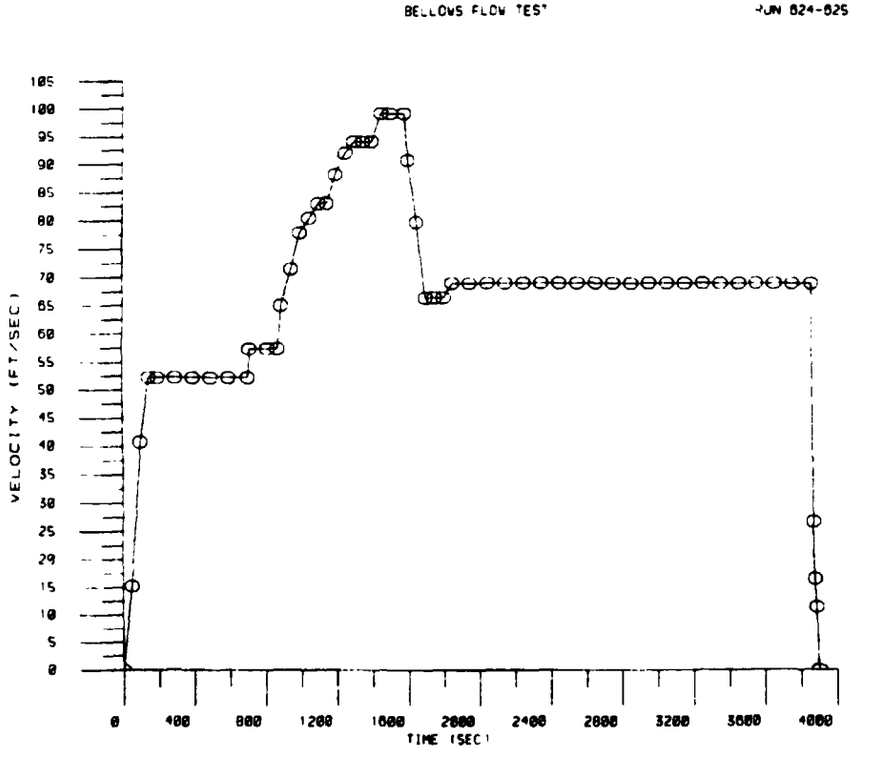

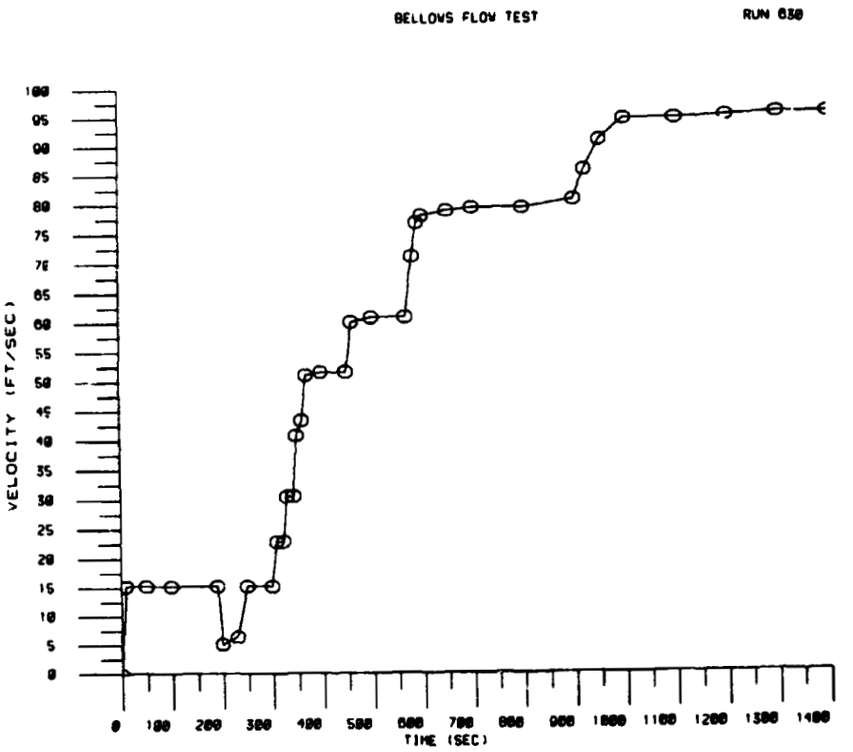

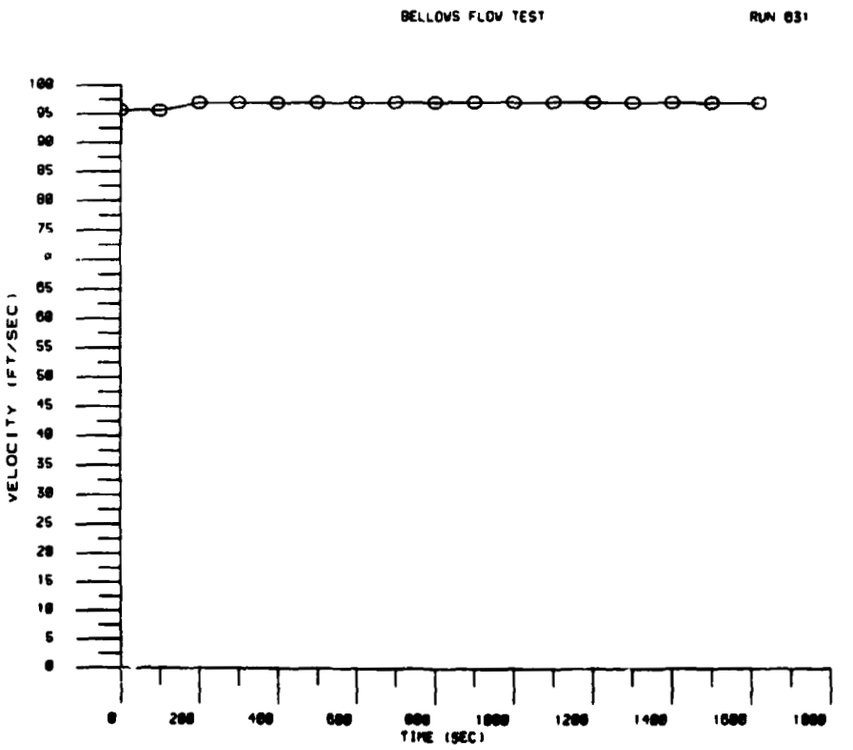

BELLOWS FLOW TEST RUN 632

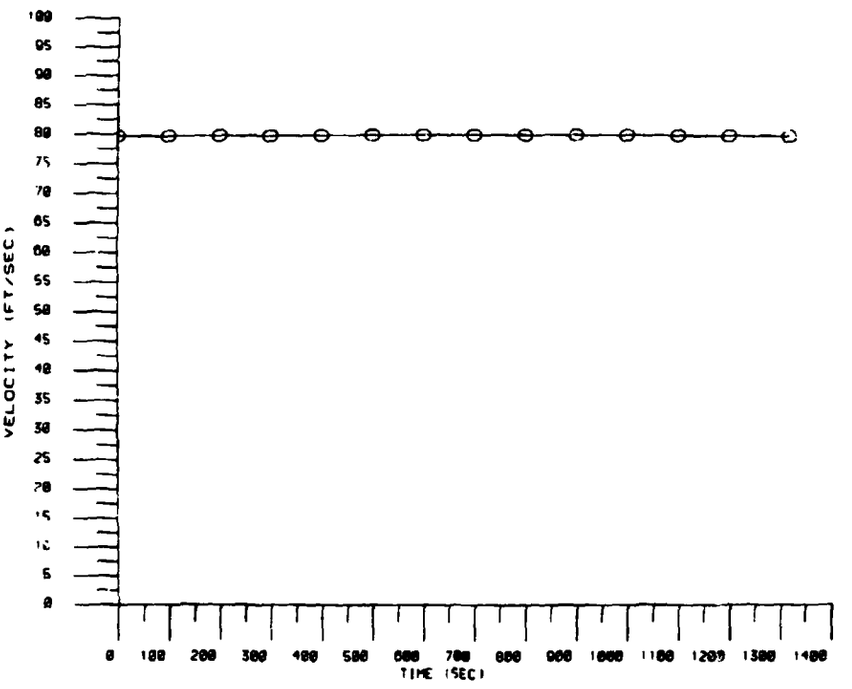

BELLOWS FLOW TEST RUN 637-638

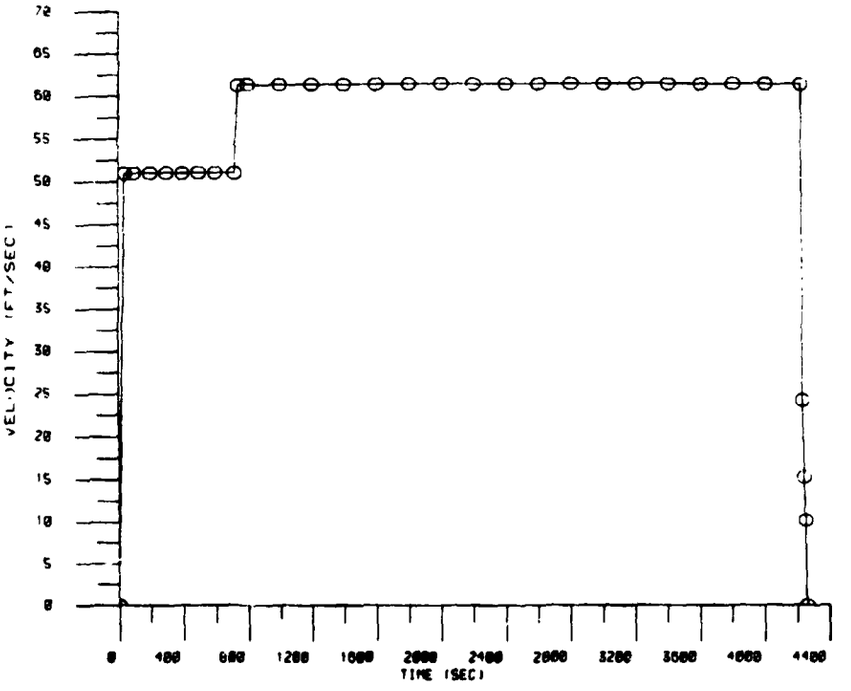

BELLOWS FLOW TEST RUN 843-844

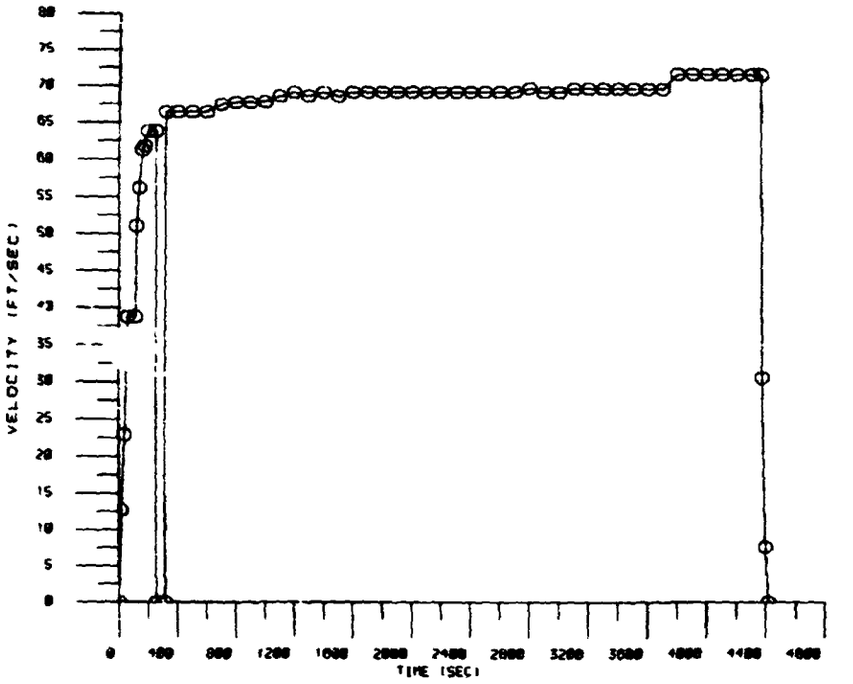

BELLOWS FLOW TEST RUN 849-852

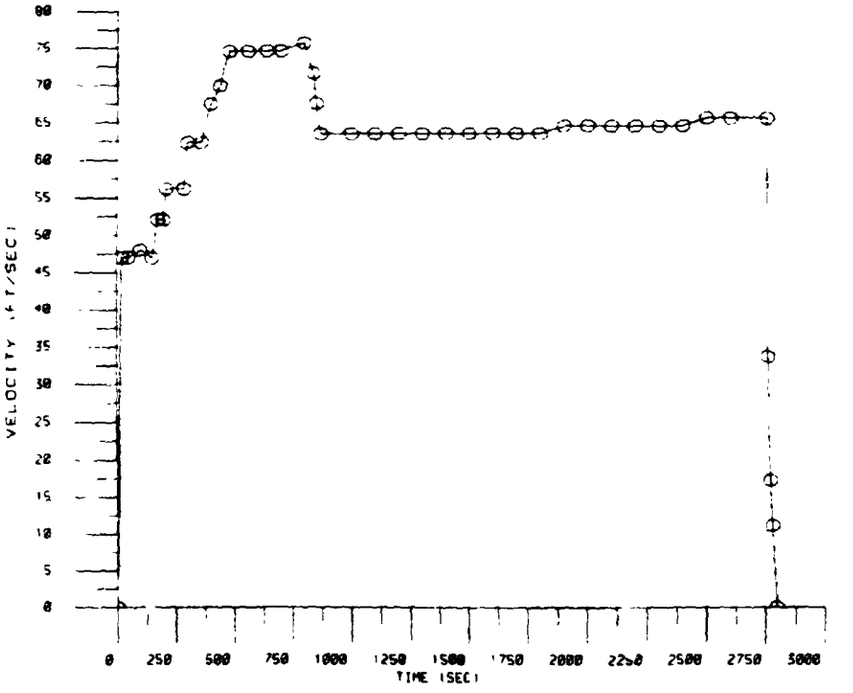

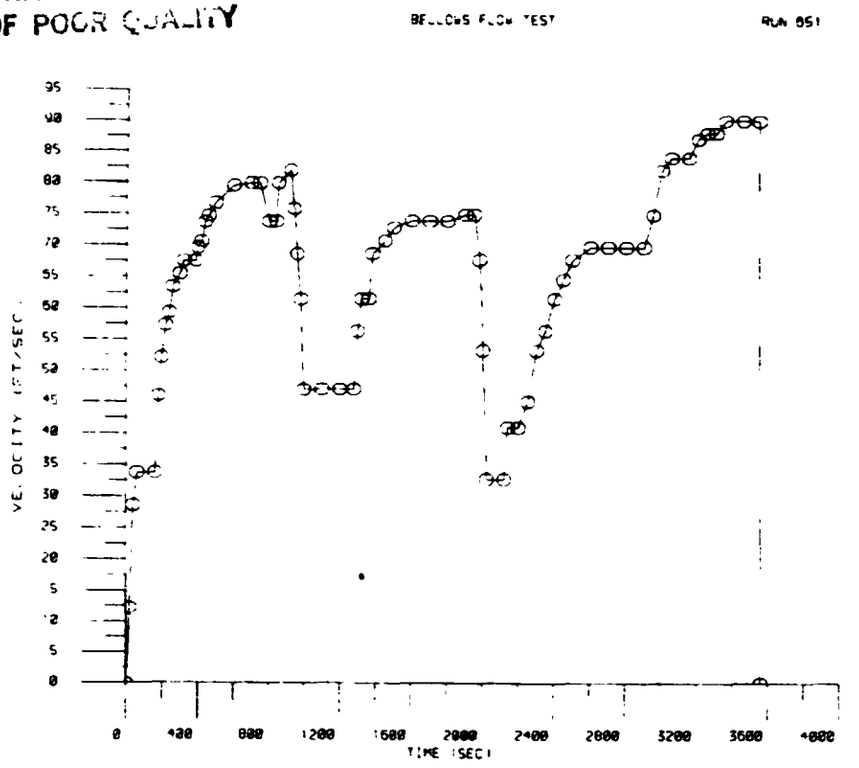

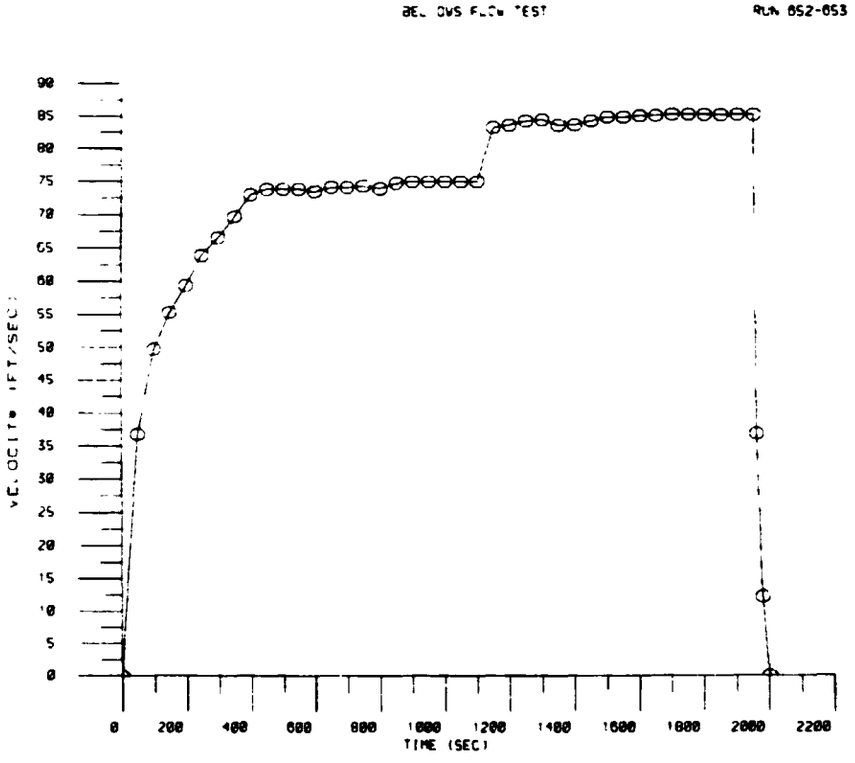

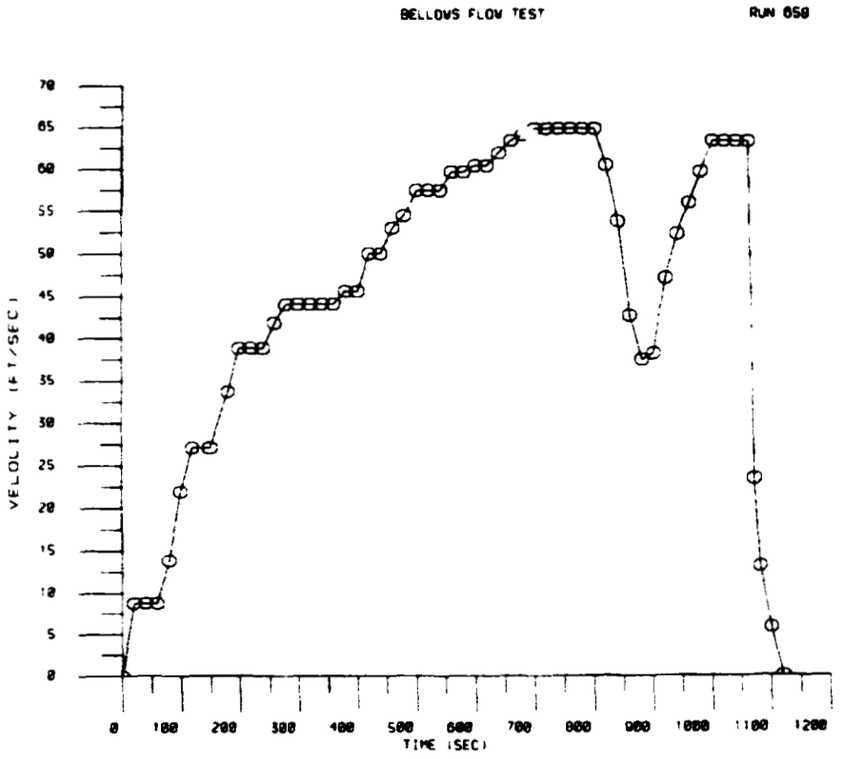

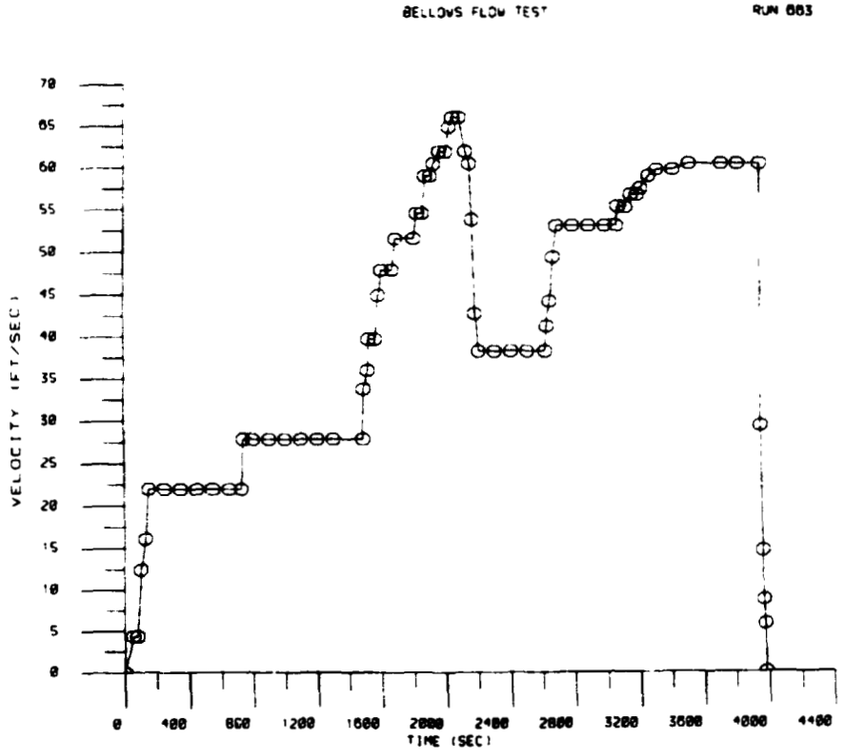

APPENDIX F

FREQUENCY VERSUS VELOCITY PLOTS AND POWER-SPECTRAL-DENSITY PLOTS FOR MSFC BELLOWS FLOW TESTS

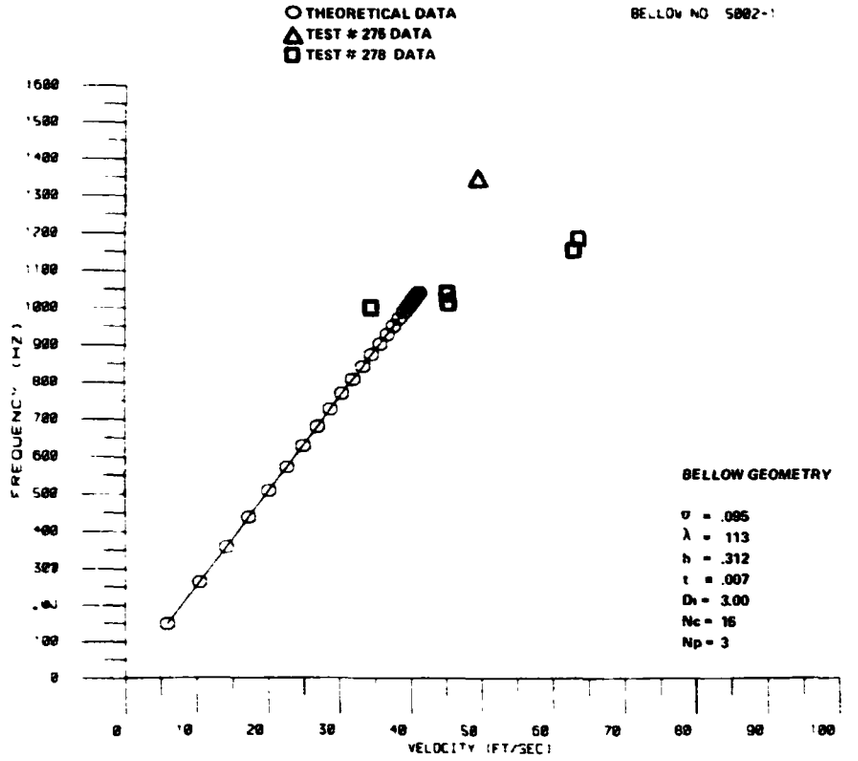

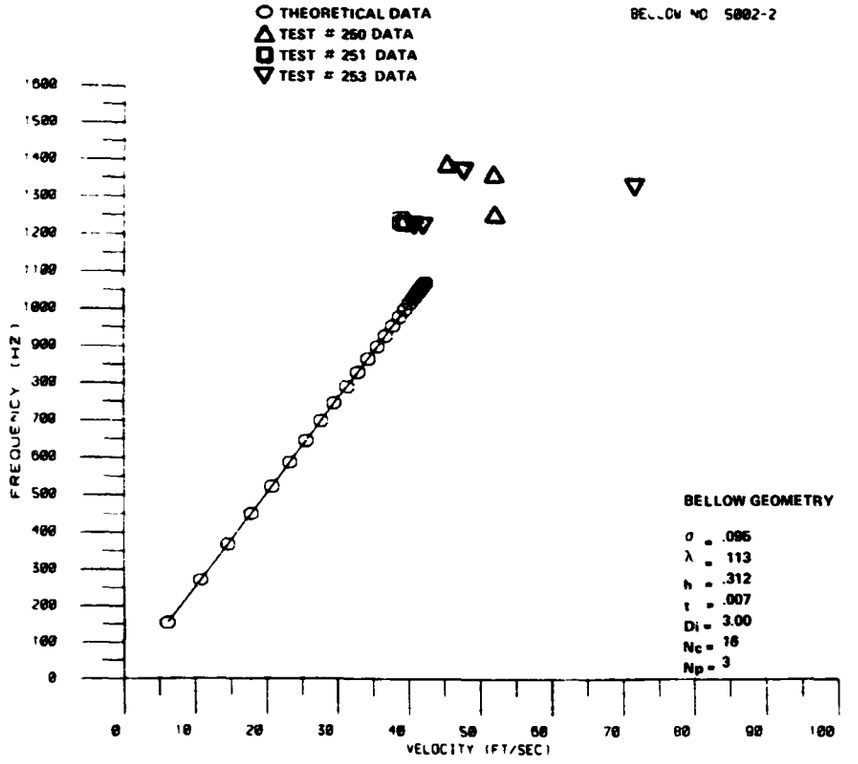

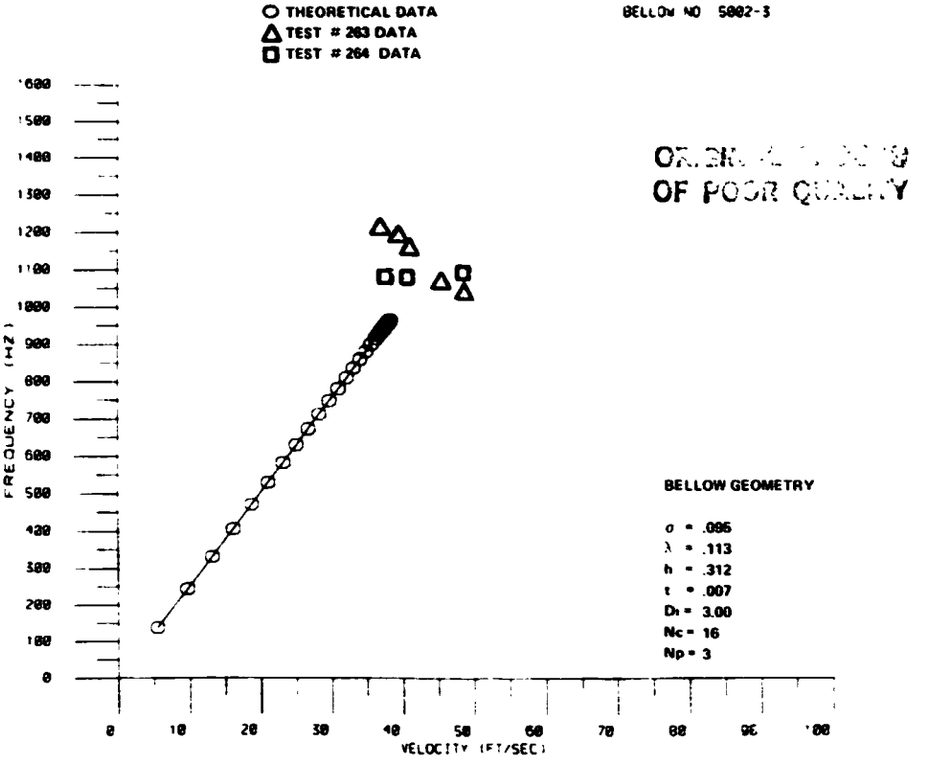

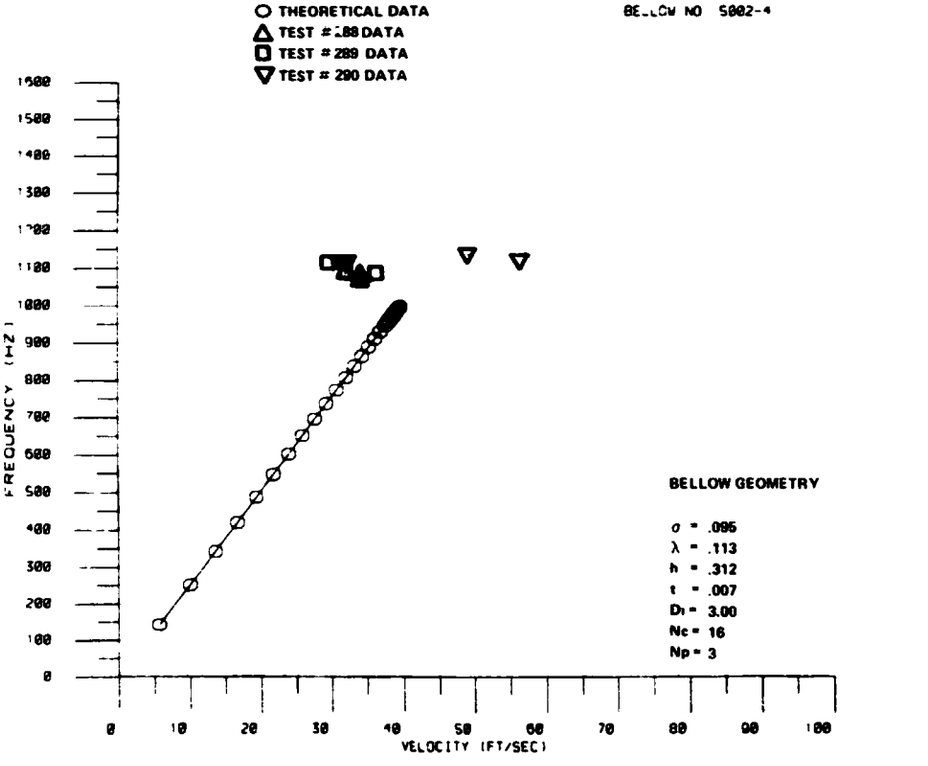

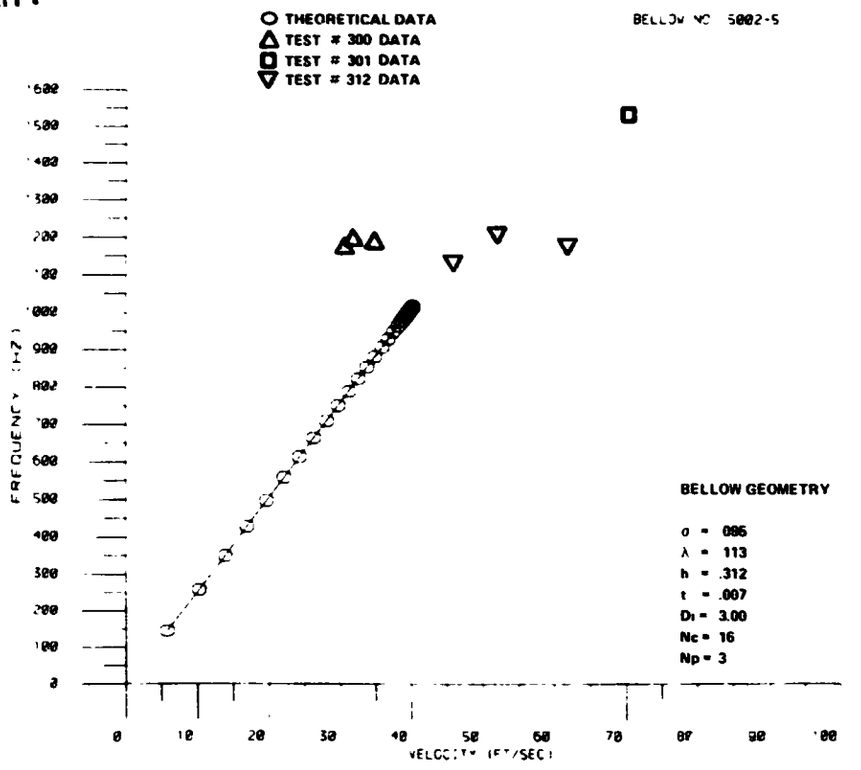

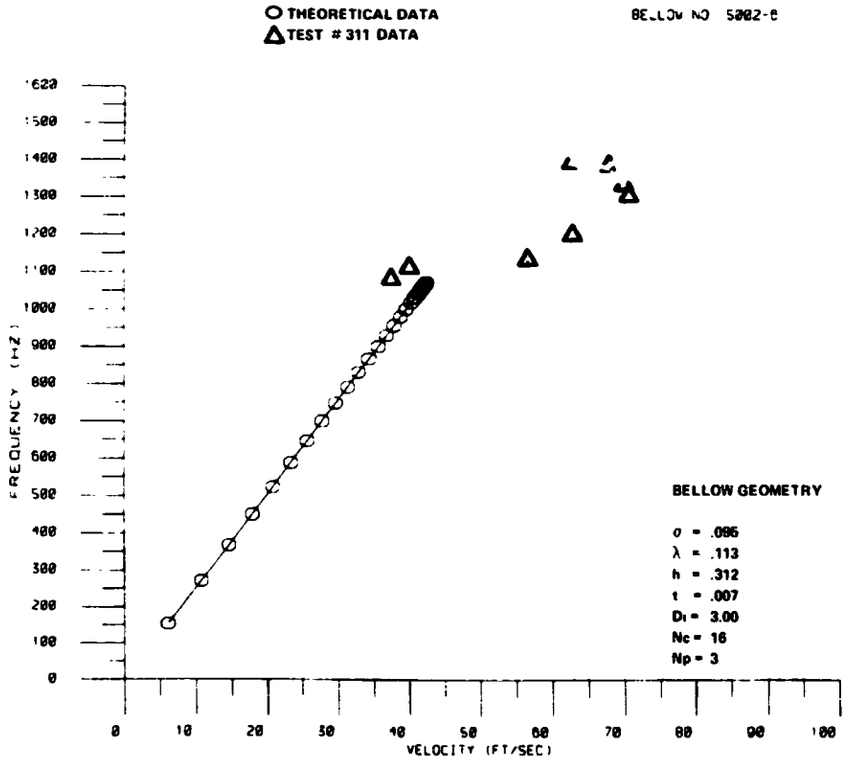

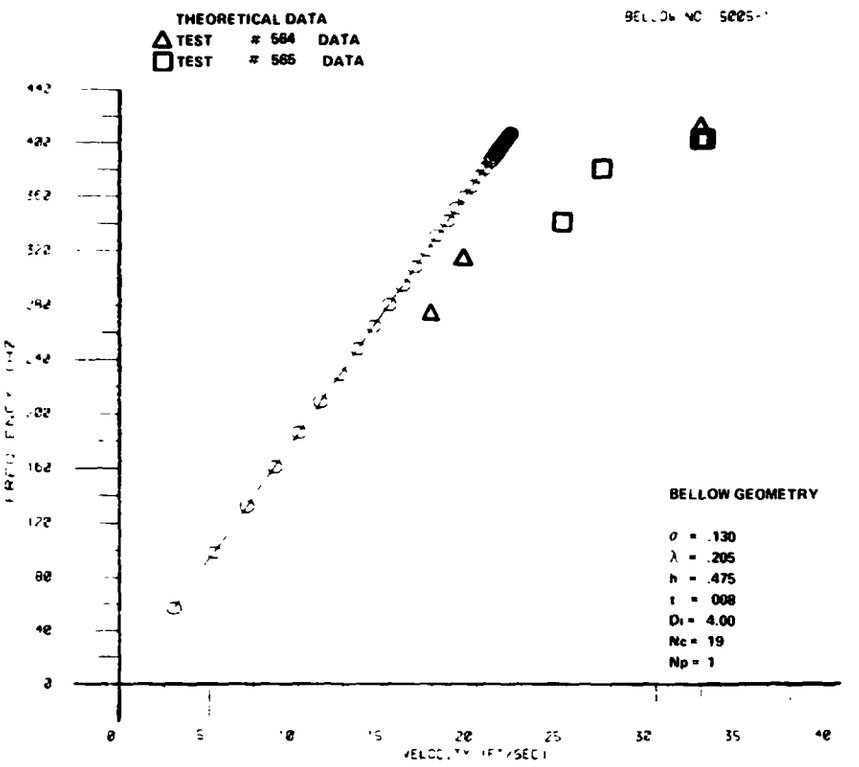

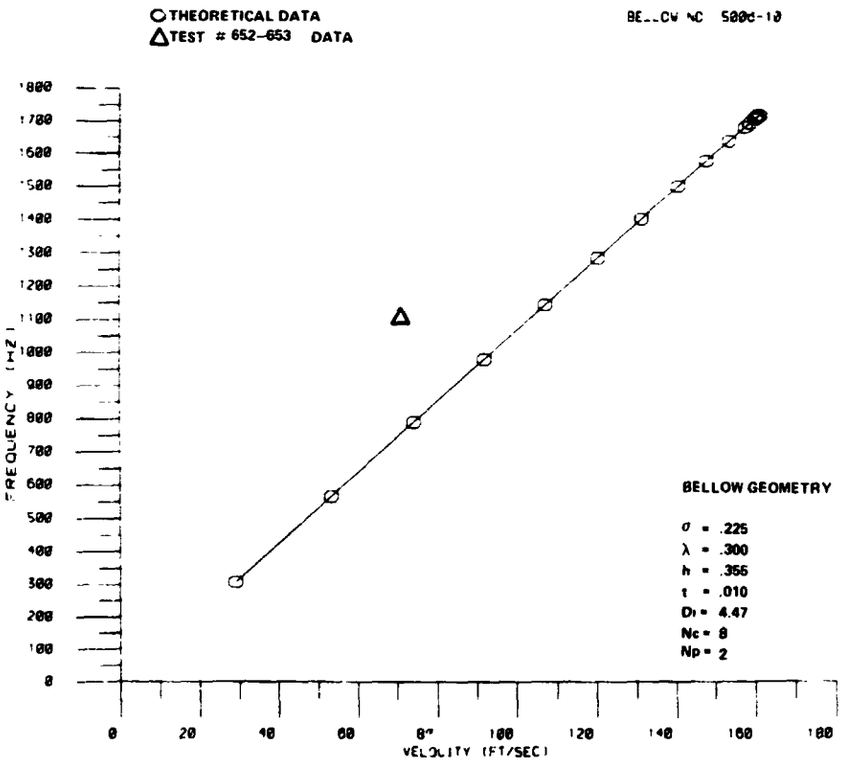

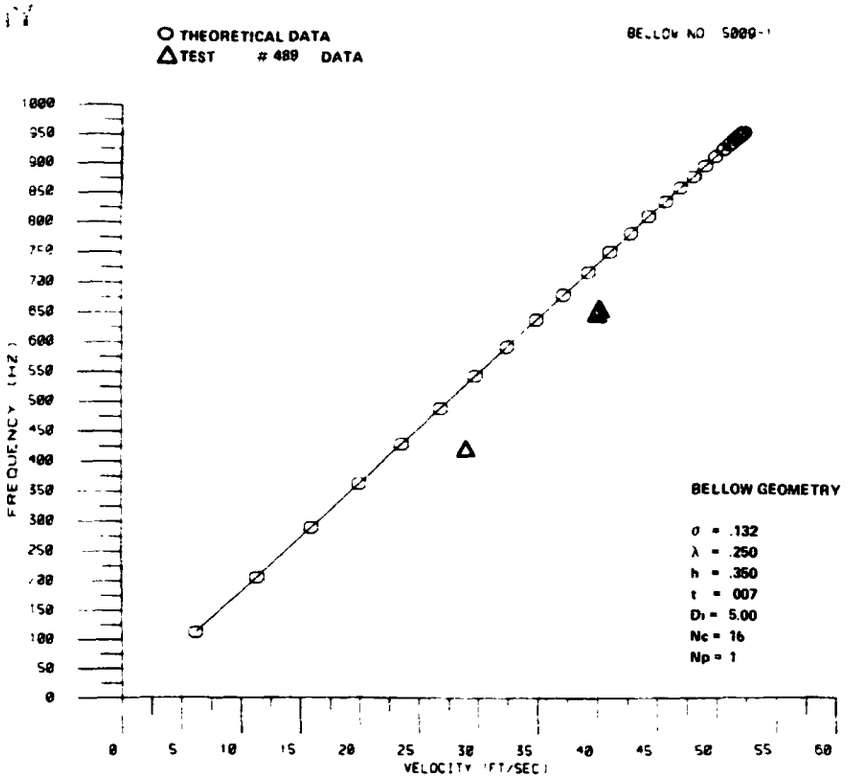

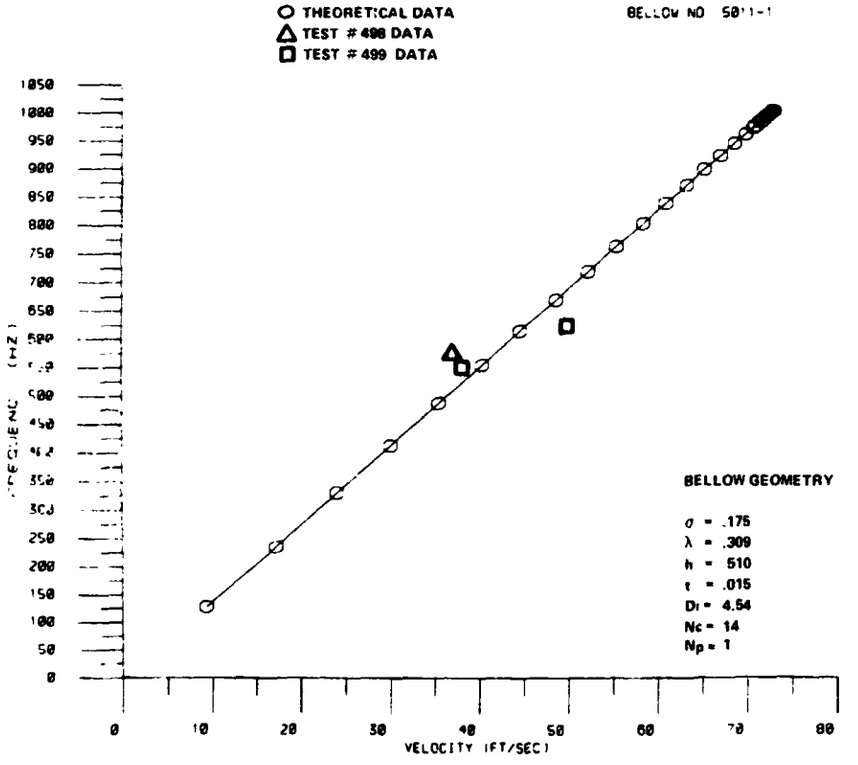

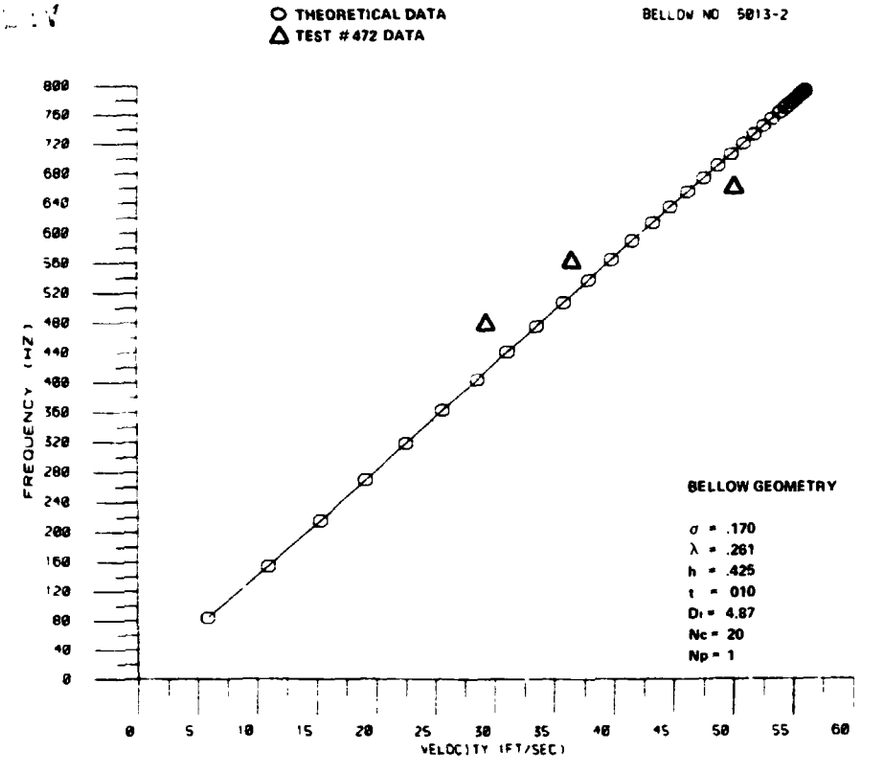

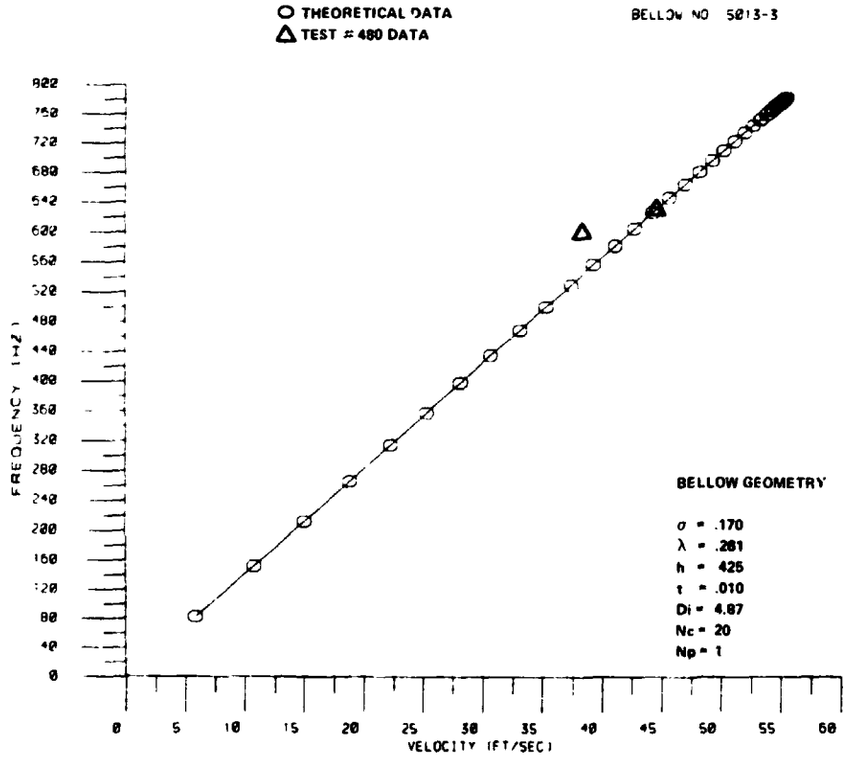

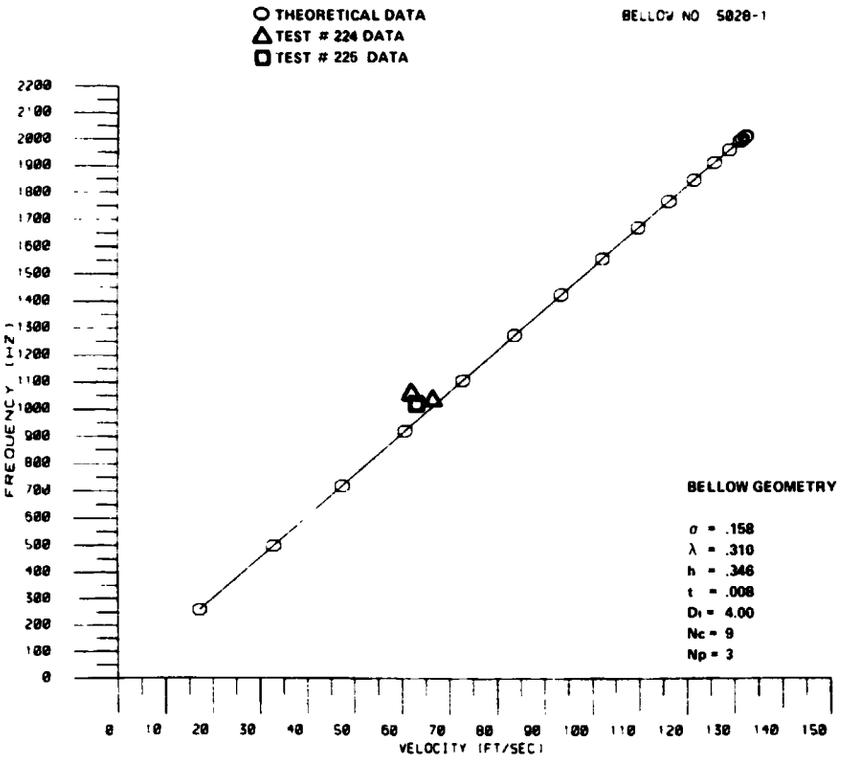

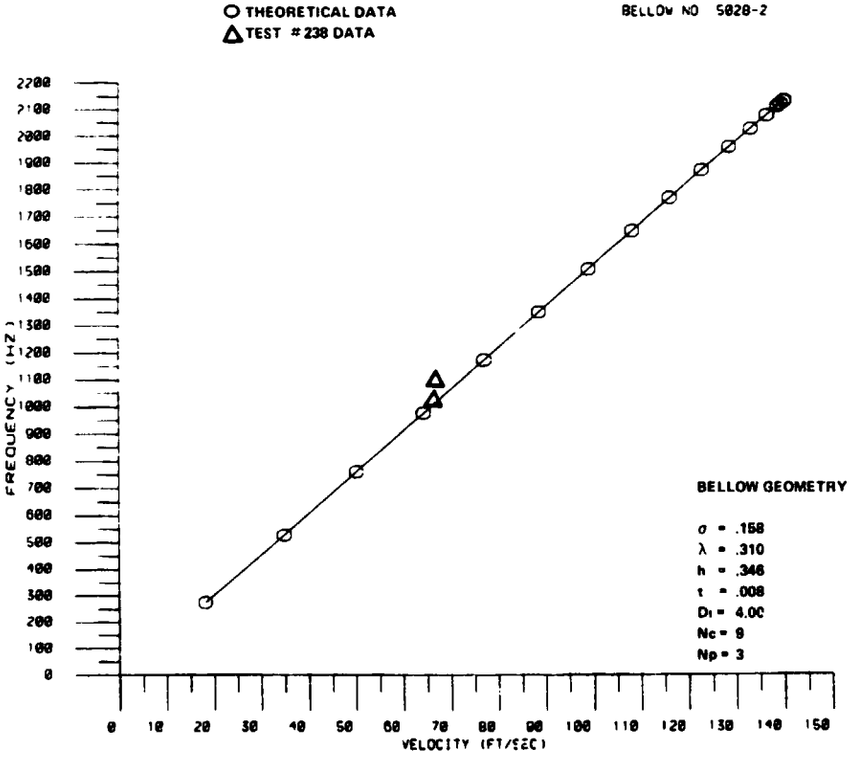

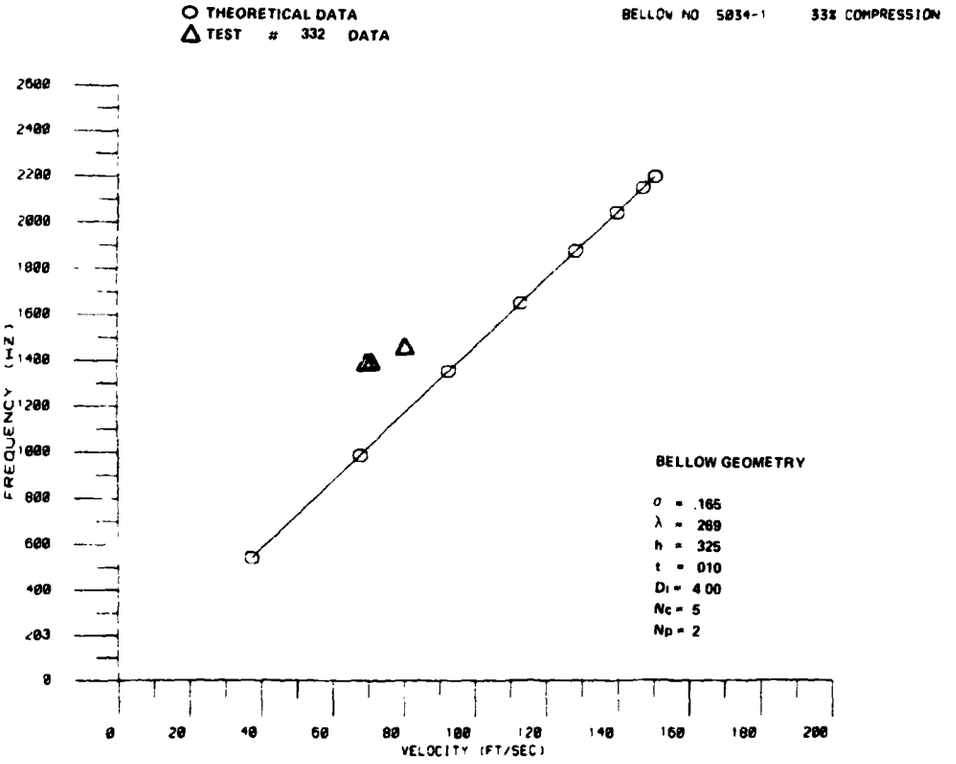

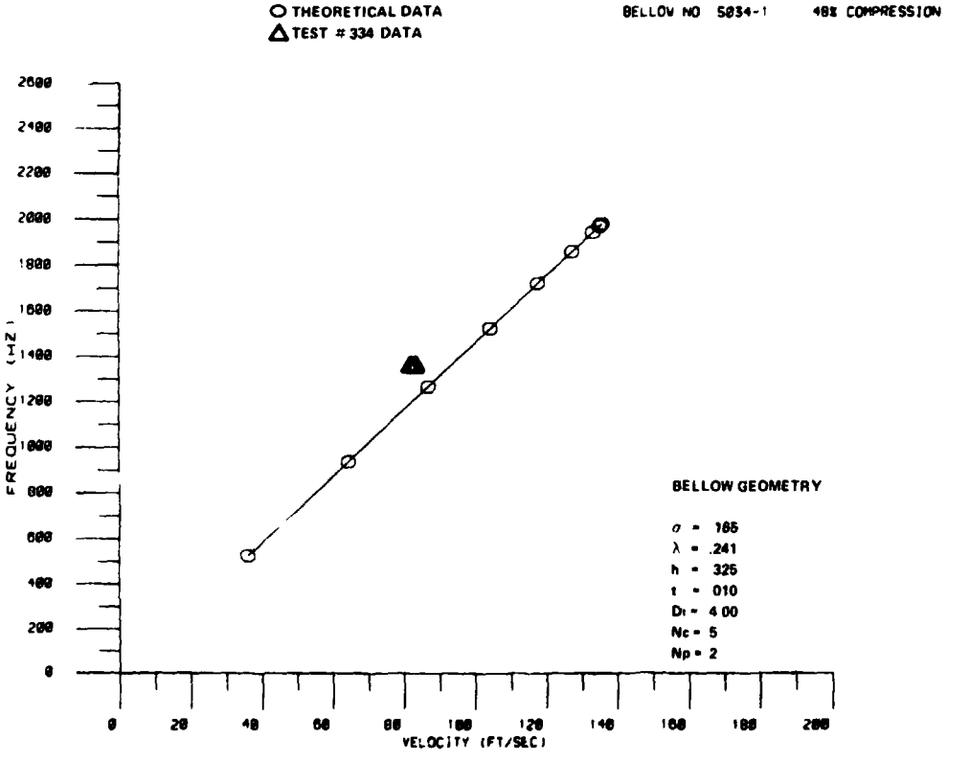

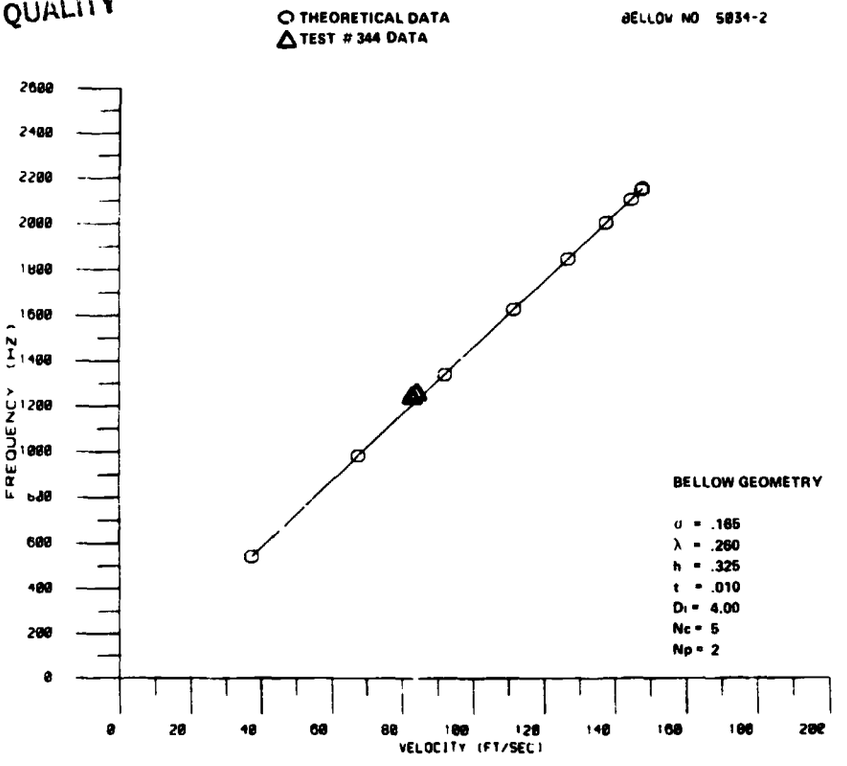

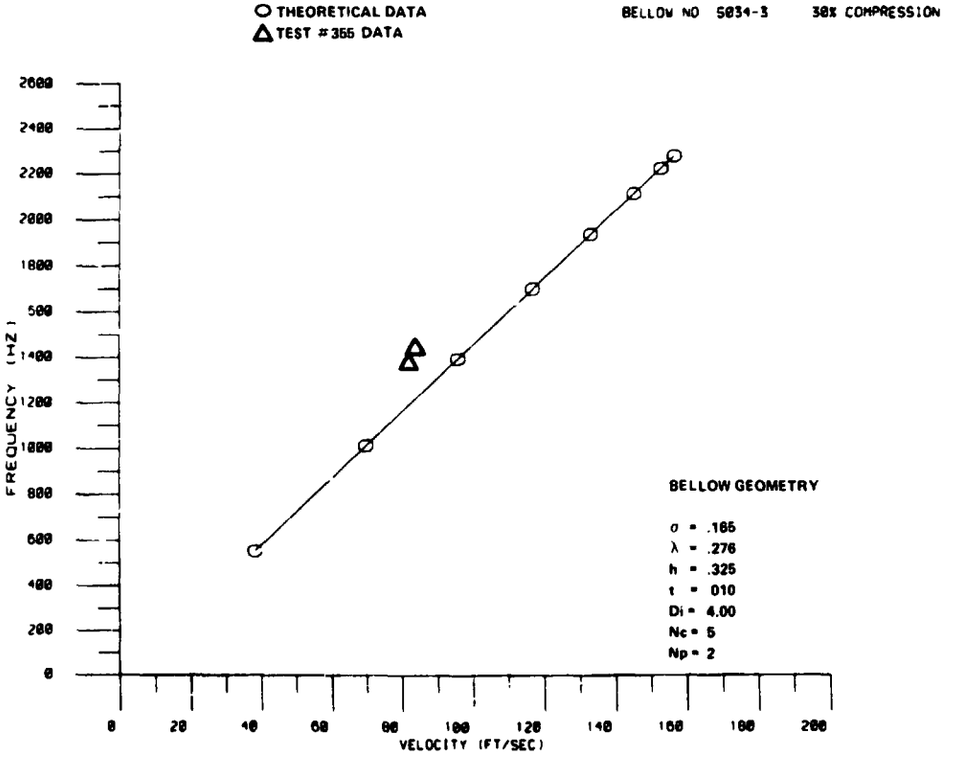

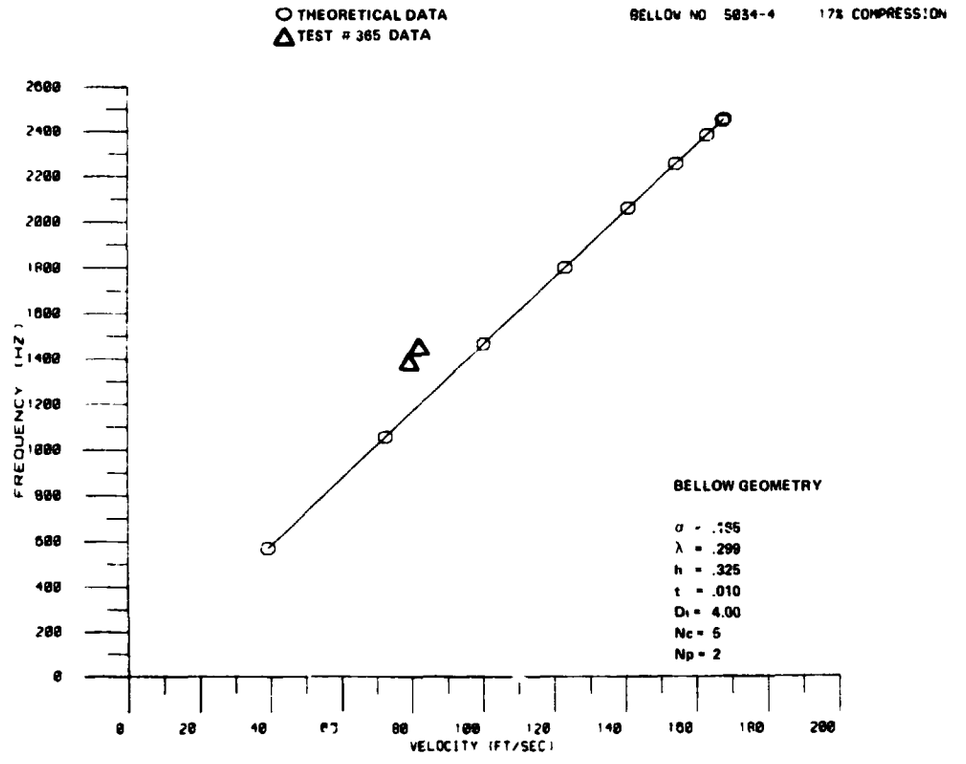

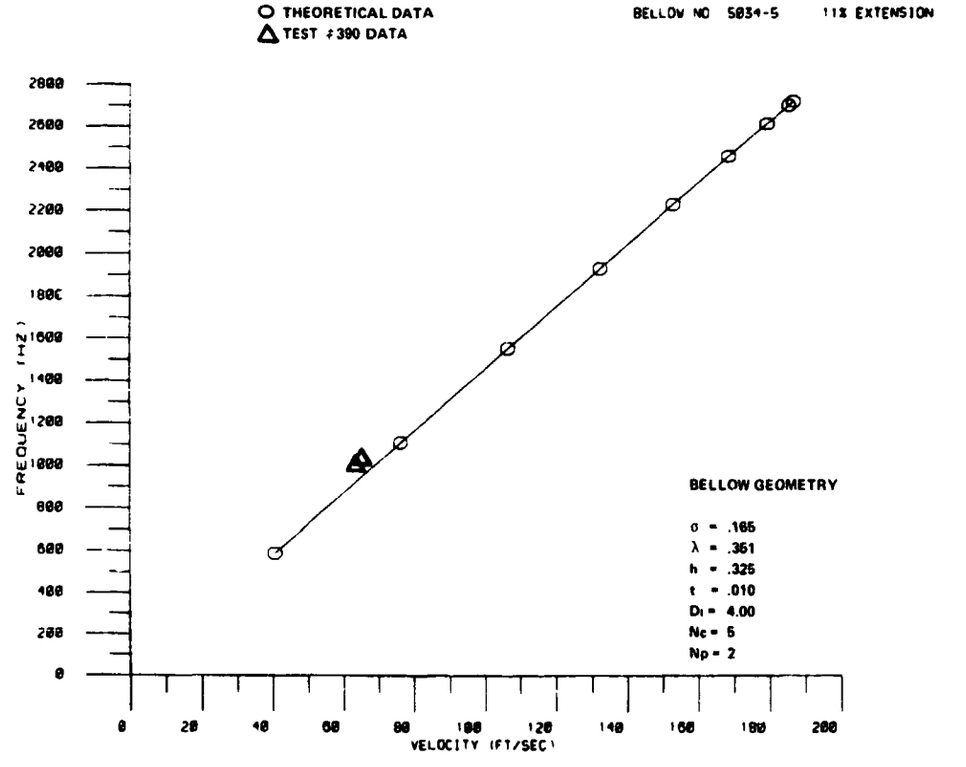

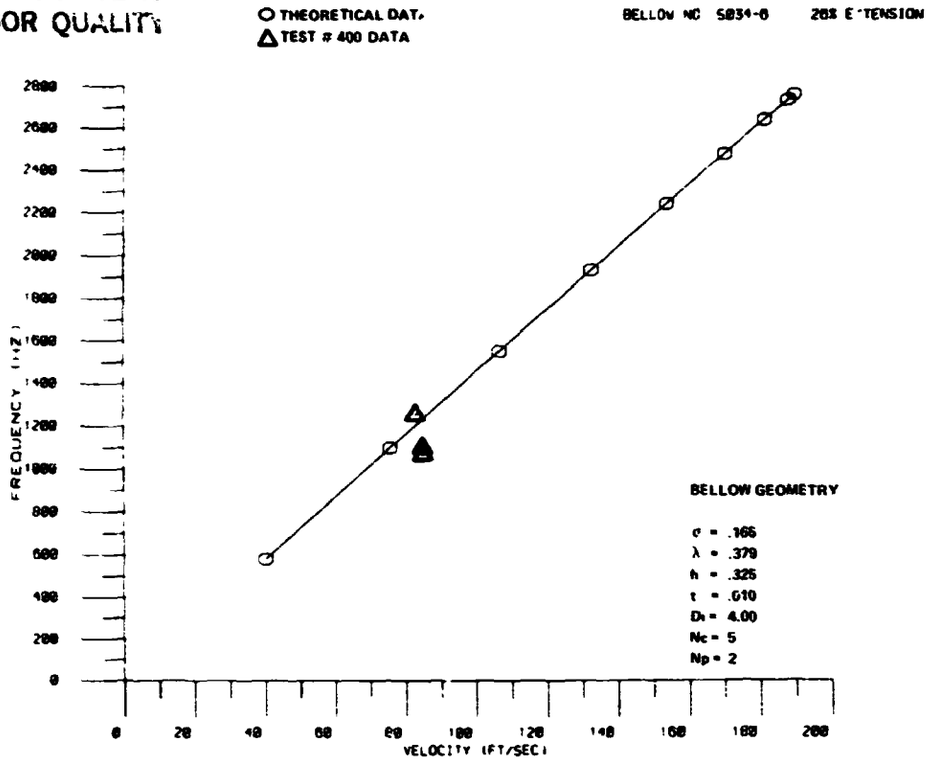

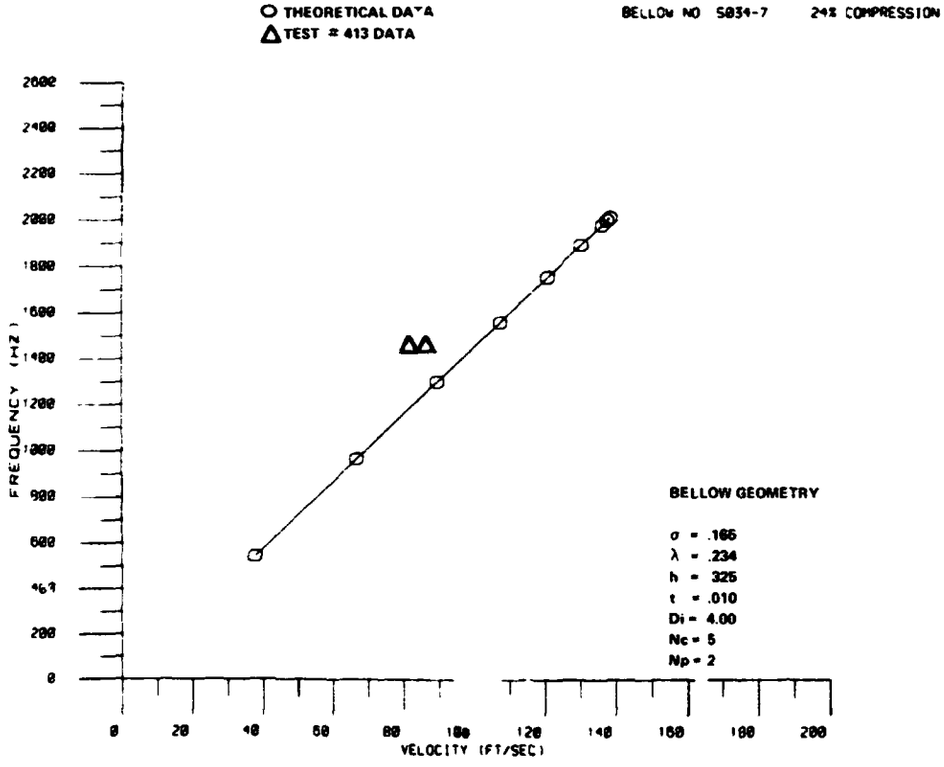

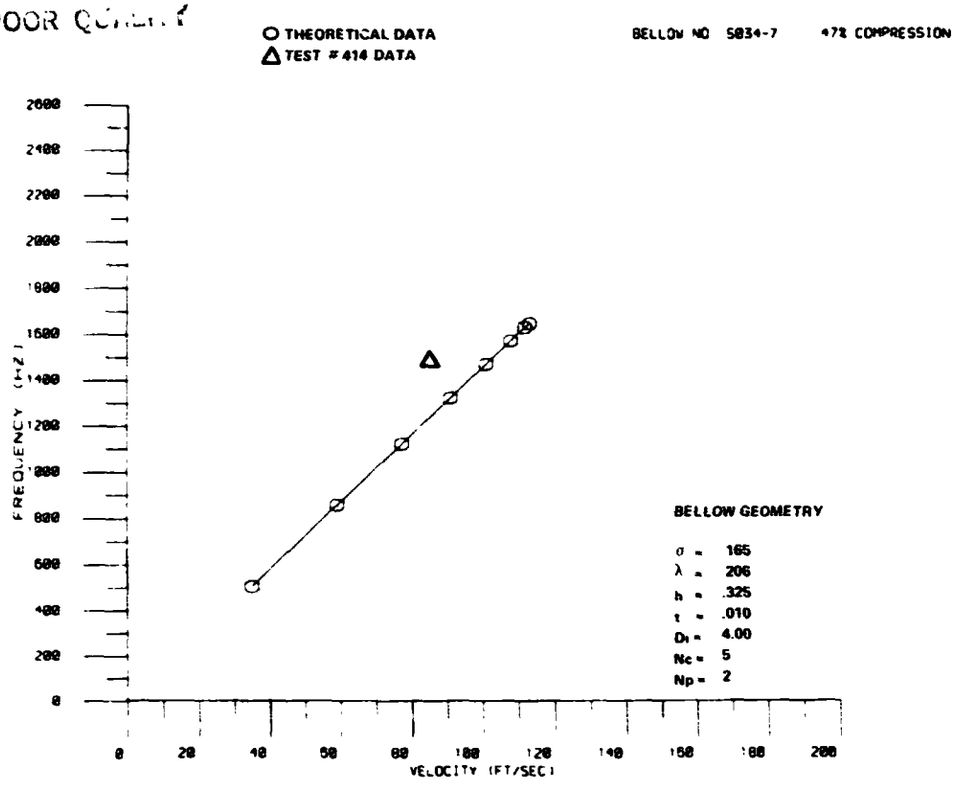

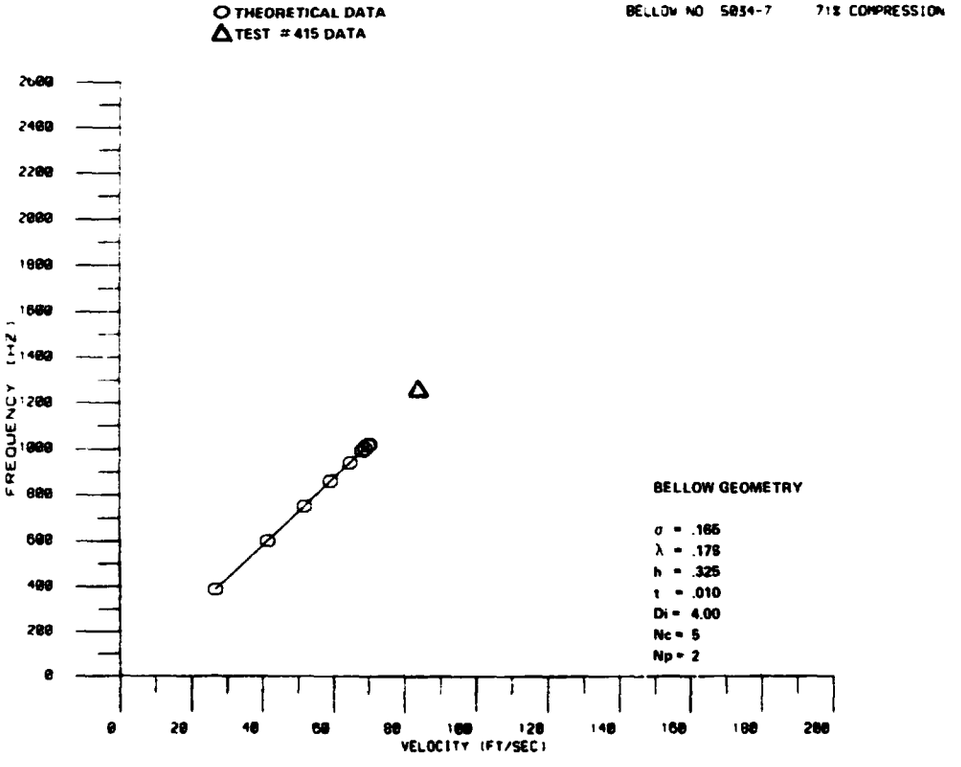

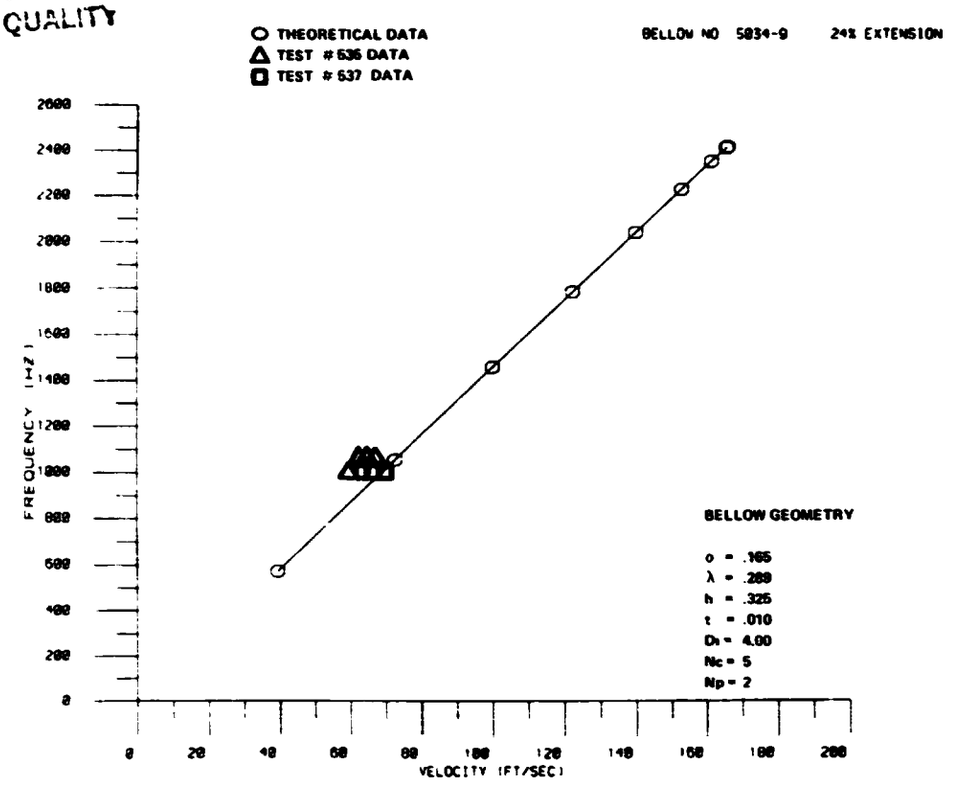

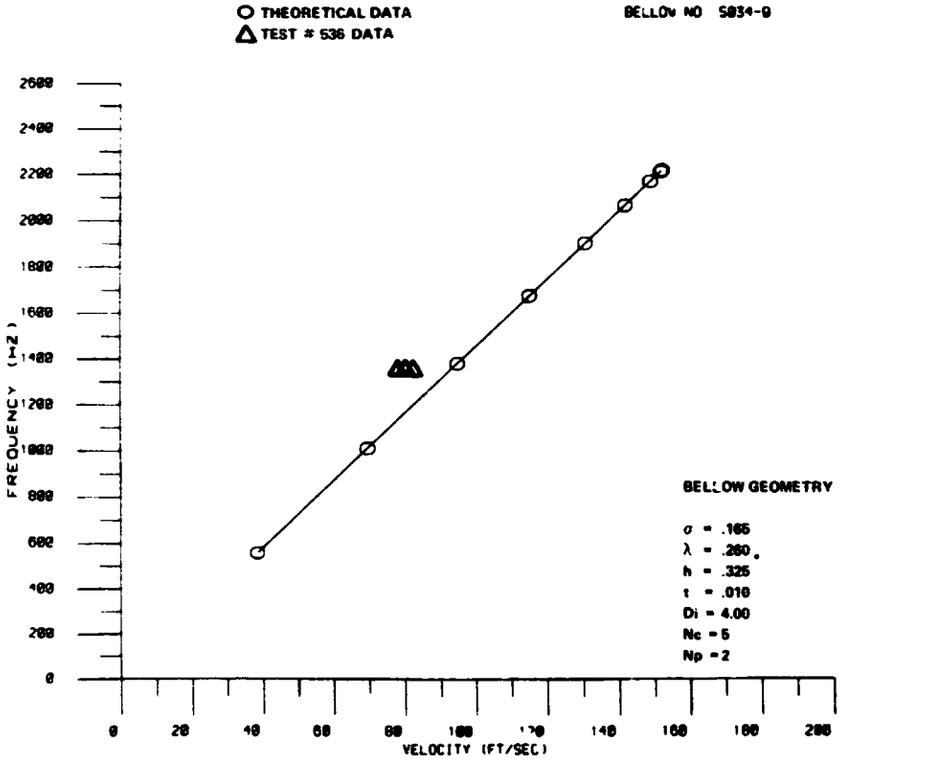

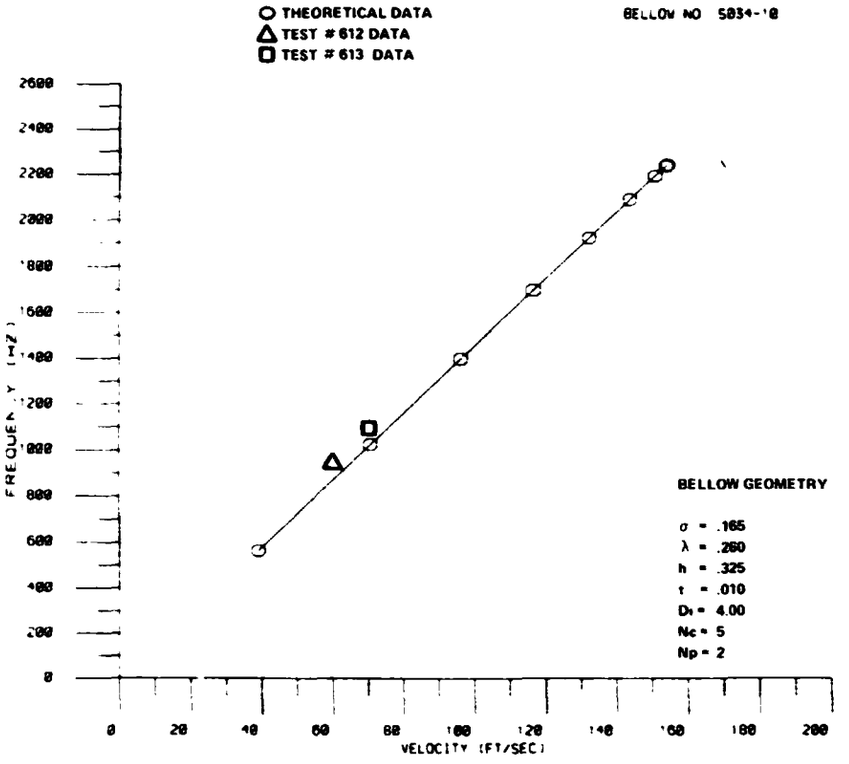

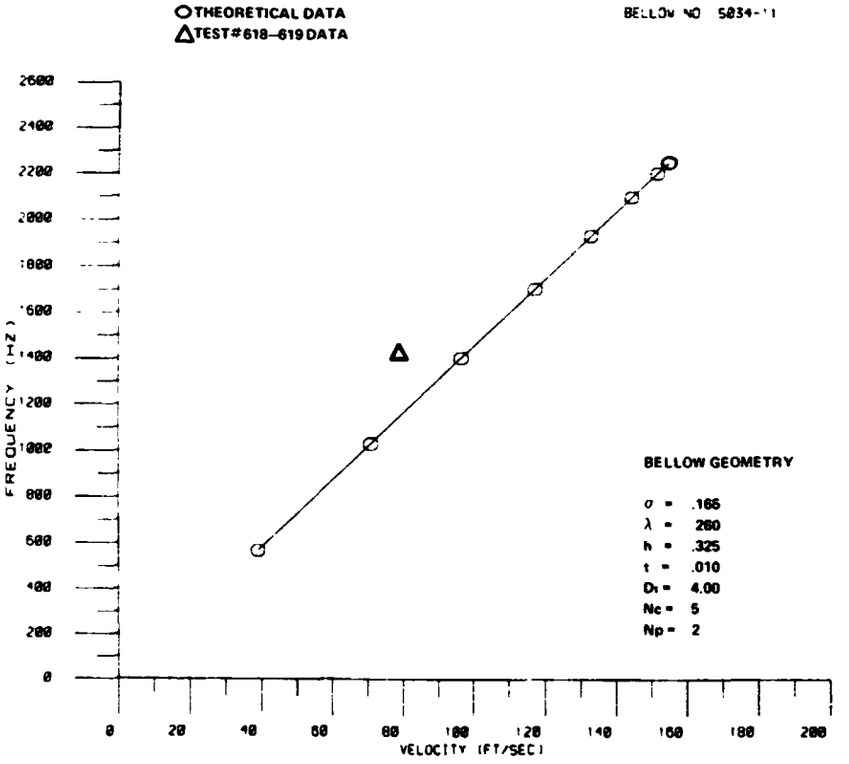

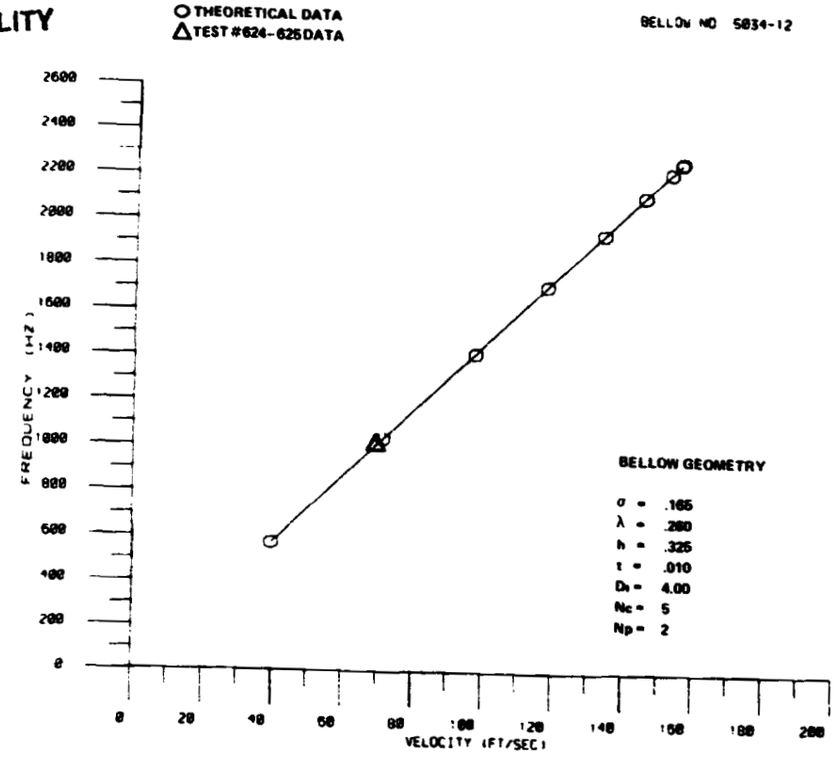

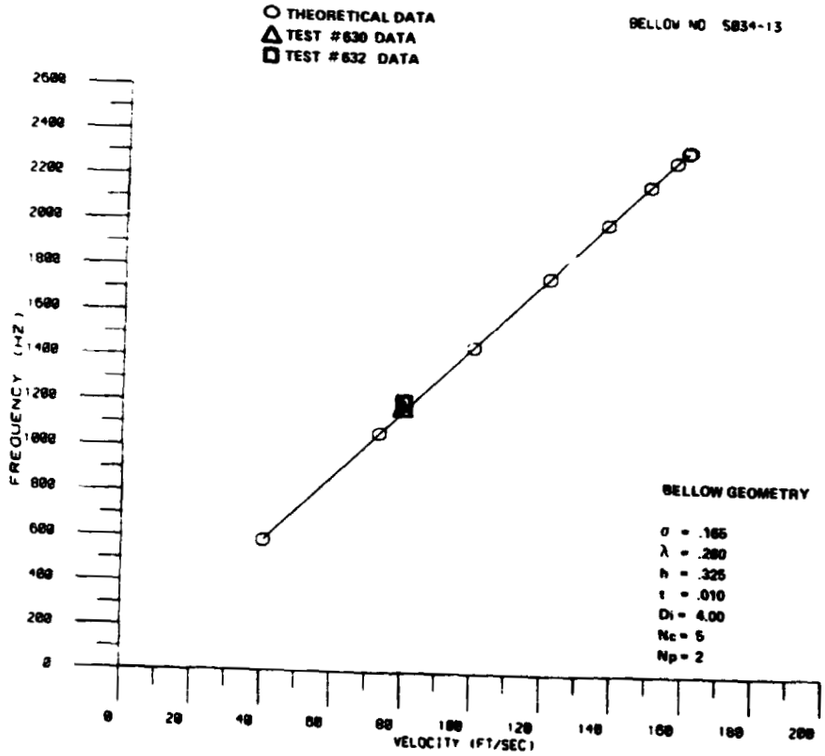

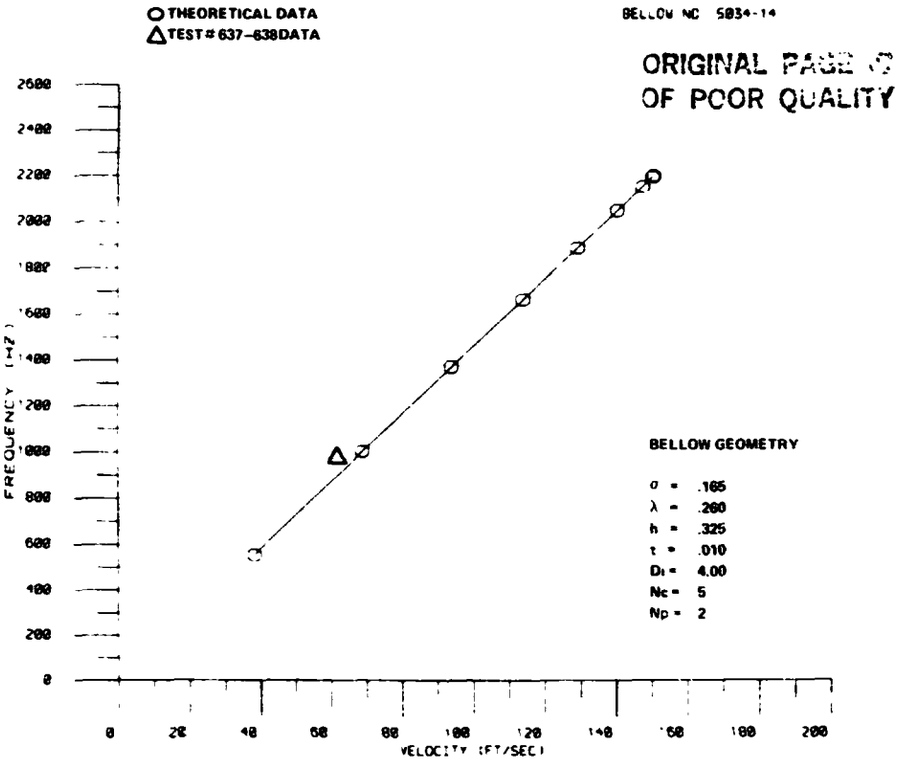
O THEORETICAL DATA
△ TEST # 637–638 DATA
BELLOW NO 5834-14
ORIGINAL PAGE IS
OF POOR QUALITY
FREQUENCY (HZ)
VELOCITY (FT/SEC)
BELLOW GEOMETRY
σ = .165
λ = .260
h = .325
t = .010
Di = 4.00
Nc = 5
Np = 2

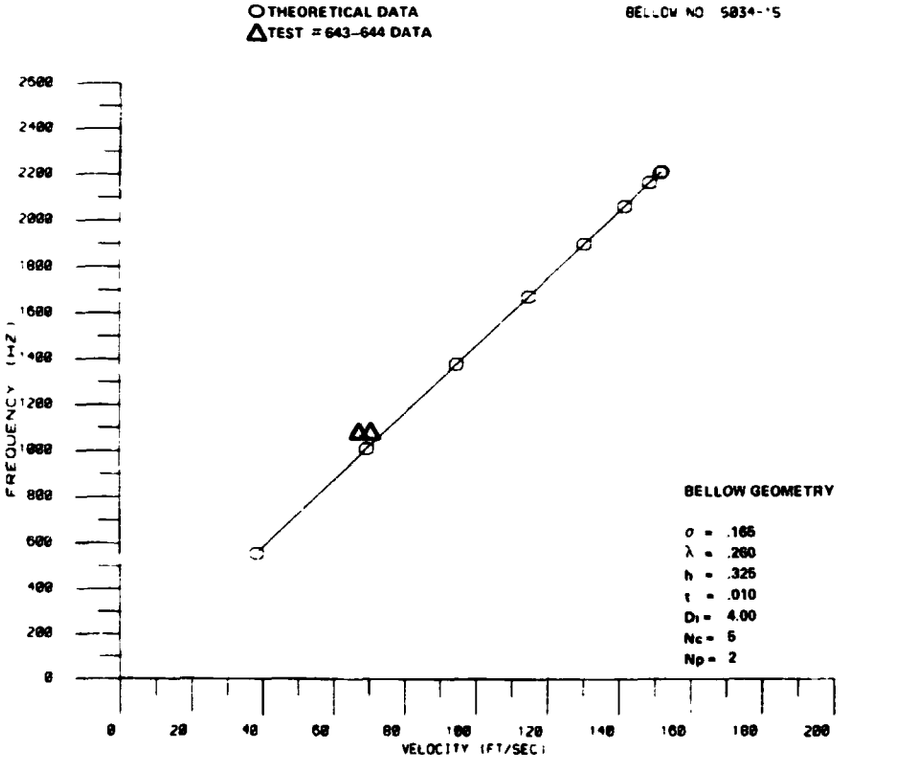
O THEORETICAL DATA
△ TEST = 643–644 DATA
BELLOW NO 5834-15
FREQUENCY (HZ)
VELOCITY (FT/SEC)
BELLOW GEOMETRY
σ = .165
λ = .260
h = .325
t = .010
Di = 4.00
Nc = 5
Np = 2

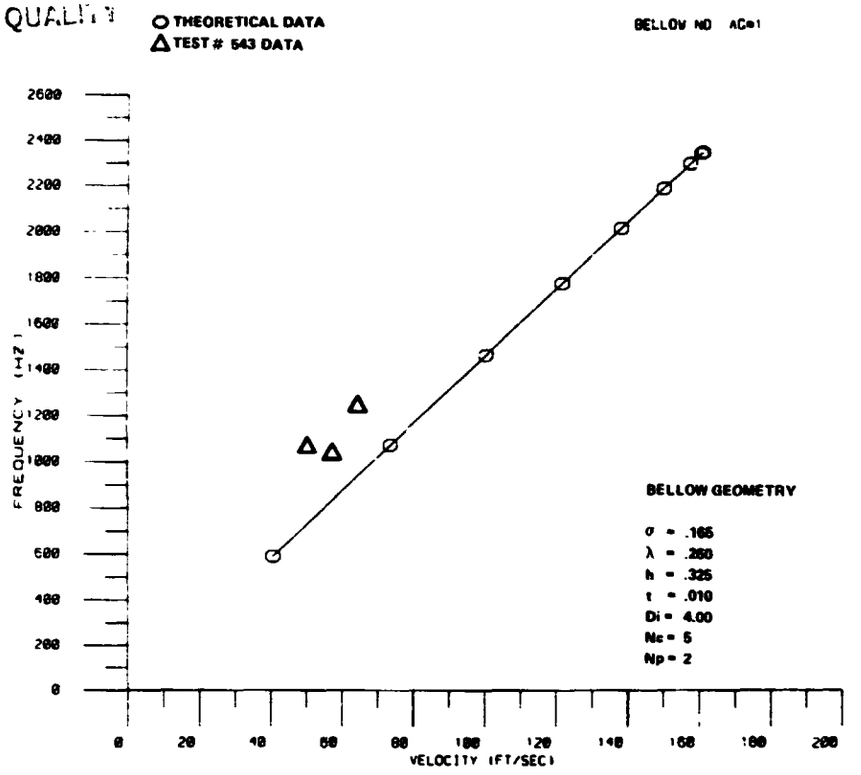

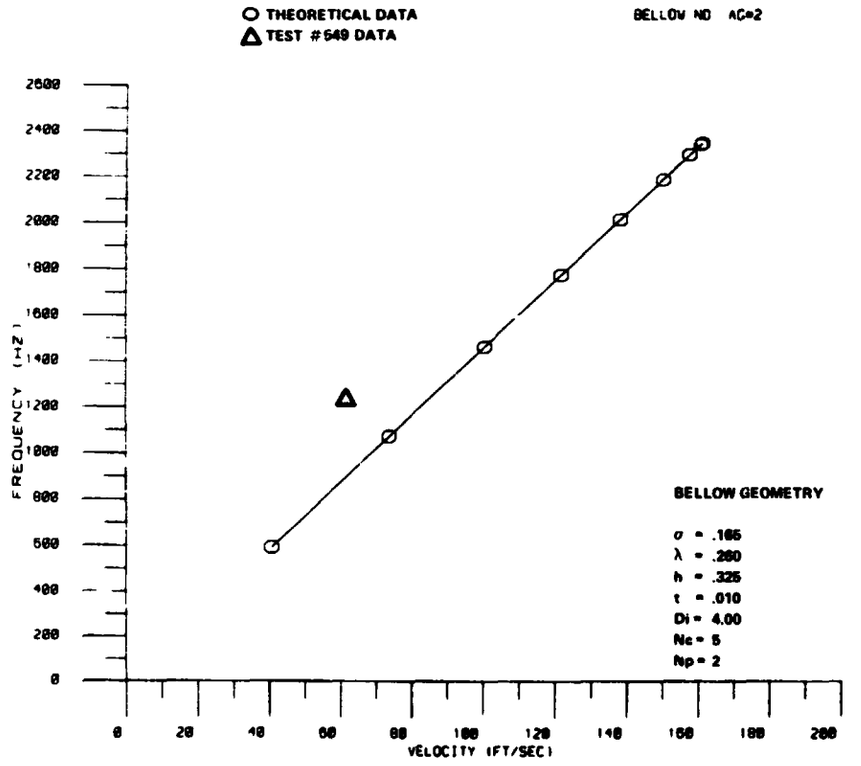

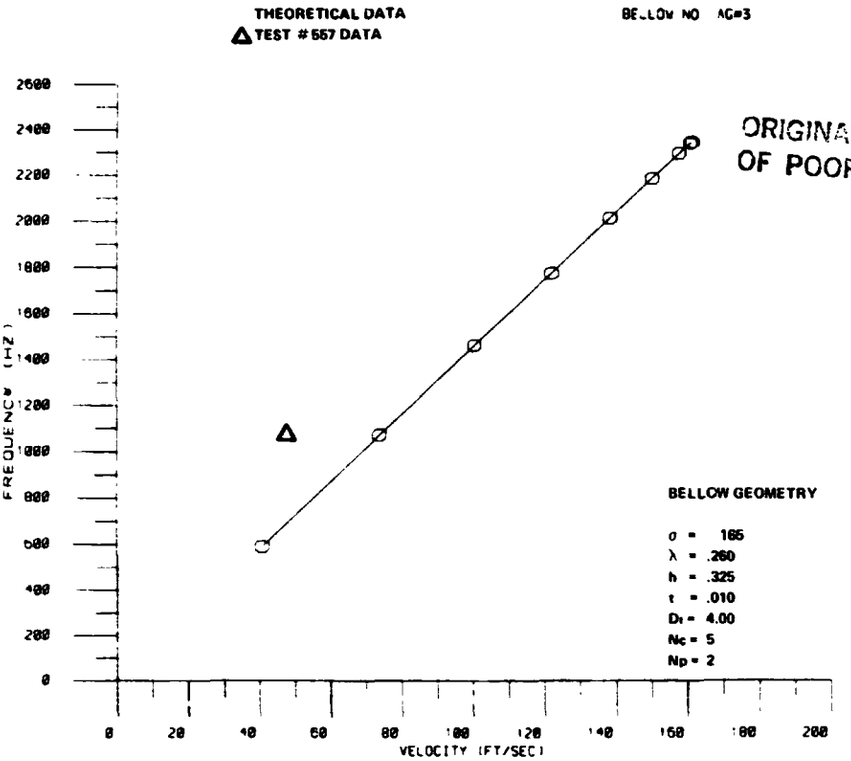

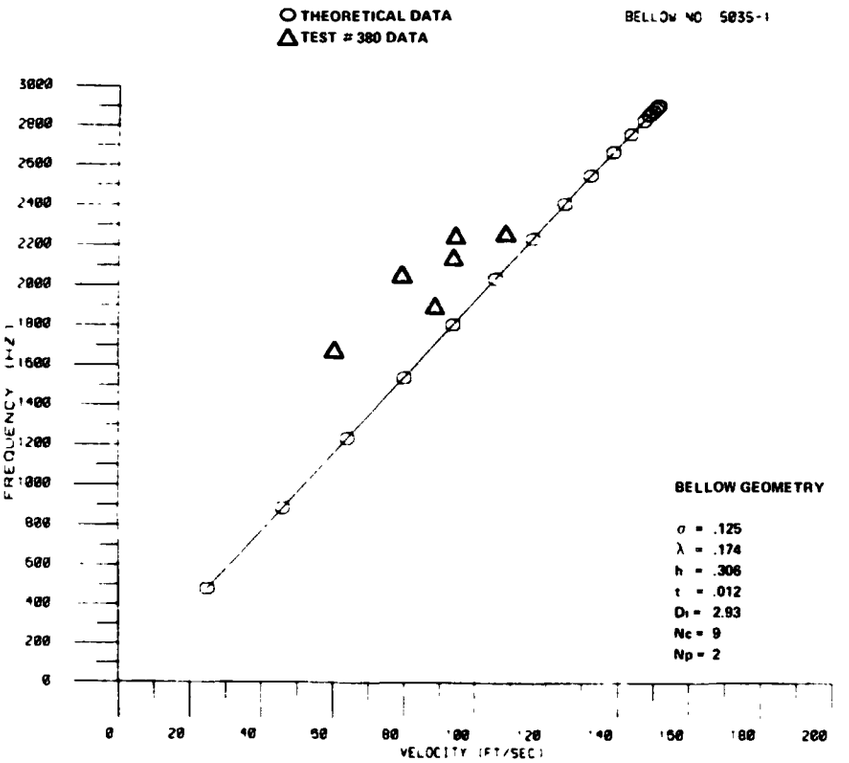

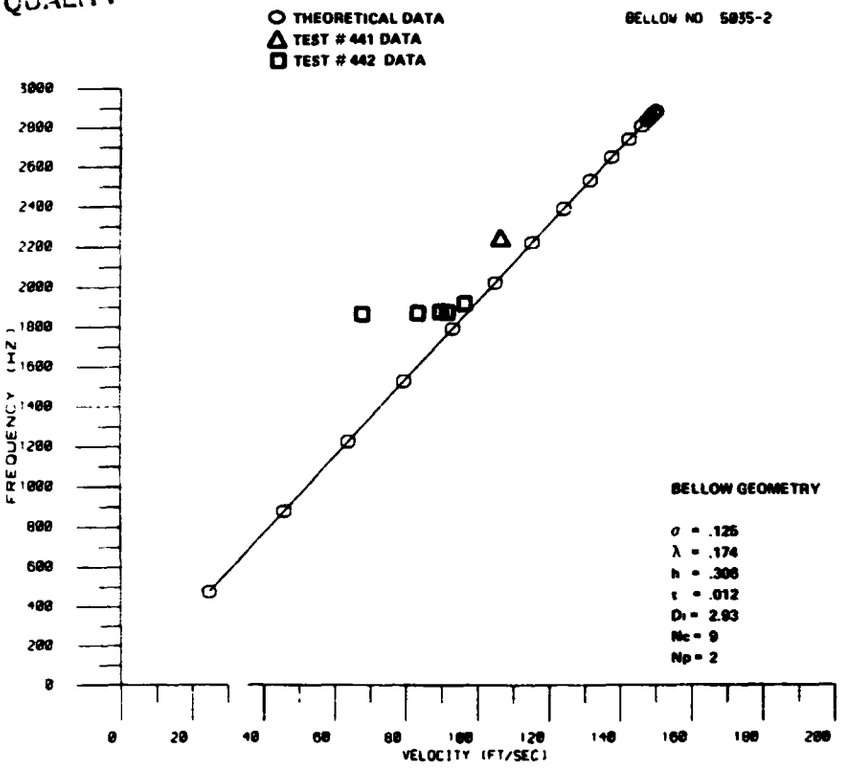

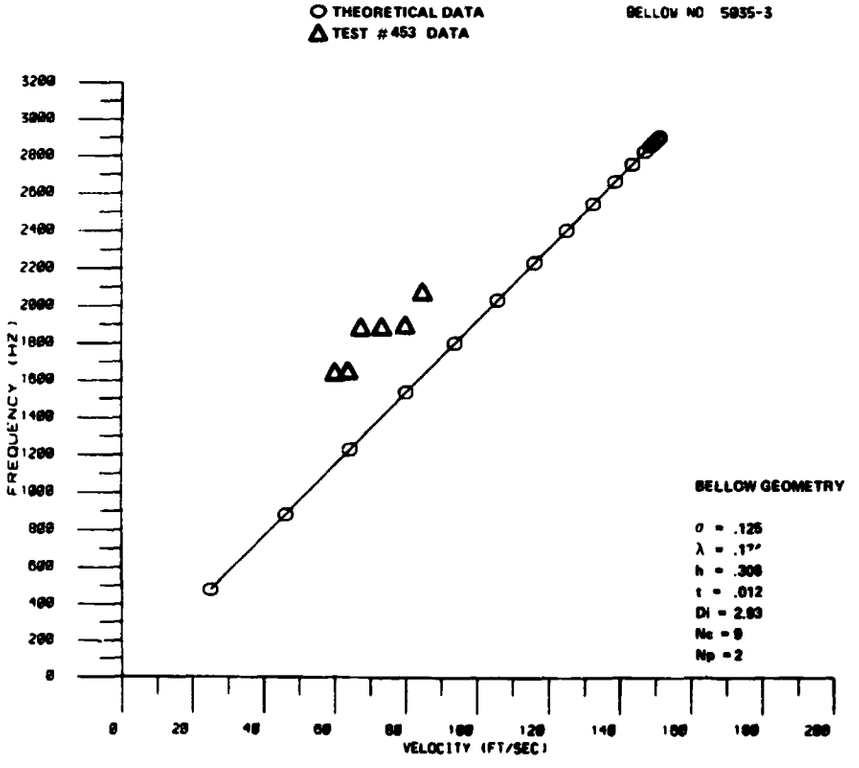

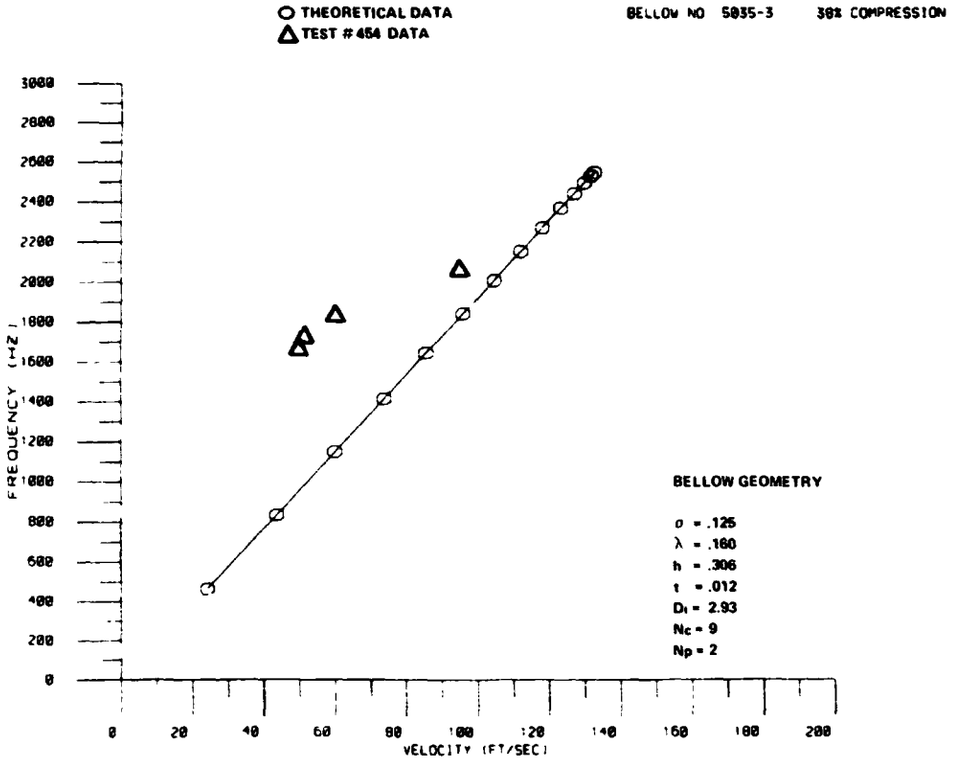

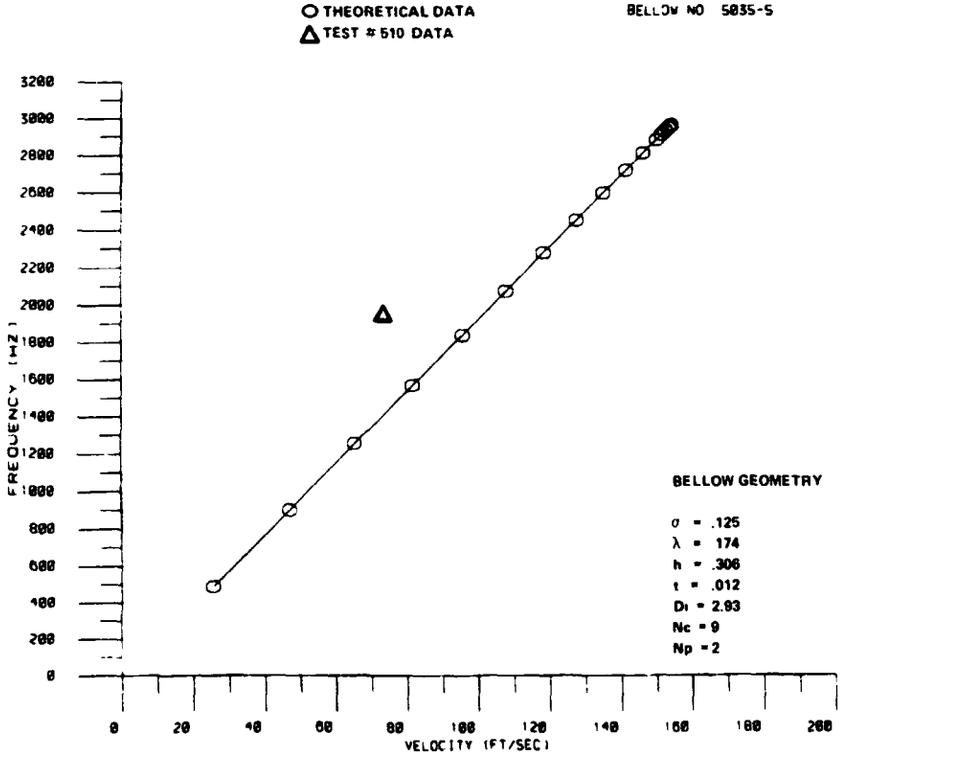

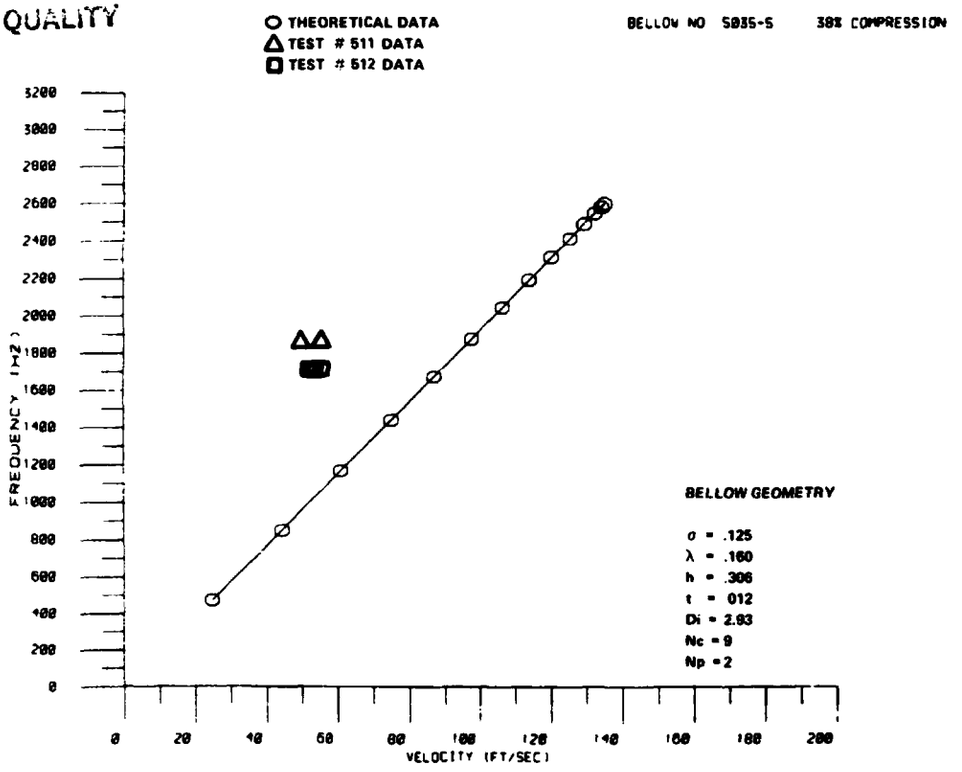

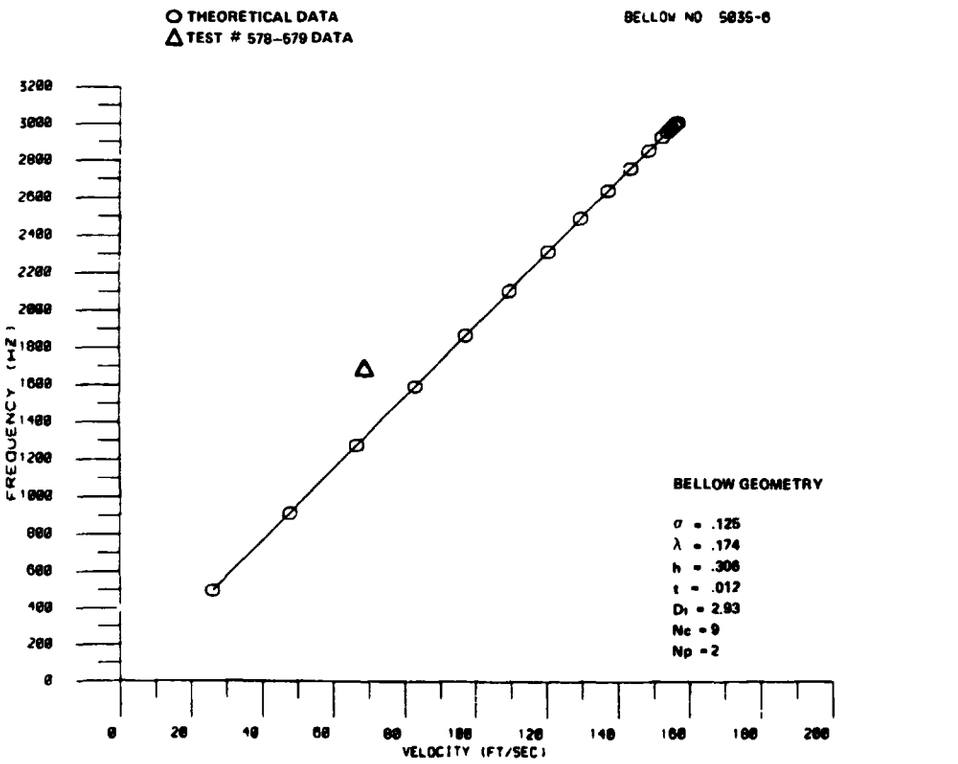

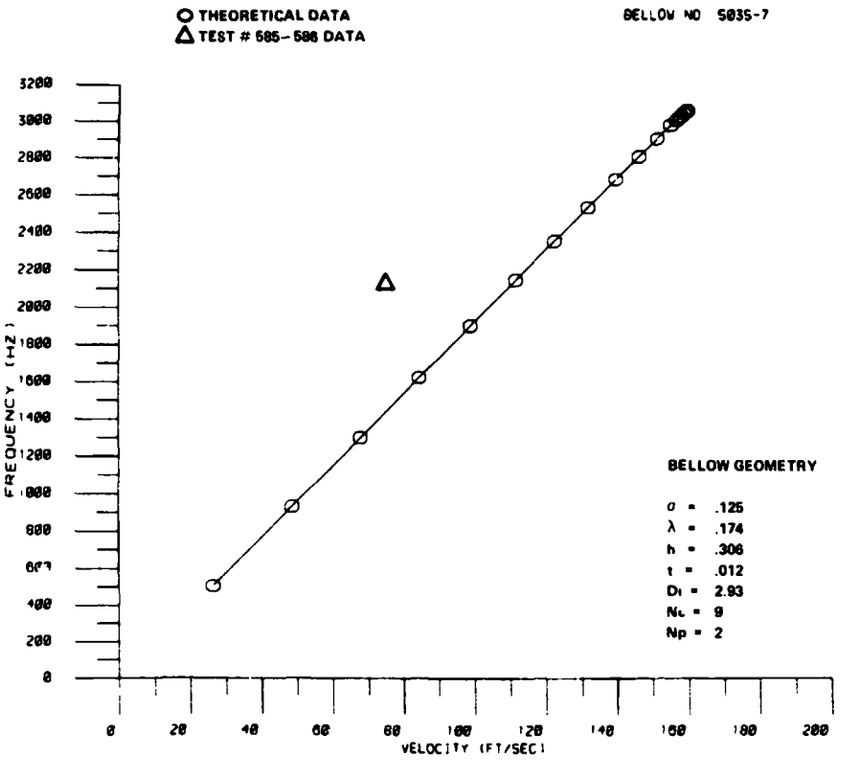

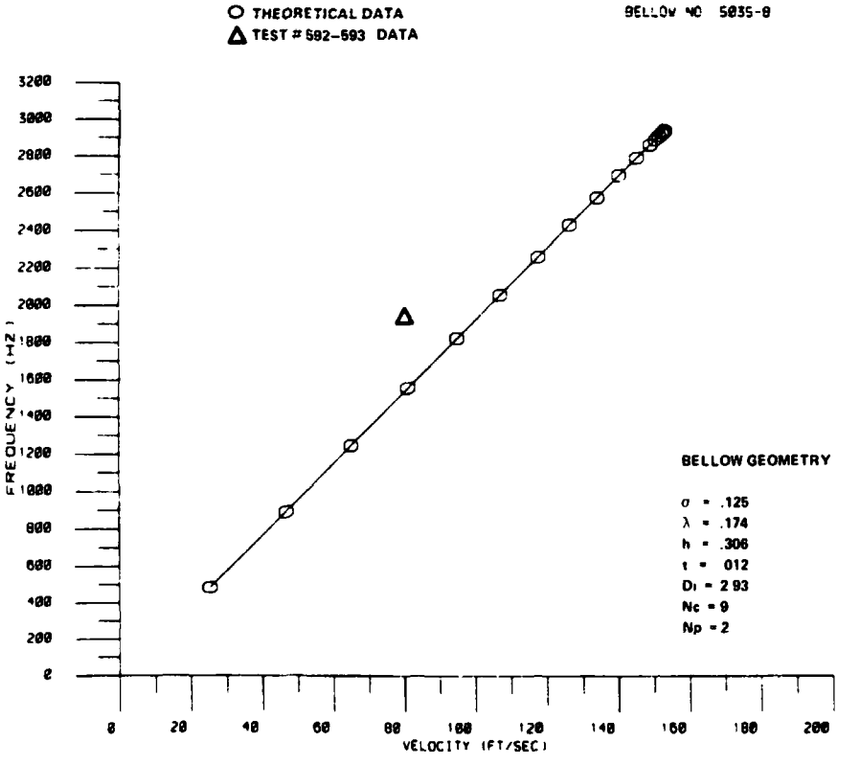

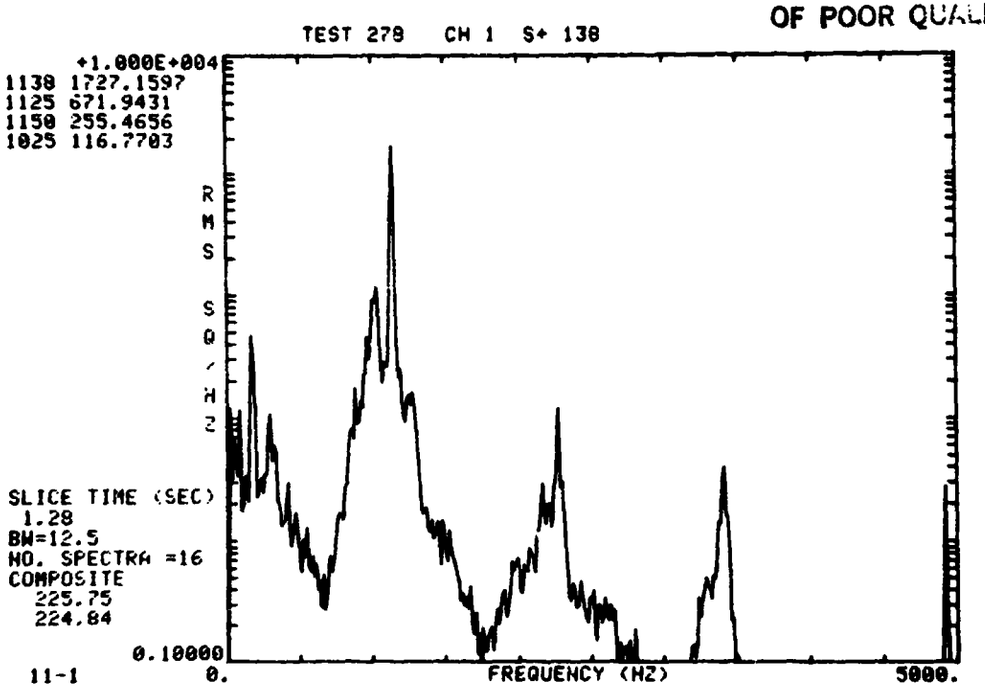

POWER-SPECTRAL-DENSITY PLOT
BELLOWS NO. 5002-1 90° ELBOW-L/D = 8.17

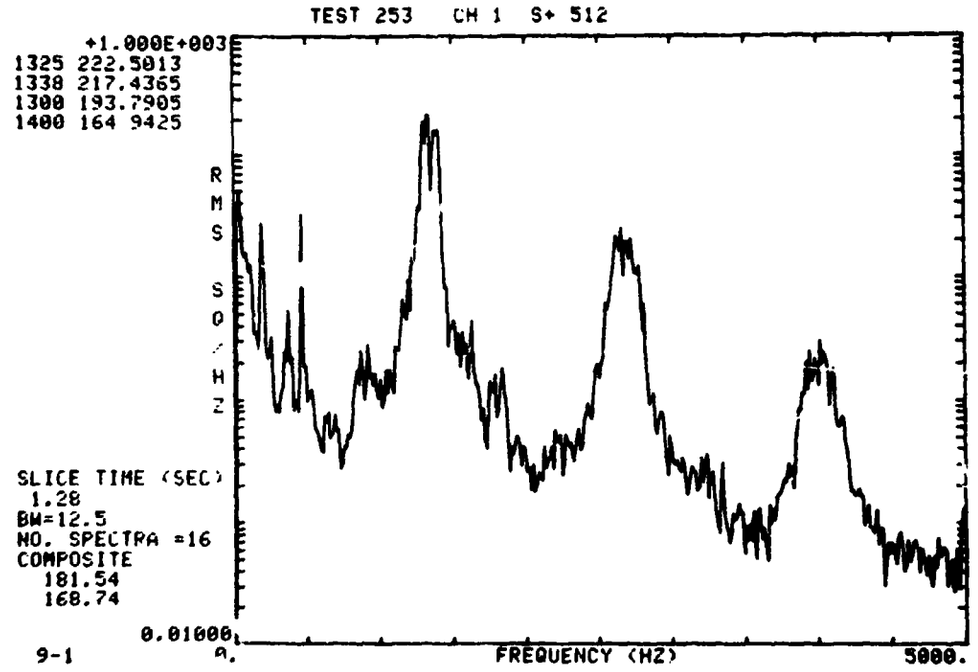

POWER-SPECTRAL-DENSITY PLOT
BELLOWS NO. 5002-2 90° ELBOW-L/D = 28.3

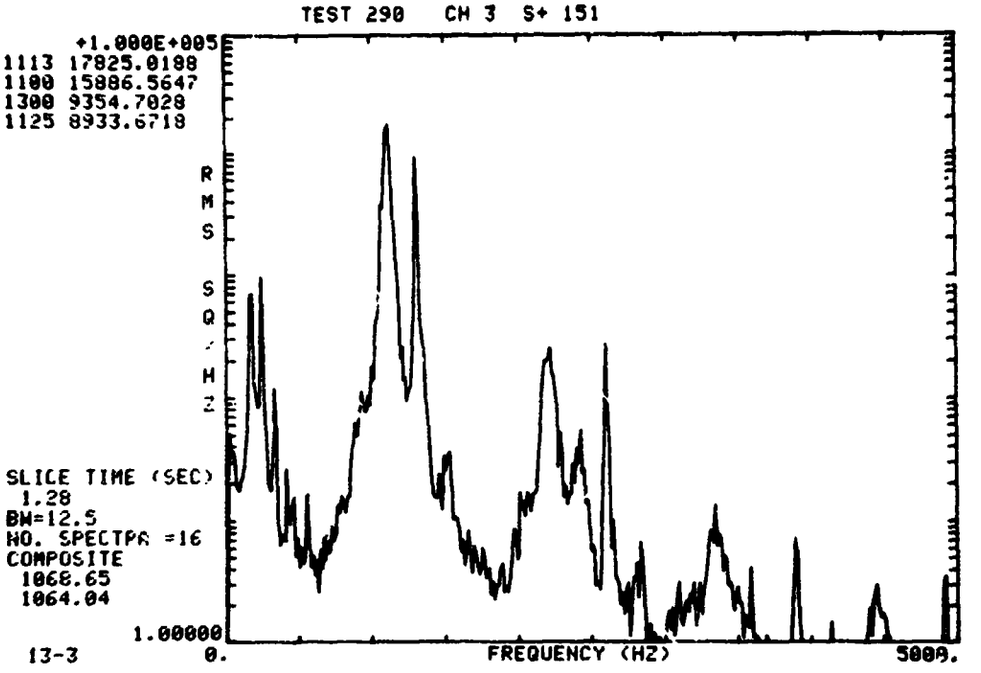

POWER-SPECTRAL-DENSITY PLOT
BELLOWS NO. 5002-4 90° ELBOW-L/D = 2.17

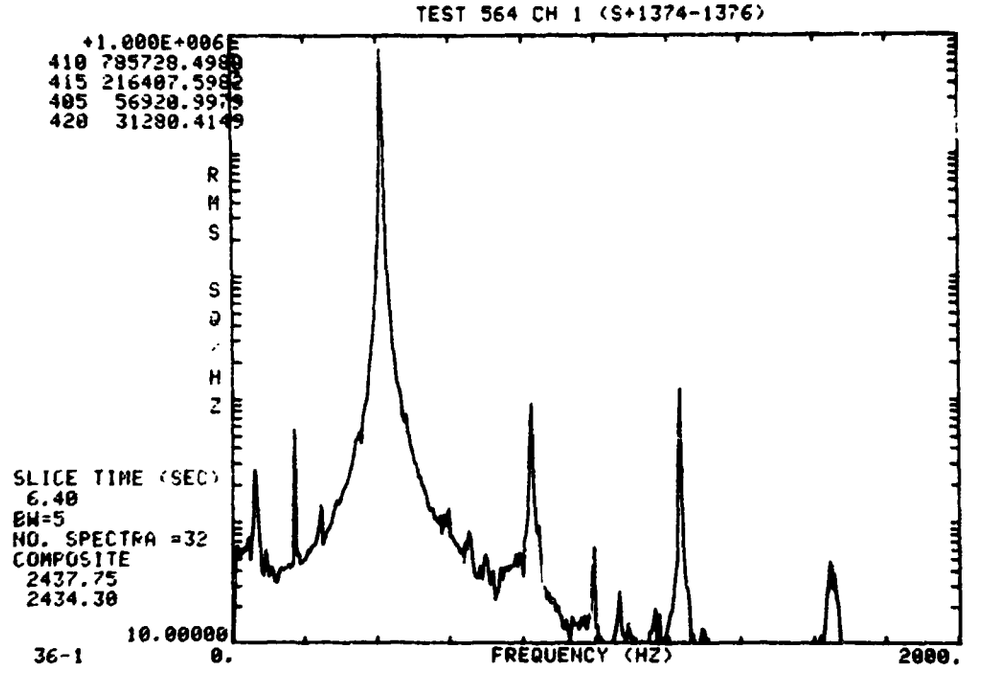

POWER-SPECTRAL-DENSITY PLOT
BELLOWS NO. 5005-1

ORIGINAL PAGE IS
OF POOR QUALITY

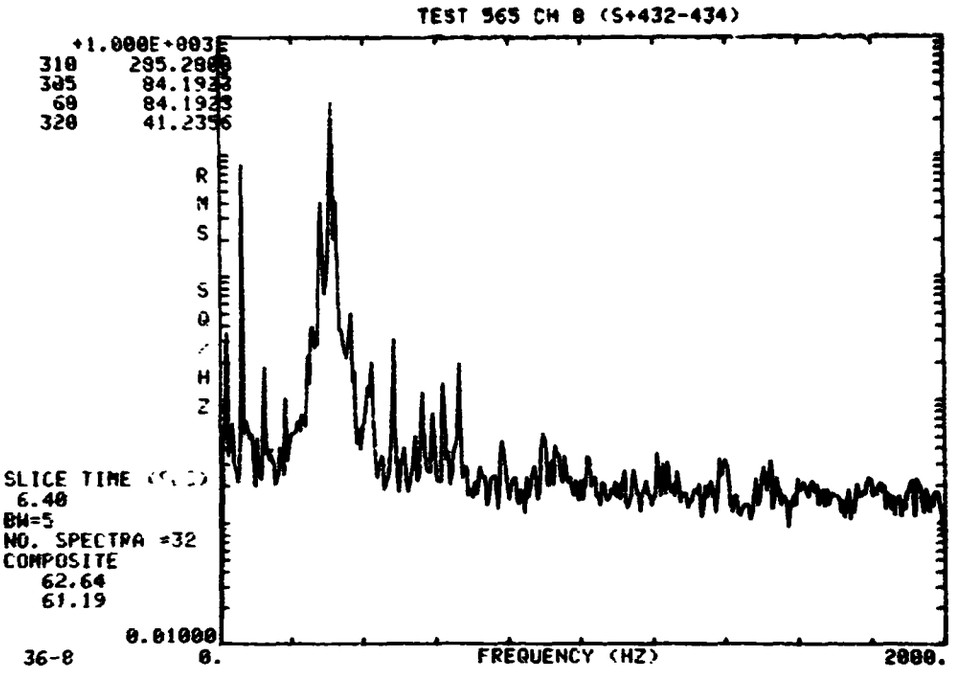

POWER-SPECTRAL-DENSITY PLOT
BELLOWS NO. 5005-1

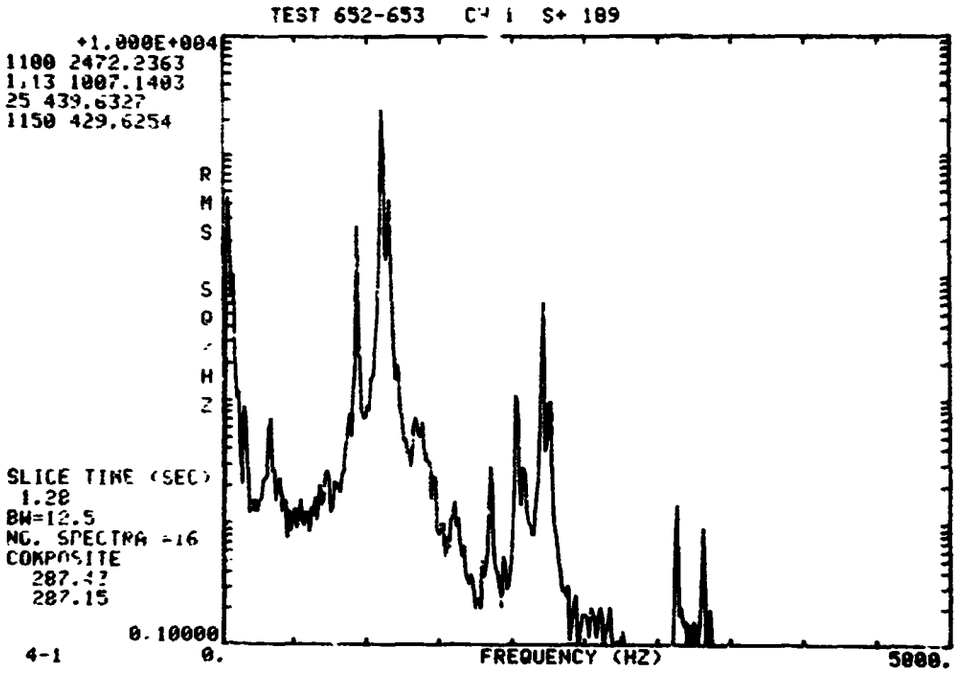

POWER-SPECTRAL-DENSITY PLOT
BELLOWS NO. 5006-10

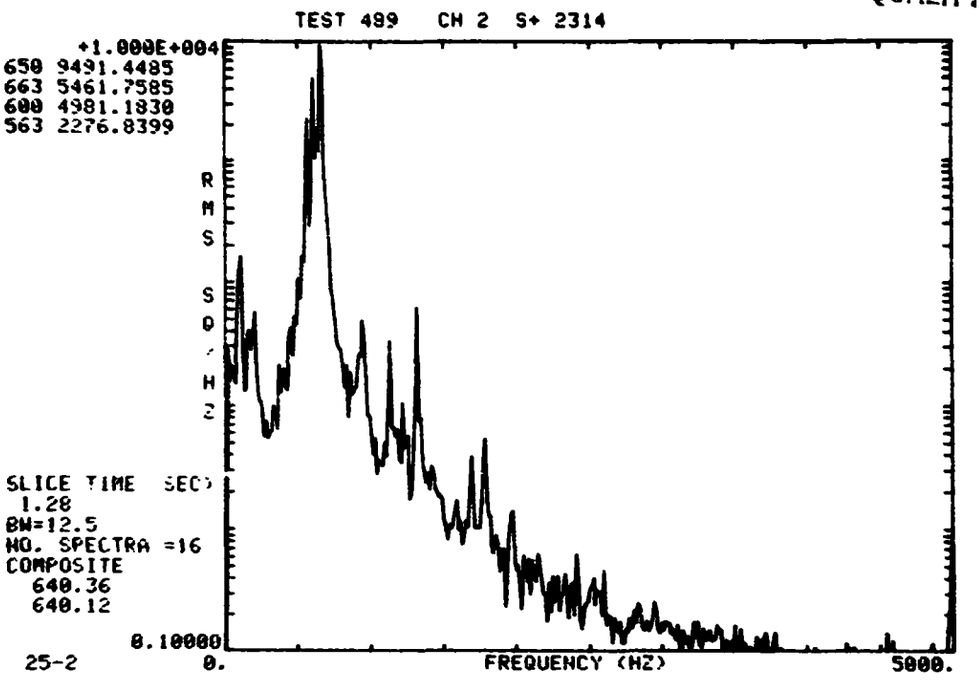

POWER-SPECTRAL-DENSITY PLOT
BELLOWS NO. 5009-1

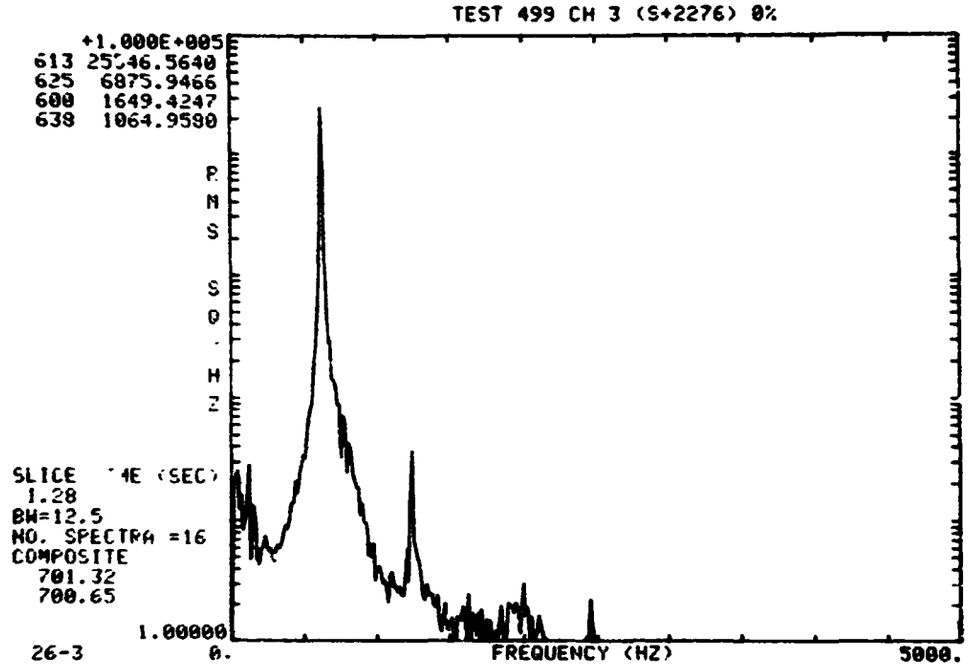

POWER-SPECTRAL-DENSITY PLOT
BELLOWS NO. 5011-1

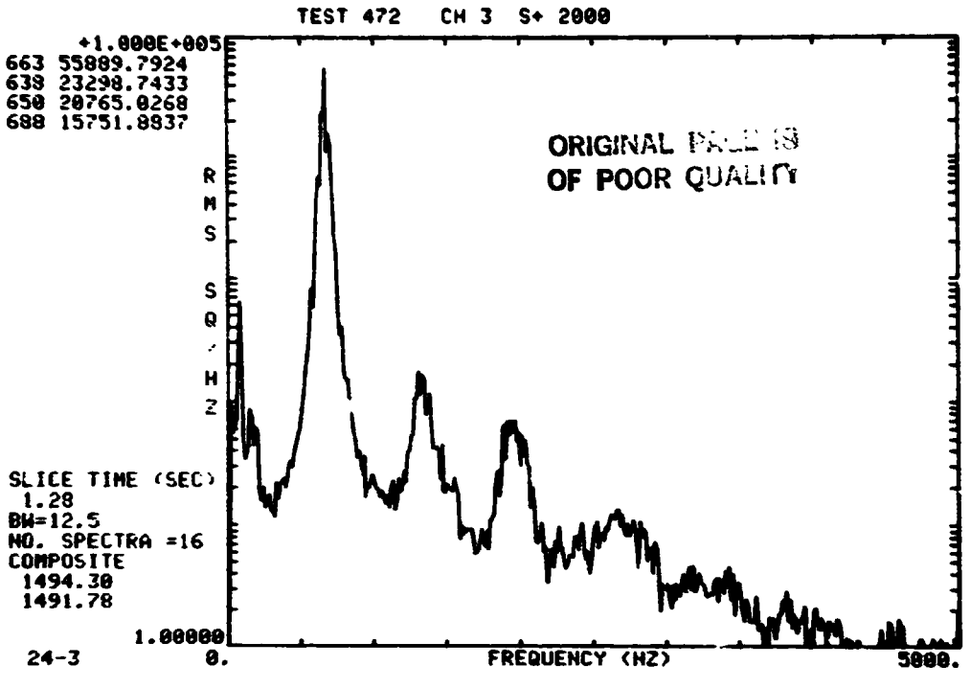

POWER-SPECTRAL-DENSITY PLOT
BELLOWS NO. 5013-2

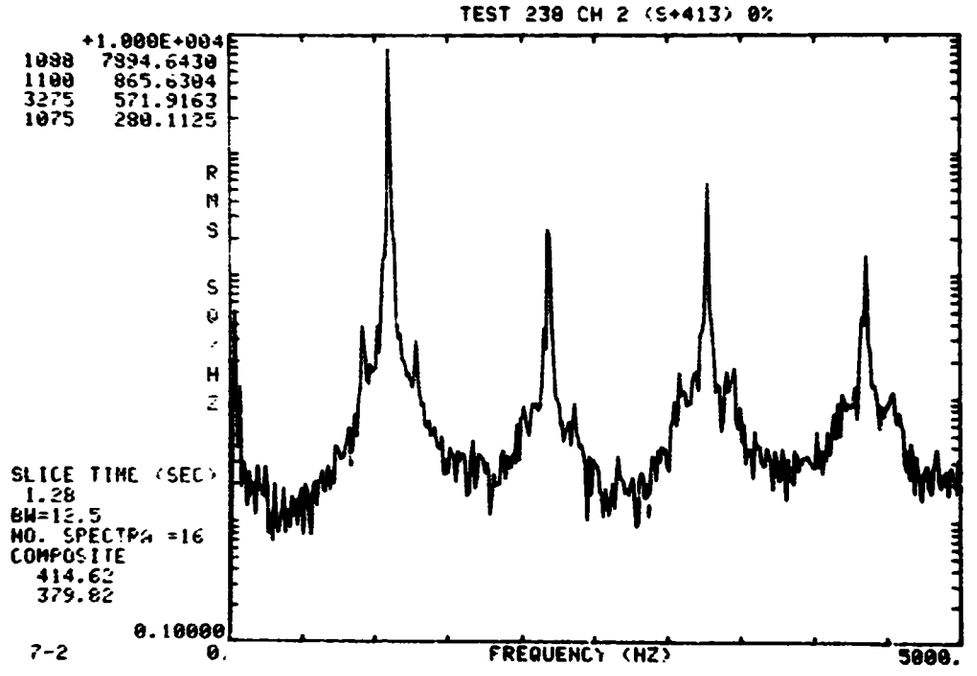

POWER-SPECTRAL-DENSITY PLOT
BELLOWS NO. 5028-2

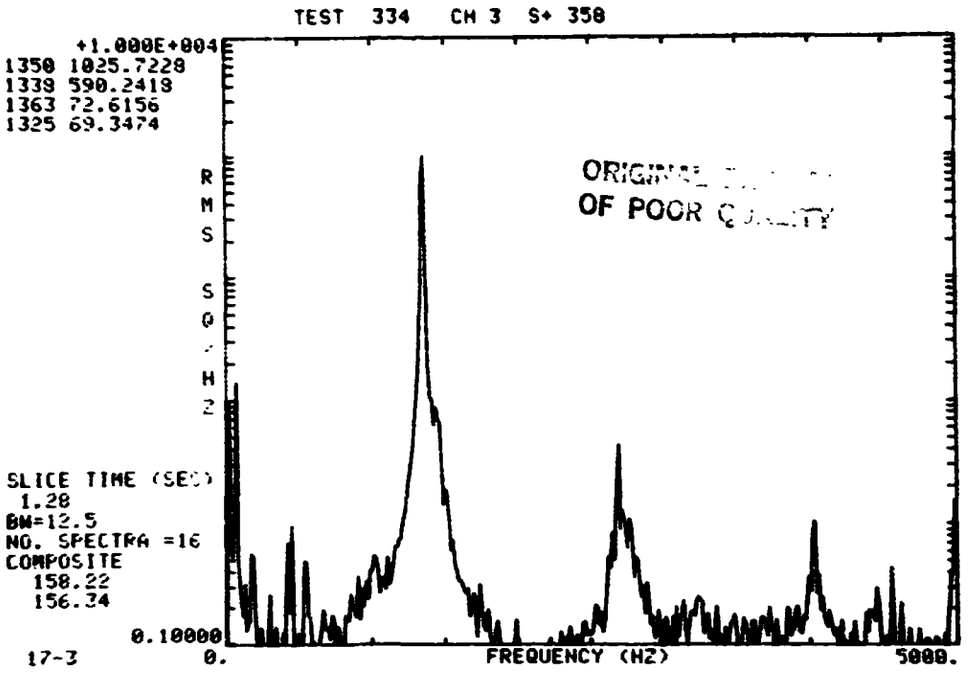

POWER-SPECTRAL-DENSITY PLOT
BELLOWS NO. 5034-1 COMPRESSED 48%

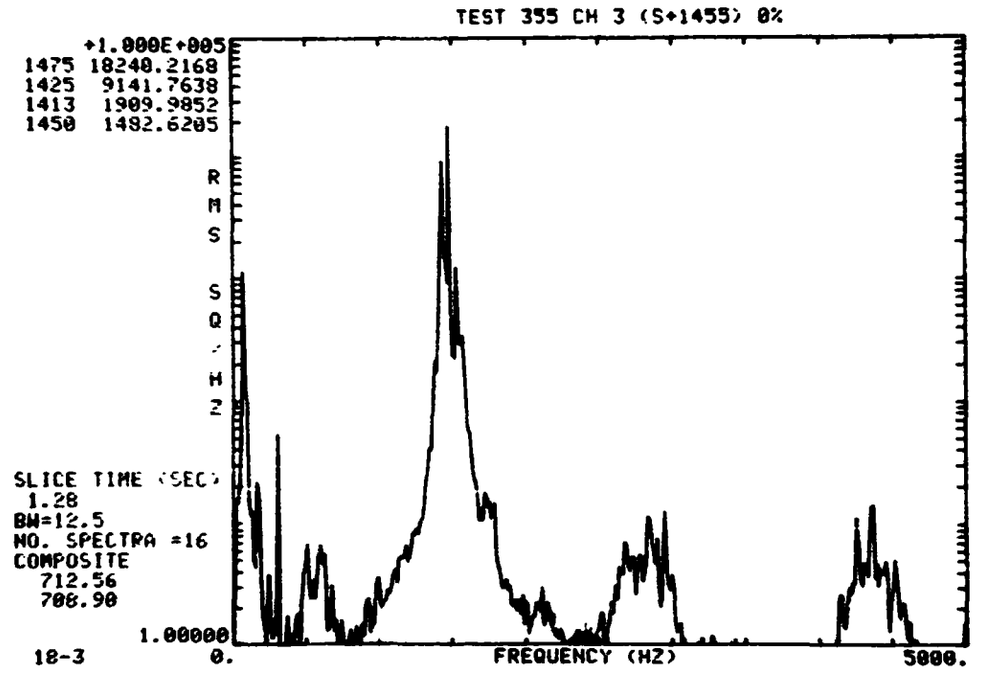

POWER-SPECTRAL-DENSITY PLOT
BELLOWS NO. 5034-3 COMPRESSED 30%

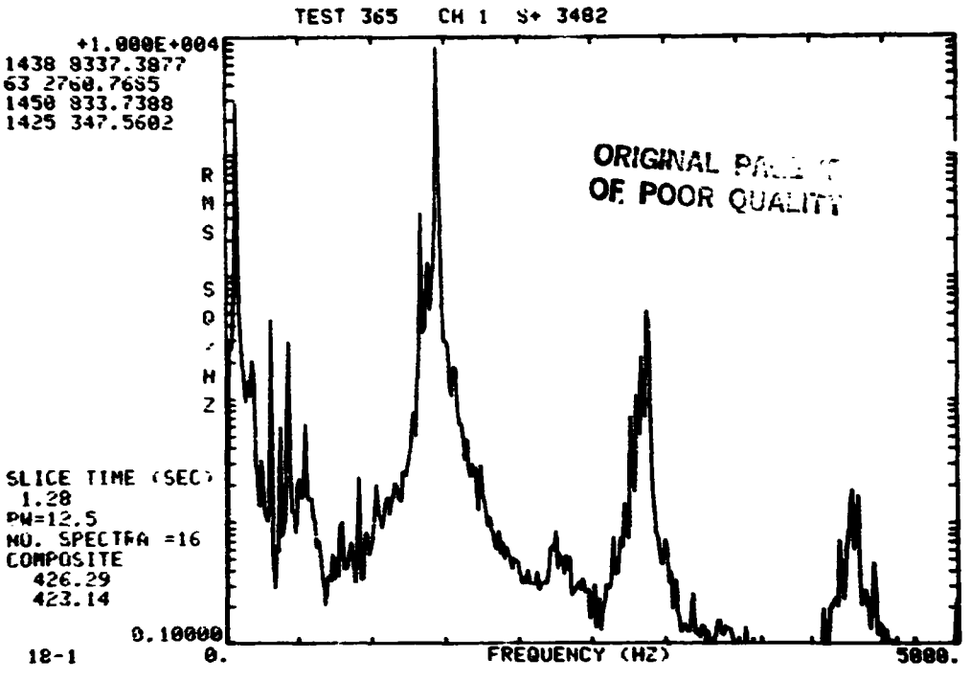

POWER-SPECTRAL-DENSITY PLOT
BELLOWS NO. 5034-4 COMPRESSED 17%

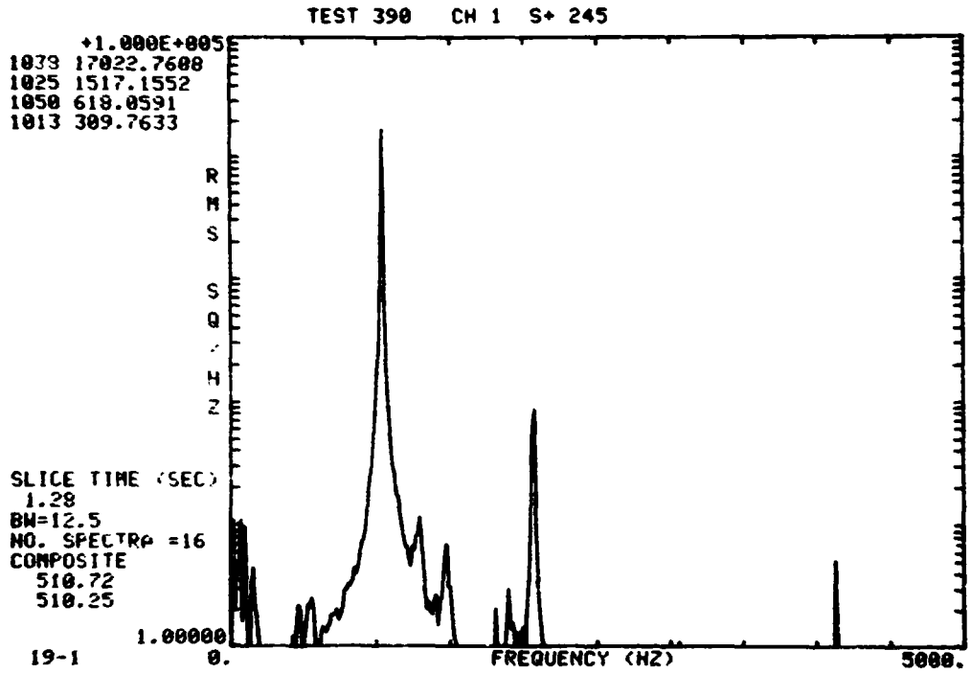

POWER-SPECTRAL-DENSITY PLOT
BELLOWS NO. 5034-5 EXTENDED 11%

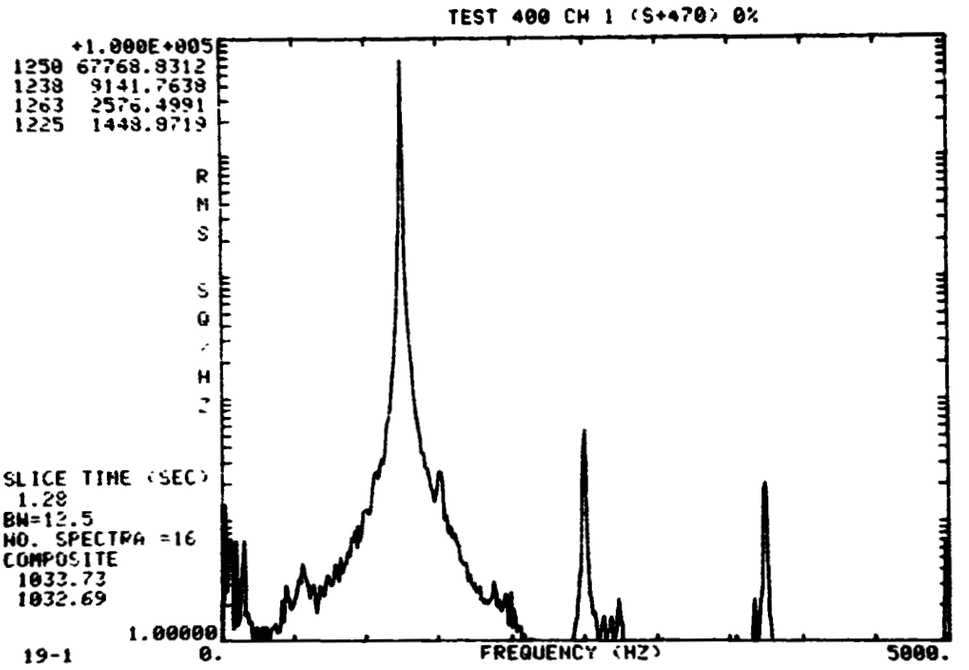

POWER-SPECTRAL-DENSITY PLOT
BELLOWS NO. 5034-6 EXTENDED 26%

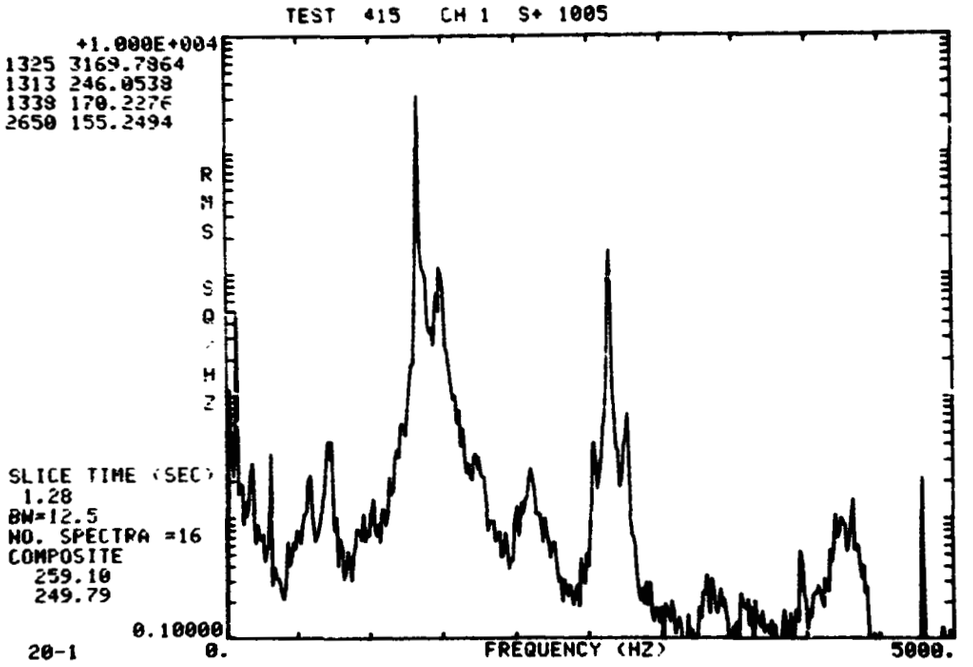

POWER-SPECTRAL-DENSITY PLOT
BELLOWS NO. 5034-7 COMPRESSED 71%

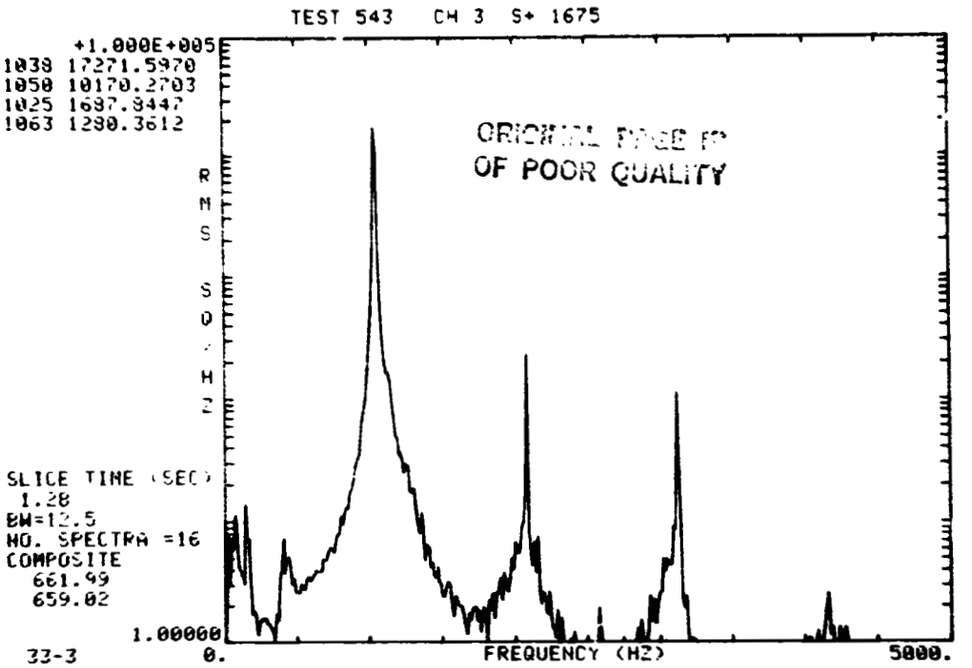

POWER-SPECTRAL-DENSITY PLOT
BELLOWS NO. AG #1

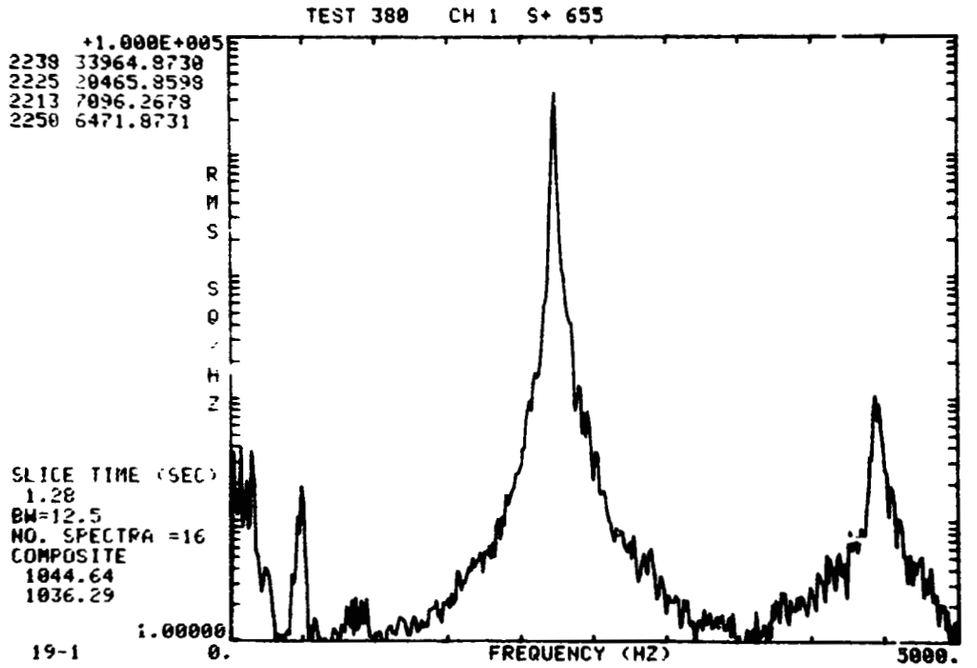

POWER-SPECTRAL-DENSITY PLOT
BELLOWS NO. 5035-1

APPENDIX G

FATIGUE LIFE DATA FOR MSFC TEST BELLOWS

MSFC TEST BELLOWS

BELLOWS NO.	f_F (HZ)	TIME TO FAILURE (SEC)	CYCLES TO FAILURE ($X10^6$)	MATERIAL	ACTUAL STRESS (PSI)	VARIATION
5002-1	62	148-158	.17-.18	321	29,800	ELBOW
5002-2	72	525-535	.70-.71	321	28,300	ELBOW
5002-3	48	313-333	.34-.36	321	29,000	ELBOW
5002-4	56	2255-2309	2.5-2.6	321	27,800	ELBOW
5002-5	70	10460-10585	16.0-16.1	321	26,500	ELBOW
5002-6	70	730-736	.95-.96	321	28,100	ELBOW
5005-1	33.2	1841-1863	.78-.79	321	28,200	
5005-2	65.2	75-100	----	321	~33,000	ELBOW
5006-10	77.7	1500-1530	1.7	321	27,900	
5009-1	40.5	2728-2743	1.8	321	27,900	
5011-1	49.4	3107-3133	1.9	321	27,600	
5013-2	50	2007-2027	1.3	321	28,000	
5013-3	45	749-760	.47-.48	321	28,800	
5028-1	65.8	787	----	21-6-9	~33,000	ELBOW
5028-2	66.6	150	.16	21-6-9	37,000	ELBOW
5034-1	82.5	1672	2.3	21-6-9	31,200	λ
5034-2	84	1427-1467	1.9-2.0	21-6-9	31,200	
5034-3	84.2	3391-3402	5.0	21-6-9	31,000	λ
5034-4	84.4	3683	5.3	21-6-9	31,000	λ
5034-5	65.5	353-373	.37-.39	21-6-9	34,000	λ
5034-6	85.5	226-256	.28-.32	21-6-9	34,200	λ
5034-7	85	2199	2.9	21-6-9	31,000	λ
5034-8	85.8	560-590	.74-.78	21-6-9	31,900	
5034-10	70.9	3580-3760	3.9-4.1	21-6-9	31,000	
5034-13	79.5	1375-1495	1.6-1.8	21.6-9	31,200	
5034-15	69	4180	4.5	21-6-9	31,000	
AG#1	57.8	1604-1634	1.7	21-6-9	31,400	
AG#2	74.8	20099-20124	----	21-6-9	----	
AG#3	80.5	11248-11278	----	21-6-9	----	
5035-1	113	1976-1996	4.4-4.5	21-6-9	31,000	
5035-2	110	437-477	.93-1.1	21-6-9	31,800	
5035-3	94	7916-8036	16.3-16.6	21-6-9	31,000	λ

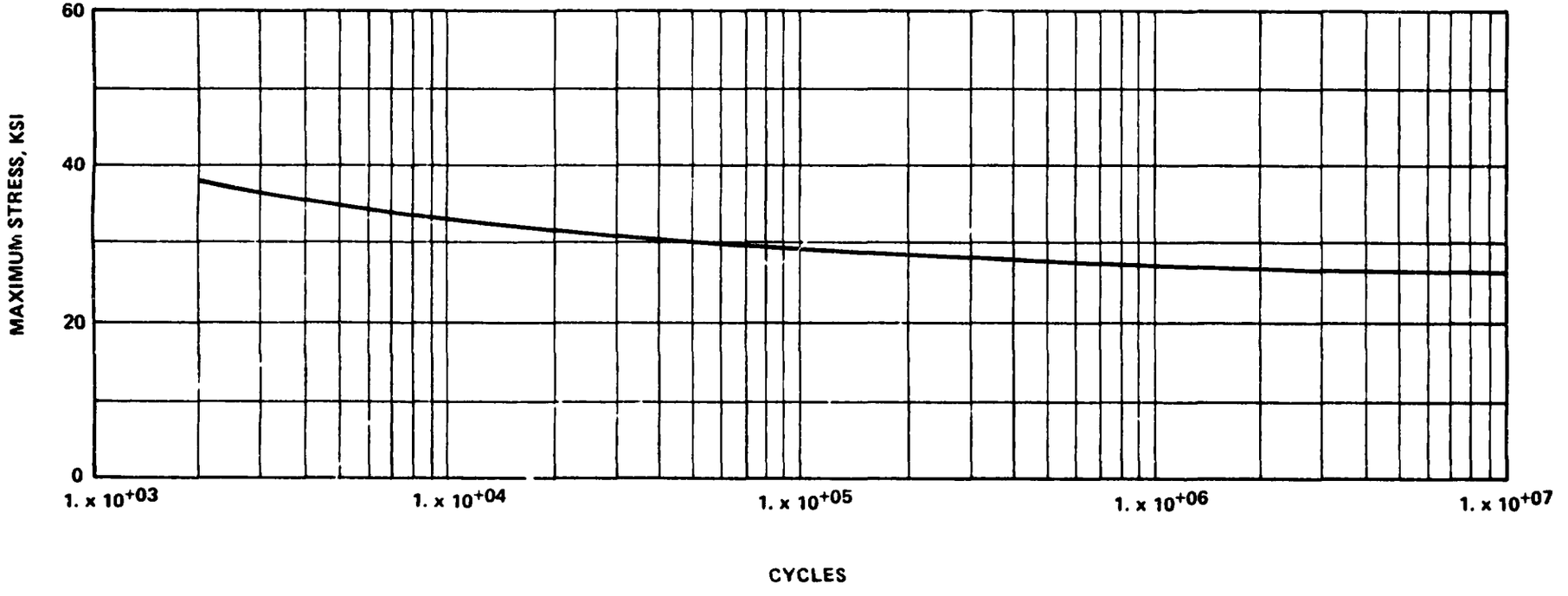

S-N Diagram for 321 S.S. (at 70 F)

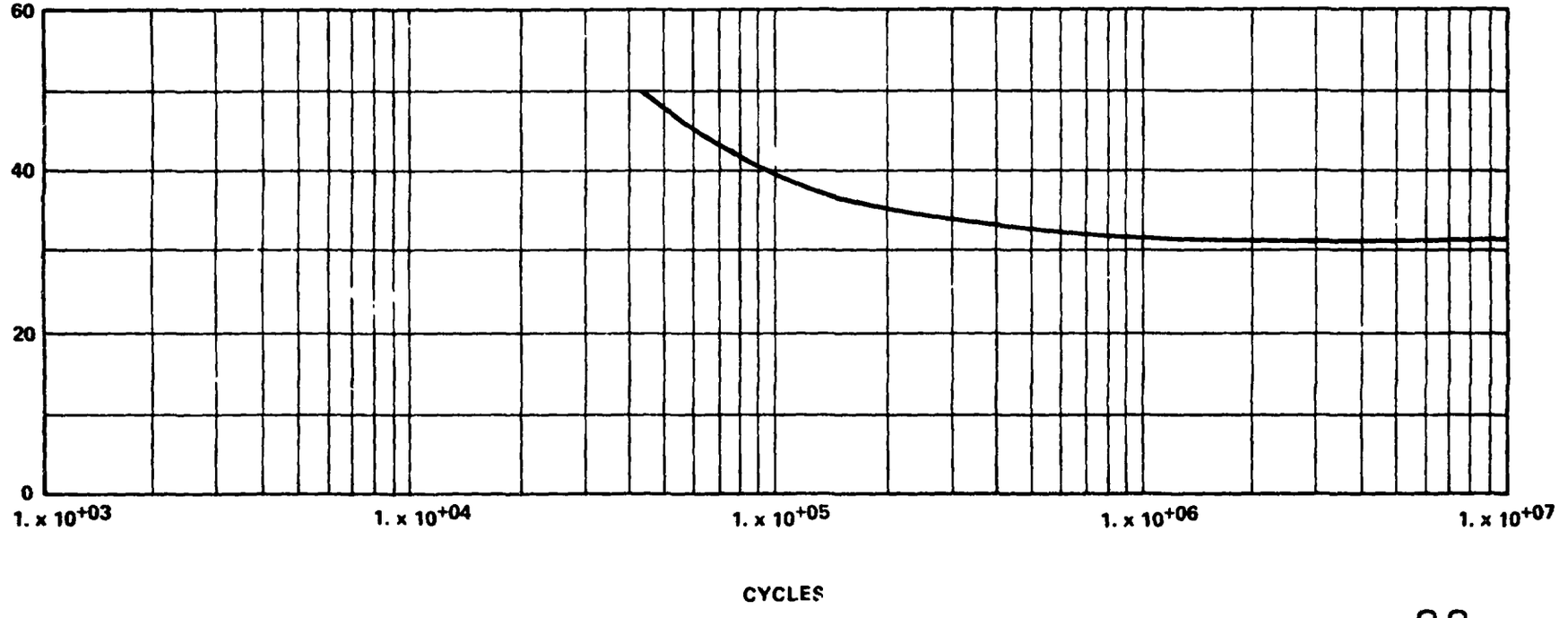

S-N Diagram for 21-6-9 Alloy (at 70 F)

APPENDIX H

BELLOWS FLOW-INDUCED VIBRATION COMPUTER PROGRAM

```
C***THIS IS THE FIS DECK
C      THIS PROGRAM PREDICTS FATIGUE LIFE OF BELLOWS WHEN EXPOSED TO
C       FLOW-INDUCED VIBRATION.
C  INPUT
C      JFLAG = 1(COMPUTE KA), 2(USE GIVEN KA). KA IS
C        OVERALL SPRING RATE, LB/IN
C      NFLUID = 1(GAS), 2(LIQUID)
C      NDEG = NUMBER OF BELLOWS LONGITUDINAL DEGREES OF FREEDOM, 2*NC-1
C      NC = NUMBER OF BELLOWS CONVOLUTES
C      SIGMA = CONVOLUTE WIDTH, IN.
C      LAMBDA = DISTANCE BETWEEN ADJACENT CONVOLUTE CROWNS, IN.
C      H = MEAN DISC HEIGHT, IN.
C      T = THICKNESS PER CONVOLUTE PLY, IN.
C      NPLY = NUMBER OF PLYS IN THE BELLOWS CONVOLUTES
C      DI = BELLOWS INSIDE DIAMETER, IN.
C      DO = BELLOWS OUTSIDE DIAMETER, IN.
C      E = YOUNG'S MODULUS OF THE BELLOWS MATERIAL, LB/SQ IN.
C      RHOM = WEIGHT DENSITY OF THE BELLOWS MATERIAL, LB/CU IN.
C      LOVERD = LENGTH FROM TERMINATION OF ELBOW TO FIRST CONVOLUTE
C        DIVIDED BY THE I.D. OF PIPE JUST BEFORE THE BELLOW.
C      CE = DIMENSIONLESS ELBOW FACTOR
C      IF NFLUID = 1(GAS), THE PERFECT GAS EQUATION OF STATE IS USED FOR
C        CALCULATING GAS DENSITY AT THE STATE DEFINED BY P AND TEMP.
C        IT IS ASSUMED THAT THE GAS PROPERTIES ARE KNOWN AT A REFERENCE
C        STATE DEFINED BY RHOREF, PREF, AND TREF.
C        P = GAS PRESSURE, PSIG
C        TEMP = GAS TEMPERATURE, DEG. F.
C        PREF AND TREF = REFERENCE GAS STATE, PSIA AND DEG. F.
C      RHOREF = GAS DENSITY AT REFERENCE STATE,LB/CU FT.
C        GAMMA = RATIO OF SPECIFIC HEATS FOR GAS
C      IF NFLUID = 2(LIQUID), THE LIQUID DENSITY MUST BE KNOWN APRIORI AT
C        THE LIQUID STATE(P AND TEMP)
C        P = LIQUID PRESSURE, PSIG
C        TEMP = LIQUID TEMPERATURE, DEG. F.
C        RHOF = LIQUID DENSITY AT P AND TEMP, LB/CU FT.
C * * * * * * * * * * * * * * * * * * * * * * * * * * * * * * * * * * * * *
      IMPLICIT INTEGER*2(I-N,#)
      IMPLICIT REAL(A-H,O-Z)
      REAL MODER,MASS,MFLUID,MFLUDR,MMETAL,MCF,MASSR
      REAL KA,K,N1,LOVERD
      TRACE LABELS
      INTEGER*2 ANS,DEV
      INTEGER*1 TITLE(80),DFILE(20),OFILE(20)
      DIMENSION FREQ(75),V(75,3),SI(75)
      DIMENSION VELR(50),MCF(50),SI2(50),VSPEC(20),FISVEL(20)
      COMMON NPLY,SSR,NFLUID,P,RHOF,JCURVE,JOP,Q
      REAL NC,NPLY,LAMBDA,FLUID1,FLUID2,MFLUID,MMETAL,KA,K,MASS
C * * * * * * * * * * * * * * * * * * * * * * * * * * * * * * * * * * * * *
      CALL GONEW(6)
```

```
      CALL BFDEV(6,'DC1 ')
      CALL BFDEV(5,'DK1 ')
      CALL BFDEV(4,'KBO ')
      CALL BFDEV(3,'LPO ')
      WRITE(6,1000)
 1000 FORMAT(1X 'INPUT DATA FILE NAME - XXXXXX.DAT',/,1X,'[illegible].DAT')
      READ(4,*)DFILE
      CALL BFACT(5,DFILE)
      READ(5,1010)(TITLE(I),I=1,80)
 1010 FORMAT(80A1)
      READ(5,1020)JFLAG,NFLUID,NDEG
 1020 FORMAT(3I5)
      READ(5,1030)NC,NPLY,SIGMA,LAMBDA,H,T
      READ(5,1030)DI,DO,E,RHOM,KA,LOVERD
 1030 FORMAT(6F10.0)
      GO TO (10,11),NFLUID
   10 READ(5,1030)P,TEMP,PREF,TREF,RHOREF,GAMMA
      GO TO 12
   11 READ(5,1030)P,TEMP,RHOF
   12 CONTINUE
      CALL BFCLO(5)
C * * CALCULATION OF NATURAL FREQUENCIES AND EXCITATION VELOCITIES * * *
      PI=3.1415927
      G=32.174049
      DMEAN=(DI+DO)/2.
      GO TO (30,35),JFLAG
   30 KA=DMEAN*E*(NPLY/NC)*(T/H)**3
   35 K=2.*NC*KA*12.
      A=(SIGMA-T*NPLY)/2.
      MMETAL=PI*RHOM*T*NPLY*DMEAN*(PI*A+H-2.*A)/G
      GO TO (36,37),NFLUID
   36 RHOF=RHOREF*(P+14.7)*((TREF+460.)/(TEMP+460.))/(PREF*1728.)
      GO TO 38
   37 RHOF=RHOF/1728.
   38 FLUID1=0.0
      DELTA=LAMBDA - SIGMA
      FLUID2=0.68*RHOF*DMEAN*(H**3)/(G*DELTA)
      STOP=0.3
      STLO=0.1
      STCRIT=0.2
      AMODE=1.
      MODER=NC
      MFLUDR=(FLUID2*MODER)/NC
      MASSR=MFLUDR+MMETAL
      FREQC=(SQRT(2.*K/MASSR))/(2.*PI)
      VELC=FREQC*SIGMA/(STCRIT*12.)
      WRITE(6,*)
      DO 60 MODE=1,NDEG
      MFLUID=FLUID2*(AMODE/NC)
      MASS=MFLUID+MMETAL
```

```
      B1=SQRT(2.*(1.+COS((PI*(2.*NC-MODE))/(2.*NC))))
      FREQ(MODE)=SQRT(K/MASS)*B1/(2.*PI)
      DO 55 J=1,3
      GO TO(40,45,50),J
   40 V(MODE,J)=FREQ(MODE)*SIGMA/(STUP*12.)
      GO TO 55
   45 V(MODE,J)=FREQ(MODE)*SIGMA/(STCRIT*12.)
      GO TO 55
   50 V(MODE,J)=FREQ(MODE)*SIGMA/(STLO*12.)
   55 CONTINUE
      VELR(MODE)=V(MODE,2)/VELC
      MCR(MODE)=2.*VELR(MODE)
   60 AMODE=AMODE+1.
C * * * * * * * * * * * * * * * * * * * * * * * * * * * * * * * * * * * * * * *
C     THEORETICAL FLOW-INDUCED STRESS FOR CRITICAL STROUHAL NUMBER
      SSR=KA*NC/(DMEAN*NPLY)
      IF(NFLUID-1)70,65,70
   65 R1=D1/2.
      HR1=H/R1
      CO=SQRT(GAMMA*(P+14.7)*G/(RHOF*12.))
      CALL ACOURE(HR1,R1,CO,FREQCO,QADJUS)
   70 AMODE=1.0
      C1=.13
      C2=.462
      C3=1.0
      C4=10.
      C5=.05
      C6=1.25
      C7=5.5
      CM=1.
      N1=1.0
      IF(LOVERD.EQ.0.0) N1=0.0
      CE=1.+(N1*4.//(2.+LOVERD))
      DO 100 MODE=1,NDEG
      IF(NPLY.GT.1.) GO TO 75
      CNP=1.
      GO TO 80
   75 VP=V(MODE,2)/VELC
      AA=1.+(C7*VP**2)
      CNP=1.0-(C6*SIGMA/H)/AA
   80 VP=V(MODE,3)/VELC
      BB=C1/(C2+VP**2)
      CC=C3*ABS(SIN(PI*VP))/(C4+VP**2)
      CST=BB+CC+C5
      PD=12.*RHOF*(V(MODE,3)**2)/(2.*G)
      DD=CST*H*T*PD/(VP*H*SSR*DELTA)
      EE=1.+.1*((400./SSR)**2)
      FTS=EE*DD*CNP*CM*CE/NPLY
      IF(NFLUID-1)90,85,90
   85 IF (FREQ(MODE).GE.FREQCO) FTS=FTS*QADJUS
```


C - 3

```
151        90 SI(MODE)=FIS
152           AMODE=AMODE+1.
153       100 CONTINUE
154           WRITE (6,500)
155       500 FORMAT(' DO YOU WANT THE STRESS AT A SPECIFIC
156          $ FLUID VELOCITY ? (YES=1,NO=2) ')
157           READ (5,*) FAIL
158           GO TO (510,600), FAIL
159       510 CONTINUE
160           WRITE(6,520)
161       520 FORMAT(' HOW MANY SPECIFIC FLUID VELOCITIES ? ')
162           READ(5,*) NN
163           WRITE(6,530)
164       530 FORMAT(' INPUT FLUID VELOCITY(S) IN FT/SEC ')
165           DO 600 I=1,NN
166           READ(5,*) VSPEC(I)
167           IF (VSPEC(I).EQ.0.) GO TO 560
168           IF (NPLY.GT.1.) GO TO 540
169           CNP=1.
170           GO TO 550
171       540 VP=VSPEC(I)/VELC
172           AA=1.+(C7*VP**2)
173           CNP=1.0-(C6*SIGMA/H)/AA
174       550 VP=VSPEC(I)/VELC
175           BB=C1/(C2+VP**2)
176           CC=C3*ABS(SIN(PI*VP))/(C4+VP**2)
177           CST=BB+CC+C5
178           PD=12.*RHOF*(VSPEC(I)**2)/(2.*G)
179           DD=CST*H*T*PD/(VP*H*SSR*DELTA)
180           EE=1.+.1*((400./SSR)**2)
181           FIS=EE*DD*E*CNP*CM*CC/NPLY
182           FISVEL(I)=FIS
183           GO TO 570
184       560 FISVEL(I)=0.0
185       570 IF(I.EQ.NN) GO TO 610
186       600 CONTINUE
187       610 CALL ERASE
188           WRITE(6,1010)(TITLE(I),I=1,80)
189           WRITE(6,940) SIGMA,LAMBDA,H,T,DI,DO,NC,NPLY,E
190           WRITE(6,950)KA,RHOM,P,TEMP,RHOF,NFLUID,CE
191           WRITE(6,960)
192           DO 620 MODE=1,NDEG
193       620 WRITE(6,970)MODE,SI(MODE),FREQ(MODE),V(MODE,1),V(MODE,2),V(MODE,3
194          1)
195           IF (NFLUID-1)710,700,710
196       700 WRITE(6,980)FREQCO,QADJUS
197           IF (FAIL.EQ.2) GO TO 800
198           WRITE(6,991) (VSPEC(I),FISVEL(I),I=1,NN)
199           GO TO 800
200       710 IF (FAIL.EQ.2) GO TO 800
```

```
      WRITE(6,990) (VSPEC(I),FISVEL(I),I=1,NN)
  800 WRITE(6,810)
  810 FORMAT(//,1X,'WHERE DO YOU WANT OUTPUT SENT? 0-EXIT,1-FILE,
     +2-PRINTER')
     1')
      READ(4,*) ANS
      IF(ANS.EQ.0) GO TO 2000
      IF(ANS.EQ.1) DEV=5
      IF(ANS.EQ.2) DEV=3
      IF(ANS.EQ.1) GO TO 820
      GO TO 900
  820 WRITE(6,830)
  830 FORMAT(1X,'OUTPUT FILE NAME?')
      READ(4,*) OFILE
      CALL BFNEW(5,OFILE)
  900 WRITE(DEV,1010)(TITLE(I),I=1,80)
      WRITE(DEV,940)SIGMA,LAMBDA,H,T,DI,DO,NC,NPLY,E
      WRITE(DEV,950)KA,RHOM,P,TEMP,RHOF,NFLUID,CE
      WRITE(DEV,960)
      DO 910 MODE=1,NDEG
  910 WRITE(DEV,970)MODE,SI(MODE),FREQ(MODE),V(MODE,1),V(MODE,2),V(MODE
     1,3)
      IF(NFLUID-1) 930,920,930
  920 WRITE(DEV,980)FREQCO,QAOJUS
  930 CALL BFCLO(5)
  940 FORMAT(29X,18HBELLOWS PARAMETERS//
     $        19X,26HSIGMA(CONVOLUTE WIDTH, IN),11X,F6.3,/
     $            19X,27HLAMBDA(CONVOLUTE PITCH, IN),10X,F6.3,/
     $            19X,23HH(MEAN DISC HEIGHT, IN),14X,F6.3,/
     $            19X,30HT(CONVOLUTE THICKNESS/PLY, IN),7X,F6.3,/
     $            19X,23HDI(INSIDE DIAMETER, IN),14X,F6.3,/
     $            19X,24HDO(OUTSIDE DIAMETER, IN),13X,F6.3,/
     $            19X,24HNC(NUMBER OF CONVOLUTES),12X,F7.3,/
     $            19X,21HNPLY(NUMBER OF PLIES),15X,F7.3,/
     $            19X,28HE(YOUNG'S MODULUS, LB/SQ.IN),4X,E11.4)
  950 FORMAT(19X,30HKA(OVERALL SPRING RATE, LB/IN),2X,F11.3,/
     $        19X,32HRHOM(MATERIAL DENSITY, LB/CU.IN),4X,F7.3,//
     $        30X,16HFLUID PARAMETERS,//
     $        19X,1/HP(PRESSURE, PSIG),19X,F7.3,/
     $            19X,24HTEMP(TEMPERATURE, DEG F),11X,F8.3,/
     $            19X,29HRHOF(FLUID DENSITY, LB/CU.IN),3X,E11.4,/
     $            19X,23HNFLUID(1=GAS, 2=LIQUID),19X,I1,/
     $            19X,'CE(ELBOW FACTOR, DIMENSIONLESS)',6X,F6.3//
     $        25X,'THEORETICAL BELLOWS PERFORMANCE',/)
  960 FORMAT(1X,/9HMODE NO.  FLOW-IND. STRESS  NATURAL FREQUENCY      F
     $LOW EXCITATION RANGE,FT/SEC,/,18X,3HPSI,
     $        16X,2HHZ,13X,5HLOWER,5X,8HCRITICAL,4X,5HUPPER,/)
  970 FORMAT(3X,12,8X,E11.4,7X,F11.3,5X,3F11.3)
  980 FORMAT(//,3X,'FIRST MODE RADIAL ACOUSTIC RESONANT FREQUENCY=',F9
     +.3,4X,' QAOJUS=',F5.2,/)

  990 FORMAT(/,'   STRESS AT ',F7.1,' FT/SEC IS ',E11.4,' PSI ')
  991 FORMAT(/,'   UNADJUSTED STRESS AT  ',F7.1,' FT/SEC IS ',E11.4,
     +  ' PSI ')
 2000 CONTINUE
      END
```

```
1
2           SUBROUTINE ACOURE (X,Y,Z,FREQCO,QADJUS)
3           IMPLICIT INTEGER*2(I-N,$)
4           IMPLICIT REAL(A-H,O-Z)
5           PI=3.1415927
6           HRI=X
7           RI=Y
8           CO=Z
9           IF(HRI.LE.0.55) GO TO 20
10        10 FNCO=1.972-1.222*HRI
11          GO TO 30
12        20 FNCO=3.8-4.545*HRI
13        30 FREQCO=12.*FNCO*CO/(2.*PI*RI)
14          QADJUS=5.0
15          RETURN
16          END
```

GENERAL CARD DESIGN
(1 - 80 SPACES)

EXAMPLE - INPUT DATA DECK

```
1BELLOW PROG LOX FEED LINE AT 294PSIG, -296F, 25.4FPS, 21-6-9, ARROW
 1  2  9
   NC            NPLY             σ              λ              H              T
.500000 +01 .300000 +01 .300000 +00 .604000 +00 .682000 +00 .160000 -01
    DI            DO               E            RHOM        KA (EXP)      LOVERD
.171200 +02 .185800 +02 .290000 +08 .280000 +00 .000000 +00 .000000 +00
     P            TEMP           RHOF
.294000 +03-.296000 +03 .714000 +02
```

(IDENTIFICATION)

(KA, NFLUID, 2NC-1)

APPENDIX I

STRAIN VERSUS FORCE PLOTS AND STRAIN VERSUS PRESSURE PLOTS FOR MSFC BELLOWS BENCH TESTS

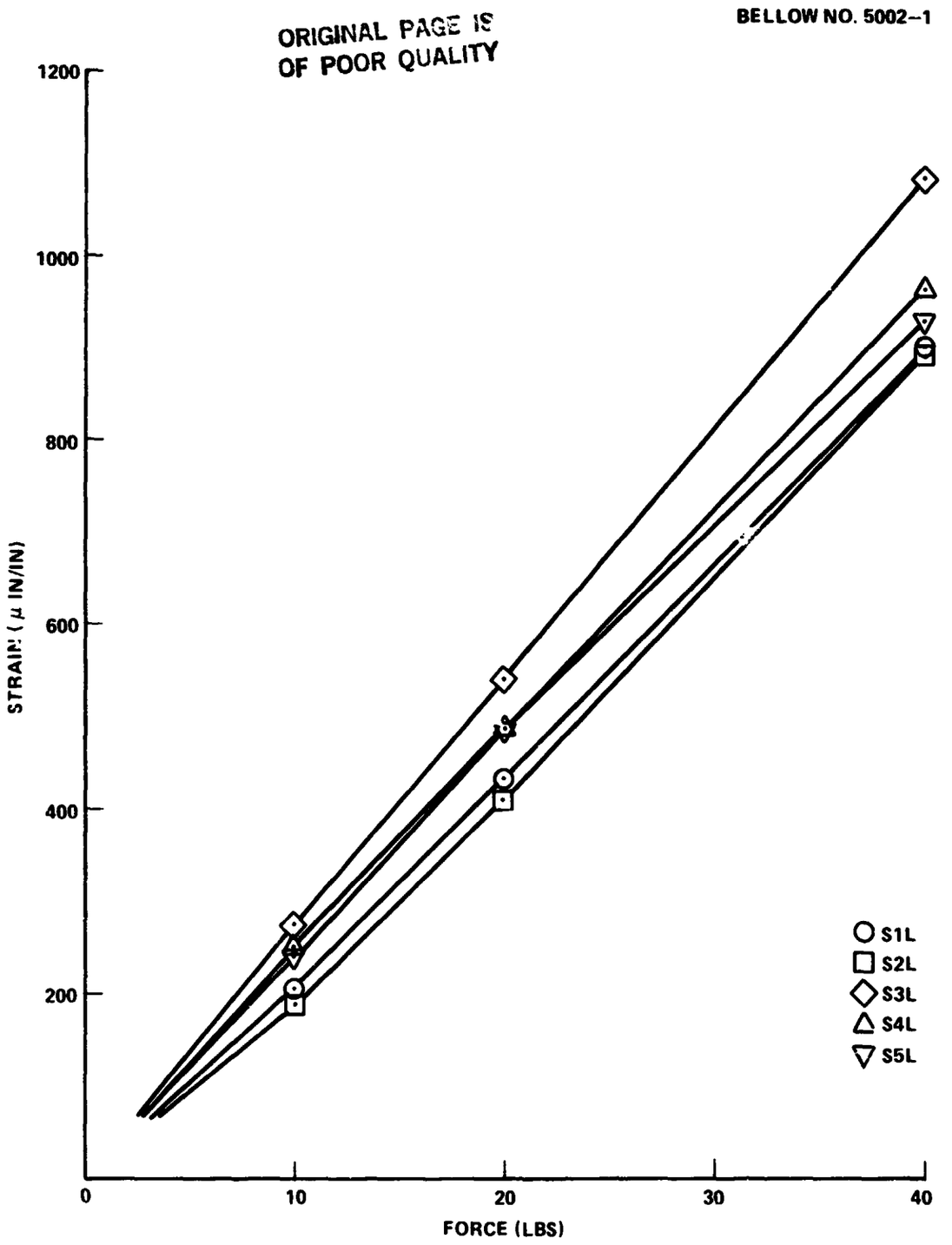

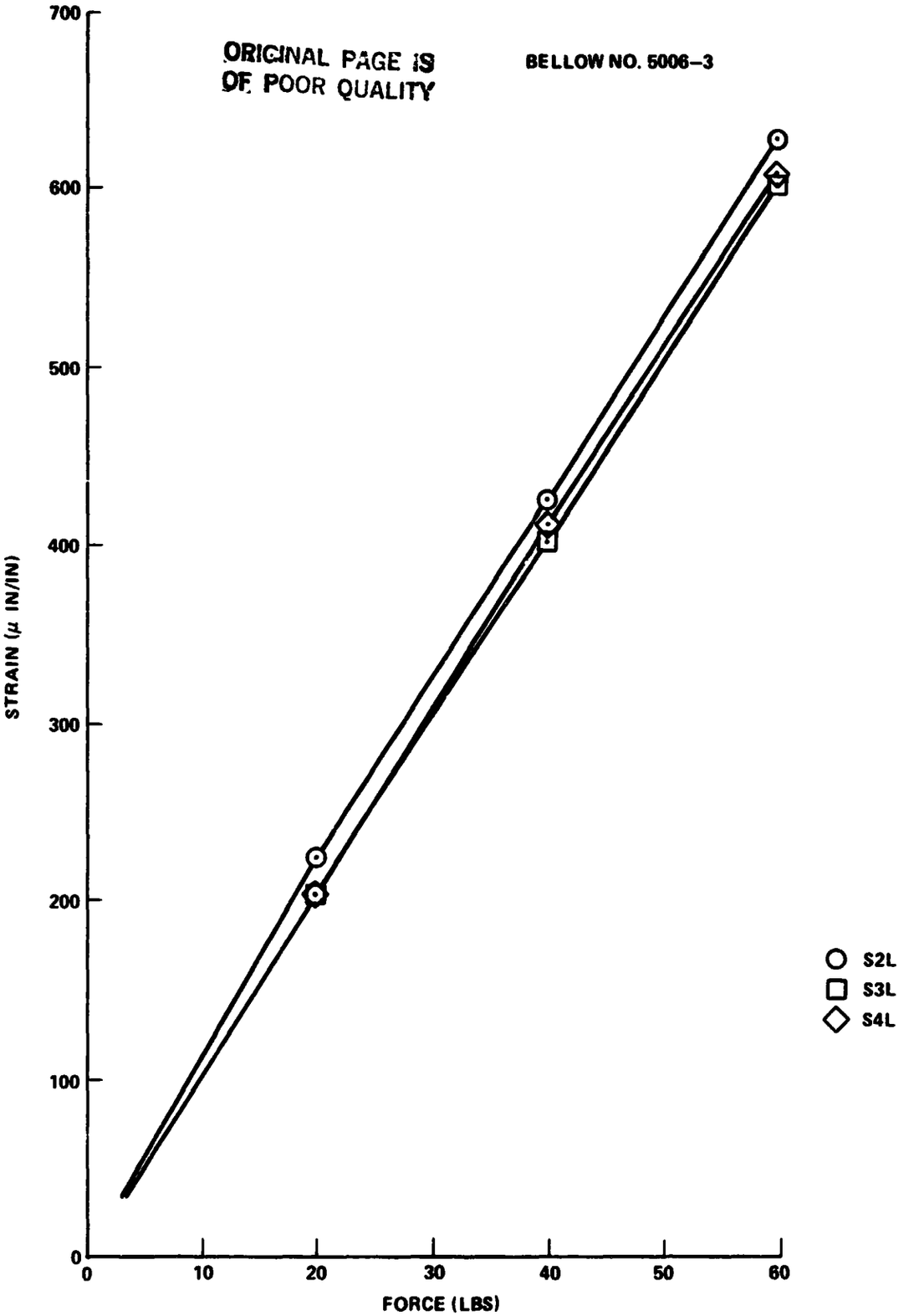
ORIGINAL PAGE IS
OF POOR QUALITY
BELLOW NO. 5006-3
700
600
500
400
300
200
100
0
STRAIN (μ IN/IN)
0
10
20
30
40
50
60
FORCE (LBS)
S2L
S3L
S4L

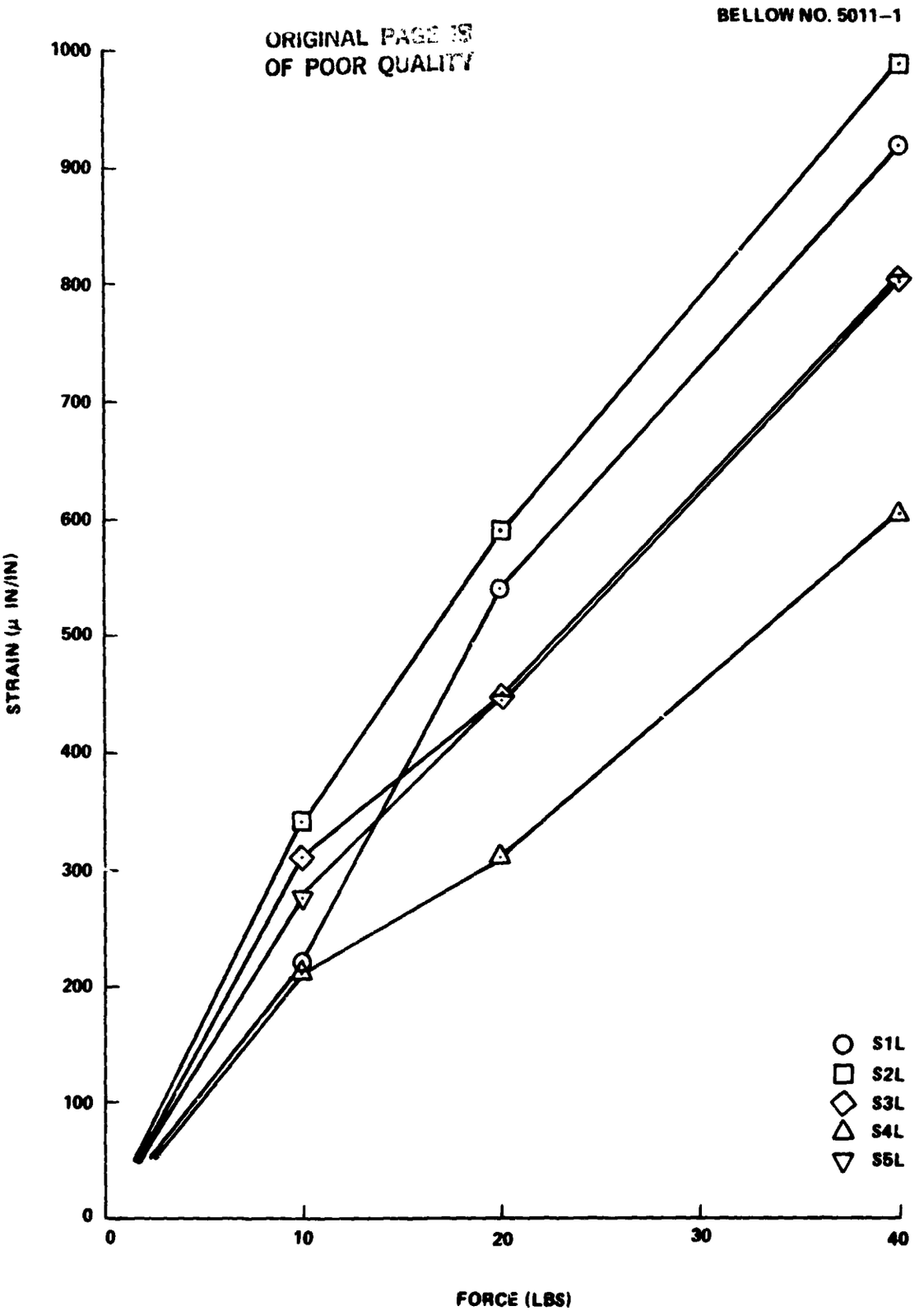

BELLOW NO. 5012–1

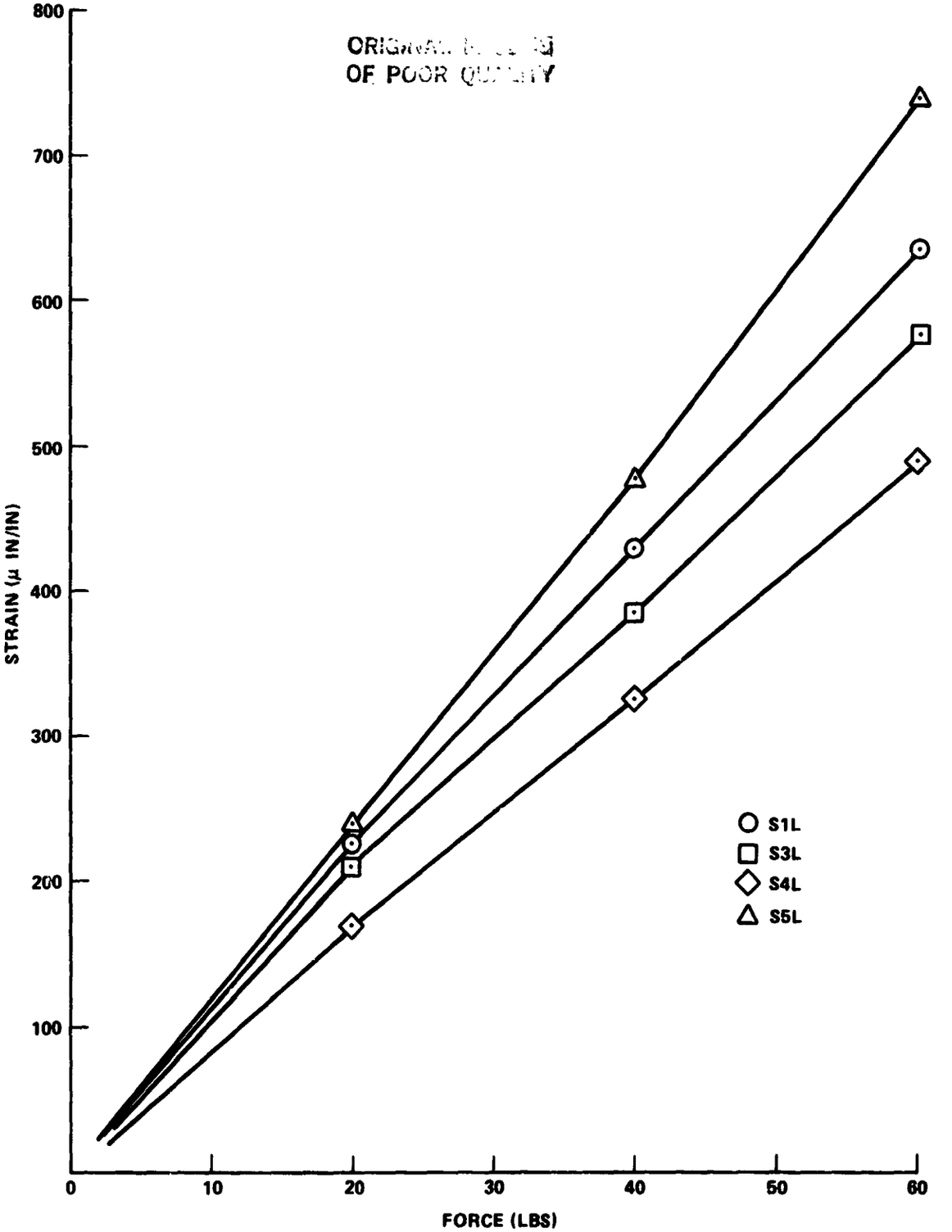

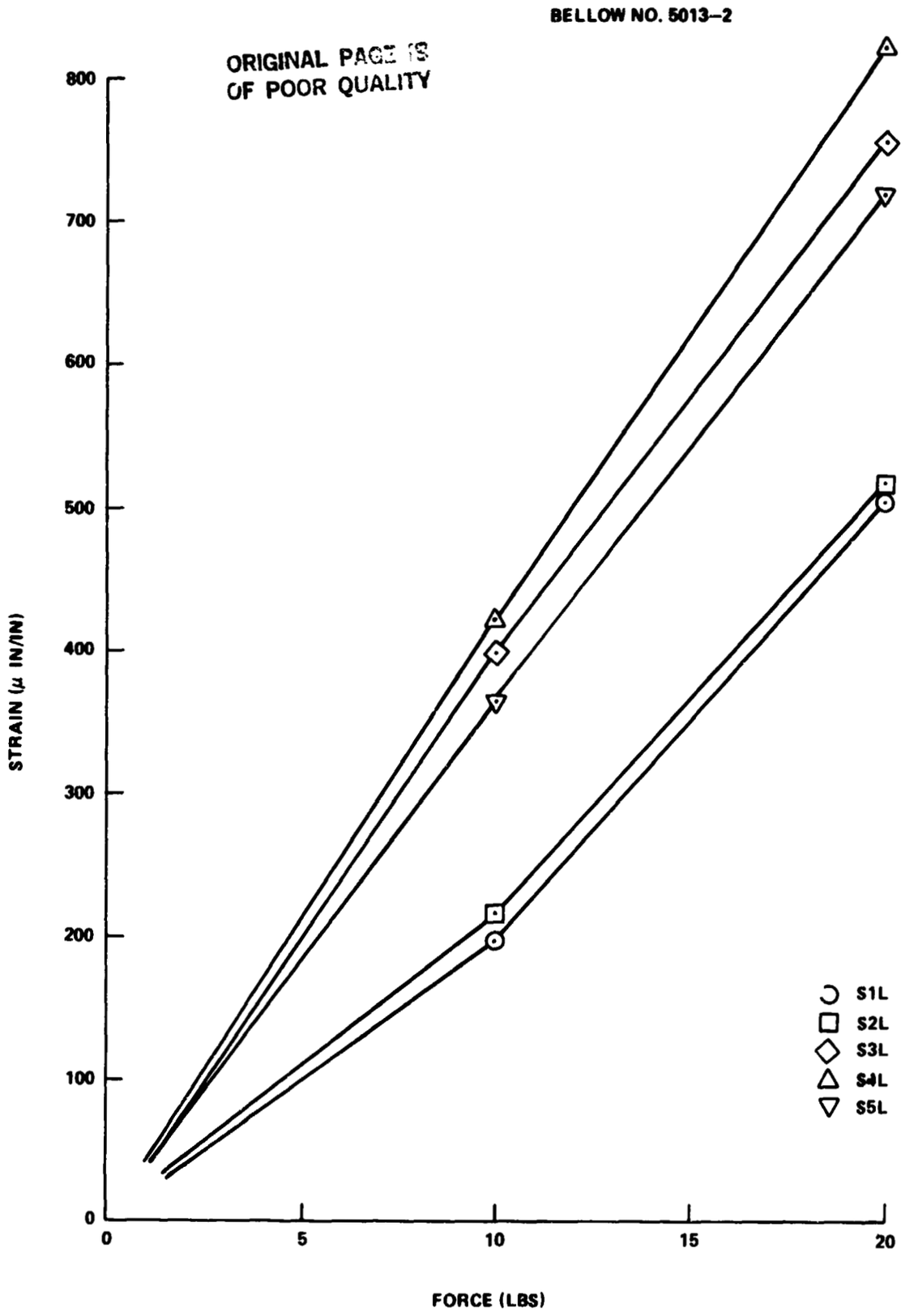
BELLOW NO. 5013–2
ORIGINAL PAGE IS
OF POOR QUALITY
800
700
600
500
400
300
200
100
0
STRAIN (μ IN/IN)
0
5
10
15
20
FORCE (LBS)
S1L
S2L
S3L
S4L
S5L

BELLOW NO. 5028-1

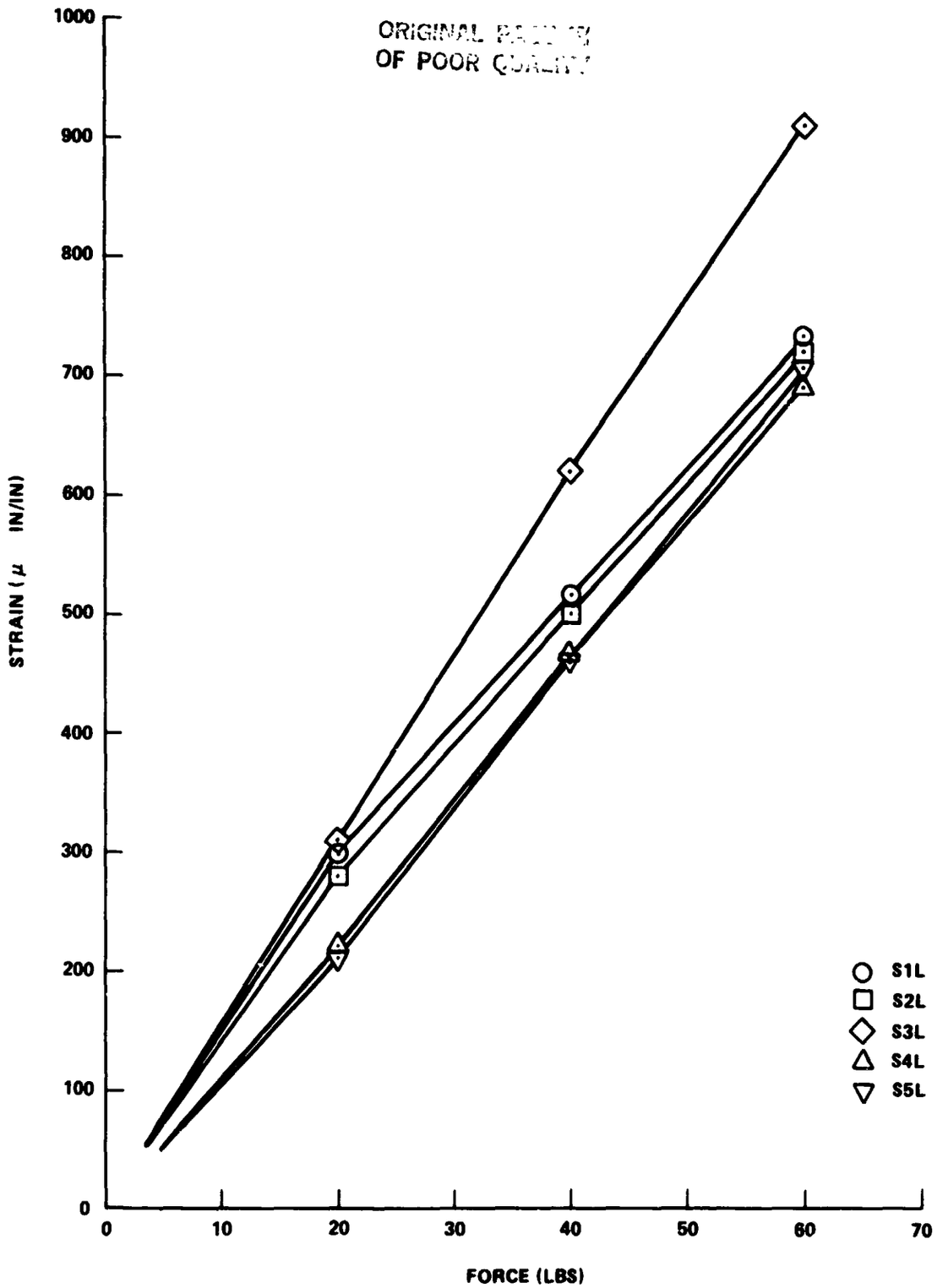

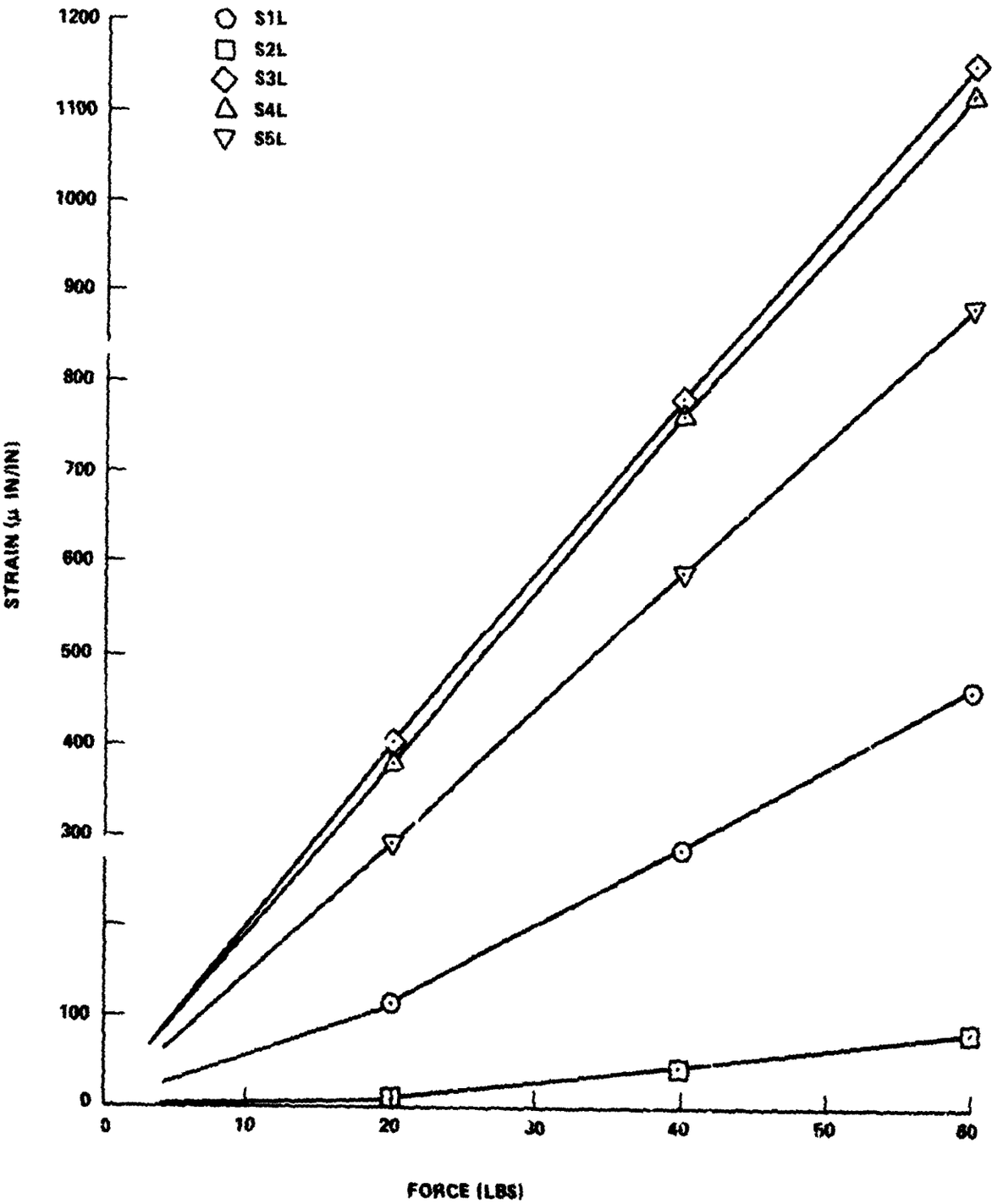

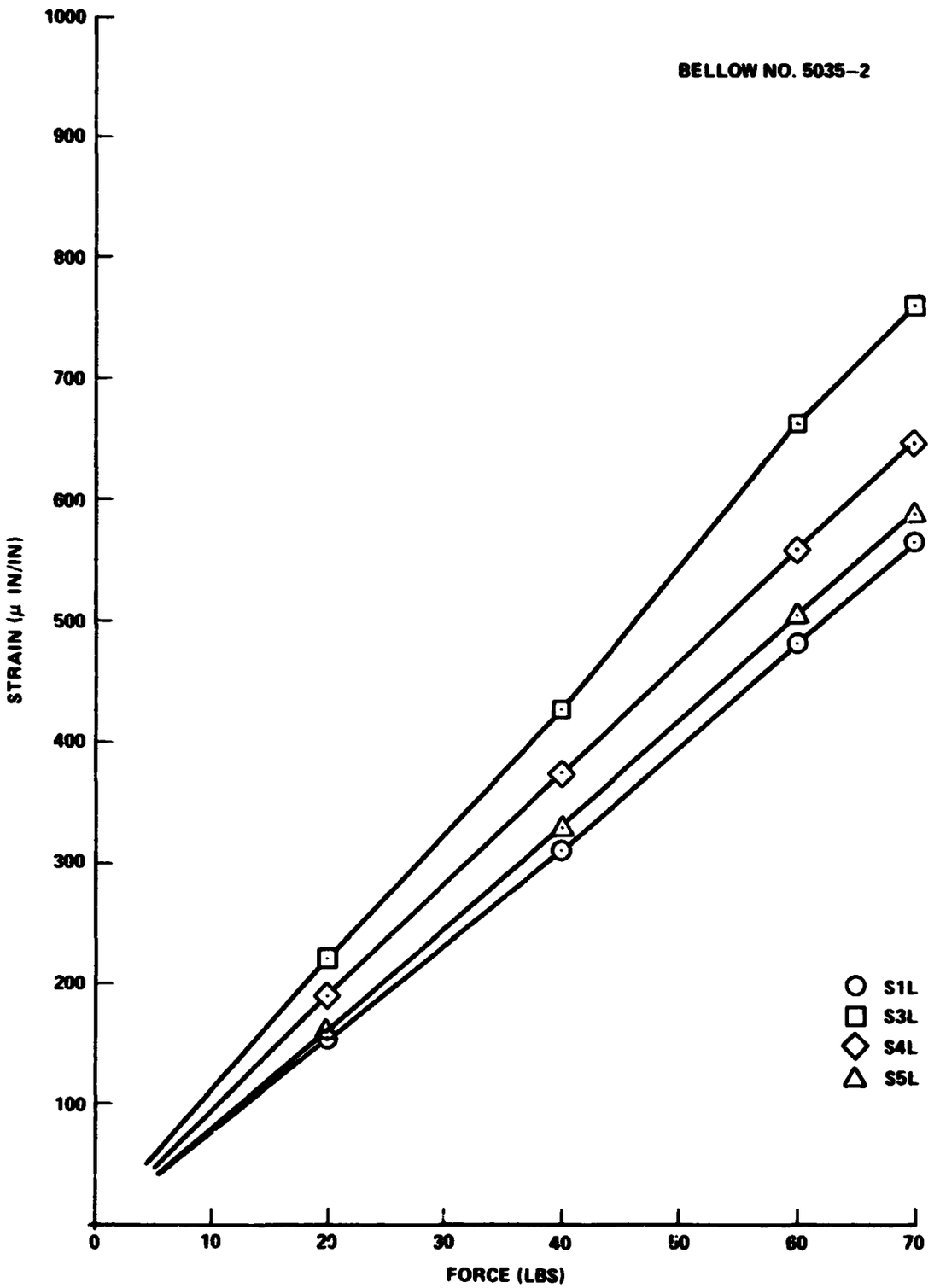
BELLOW NO. 5035–2
STRAIN (μ IN/IN)
1000
900
800
700
600
500
400
300
200
100
0
10
20
30
40
50
60
70
FORCE (LBS)
S1L
S3L
S4L
S5L

ORIGINAL PAGE IS
OF POOR QUALITY

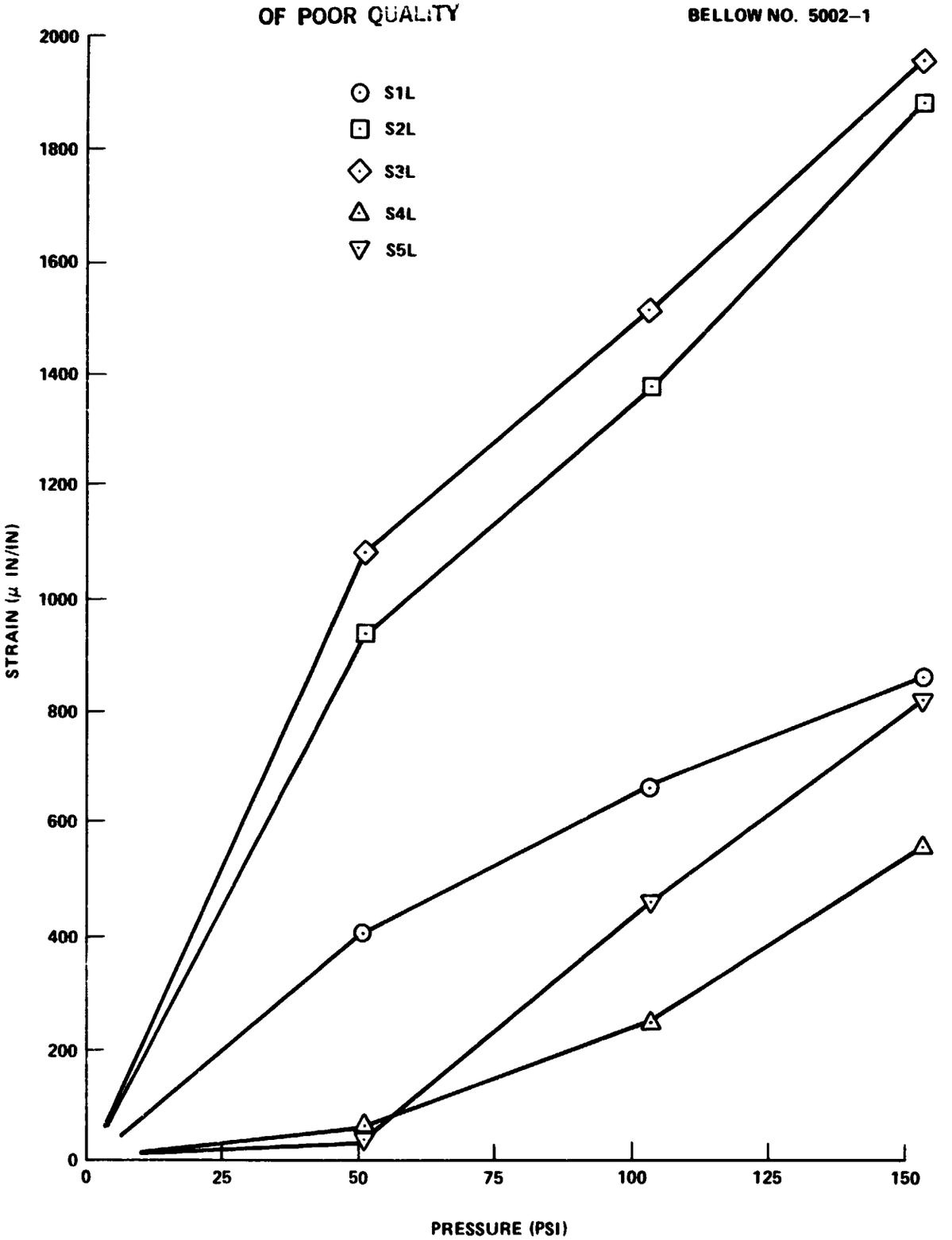

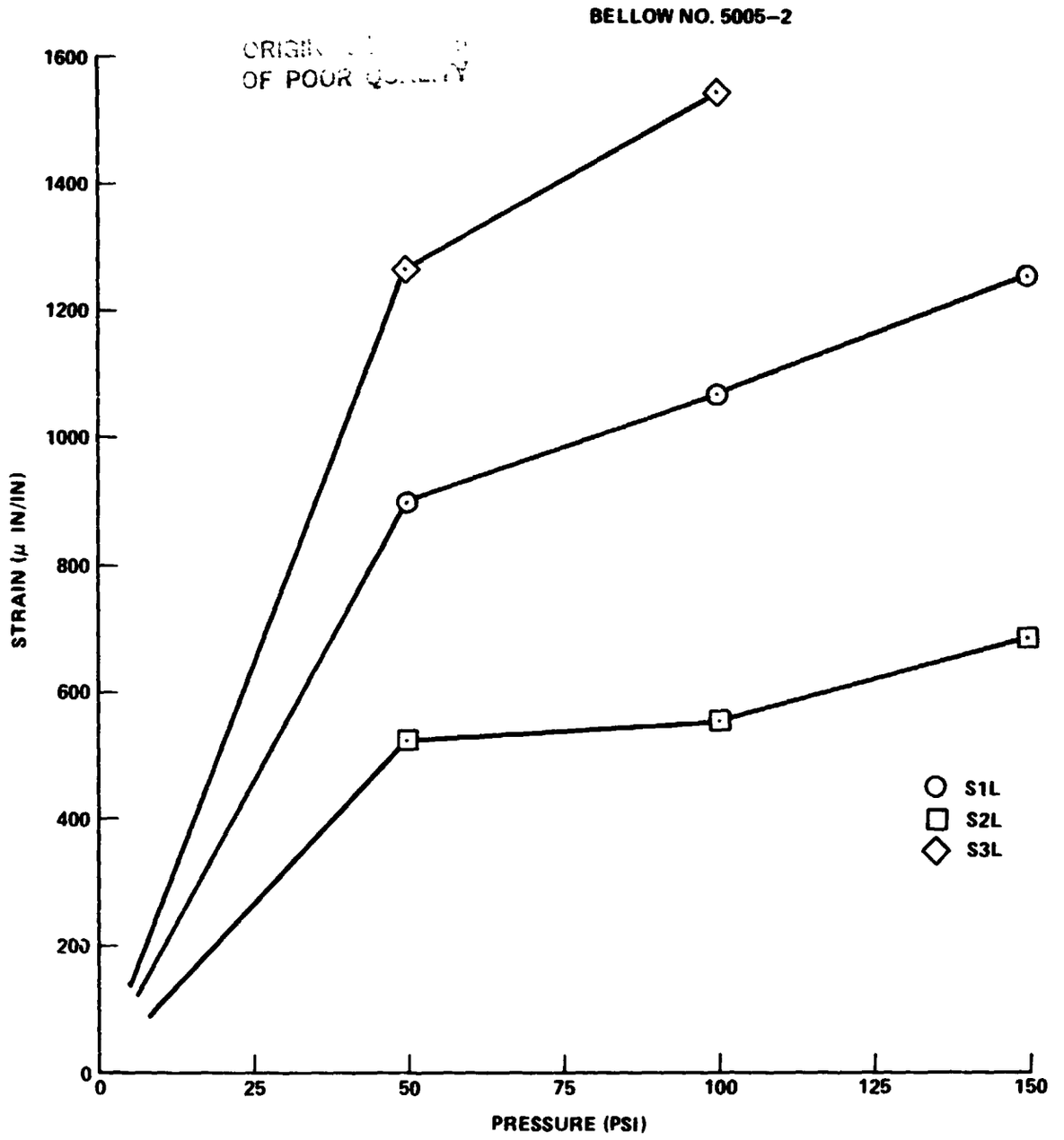
BELLOW NO. 5005–2
ORIGINAL PAGE IS
OF POOR QUALITY
1600
1400
1200
1000
800
600
400
200
0
STRAIN (μ IN/IN)
0
25
50
75
100
125
150
PRESSURE (PSI)
S1L
S2L
S3L

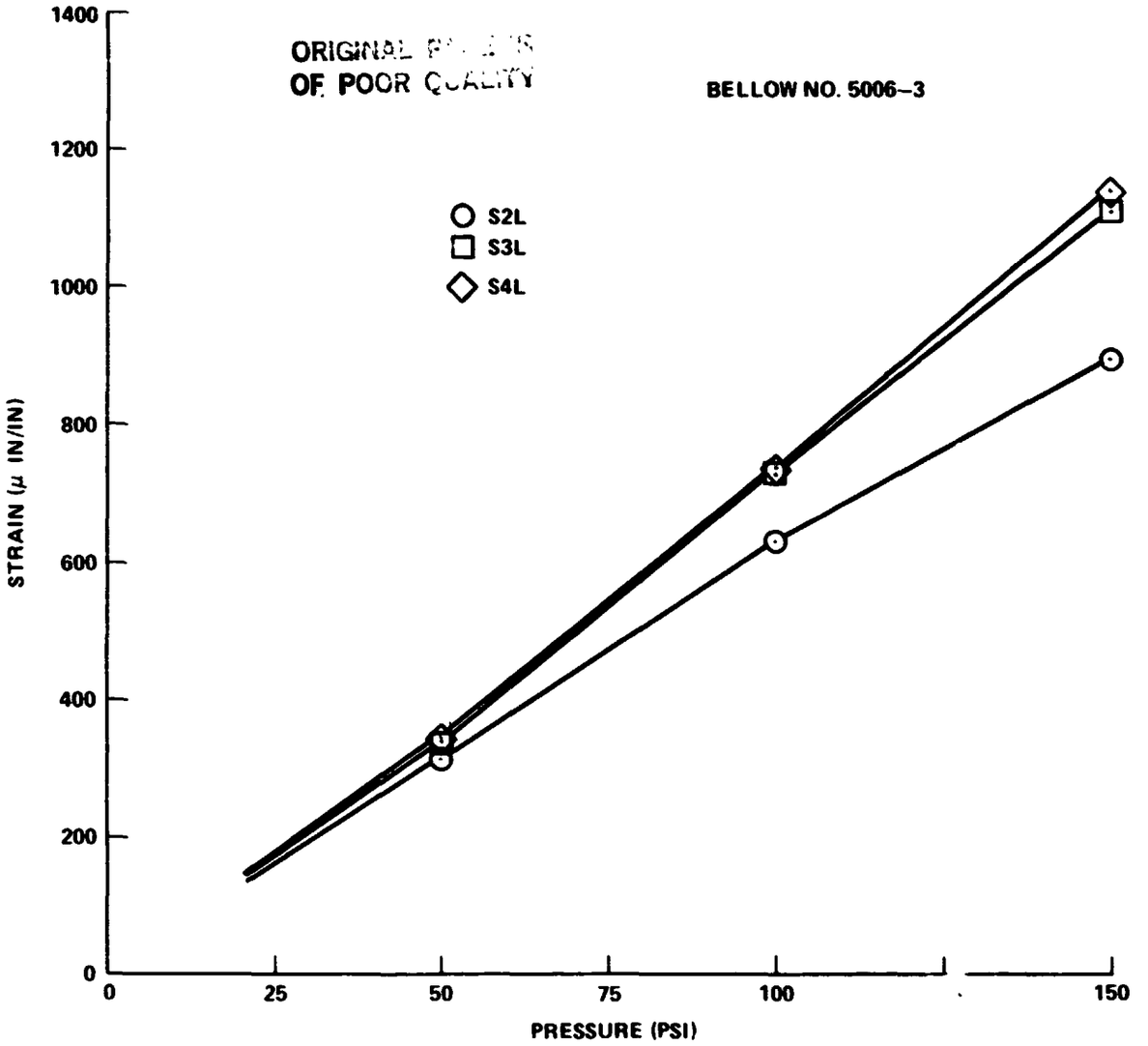
ORIGINAL PAGE IS
OF POOR QUALITY
BELLOW NO. 5006–3
S2L
S3L
S4L
STRAIN (μ IN/IN)
PRESSURE (PSI)
0
200
400
600
800
1000
1200
1400
0
25
50
75
100
150

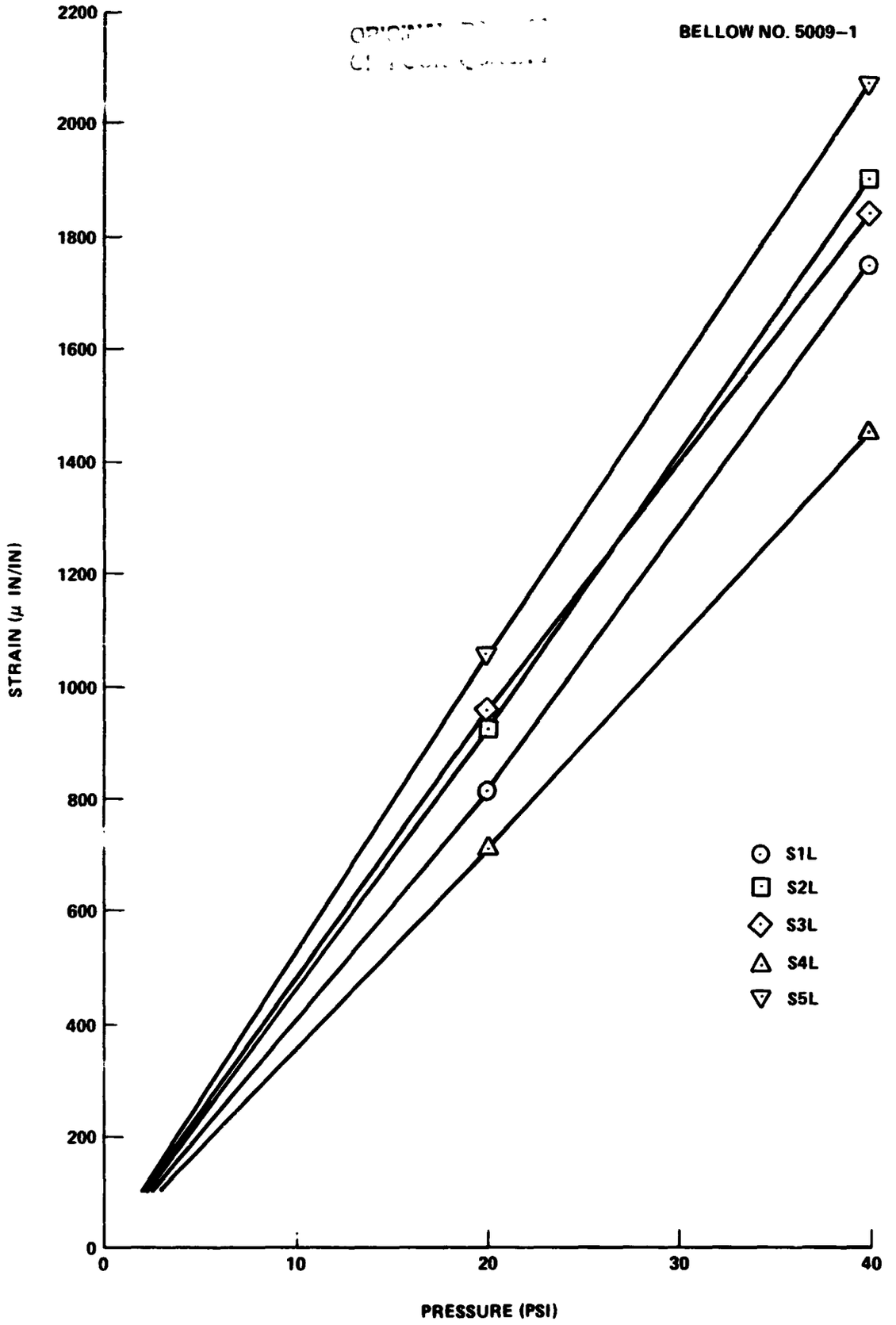
BELLOW NO. 5009–1
STRAIN (μ IN/IN)
2200
2000
1800
1600
1400
1200
1000
800
600
400
200
0
0
10
20
30
40
PRESSURE (PSI)
S1L
S2L
S3L
S4L
S5L

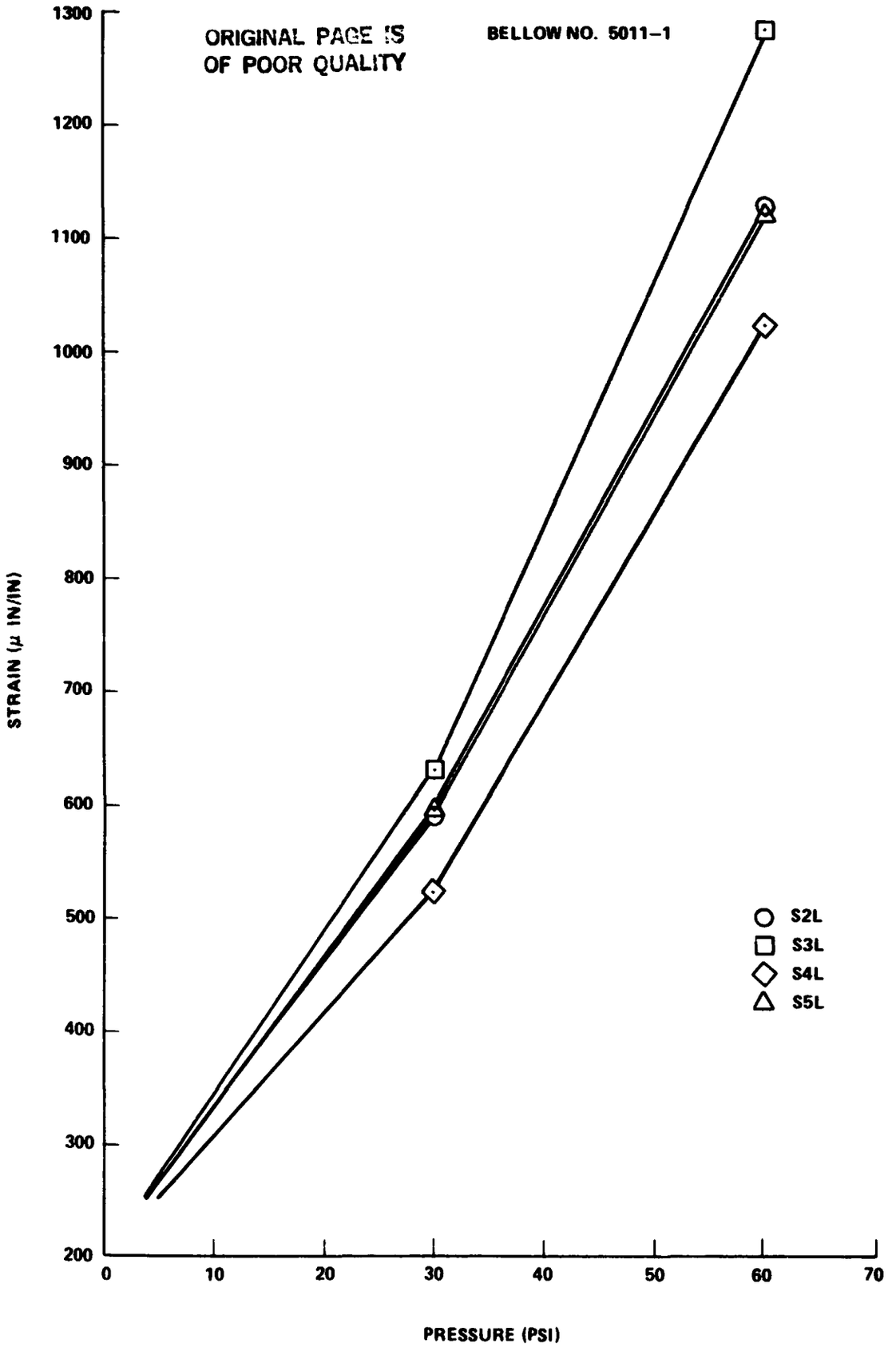
ORIGINAL PAGE IS
OF POOR QUALITY
BELLOW NO. 5011-1
1300
1200
1100
1000
900
800
700
600
500
400
300
200
STRAIN (μ IN/IN)
0
10
20
30
40
50
60
70
PRESSURE (PSI)
S2L
S3L
S4L
S5L

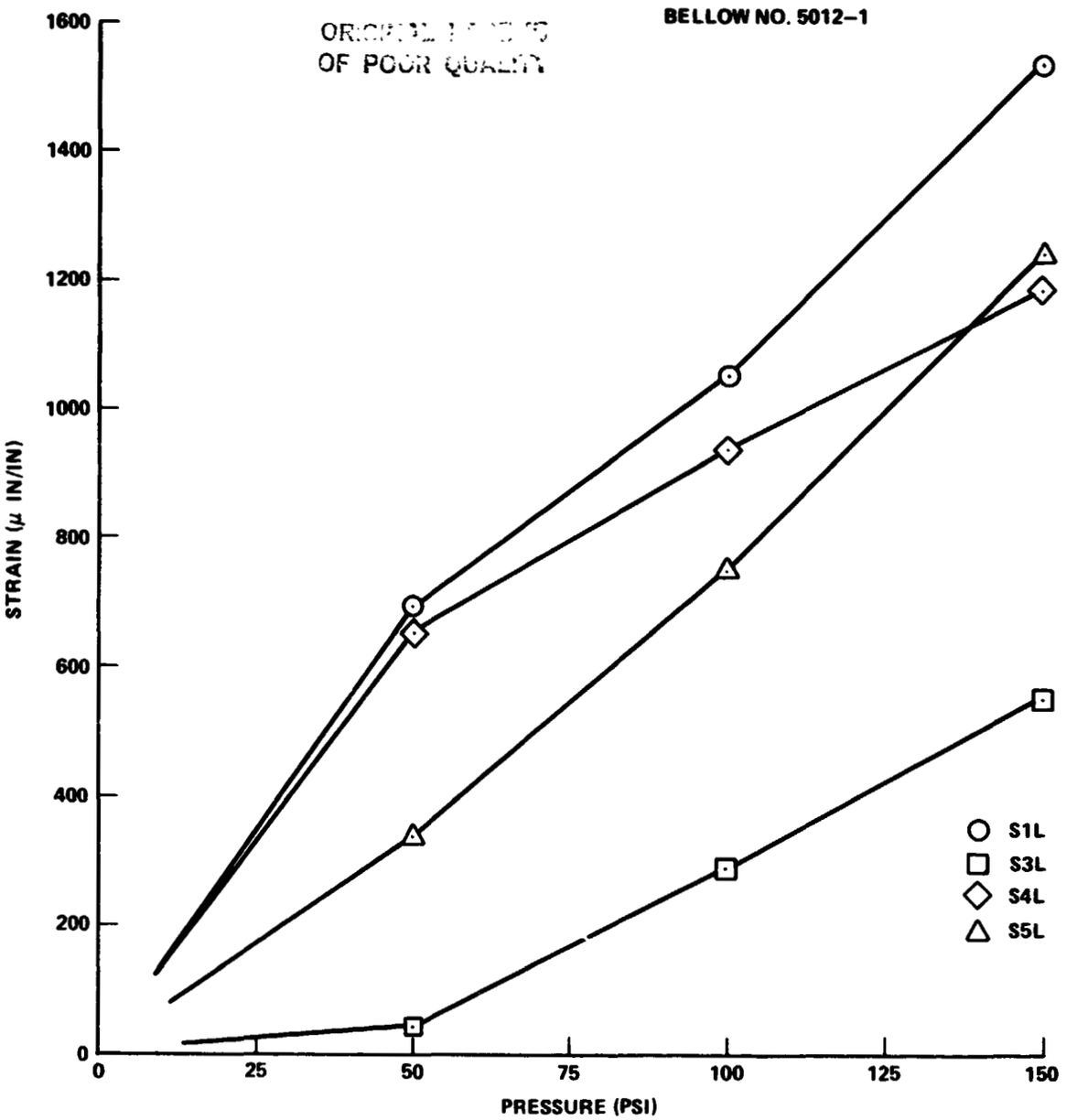
BELLOW NO. 5012–1
ORIGINAL PAGE IS
OF POOR QUALITY
STRAIN (μ IN/IN)
1600
1400
1200
1000
800
600
400
200
0
0
25
50
75
100
125
150
PRESSURE (PSI)
S1L
S3L
S4L
S5L

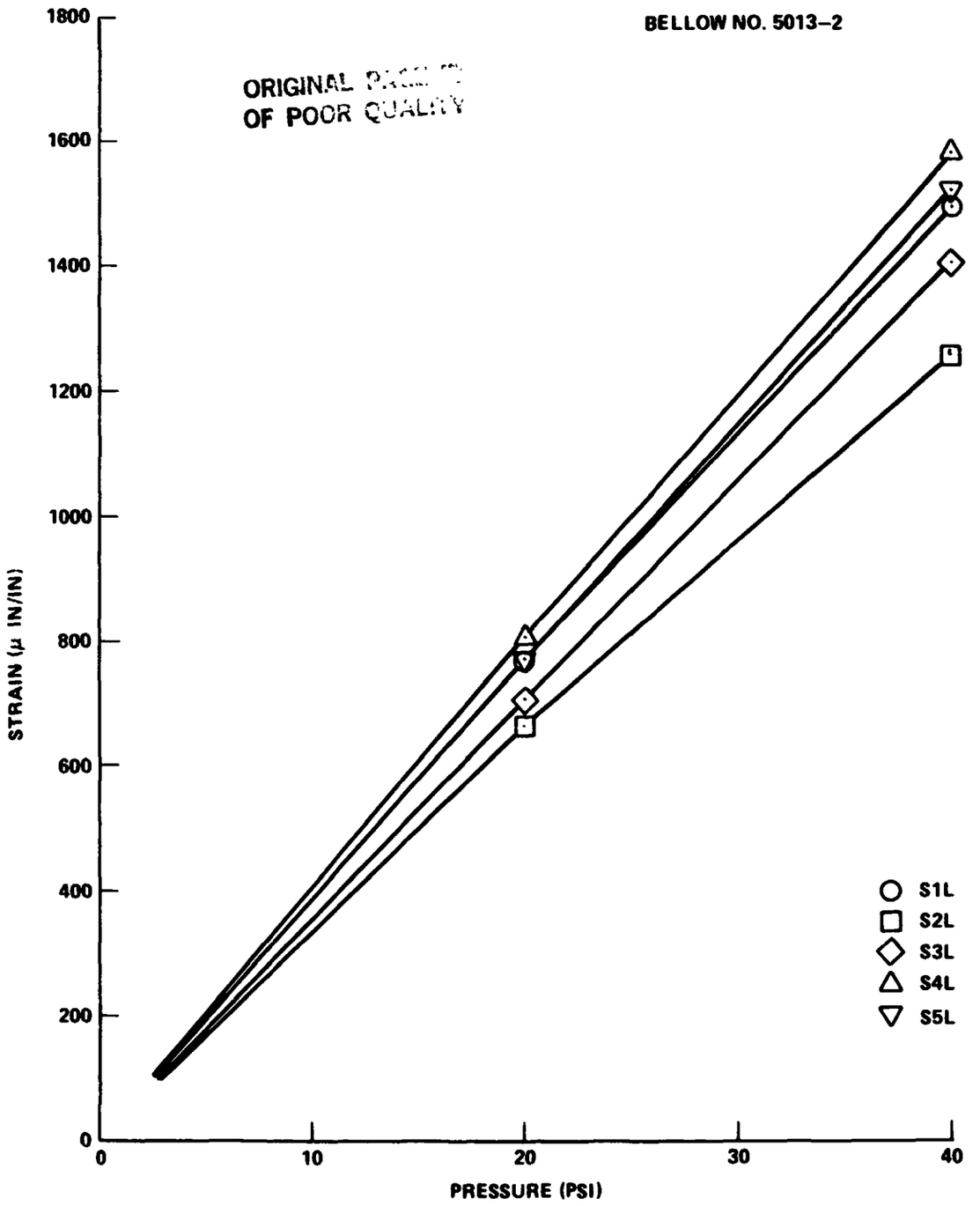
BELLOW NO. 5013–2
ORIGINAL PAGE IS
OF POOR QUALITY
1800
1600
1400
1200
1000
800
600
400
200
0
STRAIN (μ IN/IN)
0
10
20
30
40
PRESSURE (PSI)
S1L
S2L
S3L
S4L
S5L

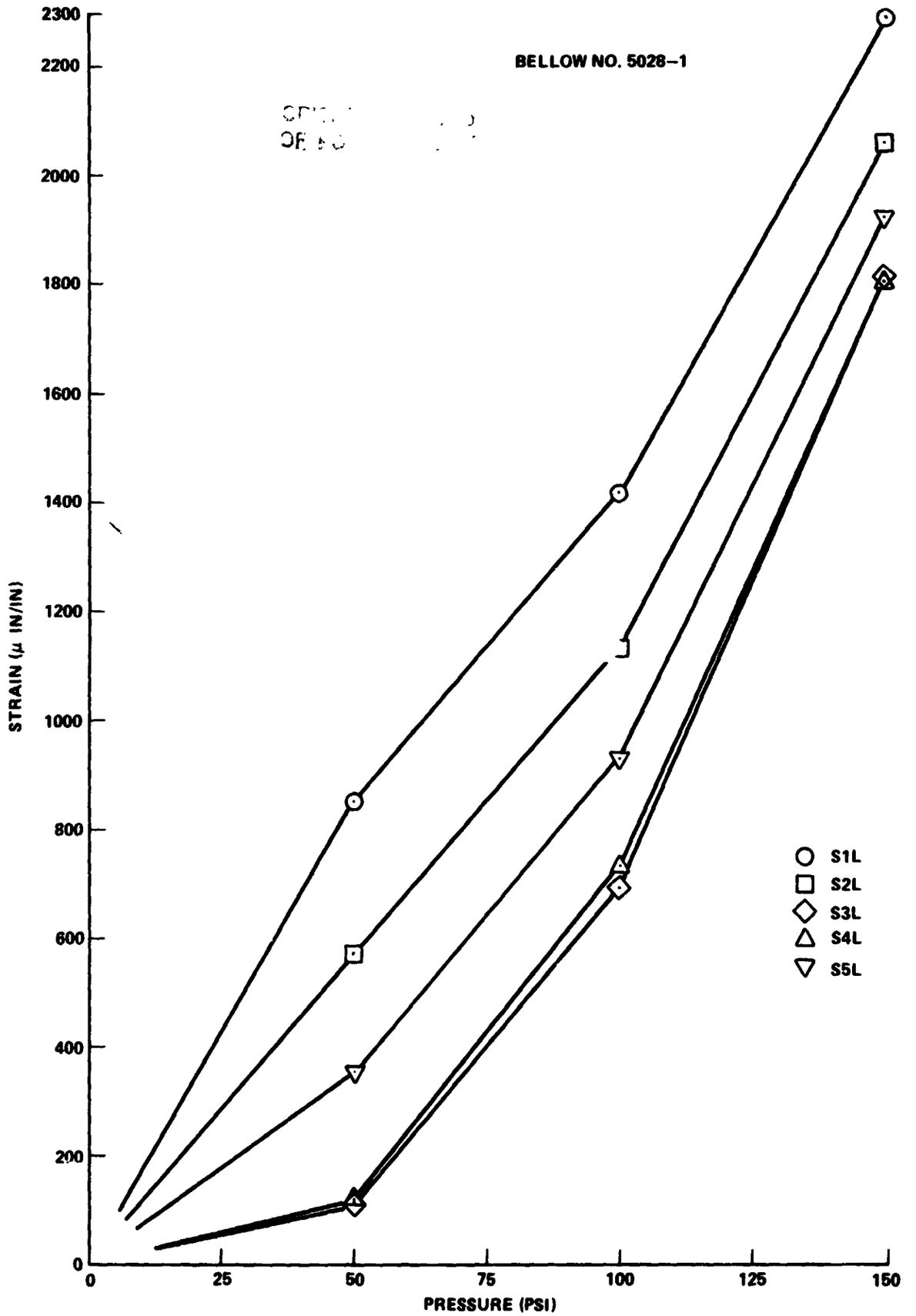
BELLOW NO. 5028–1
STRAIN (μ IN/IN)
PRESSURE (PSI)
2300
2200
2000
1800
1600
1400
1200
1000
800
600
400
200
0
0
25
50
75
100
125
150
S1L
S2L
S3L
S4L
S5L

BELLOW NO. 5034–1

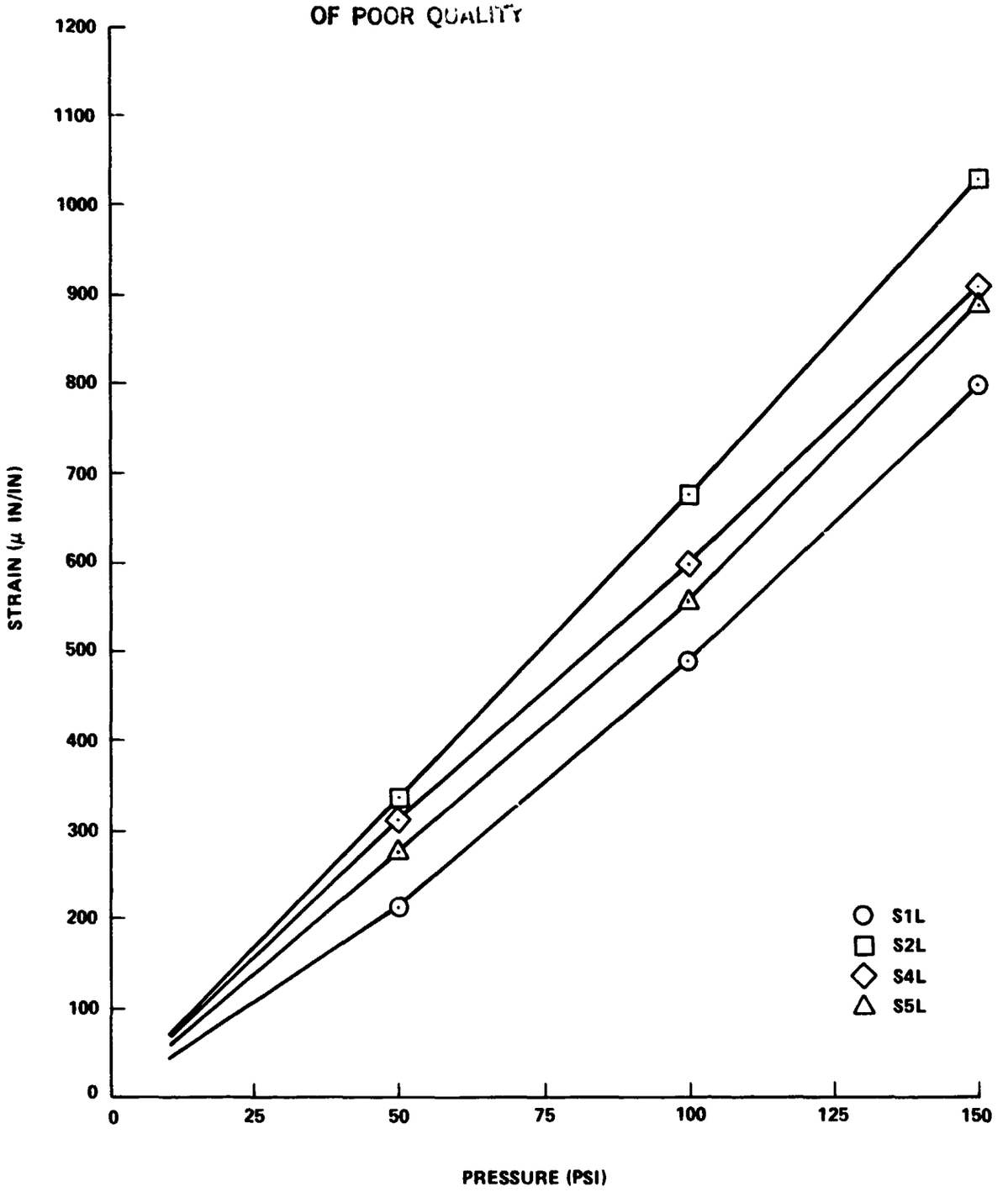

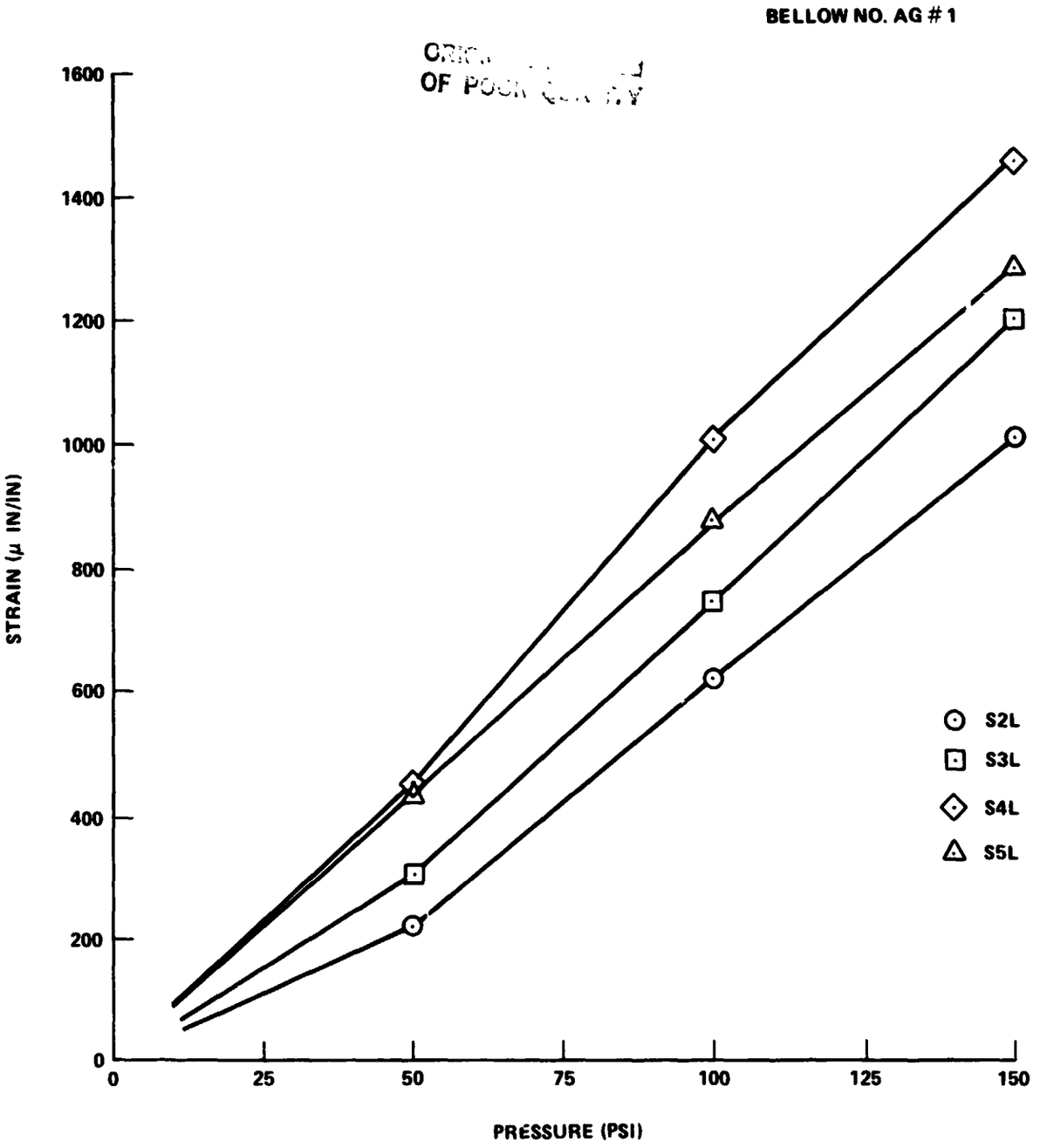
BELLOW NO. AG # 1
1600
1400
1200
1000
800
600
400
200
0
STRAIN (μ IN/IN)
0
25
50
75
100
125
150
PRESSURE (PSI)
S2L
S3L
S4L
S5L

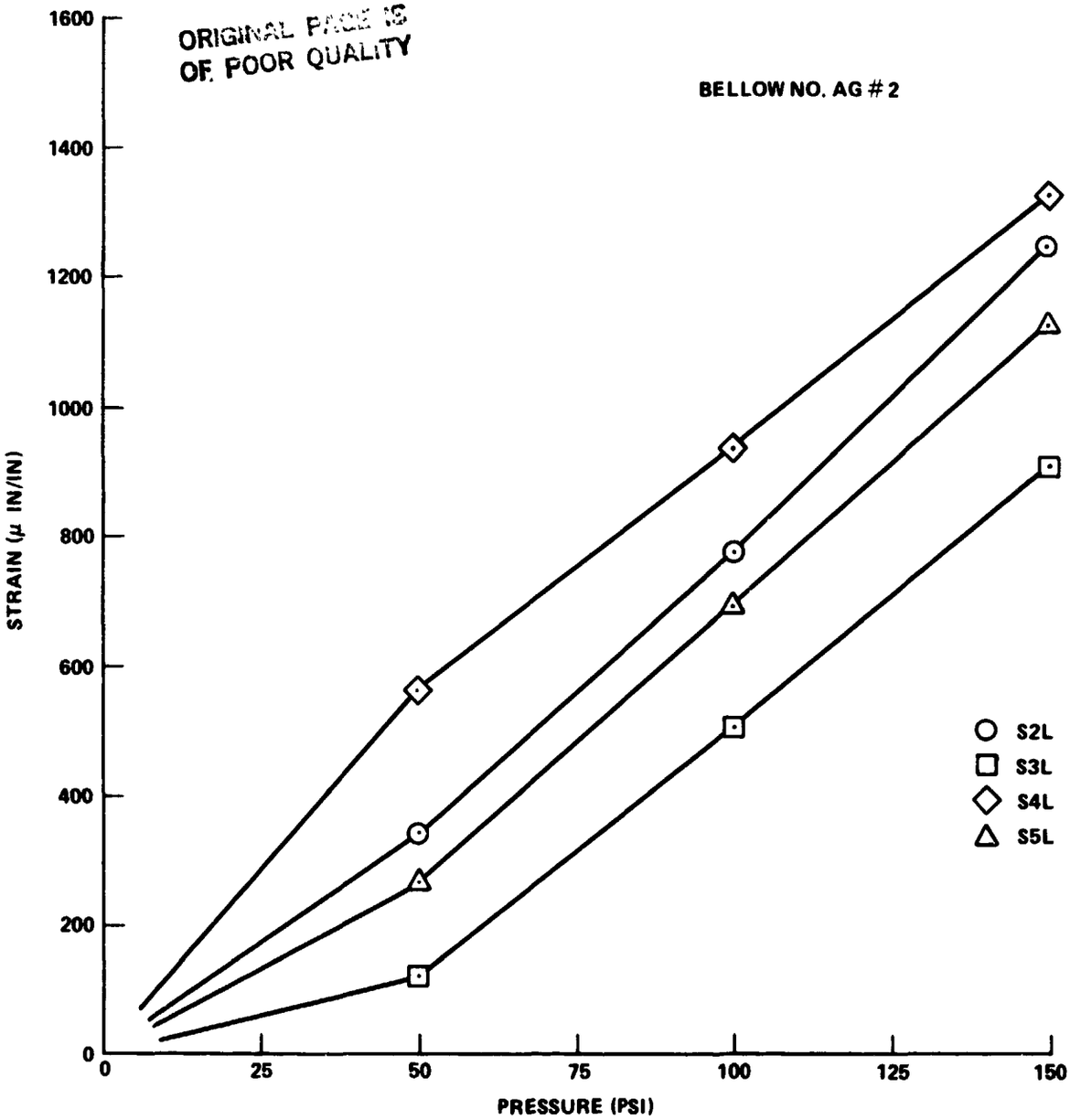

BELLOW NO. AC #3

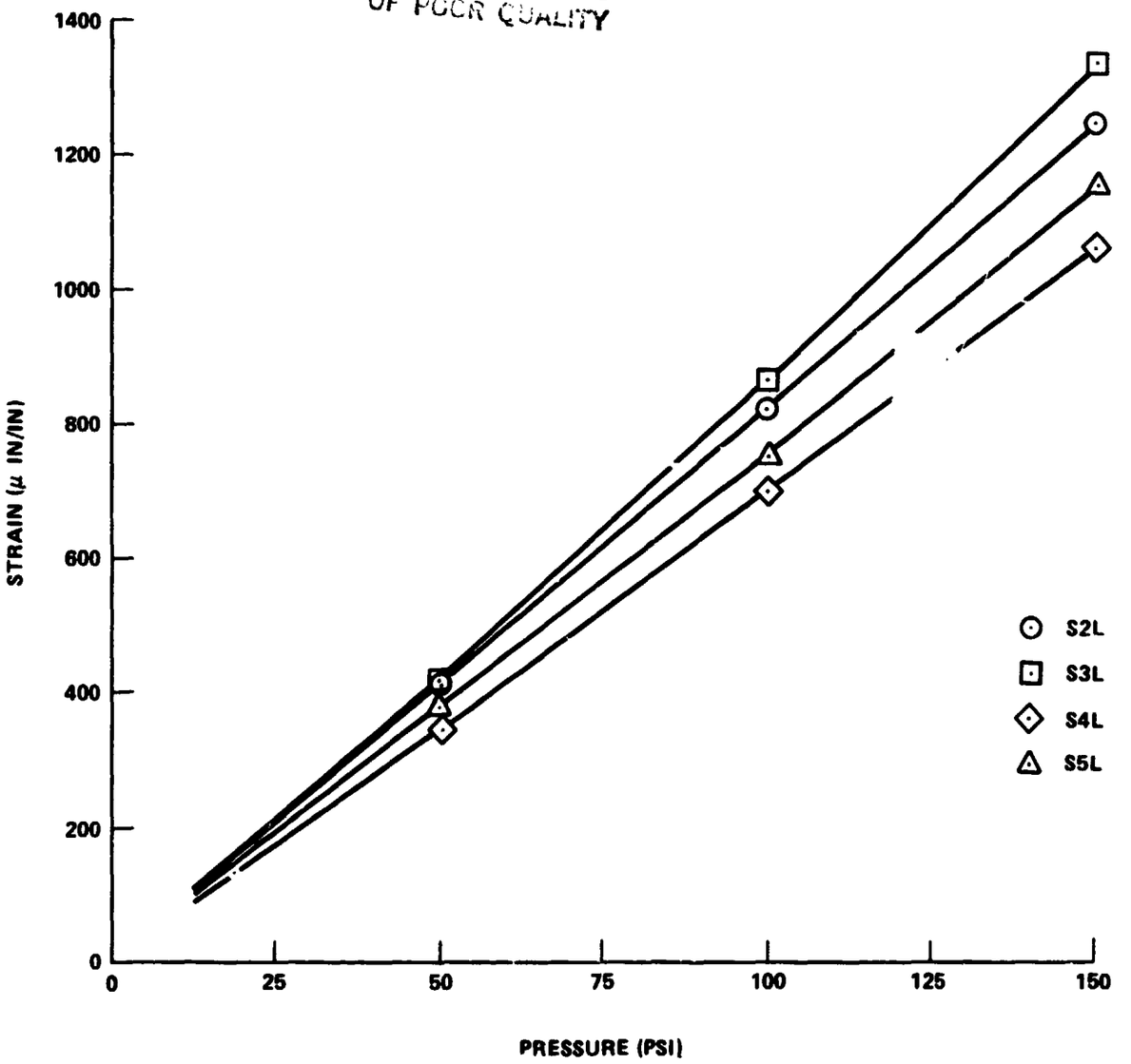

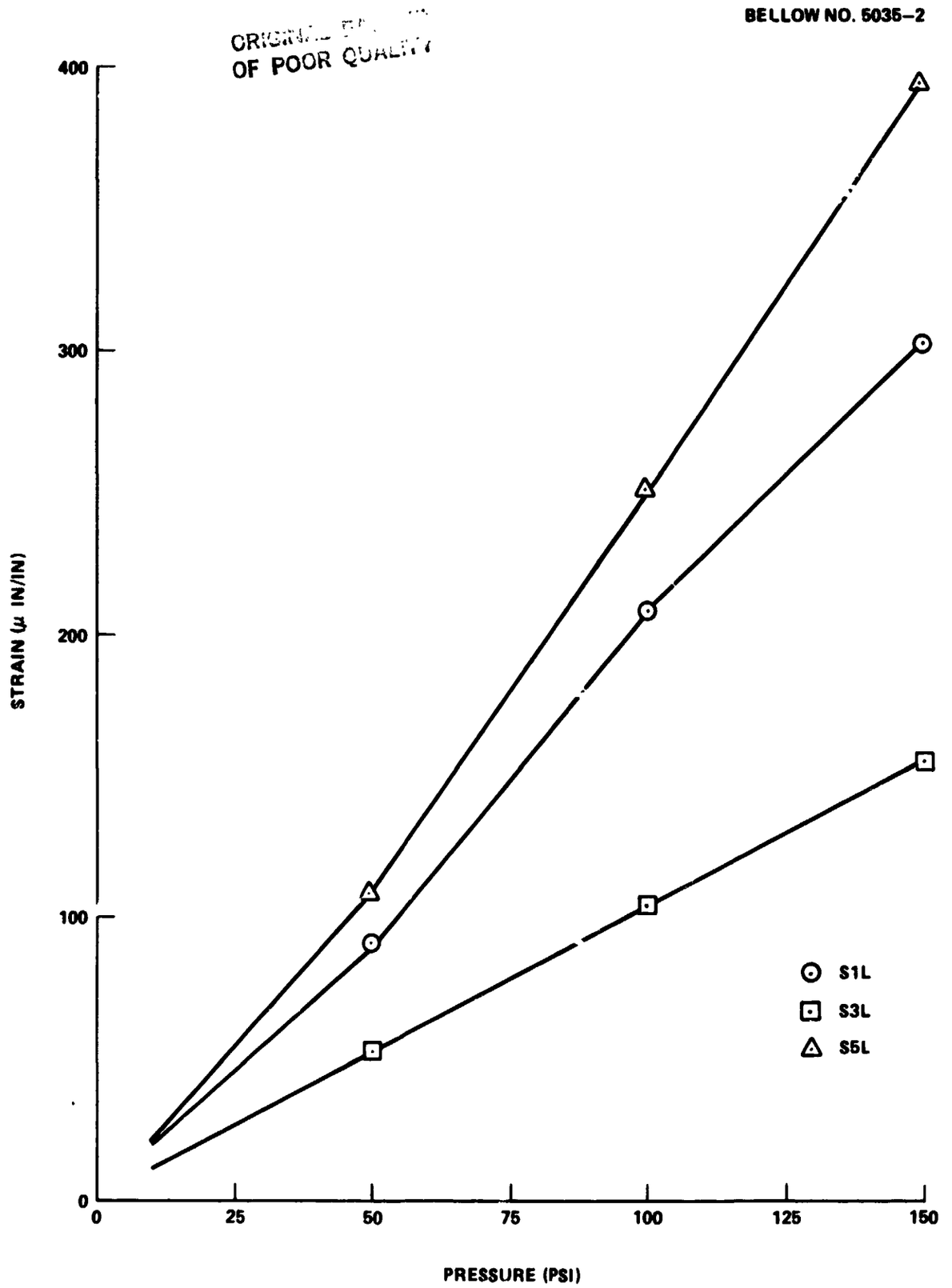

APPENDIX J

FREQUENCY VERSUS VELOCITY PLOTS FOR TYPICAL SwRI BELLOWS FLOW TESTS

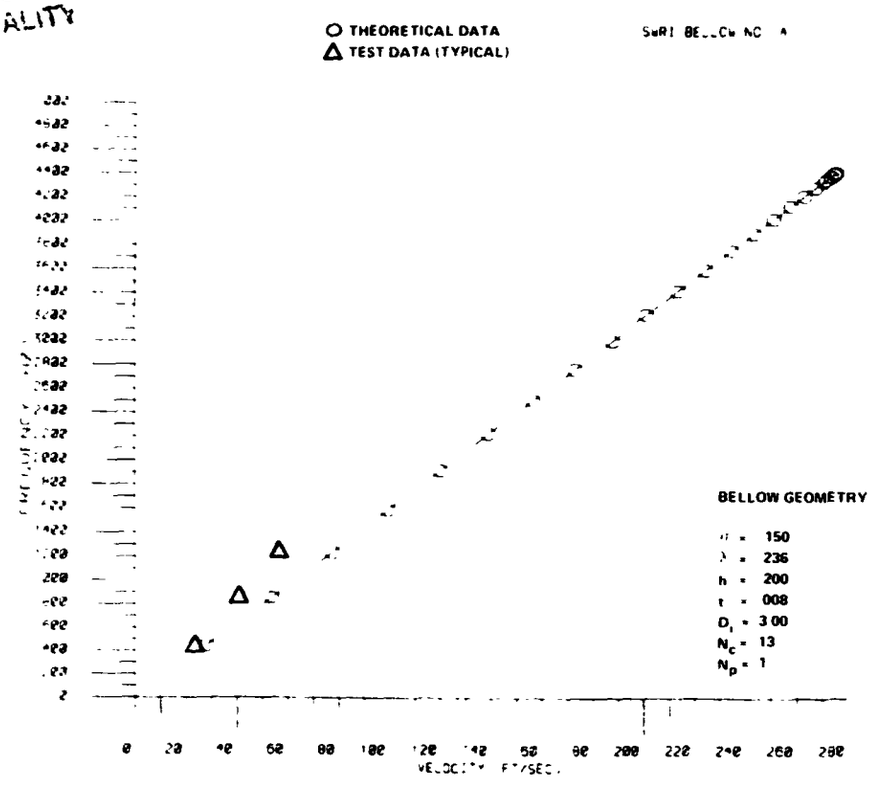

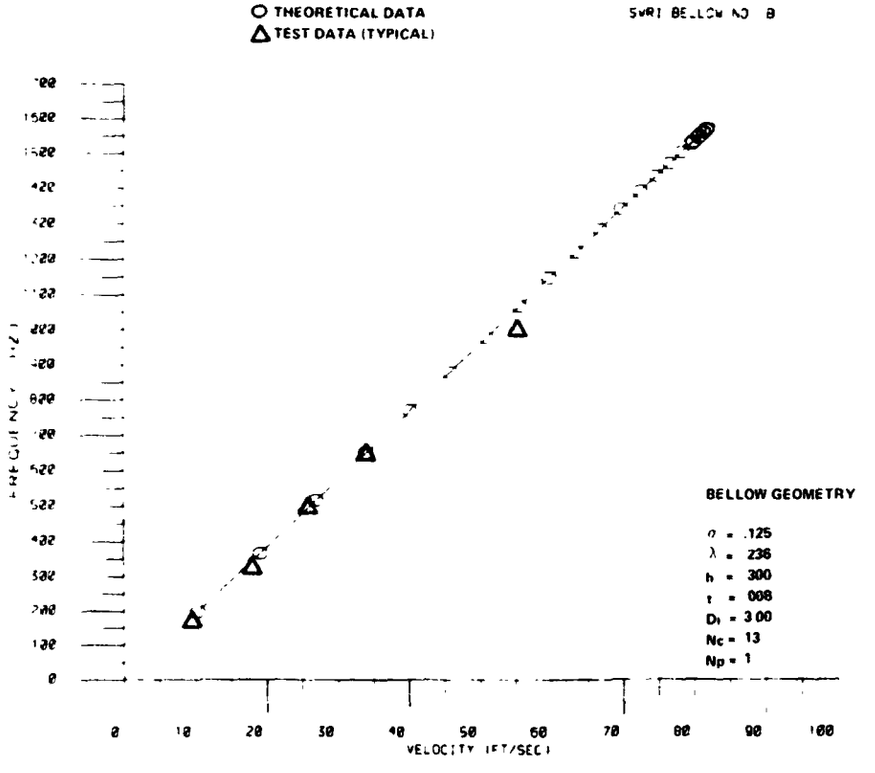

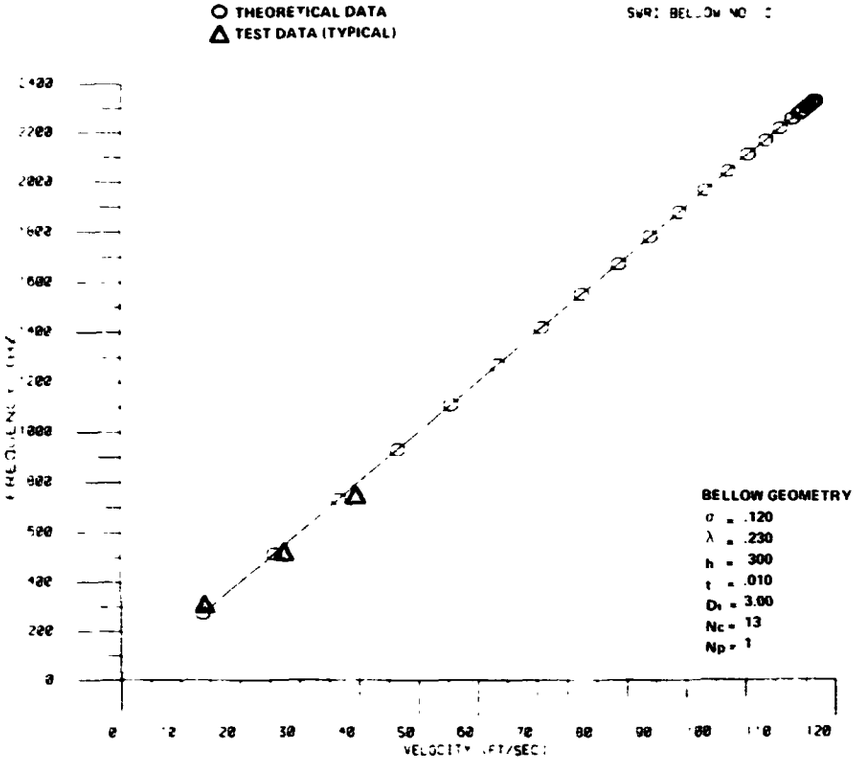

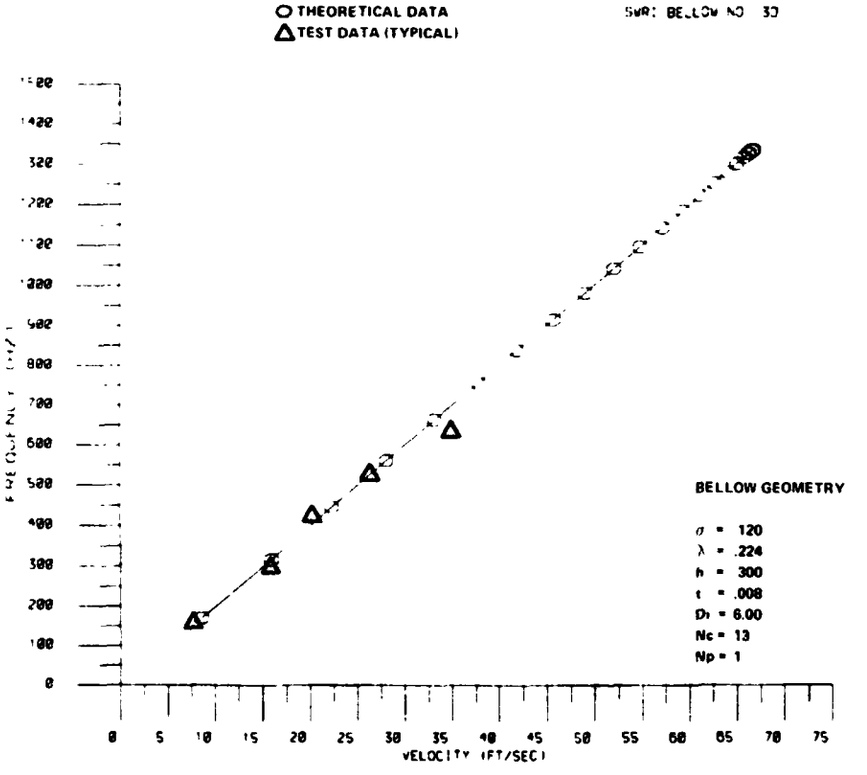

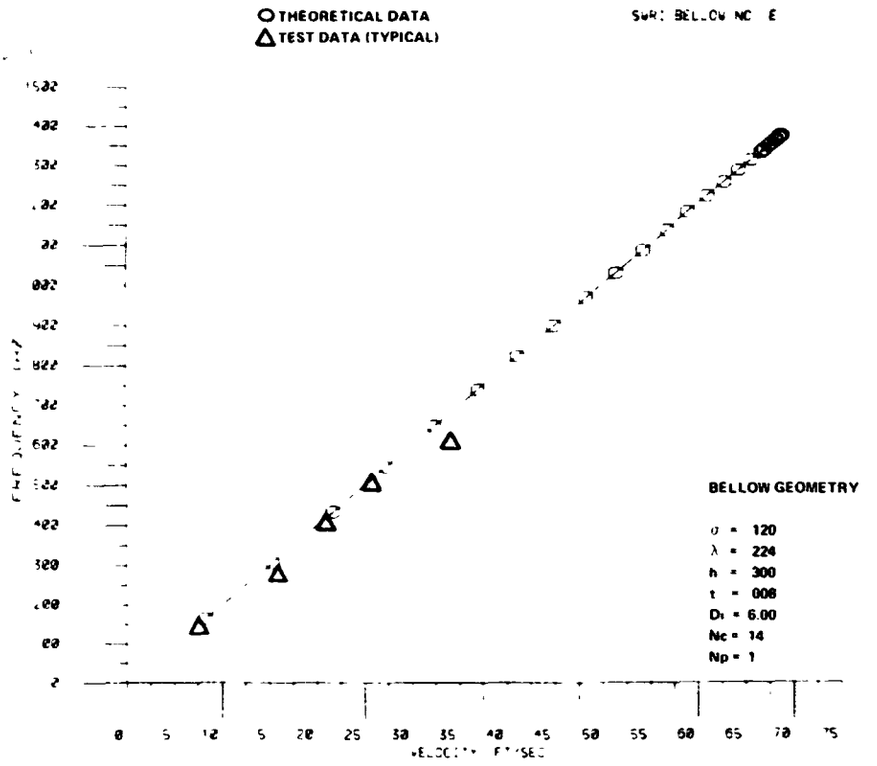

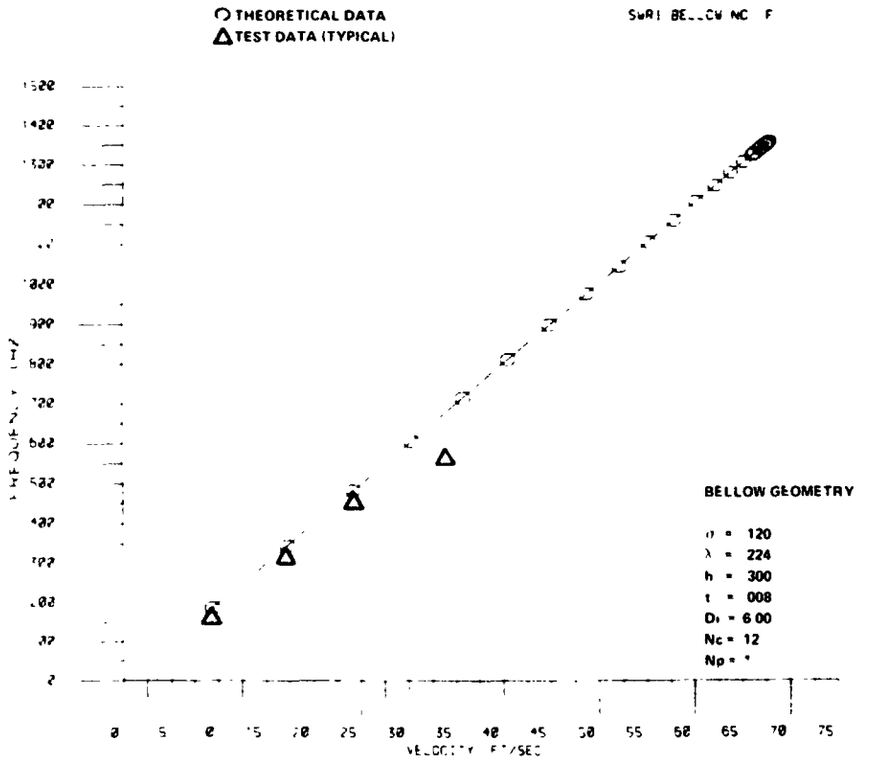

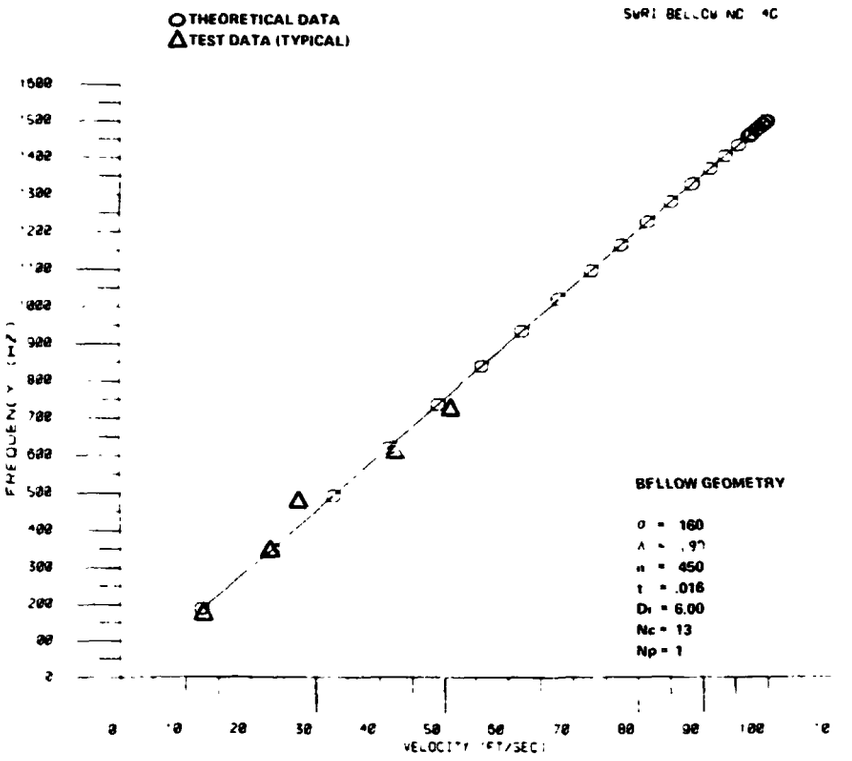
THEORETICAL DATA
TEST DATA (TYPICAL)
BELLOW GEOMETRY
θ = 160
λ = .97
n = 450
t = .016
Dᵢ = 6.00
Nc = 13
Np = 1
VELOCITY (FT/SEC)

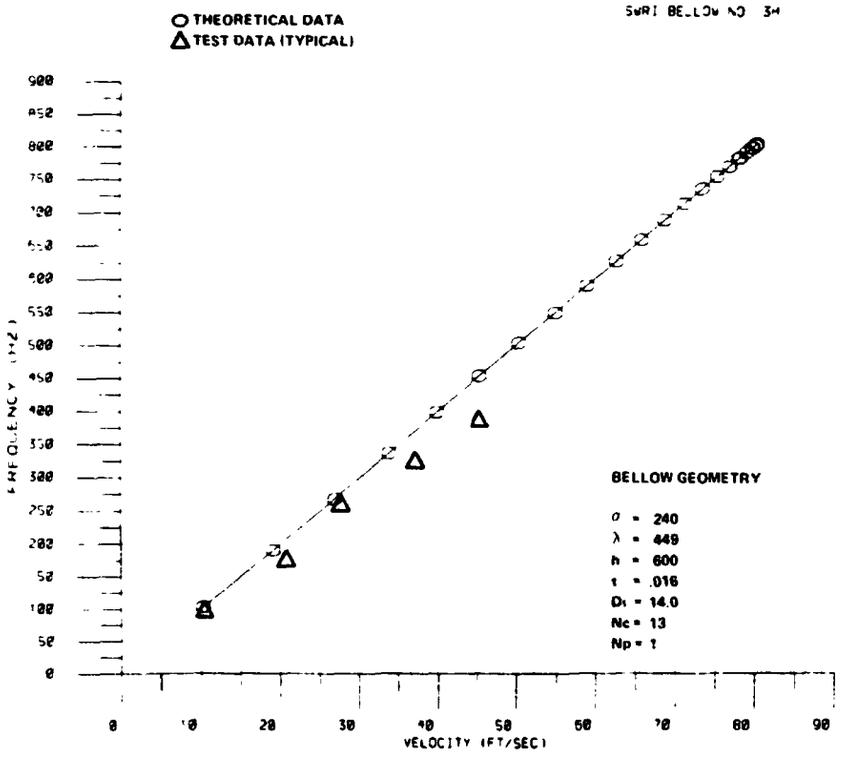
THEORETICAL DATA
TEST DATA (TYPICAL)
BELLOW GEOMETRY
θ = 240
λ = 449
h = 600
t = .016
Dᵢ = 14.0
Nc = 13
Np = 1
VELOCITY (FT/SEC)

ORIGINAL PAGE IS
OF POOR QUALITY

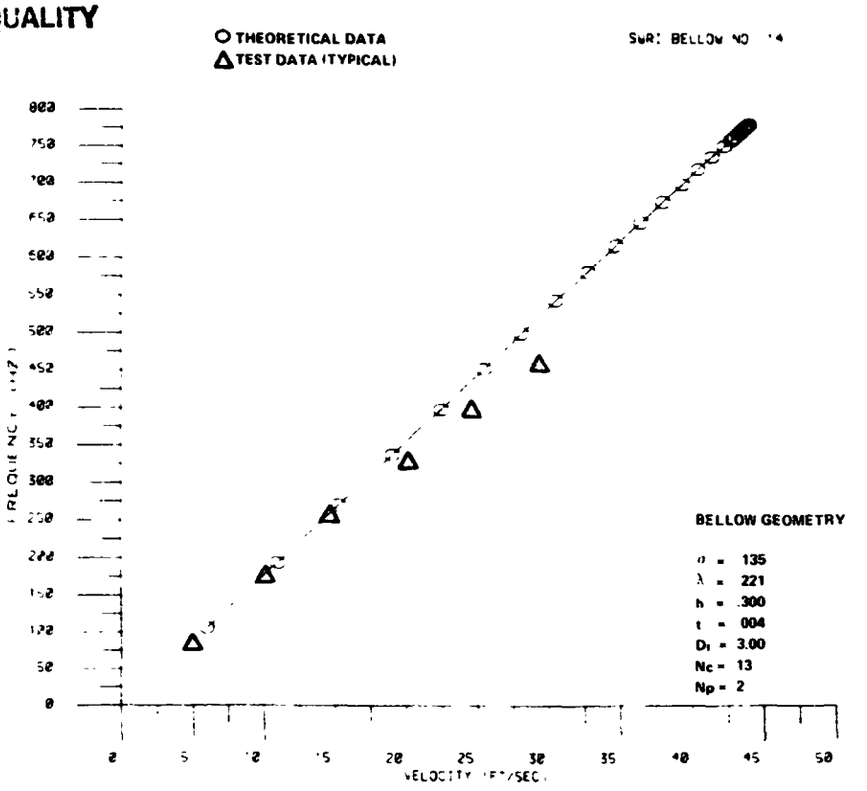

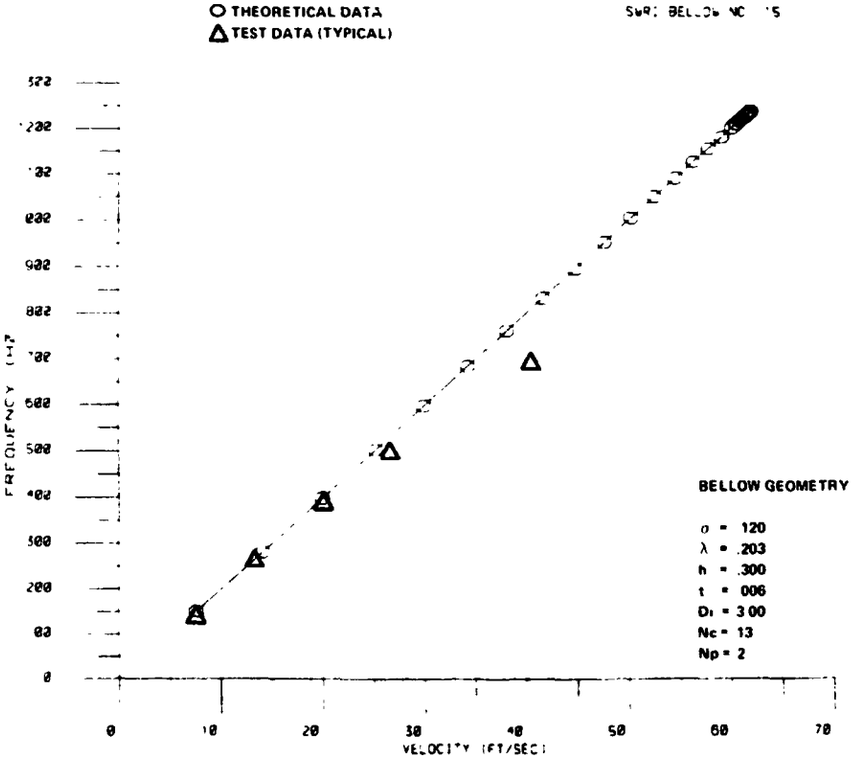

APPROVAL

BELLOWS FLOW-INDUCED VIBRATIONS

By Dr. C. R. Gerlach, P. J. Tygielski and H. M. Smyly

The information in this report has been reviewed for technical content. Review of any information concerning Department of Defense or nuclear energy activities or programs has been made by the MSFC Security Classification Officer This report, in its entirety, has been determined to be unclassified.

A. A. McCOOL
Director, Structures and Propulsion Laboratory

☆ U.S. GOVERNMENT PRINTING OFFICE 1983—746-070/97